Mechanisms of Interleukin-13 Inhibition of Allergic Inflammation

Kate Louise Tomlinson

Leukocyte Biology

NHLI

Imperial College London

A Thesis Submitted for the Degree of Doctor of Philosophy

DECLARATION

The work presented in this thesis was conducted by me with the following exceptions; total IgE, HDM specific IgG2a and HDM specific IgG2b ELISAs were performed by Kieran Jones; AB/PAS, Masson's trichrome staining and the subsequent image analyses were performed in part by me, Remi Okoye, Gemma Greenslade and Daniel Sutton; RNA isolation and real-time PCR analysis was conducted by me and Gareth Davies. All experimental work was performed at UCB, Slough.

ABSTRACT

Interleukin-13 (IL-13) is a Th2 cytokine proposed to mediate aspects of asthma pathogenesis such as airway inflammation, hyperreactivity (AHR), remodelling and mucus hypersecretion. These features of asthma have been reproduced in mice chronically exposed to house dust mite extract (HDM) in which IL-13 was demonstrated to be up-regulated. The aim of this thesis was to investigate the role of IL-13 in HDM induced allergic airways disease (AAD). This was accomplished using high affinity neutralising anti-mouse IL-13 monoclonal antibodies (mAb). Prophylactic anti-IL-13 mAb administration during HDM exposure inhibited airway eosinophilia, AHR, goblet cell up-regulation and airway remodelling. Furthermore, therapeutic neutralisation of IL-13 after the induction of AAD reduced airway inflammation, AHR, goblet cell frequency and remodelling; thus implicating IL-13 in both the initiation and maintenance of AAD.

To investigate the mechanisms of IL-13 inhibition in AAD the expression and distribution of IL-13 receptors, IL-13Rα1 and IL-13Rα2, were investigated in lungs from sham and HDM exposed mice. IL-13Rα2 but not IL-13Rα1 mRNA was up-regulated following induction of AAD. Immunofluorescence staining for IL-13Rα2 protein revealed expression in the airway epithelium of sham mice and abundance throughout the lung tissue in mice with AAD. The key signalling receptor IL-13Rα1 was detected in alveolar macrophages (AM) in both sham and HDM exposed mice, however surface expression of IL-13Rα1 was lost during AAD.

The function of IL-13Rα1+ AM *in vivo* was explored by depletion of AM using clodronate liposomes. The absence of AM during IL-13 or HDM induced inflammation resulted in exacerbated airway pathophysiology suggesting AM may regulate allergic airways inflammation.

In summary, HDM induced pathophysiology in mice is largely dependent on IL-13. Based on receptor expression, AM were identified as IL-13 responsive cells, however AM depletion exacerbated AAD indicating AM, or a subset of, are not driving IL-13 pathology and may in fact be protective.

ACKNOWLEDGMENTS

I would like to thank UCB for giving me the opportunity to embark upon this project, and the many people at UCB who have helped me over the years. There are too many names to mention, but I have received much help in the lab learning new techniques and advice from those no longer lab dwelling.

I would also like to thank Prof Clare Lloyd and her team for welcoming me into the group, despite my infrequent presence. Through my time at the NHLI I have met some great people, received valuable input into my work and learnt a lot. I am particularly grateful to Clare for all her guidance over the course of this project.

And finally, but my no means least I would like to thank my new husband, James, for supporting me throughout this project; especially during the last 6 months in which he has had to assume the roles of wedding planner, housekeeper and chef.

CONTENTS

i. Table of Contents

DECLARATION 2

ABSTRACT 3

ACKNOWLEDGMENTS 4

CONTENTS 5

i. Table of Contents 5

ii. List of Tables 9

iii. Table of Figures 10

ABBREVIATIONS 13

1. INTRODUCTION 18

1.1 Asthma 19

1.2 IL-13 23

1.2.1 IL-13 in asthma *23*

1.2.2 IL-13 activities *24*

1.2.3 IL-13 receptors *31*

1.2.4 Modulation of IL-13 *36*

1.3 HDM induced AAD 43

1.4 Hypothesis 49

1.5 Aims 49

2. MATERIALS AND METHODS 50

2.1 Animals 51

2.2 HDM exposure 51

2.3 Anti-IL-13 mAbs and treatment 51

2.4 Assessment of AHR 51

2.5 Collection of samples 52

2.6 Lung digest 53

2.7 Flow cytometry 53

2.8 Cytokine analysis 56

2.9 Detection of serum immunoglobulins 56

2.10 Histology **57**
2.10.1 Paraffin sections *57*
2.10.2 Frozen sections *60*
2.10.3 BAL cytospins *60*
2.10.4 Immunofluorescence *60*
2.11 cDNA Synthesis and real-time PCR **61**
2.12 Statistical Analysis **62**
3. CHARACTERISATION OF HDM INDUCED AAD **63**
3.1 Introduction **64**
3.1.1 Aim *65*
3.2 Methods **66**
3.2.1 HDM exposure. *66*
3.2.2 IL-13 Immunofluorescence staining. *66*
3.3 Results **68**
3.3.1 Chronic exposure to HDM induces AHR *68*
3.3.2 Chronic exposure to HDM induces pulmonary inflammation *68*
3.3.3 HDM induced pulmonary inflammation is Th2 biased *71*
3.3.4 HDM induced cytokine profile *71*
3.3.5 HDM induced antibody production *77*
3.3.6 HDM induced airway remodelling *79*
3.3.7 HDM exposure up-regulates IL-13 *82*
3.4 Discussion **91**
3.4.1 HDM exposure induces allergic airways disease *91*
3.4.2 HDM exposure up-regulates IL-13 *95*
4. THE ROLE OF IL-13 IN HDM INDUCED AAD **99**
4.1 Introduction **100**
4.1.1 Aim *102*
4.2 Methods **104**
4.2.1 Mice and HDM sensitisation. *104*
4.3 Results **106**
4.3.1 Dose response to anti-IL-13 mAb *106*
4.3.2 Direct comparison of anti-IL-13 mAbs with distinct functional epitopes. *109*
4.3.3 IL-13 neutralisation inhibits AHR *114*
4.3.4 Effects of IL-13 neutralisation on pulmonary inflammation *116*
4.3.5 Effects of IL-13 neutralisation on the cytokine milieu *121*
4.3.6 Effects of IL-13 neutralisation on antibody generation *126*

4.3.7 Effects of therapeutic IL-13 neutralisation *128*

4.4 Discussion **132**

4.4.1 Anti-IL-13 mAb dose selection *132*

4.4.2 Anti-IL-13 mAb selection *132*

4.4.3 Effects of prophylactic IL-13 neutralisation in HDM induced AAD *135*
4.4.3.1 AHR 135
4.4.3.2 Inflammation 136
4.4.3.3 Remodelling 142

4.4.4 Effects of therapeutic IL-13 neutralisation in HDM induced AAD *142*
4.4.4.1 AHR 143
4.4.4.2 Inflammation 145
4.4.4.3 Remodelling 146

5. IL-13 RECEPTOR DISTRIBUTION **149**

5.1 Introduction **150**

5.1.1 Aim *151*

5.2 Methods **152**

5.2.1 IL-13Rα2 ELISA *152*

5.2.2 IL-13Rα1 staining for flow cytometry *152*

5.3 Results **153**

5.3.1 IL-13 receptor mRNA expression following HDM exposure *153*

5.3.2 IL-13Rα2 expression following HDM exposure. *153*

5.3.3 IL-13Rα1 expression in the lungs following HDM exposure. *157*

5.3.4 Quantification of IL-13Rα1+ cells. *163*

5.3.5 IL-13Rα1+ macrophages *166*

5.3.6 IL-13Rα1 expression on non-macrophages *176*

5.4 Discussion **186**

5.4.1 IL-13Rα2 expression *186*

5.4.2 IL-13Rα1 expression *189*
5.4.2.1 IL-13Rα1 expression on macrophages. 190
5.4.2.2 IL-13Rα1 expression on monocytes 193
5.4.2.3 IL-13Rα1 expression on T cells 193

6. THE ROLE OF AM IN HDM INDUCED AAD **196**

6.1 Introduction **197**

6.1.1 Aim *198*

6.2 Methods **199**

6.2.1 Macrophage depletion. *199*
6.2.1.1 Anti-CSF-1R treatment 199
6.2.1.2 Administration of clodronate liposomes 199

6.2.2 IL-13 induced lung inflammation *199*

6.2.3 Clodronate liposome treatment of HDM exposed mice *200*

6.3 Results 202

6.3.1 Anti-CSF-1 receptor induced macrophage depletion 202

6.3.2 Clodronate liposome mediated macrophage depletion 205

6.3.3 IL-13 induced lung inflammation 209

6.3.4 IL-13 induced lung inflammation in mice pre-treated with clodronate liposomes 214

6.3.5 Prophylactic administration of clodronate liposomes during HDM induced lung inflammation 220

6.3.6 Therapeutic administration of clodronate liposomes during HDM induced lung inflammation 237

6.4 Discussion 244

6.4.1 Anti-CSF-1R induced macrophage depletion 244

6.4.2 Clodronate liposome mediated macrophage depletion 245

6.4.3 IL-13 induced lung inflammation 245

6.4.4 IL-13 induced lung inflammation in AM deficient mice 246

6.4.5 Prophylactic clodronate treatment during HDM induced lung inflammation 247

6.4.6 Therapeutic clodronate treatment during HDM induced lung inflammation 252

6.4.7 The role of AM in lung inflammation 253

6.4.7.1 Adjuvanticity of liposomes 255

6.4.7.2 Adjuvanticity of apoptotic cells 255

6.4.7.3 Pro-inflammatory macrophages replenish the AM population 256

6.4.7.4 Lack of macrophage mediated clearance of inflammatory cells 257

6.4.7.5 AM are immunosuppressive 257

7. CONCLUDING DISCUSSION 262

7.1 Summary of findings 263

7.2 Impact of project 264

7.3 Future work 265

7.3.1 Source of IL-13 during AAD 265

7.3.2 Macrophage population expansion following anti-IL-13 mAb treatment during HDM exposure 265

7.3.3 Role of IL-13Rα2 in AAD 266

7.3.4 IL-13Rα1 internalisation 267

7.3.5 AM mediated immune suppression 268

PUBLICATIONS 270

BIBLIOGRAPHY 271

ii. List of Tables

Table 1.1	**Summary of genes affected by IL-13.**	**30**
Table 1.2	**The effects of IL-13 signalling modulation.**	**36**
Table 2.1	**Antibodies used for flow cytometry.**	**55**
Table 2.2	**Antibodies used for immunoglobulin ELISAs.**	**57**
Table 2.3	**Antibodies used for immunofluorescence.**	**61**
Table 2.4	**Probes used for real-time PCR.**	**62**
Table 4.1	**Summary of IL-13 effects.**	**148**

iii. Table of Figures

Figure 1.1	**IL-13 activities.**	**25**
Figure 1.2	**Macrophage activation.**	**28**
Figure 1.3	**IL-13 and IL-4 receptor assembly.**	**34**
Figure 1.4	**Allergeneic properties of HDM.**	**45**
Figure 2.1	**Goblet cell scoring.**	**58**
Figure 2.2	**Measurement of peribronchial collagen.**	**59**
Figure 3.1	**Experimental protocol for exposure to HDM.**	**67**
Figure 3.2	**Chronic exposure to HDM induces AHR.**	**69**
Figure 3.3	**Chronic exposure to HDM induced pulmonary inflammation.**	**70**
Figure 3.4	**Chronic exposure to HDM induces a predominant Th2 response.**	**73**
Figure 3.5	**Induction of T cell cytokines following HDM exposure.**	**74**
Figure 3.6	**HDM induced chemokine expression.**	**75**
Figure 3.7	**Expression of epithelial derived cytokines following HDM exposure.**	**76**
Figure 3.8	**Generation of IgE and HDM specific antibodies following HDM exposure.**	**78**
Figure 3.9	**Up-regulation of mucus production following HDM exposure.**	**80**
Figure 3.10	**Chronic exposure to HDM induces peribronchial collagen deposition.**	**81**
Figure 3.11	**IL-13 expression following chronic HDM exposure.**	**84**
Figure 3.12	**Non-specific IL-13 staining in the lungs following exposure to HDM.**	**85**
Figure 3.13	**Non-specific IL-13 staining in BAL following exposure to HDM.**	**86**
Figure 3.14	**IL-13 expression in CD4+ cells following chronic HDM exposure.**	**87**
Figure 3.15	**IL-13 expression in CD8+ cells following chronic HDM exposure.**	**88**
Figure 3.16	**IL-13 expression in Th2 cells following chronic HDM exposure.**	**89**
Figure 3.17	**IL-13 expression in neutrophils and eosinophils following chronic HDM exposure.**	**90**
Figure 4.1	**Type II IL-4 receptor formation and mAb specificity.**	**103**
Figure 4.2	**Experimental protocols for exposure to HDM.**	**105**
Figure 4.3	**Effects of IL-13 neutralisation on BAL cells.**	**107**
Figure 4.4	**Effects of IL-13 neutralisation on airway remodelling.**	**108**
Figure 4.5	**Effects of 582 and 587 treatment on BAL cells.**	**110**
Figure 4.6	**Effects of 582 and 587 treatment on AHR.**	**111**
Figure 4.7	**Effects of 582 and 587 treatment on goblet cell frequency.**	**112**
Figure 4.8	**Effects of 582 and 587 treatment on peribronchial collagen deposition.**	**113**
Figure 4.9	**Effects of IL-13 neutralisation on AHR.**	**115**
Figure 4.10	**Effects of IL-13 neutralisation on HDM induced pulmonary inflammation.**	**117**
Figure 4.11	**Effects of IL-13 neutralisation on macrophage accumulation.**	**118**
Figure 4.12	**Effects of IL-13 neutralisation on HDM induced T and B cell accumulation.**	**119**
Figure 4.13	**Effects of IL-13 neutralisation on T helper cell phenotype.**	**120**
Figure 4.14	**Effects of IL-13 neutralisation on IL-4, IL-5 and IL-10 production.**	**122**
Figure 4.15	**Effects of IL-13 neutralisation on IFNγ, IL-12 and IL-17 production.**	**123**
Figure 4.16	**Effects of IL-13 neutralisation on chemokines.**	**124**
Figure 4.17	**Effects of IL-13 neutralisation on epithelial derived cytokines.**	**125**
Figure 4.18	**Effects of IL-13 neutralisation on antibody generation following HDM exposure.**	**127**
Figure 4.19	**Effects of therapeutic IL-13 neutralisation on AHR.**	**129**
Figure 4.20	**Effects of therapeutic IL-13 neutralisation on pulmonary inflammation.**	**130**
Figure 4.21	**Effects of therapeutic IL-13 neutralisation on airway remodelling.**	**131**
Figure 5.1	**IL-13 receptor expression following exposure to HDM.**	**154**
Figure 5.2	**IL-13Rα2 concentrations following exposure to HDM.**	**155**
Figure 5.3	**Localisation of IL-13Rα2 following exposure to HDM.**	**156**
Figure 5.4	**Localisation of IL-13Rα1 following exposure to HDM.**	**158**
Figure 5.5	**Co-localisation of IL-13Rα1 with MOMA2 in Lungs.**	**159**
Figure 5.6	**Co-localisation of IL-13Rα1 with MOMA2 in BAL.**	**160**
Figure 5.7	**Co-localisation of IL-13Rα1 to CD68+ cells in lungs.**	**161**
Figure 5.8	**Co-localisation of IL-13Rα1 to CD68+ cells in BAL.**	**162**
Figure 5.9	**Development of a flow cytometry stain for IL-13Rα1.**	**164**

Figure 5.10 Quantification of IL-13Rα1+ BAL cells. 165
Figure 5.11 IL-13Rα1 expression on BAL macrophages is reduced following HDM exposure. 168
Figure 5.12 Extracellular IL-13Rα1 expression on BAL macrophages. 169
Figure 5.13 Intracellular IL-13Rα1 expression in BAL macrophages. 170
Figure 5.14 IL-13Rα1 expression on BAL AM. 171
Figure 5.15 IL-13Rα1 expression on LD AM and IM. 172
Figure 5.16 Proportion of IL-13Rα1+ AM and IM following HDM exposure. 173
Figure 5.17 Phenotype of BAL AM. 174
Figure 5.18 Intracellular cytokine staining of BAL AM. 175
Figure 5.19 Detection of IL-13Rα1+ cells in naïve blood. 178
Figure 5.20 IL-13Rα1 expression on T cells in naïve blood. 179
Figure 5.21 IL-13Rα1 expression on CD4+ T cells in BAL and LD from HDM exposed mice. 180
Figure 5.22 Phenotype of IL-13Rα1+ CD4+ T cells in blood from sham and HDM exposed mice. 181
Figure 5.23 Phenotype of IL-13Rα1+ CD4+ T cells in BAL from sham and HDM exposed mice. 182
Figure 5.24 Phenotype of IL-13Rα1+ CD4+ T cells in LD from sham and HDM exposed mice. 183
Figure 5.25 Phenotype of IL-13Rα1+ T helper cells in BAL from HDM exposed mice. 184
Figure 5.26 Phenotype of IL-13Rα1+ T helper cells in LD from HDM exposed mice. 185
Figure 6.1 Experimental protocol for IL-13 induced lung inflammation. 200
Figure 6.2 Experimental protocol for macrophage depletion during HDM induced lung inflammation. 201
Figure 6.3 Effects of anti-CSF-1 receptor treatment on BAL macrophage frequency. 203
Figure 6.4 Effects of anti-CSF-1 receptor treatment on blood monocytes and eosinophils. 204
Figure 6.5 Effects of 1 or 2 doses of clodronate liposomes on BAL and LD macrophages. 207
Figure 6.6 Time course of clodronate induced macrophage depletion. 208
Figure 6.7 IL-13 induced accumulation of eosinophils and T cells. 210
Figure 6.8 Effects of IL-13 on accumulation of total leukocytes, macrophages and neutrophils. 211
Figure 6.9 IL-13 induced mediator release. 212
Figure 6.10 IL-13 induced release of epithelial cytokines. 213
Figure 6.11 Administration of clodronate liposomes reduced AM in IL-13 treated mice. 215
Figure 6.12 Administration of clodronate liposomes increased BAL cellularity in IL-13 treated mice. 216
Figure 6.13 Effect of clodronate liposomes on IL-13 induced cytokines in BAL. 217
Figure 6.14 Effect of clodronate liposomes on IL-13 induced mediators. 218
Figure 6.15 Effect of clodronate liposomes on IL-13 induced goblet cell up-regulation. 219
Figure 6.16 Administration of clodronate liposomes increased HDM induced AHR. 223
Figure 6.17 Administration of clodronate liposomes exacerbated HDM induced inflammation. 224
Figure 6.18 Administration of clodronate liposomes exacerbated T cell accumulation in HDM exposed mice. 225
Figure 6.19 Administration of clodronate liposomes increased macrophage accumulation in HDM exposed mice. 226
Figure 6.20 AM and IM frequencies following administration of clodronate liposomes to HDM exposed mice. 227
Figure 6.21 CD11b expression on pulmonary macrophages following administration of clodronate liposomes to HDM exposed mice. 228
Figure 6.22 Clodronate liposomes increased accumulation of CD11b+ AM in HDM exposed mice. 229
Figure 6.23 Effects of clodronate liposomes on HDM induced Th2 cytokines. 230
Figure 6.24 Effects of clodronate liposomes on HDM induced IFNγ, IL-10 and IL-12 production. 231
Figure 6.25 Effects of clodronate liposomes on HDM induced chemokines. 232
Figure 6.26 Effects of clodronate liposomes on HDM induced epithelial derived cytokines. 233
Figure 6.27 Effects of clodronate liposomes on the generation of HDM specific antibodies. 234

Figure 6.28 **Effects of clodronate liposomes on HDM induced goblet cell hyperplasia.** **235**
Figure 6.29 **Effects of clodronate liposomes on HDM induced peribronchial collagen deposition.** **236**
Figure 6.30 **Therapeutic administration of clodronate liposomes does not affect HDM induced AHR.** **239**
Figure 6.31 **Therapeutic administration of clodronate liposomes exacerbated HDM induced inflammation.** **240**
Figure 6.32 **Therapeutic administration of clodronate liposomes exacerbated T cell accumulation in HDM exposed mice.** **241**
Figure 6.33 **Effects of therapeutic clodronate liposomes on macrophage accumulation in HDM exposed mice.** **242**
Figure 6.34 **Therapeutic clodronate liposomes increased accumulation of CD11b+ AM in HDM exposed mice.** **243**
Figure 6.35 **Potential mechanisms by which administration of clodronate liposomes may exacerbate airway inflammation.** **254**

ABBREVIATIONS

AAD	Allergic airways disease
AAM	Alternatively activated macrophage
AB/PAS	Alcian blue/periodic acid Schiff
ADCC	Antibody dependent cell cytotoxicity
AHR	Airway hyperreactivity
AM	Alveolar macrophage
ANOVA	Analysis of variance
AP-1	Activating protein-1
APC	Allophycocyanin
APC	Antigen presenting cell
ASM	Airway smooth muscle
αSMA	α-Smooth muscle actin
BAL	Broncho-alveolar lavage
BSA	Bovine serum albumin
C (3, 3a, 5, 5a)	Complement
CAM	Classically activated macrophage
CD	Cluster of differentiation antigen
cDNA	clonal DNA
C_{dyn}	Dynamic compliance
CLCA3	Calcium-activated chloride channel-3
CLR	C-type lectin receptor
COX	Cyclooxygenase
CS	Corticosteroid
CSF	Colony-stimulating factor
CTACK	Cutaneous T-cell-attracting chemokine
Cy	Cyanine
Cys-LT	Cysteinyl leukotriene
DAMP	Damage associated molecular patterns
DAPI	4’,6-Diamidino-2-phenylindole
DC	Dendritic cell
DC-SIGN	DC-specific intercellular adhesion molecule-3-grabbing non-integrin

DNA	Deoxyribonucleic acid
EAR	Early phase asthmatic response
ECM	Extracellular matrix
EDTA	Ethylenediaminetetraacetic acid
ELISA	Enzyme-linked immunosorbent assay
Erg-1	Early growth response-1
ERK	Extracellular signal-related kinase
FACS	Fluorescence-activated cell sorting
FCS	Foetal calf serum
F_ENO	Fractional expiratory nitric oxide
FEV_1	Forced expiratory volume in 1s
FGF	Fibroblast growth factor
FITC	Fluorescein isothiocyanate
FKBP	FK506 binding protein
FoxP3	Forkhead box P3
GATA-3	GATA-binding protein 3
G-CSF	Granulocyte colony-stimulating factor
GDP	Guanosine diphosphate
GM-CSF	Granulocyte-macrophage colony-stimulating factor
HBSS	Hank's balanced salt solution
HDM	House dust mite
HEPES	4-(2-hydroxyethyl)-1-piperazineethanesulfonic acid
hi	High
HRP	Horseradish peroxidase
IF	Immunofluorescence
IFNγ	Interferon-γ
Ig	Immunoglobulin
IL	Interleukin
IM	Interstitial macrophage
i.m.	Intra-muscular
i.n.	Intra-nasal
iNKT	Invariant natural killer T cell
iNOS	Inducible nitric oxide synthase

i.p.	Intra-peritoneal
IRS	Insulin receptor substrate
i.t.	Intra-tracheal
JAK	Janus activating kinase
KC	Keratinocyte chemoattractant
K_D	Dissociation constant
KLF	Kruppel-like factor
LAR	Late phase asthmatic response
LD	Lung digest
LH	Lung homogenate
lo	Low
LPS	Lipopolysaccharide
LT	Leukotriene
mAb	Monoclonal antibody
MAPK	Mitogen-activating protein kinase
MCh	Methacholine
MCP	Monocyte chemotactic protein
MDC	Macrophage derived chemokine
MFI	Mean fluorescence intensity
MHC	Major histocompatibility complex
min	minute
MIP-1	Macrophage inflammatory protein-1
MMP	Matrix Metalloproteinase
mRNA	Messenger ribonucleic acid
NHP	Non-human primate
NK	Natural killer
NLR	NOD-like receptor
NO	Nitric oxide
NOD	Nucleotide-binding oligomerization domain
n.s.	Non-significant
OD	Optical density
OCT	Optimum cutting temperature formulation
OSM	Oncostatin M
OVA	Ovalbumin

pAb	Polyclonal antibody
PAR	Protease activated receptor
PAMP	Pathogen associated molecular patterns
PBS	Phosphate buffered saline
PCR	Polymerase chain reaction
PDGF	Platelet-derived growth factor
PE	Phycoerythrin
Penh	Enhanced pause
PerCP	Peridinin chlorophyll protein
PGE_2	Prostaglandin E_2
PI3K	Phosphatidylinositol 3-kinase
PMA	Phorbol 12-myristate 13-acetate
PRR	Pattern recognition receptor
RANTES	Regulated upon activation, normal T-cell expressed, and secreted
RELMα	Resistin-like molecule-α
R/C	Lung resistance and dynamic compliance
R_L	Lung resistance
RNA	Ribonucleic acid
RORγt	Retinoic acid receptor-related orphan receptor-γt
RPE	R-phycoerythrin
RPMI	Roswell Park Memorial Institute media
rRNA	Ribosomal ribonucleic acid
RT	Room temperature
SEA	*Schistosoma mansoni* egg antigen
SEM	Standard error of the mean
s.c.	sub-cutaneous
SP-A, -D	Surfactant protein-A, -D
STAT	Signal transducer and activator of transcription
TARC	Thymus and activation regulated chemokine
TBS	Tris-buffered saline
TGF	Transforming growth factor
Th	T helper cell
TLR	Toll-like receptor

TMB	3,3',5,5'-Tetramethylbenzidine
TNFα	Tumour necrosis factor-α
T.O.C.	Time of challenge
Treg	Regulatory T cell
TRPC	Transient receptor potential cation channel
TSLP	Thymic stromal lymphopoietin
TYK	Protein tyrosine kinase
VCAM	Vascular cell adhesion molecule
VLA	Very late antigen
w/v	weight per volume

1. INTRODUCTION

1.1 Asthma

Asthma is a chronic inflammatory disease of the conducting airways characterised by airflow obstruction that is reversible spontaneously or with treatment, although a degree of fixed airflow obstruction is often associated with severe disease (Backman *et al.*, 1997). This airflow obstruction is due in part to excessive bronchoconstriction in response to inhaled stimuli such as allergens, pollutants or cold air; i.e. airway hyperreactivity (AHR), and results in symptoms of episodic wheezing, breathlessness, coughing and chest tightness (O'Byrne & Inman, 2003;GINA, 2006). In addition, patients with asthma exhibit reduced basal lung function and the age related rate of decline in lung function is accelerated (James *et al.*, 2005).

Asthma is a heterogeneous disease of unknown aetiology however the majority of cases are coupled with atopy (Wenzel, 2006); the predisposition to mount an excessive IgE response to otherwise innocuous allergens. Non-atopic asthma is more common in patients with late-onset disease and is not associated with reactivity to known allergens (Wenzel, 2006). Despite these apparent differences much of the underlying pathology is common to both atopic and non-atoptic asthma. The development of asthma is likely to result from a complex interaction between genetic and environmental factors such as susceptibility to atopy, viral infections and exposure to pollutants and allergens.

The underlying pathology of lung tissue from asthmatic patients exhibits peribronchial inflammation and persistent structural changes to the airway walls; termed airway remodelling. Airway remodelling encompasses changes in the epithelium, basement membrane and airway smooth muscle (ASM) which leads to significant thickening of the airway walls. This in turn may contribute to airflow restriction and decline in lung function. The airway epithelium is thickened; increased epithelial turnover and epithelial shedding have also been reported, thus potentially compromising barrier function (James & Wenzel, 2007;Bergeron *et al.*, 2009). Hyperplasia of goblet cells and submucosal glands is characteristic of asthma and together with the associated hypersecretion of mucus can lead to the formation of mucus plugs and thus contribute to airflow limitation (Ordonez *et al.*, 2001). Thickening of the basement membrane occurs as a result of subepithelial fibrosis and specifically the deposition of extracellular matrix proteins such as collagens. In

addition, asthmatic airways exhibit increased smooth muscle mass as a result of ASM hypertrophy and hyperplasia (James & Wenzel, 2007). Whilst airway wall thickness is closely associated with disease severity; whether remodelling is deleterious to disease or protective remains contentious (Niimi *et al.*, 2000;Little *et al.*, 2002). Structurally, airway remodelling results in stiffening of the airway wall which may limit bronchoconstriction however increased ASM mass may heighten bronchoconstriction (James & Wenzel, 2007). In addition, cells implicated in the remodelling process such as epithelial cells, ASM cells and fibroblasts may perpetuate the inflammatory process by releasing proinflammatory mediators (Holgate *et al.*, 2000;Bergeron *et al.*, 2009). Increasing evidence implicates the airway epithelium in the pathogenesis of asthma and has lead to the proposal that epithelial damage followed by impaired repair is responsible for initiation and propagation of the disease. Thus the damaged epithelium not only permits allergen sensitisation but drives fibrosis in a bid to maintain barrier function (Holgate *et al.*, 2000). Furthermore, it has recently been demonstrated that repeated bronchoconstriction induces epithelial stress, which stimulates airway remodelling even in the absence of allergen induced inflammation (Grainge *et al.*, 2011). However, it is unknown whether structural changes in the airway wall precede airway inflammation or arise from an aberrant tissue repair response driven by persistent inflammation (James & Wenzel, 2007;Holgate *et al.*, 2000). It is likely inflammation, AHR and remodelling are interdependent and self-perpetuating in the pathogenesis of asthma.

The inflammatory response underpinning asthma is orchestrated by a T helper 2 (Th2) response. In allergic asthmatics this response is frequently directed against innocuous inhaled peptides, such as those found in house dust mites (HDM) and grass pollens, however strikingly similar immunopathology is also present in non-atopic asthmatics (Kay, 2006). Evidence for Th2 involvement in asthma primarily comes from the presence of Th2 cells in the airways and the associated elevation of the Th2 cytokines interleukin (IL)-4, IL-5 and IL-13 (Robinson *et al.*, 1992;Brightling *et al.*, 2002). In turn, these mediators drive some of the fundamental characteristics of asthma such as IgE production, eosinophilia, AHR and airway remodelling. IL-4 is increased in broncho-alveolar lavage (BAL) from asthma patients and is a requisite for Th2 differentiation and B cell isotype switching to IgE (Steinke, 2004). IL-5 is also up-regulated in asthma and, together with eotaxin, is primarily involved in the

development, recruitment, activation and survival of eosinophils (Robinson *et al.*, 1992;Rothenberg & Hogan, 2006).

Several recent findings have shed light on the mechanisms involved in priming Th2 responses. The central role of airway dendritic cells (DC) in sampling allergen and subsequently migrating to draining lymph nodes to present allergen and prime Th2 responses has been well demonstrated by Lambrecht *et al.* (Lambrecht & Hammad, 2009;van Rijt *et al.*, 2005). In addition, basophils may play a role in priming the allergic response. Although it is debated whether basophils are capable of presenting antigen themselves, they are able to migrate to the draining lymph node where they may provide an early source of IL-4 to direct the immune response towards Th2 differentiation (Hammad *et al.*, 2010;Sokol *et al.*, 2009;Yoshimoto *et al.*, 2009;Perrigoue *et al.*, 2009). In addition, the recent discovery of innate helper cells in mice may provide a novel mechanism by which Th2 responses are initiated and amplified at mucosal surfaces. Several subpopulations of innate lymphoid cells have been described that respond to epithelial derived cytokines such as IL-25, IL-33 and thymic stromal lymphopoietin (TSLP) by producing Th2 cytokines (IL-4, IL-5 and IL-13) (Price *et al.*, 2010;Neill *et al.*, 2010;Saenz *et al.*, 2010b;Moro *et al.*, 2010). Furthermore, innate lymphoid cells have recently been demonstrated to be potent inducers of AHR, via IL-13 production, under certain circumstances (Chang 2011). Although these cells have yet to be identified in man, and their function in allergic lung inflammation unreported to date, their purpose may be to provide immediate, "substitute help" following epithelial damage, prior to the development of an antigen specific T cell response (Saenz *et al.*, 2010a;Eberl, 2010).

Despite the Th2 dominance in asthma, other T helper cell phenotypes have been demonstrated to be present in the lungs which may play a role in pathogenesis of the disease. Th1 cells are elevated in BAL from asthmatics and further increased in sputum after exacerbation in patients with severe disease (Krug *et al.*, 1996;Mamessier *et al.*, 2008). However, the role of Th1 cells and their primary cytokine interferon-γ (IFNγ) is unclear. While Th1 cells can suppress Th2 responses, some studies have implicated IFNγ in AHR (Vock *et al.*, 2010). Th17 cells have been isolated from biopsies from severe asthmatic patients (Pene *et al.*, 2008). Furthermore, IL-17A is up-regulated in asthma and correlates with sputum

neutrophilia and disease severity, thus implicating Th17 cells in the pathogenesis of severe rather than mild-moderate asthma (Molet *et al.*, 2001;Bullens *et al.*, 2006;Al-Ramli *et al.*, 2009).

Airway eosinophilia is one of the principal characteristics of asthma. Eosinophils are increased in BAL and blood from asthmatic patients and correlate with disease severity (Bousquet *et al.*, 1990). In addition, sputum eosinophilia has been linked to increased basement membrane thickening and sensitivity to corticosteroid treatment (Berry *et al.*, 2007). The role of eosinophils in the pathogenesis of asthma however is disputed (Fattouh & Jordana, 2008;Kariyawasam & Robinson, 2007;Jacobsen *et al.*, 2007). Eosinophils represent a significant source of cytokines, mediators and cytotoxic proteins (Kariyawasam & Robinson, 2006). Production of pro-fibrotic factors such as transforming growth factor-β (TGFβ) is likely to play a direct role in airway remodelling while release of cytotoxins from degranulation may indirectly contributing disease pathogenesis by causing tissue damage (Kariyawasam & Robinson, 2007).

Mast cells are fundamental in eliciting pulmonary responses to allergen. Upon exposure to allergen IgE, bound to the surface of mast cells via FcεRI, cross-links thus inducing degranulation. Release of intracellular stores of pro-inflammatory mediators by degranulation elicits the early phase asthmatic response (EAR) and the recruitment of cells which subsequently drive the late phase response (LAR). Importantly, mast cells are located within the ASM of asthmatic patients and stain positively for IL-4 and IL-13 (Brightling *et al.*, 2003). Hence, they are also proposed to play a role in airway remodelling and AHR by directly modulating ASM in addition to perpetuating inflammation.

There is increasing evidence neutrophils are involved in asthma pathogenesis, specifically severe asthma. The number of BAL neutrophils is elevated in severe but not mild-moderate asthma, unless the patient is experiencing an acute exacerbation. Moreover, sputum neutrophilia has been correlated to fixed airflow obstruction, but not AHR (Fahy, 2009).

Current therapy for asthma consists of reliever and controller medication (GINA, 2006). Reliever medications are commonly fast acting inhaled β_2 agonists used to

relax the ASM during bronchospasm. In addition, many patients require controller medications; anti-inflammatories such as corticosteroids (CS), often taken daily to control asthma symptoms. Depending on the severity of disease, CS therapy can be inhaled or oral. Long-acting β_2 agonists may also be used as controller therapy in conjunction with CS to improve lung function. In persistent asthma add on therapies such as leukotriene modifiers, theophylline or anti-IgE may be employed. However, disease symptoms remain poorly controlled in approximately 10% of asthma patients with severe disease (Wenzel, 2005). Furthermore, current therapies fail to modify the course on the disease, but merely control symptoms hence there is an unmet clinical need for therapies that can halt or even reverse the pathogenesis of asthma. In order to address this, a great deal of research has focused on targeting the underlying Th2 response by neutralising key Th2 cytokines such as IL-4, IL-5 and IL-13.

1.2 IL-13

IL-13 was originally identified as an IL-4 related cytokine produced in activated human T cells that was capable of inducing monocyte differentiation and B cell differentiation and proliferation (Minty *et al.*, 1993;McKenzie *et al.*, 1993). IL-13 was subsequently demonstrated to be both sufficient and necessary for the induction of asthma-like pathology in mice (Wills-Karp *et al.*, 1998;Grunig *et al.*, 1998). Since its discovery, a plethora of functions have been ascribed to IL-13 and the cytokine has consequently been proposed to be a central mediator in the pathogenesis of asthma (Wynn, 2003;Wills-Karp, 2004;Kasaian & Miller, 2008;Brightling *et al.*, 2010).

1.2.1 IL-13 in asthma

In patients with atopic asthma BAL IL-13 mRNA and protein is elevated following allergen challenge, compared to non-asthmatic controls (Huang *et al.*, 1995;Batra *et al.*, 2004). Furthermore, post-challenge BAL IL-13 concentration positively correlates with BAL eosinophilia (Kroegel *et al.*, 1996). Expression of IL-13 mRNA in bronchial biopsies has been demonstrated to be greater in asthmatic patients compared to non-asthmatic controls; moreover IL-13 mRNA expression is equivalent in atopic and non-atopic asthmatics and positively correlates with lung eosinophilia (Humbert *et al.*, 1997). Berry *et al.* and Saha *et al.* have also detected IL-13 in sputum and an increase in the number of IL-13 positive cells in the submucosa and ASM bundles in biopsies from asthmatic patients (Berry *et al.*, 2004;Saha *et al.*,

2008). These IL-13 expressing cells have been identified predominantly as submucosal eosinophils and mast cells in the ASM (Berry *et al.*, 2004;Brightling *et al.*, 2003). Furthermore, peripheral blood eosinophils from asthmatic but not control patients express IL-13 (Schmid-Grendelmeier *et al.*, 2002). However in BAL, up-regulation of IL-13 mRNA post-allergen challenge is significant in cells enriched for alveolar macrophages (AM) (Prieto *et al.*, 2000). In addition to T cells, eosinophils, mast cells and AM multiple other cell types are reported to be capable of producing IL-13 including basophils, DC, invariant natural killer T cells (iNKT), innate lymphoid cells and stromal cells such as ASM and epithelium (Ochensberger *et al.*, 1996;Gibbs *et al.*, 1996;Schroeder *et al.*, 2010;de Saint-Vis *et al.*, 1998;Kim *et al.*, 2008;Price *et al.*, 2010;Moro *et al.*, 2010;Saenz *et al.*, 2010b;Neill *et al.*, 2010;Grunstein *et al.*, 2002;Semlali *et al.*, 2010).

1.2.2 IL-13 activities

IL-13 is capable of mediating many aspects of asthma pathology through its actions on both haematopoietic and stromal cells in the lung (Figure 1.1). In mice administration of exogenous IL-13 into the airways is sufficient to provoke symptoms of allergic airways disease (AAD) such as BAL eosinophilia, neutrophilia, goblet cell metaplasia and AHR (Grunig *et al.*, 1998;Wills-Karp *et al.*, 1998). In longer term studies, transgenic over-expression of IL-13 or adenoviral expression of IL-13 in the lungs induced additional pathologies; accumulation of BAL T cells, epithelial cell hypertrophy, subepithelial fibrosis, increased baseline airways resistance and up-regulation of eotaxin, keratinocyte chemoattractant (KC), IL-10 and IL-12 (Zhu *et al.*, 1999;Kuperman *et al.*, 2002;Therien *et al.*, 2008). See Table 1.1 for a summary of genes affected by IL-13 in cell types relevant to the pathogenesis of asthma.

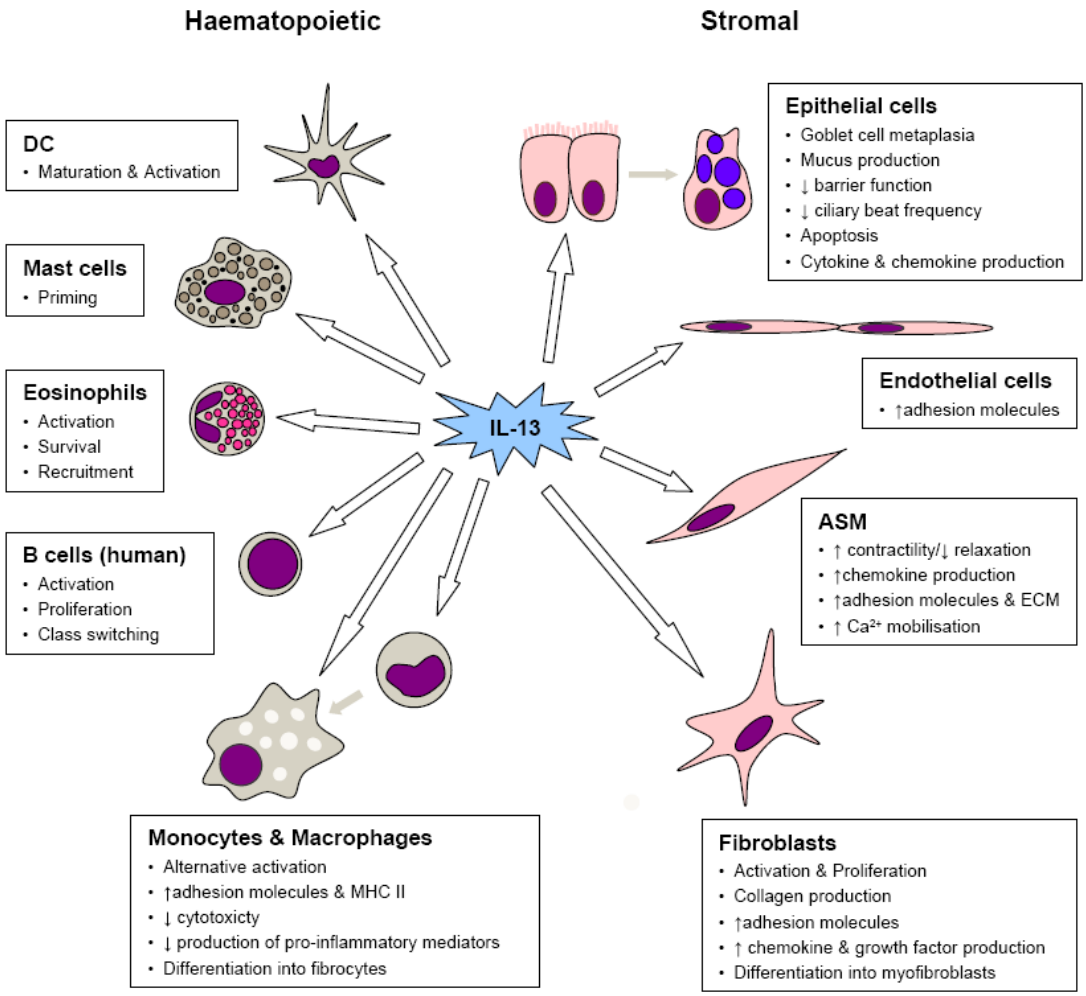


Figure 1.1 IL-13 activities. Summary of mechanisms by which IL-13 may contribute to the pathogenesis of asthma.

IL-13 propagates Th2 immunity without directly activating, polarising or inducing proliferation of T cells themselves but can perpetuate inflammation via a multitude of activities (Zurawski & de Vries, 1994;de Vries, 1998). Despite initial reports suggesting T cells to be unresponsive to IL-13, more recently Th17 cells have been reported to respond to IL-13 by down-regulating Th17 transcription factors and up-regulating Th2 transcription factors (Newcomb *et al.*, 2009;Newcomb *et al.*, 2011). IL-13 can further enhance Th2 responses by augmenting DC maturation and activation. Specifically IL-13 up-regulates expression of MHC II, activation markers such as CD205 and co-stimulatory molecules CD40 and CD86 (Padilla *et al.*, 2005). Furthermore, IL-13 enhances DC mediated suppression of IFNγ expression by memory T cells (Webb *et al.*, 2007). In human B cells IL-13 induces activation, enhances proliferation, up-regulates CD23 and MHC II and induces IL-4 independent

class switching to IgG4 and IgE however, mouse B cells do not respond to IL-13 (Punnonen *et al.*, 1993;Zurawski & de Vries, 1994). In addition, IL-13 primes mast cells by up-regulating FcεRI which consequently increases histamine release and proliferation upon FcεRI cross-linking (Kaur *et al.*, 2006). IL-13 also contributes to recruitment of inflammatory cells, in particular eosinophils, by inducing vascular cell adhesion molecule-1 (VCAM-1) and P-selectin expression on endothelial cells (Bochner *et al.*, 1995;Woltmann *et al.*, 2000).

IL-13 induces eosinophilia via the release of chemoattractants such as eotaxin. This has been demonstrated by attenuation of IL-13 stimulated airway eosinophilia in mice deficient in IL-5 and/or eotaxin (Yang *et al.*, 2001;Pope *et al.*, 2005). Furthermore, allergen induced up-regulation of eotaxin is IL-13 dependent (Pope *et al.*, 2005). In addition, IL-13 itself can act as a chemoattractant for eosinophils, prolong their survival and induce activation, as indicated by up-regulation of CD69 (Horie *et al.*, 1997;Luttmann *et al.*, 1996). Interestingly, production of IL-13 by T cells from IL-5 and eotaxin deficient mice with AAD is impaired indicating eosinophils may play a role in Th2 cell development (Mattes *et al.*, 2002). In addition, eosinophil derived IL-13 has been implicated in the development of AAD although as a sole source of IL-13, this is insufficient to sustain AAD (Walsh *et al.*, 2011). This illustrates a complex interdependency between eosinophils and T cells involving IL-13 in AAD.

Much like IL-4, IL-13 can induce alternative activation of monocytes and macrophages, however, IL-13 is not essential for macrophage polarisation due to redundancy with IL-4 (Ramalingam *et al.*, 2008). (See Figure 1.2 for a diagram illustrating the key differences between classical and alternative activation of macrophages.) Upon stimulation with IL-13, monocytes up-regulate various adhesion molecules (CD11b, CD11c, VLA-5, CD18 and CD29), MHC II, and FcεRII (CD23) and down-regulate CD14, FcγRI, FcγRII and FcγRIII expression (de Waal *et al.*, 1993). In addition, IL-13 reduces antibody dependent cell cytotoxicity (ADCC) and lipopolysaccharide (LPS) induced production of pro-inflammatory cytokines (IL-1α, IL-1β, IL-6, IL-10, granulocyte colony-stimulating factor (G-CSF; CSF-3) and tumour necrosis factor (TNF)-α). Furthermore, *in vitro* incubation of human monocytes with IL-13 can promote fibrocyte differentiation (Shao *et al.*, 2008). Alternative activation of macrophages is characterised by the up-regulation of

mannose receptor, Dectin-1, MHC II, CD23, resistin-like molecule (RELM)-α, YM-1/2 and arginase-1 and induction of 15-lipooxygenase (15-LO) in mice (Gordon, 2003;Gordon & Martinez, 2010). In turn, arginase expression results in production of proline and polyamines thus contributing to collagen synthesis and cell proliferation, respectively. IL-13 inhibits the production of IL-12, IL-1, IL-6 and TNFα and reduces nitric oxide (NO) release in response to LPS stimulation (Doherty *et al.*, 1993). In addition, alternatively activated macrophages (AAM) antagonise the effects of IL-1 by via expression of IL-1 decoy receptor and IL-1ra. Furthermore, AAM produce CCL22 (macrophage derived chemokine; MDC), CCL17 (thymus and activation regulated chemokine; TARC), eotaxin, TGFβ, IL-10 and IL-13 itself (Gordon, 2003;Pope *et al.*, 2005;Holtzman *et al.*, 2009). Overall, IL-13 counteracts the effect of Th1 stimuli such as LPS and IFNγ on monocytes and macrophages, down-regulating their cytotoxic and pro-inflammatory properties. Instead, AAM are associated with trophic functions, clearance of apoptotic bodies, wound healing and tolerance. However, by the same mechanisms, AAM can perpetuate Th2 immunity by promoting recruitment of Th2 cells, eosinophils, mast cells, basophils and neutrophils and driving excessive fibrosis.

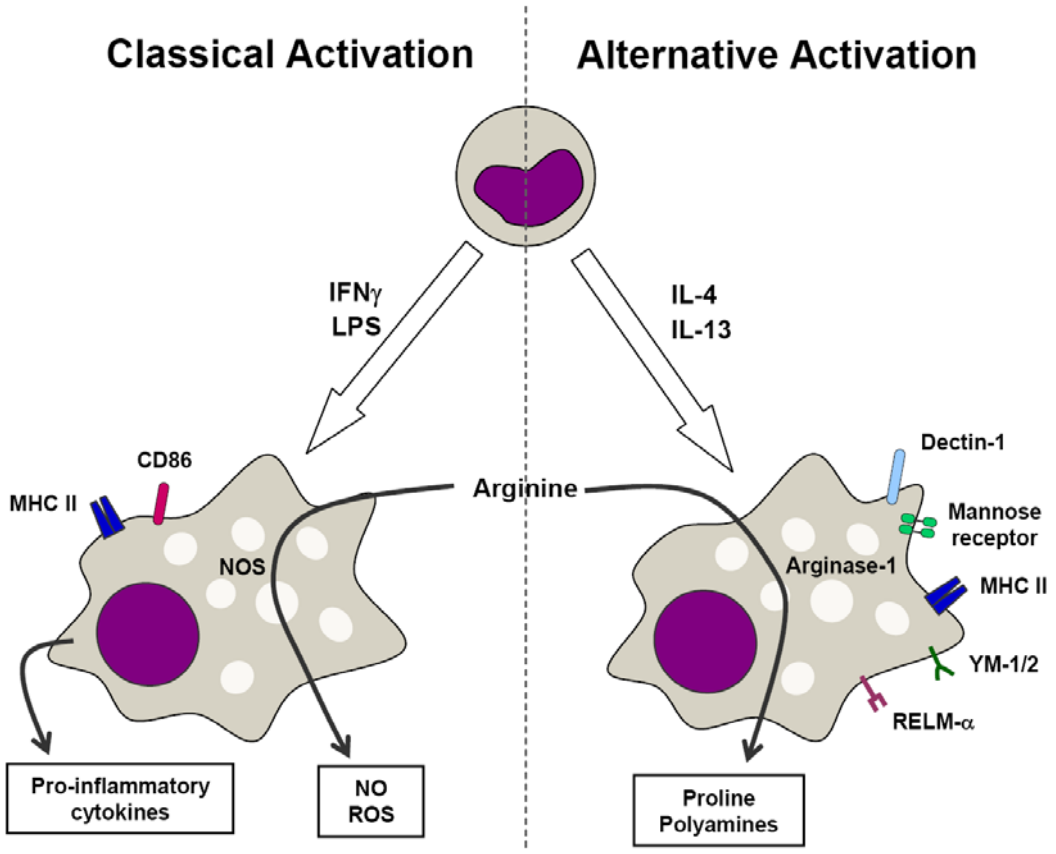


Figure 1.2 Macrophage activation. Summary of key differences between classical and alternative macrophage activation pathways. Exposure to IFNγ (interferon-γ) in the presence of LPS (lipopolysaccharide) stimulates classical activation leading to up-regulation of MHC II, CD86, NOS (nitric oxide synthase) and the subsequent production of NO (nitric oxide) and ROS (reactive oxygen species). Exposure to IL-4 or IL-13 stimulates alternative activation leading to the up-regulation of Dectin-1, mannose receptor, MHC II, YM-1/2, RELM-α, arginase-1 and the subsequent production of polyamines and proline.

IL-13 can act directly on airway epithelium. Various studies have demonstrated *ex vivo* stimulation of human epithelial cells with IL-13 up-regulates mucins and induces goblet cell metaplasia (Malavia *et al.*, 2008). IL-13 alters mucociliary differentiation by increasing the proportion of secretory cells, reduces ciliary beat frequency of epithelial cells and decreases epithelial barrier function (Laoukili *et al.*, 2001;Ahdieh *et al.*, 2001). In addition, IL-13 stimulation of epithelial cells can induce the release of eotaxin, IL-8, TGFα, TGFβ and TSLP; each of which has the potential to provoke inflammation and fibrosis of the airways (Matsukura *et al.*, 2001;Lordan *et al.*, 2002;Malavia *et al.*, 2008;Miyata *et al.*, 2009). Furthermore, IL-13 can induce apoptosis of epithelial cells which in turn also increases susceptibility to the

development of fibrosis (Borowski *et al.*, 2008). Contrary to the effects on macrophages, IL-13 has been reported to elevate inducible nitric oxide synthase (iNOS) expression and activity and reduce arginase-1 levels leading to increased nitrite production in primary bronchial epithelial cells (Chibana *et al.*, 2008). By using transgenic mice, Kuperman *et al.* demonstrated IL-13 signalling exclusively in airway epithelial cells was sufficient to induce AHR, goblet cell metaplasia and mucin expression without the induction of inflammation or fibrosis (Kuperman *et al.*, 2002).

In fibroblasts IL-13 is reported to promote differentiation to myofibroblasts, which are implicated in airway remodelling. IL-13 has been demonstrated to induce up-regulation of α-smooth muscle actin (αSMA) and collagen III mRNA however, some studies report no effects of IL-13 on αSMA and collagen production (Saito *et al.*, 2003;Borowski *et al.*, 2008;Batra *et al.*, 2004). IL-13 is capable of provoking fibroblast proliferation by at least two distinct mechanisms. Stimulation of fibroblasts with IL-13 induces release of platelet-derived growth factors (PDGF) which subsequently stimulate fibroblast and myofibroblast proliferation in an autocrine manner (Ingram *et al.*, 2006;Ingram *et al.*, 2004;Ingram *et al.*, 2003). In addition, IL-13 down regulates cyclooxygenase (COX)-1 and COX-2 expression in fibroblasts leading to reduced prostaglandin E_2 (PGE_2) production which permits the proliferation of fibroblasts (Saito *et al.*, 2003). IL-13 may also promote fibroblast activation by up-regulating the expression of CD40L and various adhesion molecules (Kaufman *et al.*, 2004;Doucet *et al.*, 1998a). IL-13 directly induces eotaxin production from fibroblasts however there are multiple mechanisms by which this response may be augmented (Wenzel *et al.*, 2002;Chibana *et al.*, 2003;Fritz *et al.*, 2009). IL-13 can synergise with TGFβ (and to a lesser extent TNFα) to up-regulate eotaxin expression in fibroblasts (Wenzel *et al.*, 2002). Similarly, oncostatin M (OSM), IL-6 and IL-11 augment IL-13 induced eotaxin production by up-regulating the expression of IL-13 receptor subunits (Fritz *et al.*, 2009). IL-13 also synergises with Leukotriene C_4 (LTC_4) to enhance eotaxin production by up-regulating cysteinyl leukotriene receptor CysLT1R expression on fibroblasts (Chibana *et al.*, 2003). Taken together these mechanisms demonstrate multiple pathways by which the actions of IL-13 on fibroblasts may contribute to asthma pathology.

Cells	Up-regulated		Down-regulated	
	Genes	**Reference**	**Genes**	**Reference**
T cells	GATA-3	Newcomb 2009	ROR-γT	Newcomb 2009
B cells	Germline ε	Punnonen 1993		
Eosinophils	CD69	Luttmann 1996		
Monocytes			IFNγ	Zurowski 1994
			IL-12	
Macrophages	YM-1	Ramalingam 2008		
	Arginase-1			
	Eotaxin-2/CCL24	Pope 2005		
Endothelia	P-selectin	Woltmann 2000		
Epithelia	Eotaxin/CCL11	Matsukura 2001	Arginase-1	Chibana 2008
	Muc5ac	Kuperman 2002		
	RELMα			
	CLCA3			
	iNOS	Chibana 2008		
Fibroblasts	YM-1	Ramalingam 2008	COX-1	Saito 2003
	RELMα		COX-2	
	IL-13Rα2			
	Collagens I & III	Borowska 2008		
	αSMA			
	PDGF-A	Ingram 2006		
	PDGF-C			
	Erg-1			
	Eotaxin/CCL11	Wenzel 2002		
	CysLT1R	Chibana 2003		
ASM	PDGF-C	Bosse 2008	KLF5	Risse 2011
	CD38	Deshpande 2004		
	IL-5	Grunstein 2002		
	Calponin	Risse 2011		
	Vinculin			
	VCAM-1	Syed 2005		
	P-selectin			
	MCP-1/CCL2			
	Eotaxin/CCL11			
	CTACK/CCL27			
	IL-13Rα2			
	IL-1R			
	Tenascins C & R			
	Collagens I, III & VI			
	CD44			
	IFNβ1			
	Vimentin			
	Tropomyosin 1 & 2			
	Actin			
	Phospholipase D			
	Calreticulin			
	TRPC 4 & 6			
	Sphingosine kinase 1			
	Rho GDP dissociation inhibitor			
	FKBP1A			
	Hisatmine H1 receptor			

Table 1.1 Summary of genes affected by IL-13. Table summarises genes up-regulated and down-regulated following IL-13 stimulation of cell types relevant to the pathogenesis of asthma. Abbreviations: ROR (retinoic acid receptor-related orphan receptor); IFN (interferon); IL (interleukin); RELM (resistin-like molecule); CLCA3 (calcium-activated chloride channel); iNOS (inducible nitric oxide synthase); COX (cyclooxygenase); SMA (smooth muscle actin); PDGF (platelet-derived growth factor); Erg (early growth response); CysLT1R (cysteinyl leukotriene 1 receptor); KLF (kruppel-like factor); VCAM (vascular cell adhesion molecule); MCP (monocyte chemotactic protein); CTACK (cutaneous T-cell-attracting chemokine); TRPC (transient receptor potential cation channels); GDP (guanosine diphosphate); FKBP (FK506 binding protein)

IL-13 stimulation of ASM cells up-regulates the expression of multiple genes including adhesion molecules, chemokines, extracellular matrix (ECM), cytoskeletal constituents and calcium regulators, thus potentially contributing to airway inflammation, remodelling and AHR (Syed *et al.*, 2005). IL-13 does not directly induce ASM proliferation and can inhibit proliferation of ASM under certain circumstances (Bosse *et al.*, 2008;Risse *et al.*, 2011). However, IL-13 does induce PDGF which can induce proliferation of ASM cells primed with fibroblast growth factor 2 (FGF2) to increase expression of PDGF receptor on ASM and hence sensitivity to PDGF (Bosse *et al.*, 2008). Importantly, IL-13 has been reported to reduce ASM responsiveness to β agonists, thus impairing relaxation and enhancing contractility induced by agonists such as carbachol, cysteinyl leukotrienes (cys-LT) and histamine (Laporte *et al.*, 2001;Tliba *et al.*, 2003;Eum *et al.*, 2005;Risse *et al.*, 2011). This enhanced contractility is due to elevated calcium signalling; perhaps via IL-13 induced up-regulation of CD38 expression and activity on ASM (Tliba *et al.*, 2003;Deshpande *et al.*, 2004). Alone, IL-13 induces transient intracellular calcium mobilisation and though this is insufficient for contraction, augmented calcium mobilisation and hence contraction is observed upon stimulation (Eum *et al.*, 2005). Interestingly, although IL-13 elevates ASM contractility it does not alter ASM phenotype by modifying the expression of contractile proteins (Risse *et al.*, 2011). In addition, IL-13 induces IL-5 and eotaxin production from ASM; which may or may not play a role in augmented contractility but are likely to contribute to airway inflammation (Grunstein *et al.*, 2002;Hirst *et al.*, 2002;Eum *et al.*, 2005). Thus, the effects of IL-13 on ASM are not only implicated in AHR but also potentially in airway inflammation and remodelling in asthma.

In summary, although IL-13 does not play a direct role in initiating Th2 polarisation, it can perpetuate an allergic response in the lungs and the associated tissue remodelling and AHR by exerting a multitude of effects on numerous distinct cell types. Hence the proposal that IL-13 is a central mediator of asthma.

1.2.3 IL-13 receptors

IL-13 has two known binding proteins; IL-13Rα1 and IL-13Rα2. The effects of IL-13 are predominantly mediated via the type II IL-4 receptor, a heterodimer comprising of IL-4Rα and IL-13Rα1 which binds both IL-13 and IL-4 (Miloux *et al.*,

1997). This shared receptor usage explains some of the overlapping functions of IL-13 and IL-4. IL-13 initially binds IL-13Rα1 with relatively low affinity and subsequently binds IL-4Rα with high affinity to form a stable complex which signals by phosphorylating signal transducer and activator of transcription 6 (STAT6) via Janus activating kinase 1 (JAK1) and protein tyrosine kinase 2 (TYK2) activation (Figure 1.3 A) (Andrews *et al.*, 2002;LaPorte *et al.*, 2008). IL-4 however, initially binds the IL-4Rα subunit which subsequently binds IL-13Rα1 to activate STAT6 (Figure 1.3 B i) (LaPorte *et al.*, 2008). Phospho-STAT6 subsequently dimerises and translocates to the nucleus where it binds DNA to induce gene transcription. In addition to STAT6 phosphorylation, there is also evidence that type II IL-4 receptor signalling activates STAT3, p38 mitogen-activated protein kinase (MAPK), extracellular signal-related kinase (ERK) and phosphatidylinositol 3-kinase δ (PI3Kδ) pathways, although activation of these pathways may be cell specific (LaPorte *et al.*, 2008;Moynihan *et al.*, 2008;Laporte *et al.*, 2001;Atherton *et al.*, 2003;Farghaly *et al.*, 2008).

In contrast to the interaction between IL-13 and IL-13Rα1, IL-13 binds IL-13Rα2 with high affinity and does not activate STAT6 (Andrews *et al.*, 2002). The role of IL-13Rα2 is complex. IL-13Rα2 has been detected in two forms; membrane bound and soluble (Figure 1.3 C). In mice soluble IL-13Rα2 (sIL-13Rα2) originates from cleavage of membrane bound IL-13Rα2 or may be synthesised directly from a splice variant and secreted as sIL-13Rα2 (Tabata *et al.*, 2006). However, this splice variant is not produced in man and hence sIL-13Rα2 is produced exclusively by cleavage of membrane bound IL-13Rα2 (O'Toole *et al.*, 2008;Chen *et al.*, 2009). Thus the functions of IL-13Rα2 are likely to differ considerably between mice and men. Due to the high binding affinity, short cytoplasmic tail and abundance of sIL-13Rα2, IL-13Rα2 was originally proposed to function primarily as a non-signalling decoy receptor, sequestering IL-13 and therefore reducing IL-13Rα1 dependent pathology (Tabata *et al.*, 2006;Daines *et al.*, 2006). Indeed, IL-13Rα2 can down-regulate IL-13 induced IL-13Rα1 signalling by directly competing for IL-13, furthermore membrane associated IL-13Rα2 internalises following IL-13 binding thus reducing the availability of IL-13 for binding IL-13Rα1 (Yasunaga *et al.*, 2003;Kawakami *et al.*, 2001). However, membrane bound IL-13Rα2 signalling has been demonstrated via

activation of an activating protein-1 (AP-1) variant which leads to TGFβ induction (Fichtner-Feigl *et al.*, 2006). Thus IL-13, via IL-13Rα2 can deliver a pro-fibrotic signal under certain, inflammation-dependent circumstances (Strober *et al.*, 2009). In addition, membrane bound IL-13Rα2 is proposed to modulate IL-4 signalling by associating with IL-4Rα where the cytoplasmic tail of IL-13Rα2 disrupts the activation of IL-4Rα associated signalling molecules (Rahaman *et al.*, 2002;Andrews *et al.*, 2006). IL-13Rα2 forms a complex with IL-4Rα only in the presence of IL-4. Similarly, IL-13Rα2 can associate with IL-13Rα1 in the presence of IL-13 and inhibit STAT6 activation, providing yet another mechanism by which IL-13Rα2 can down regulate IL-13 activity (Rahaman *et al.*, 2002). Given the multiple mechanisms by which membrane bound IL-13Rα2 can regulate IL-4 and IL-13 signalling it is interesting to note that loss of surface IL-13Rα2 could therefore render cells more sensitive to IL-4 and IL-13 stimulation. Surface IL-13Rα2 may be lost by several means, each of which is conceivably elevated in an allergic setting; i) increased activity of endogenous proteases e.g. matrix metalloproteinase (MMP) 8; ii) exposure to exogenous proteases e.g. allergens; iii) greater receptor internalisation due to the presence of IL-13 (Chen *et al.*, 2009;Daines *et al.*, 2007;Kawakami *et al.*, 2001).

IL-4 and IL-13 share the type II IL-4 receptor and hence many of their functions are overlapping, however IL-4 and IL-13 also induce various cytokine specific genes (Lewis *et al.*, 2009). Some of these discrepancies may be explained by the ability of IL-4 to use the type I IL-4 receptor which IL-13 cannot (Figure 1.3 B ii). Unlike the type II IL-4 receptor, the type I receptor activates the insulin receptor substrate-2 (IRS2) pathway in addition to STAT6 (Heller *et al.*, 2008). Aside from type I IL-4 receptor signalling, IL-4 and IL-13 deliver distinct signals, with different potencies, via the type II receptor; with IL-4 signalling being more rapid and able to signal at lower concentrations than IL-13 (LaPorte *et al.*, 2008). In addition to this intrinsic difference, the responsiveness of a specific cell to each cytokine is also governed by a fine balance between the relative abundances of receptor subunits and the cytokines themselves (Junttila *et al.*, 2008). Thus, IL-4 and IL-13 induced receptor activation is complex and the quality of signal arising can vary in what is likely to be a cell specific manner.

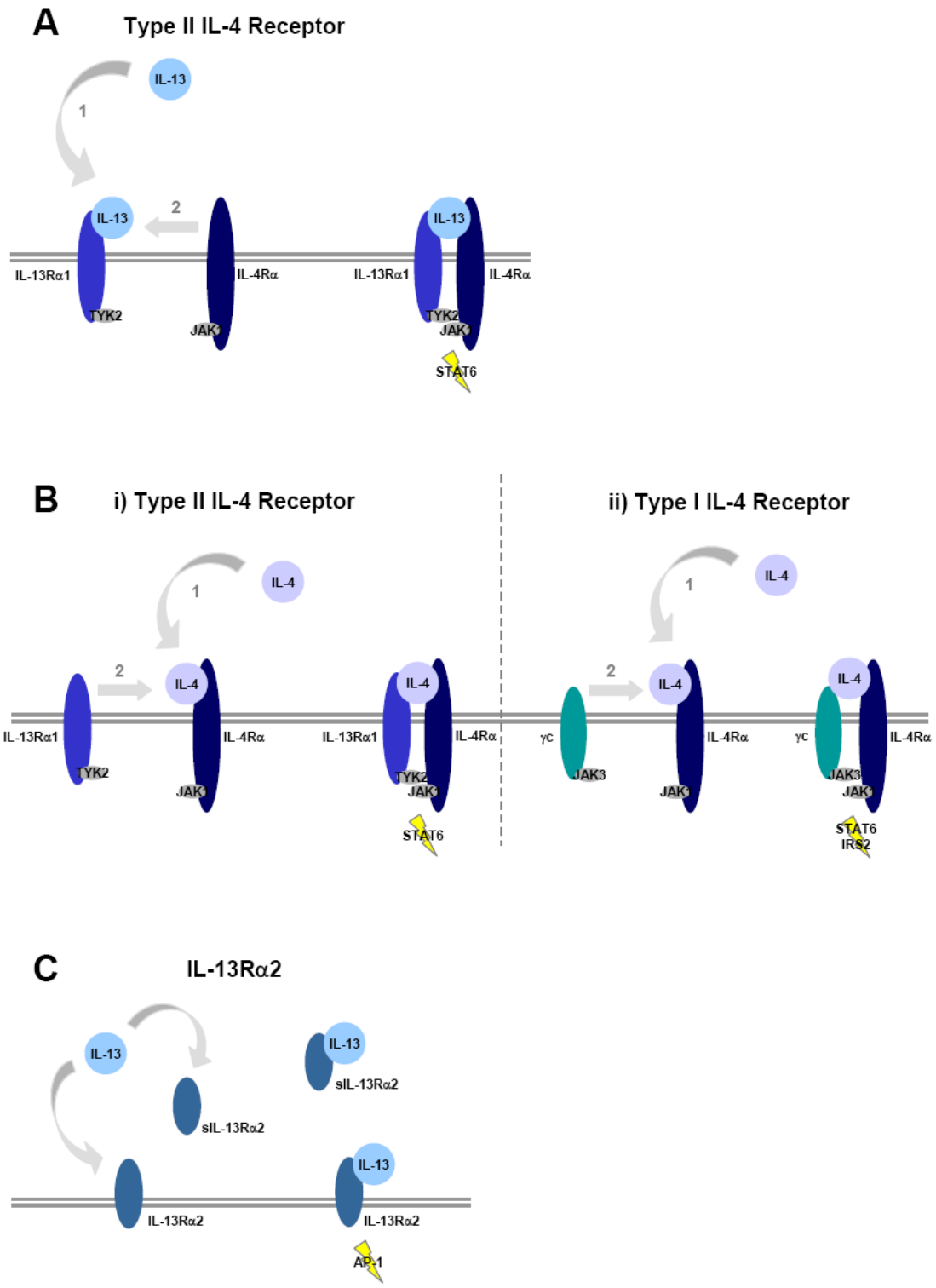


Figure 1.3 IL-13 and IL-4 receptor assembly. Figure depicts the sequential assembly of the type II IL-4 receptor in the presence of IL-13 (A) and IL-4 (B i); assembly of the type I IL-4 receptor (B ii) and IL-13 binding IL-13Rα2 (C). Arrows numbered 1 and 2 represent sequential binding where event 1 must precede event 2. Abbreviations: IL (interleukin); R (receptor); TYK (protein tyrosine kinase); JAK (janus activating kinase); STAT (signal transducer and activator of transcription); IRS (insulin receptor substrate); AP (activating protein).

Much of the evidence pertaining to expression of IL-13 receptors is based on functional responses to IL-13 *in vitro*, however several studies have directly investigated the distribution of IL-13Rα1 and IL-13Rα2. IL-13Rα1 has been detected on the surface of human B cells, specifically naïve and memory B cells, but not germinal centre B cells, and is up-regulated by stimulation with CD40L, consistent with the role of IL-13 in antibody class switching (Graber *et al.*, 1998). In contrast, mouse B cells do not express IL-13Rα1, in accordance with IL-13 being superfluous to antibody class switching in mice (Punnonen *et al.*, 1993;Zurawski & de Vries, 1994). Human monocytes have been reported to express IL-13Rα1 which is down regulated following IL-13 or IL-4 stimulation (Graber *et al.*, 1998). In addition, IL-13Rα1 and IL-4Rα subunits are present on mast cells within the bronchial submucosa; furthermore the numbers of these receptor expressing cells are higher in lung biopsies from asthmatic patients compared to healthy controls (Kotsimbos *et al.*, 1998;Kaur *et al.*, 2006). Although intracellular IL-13Rα1 protein is present in human T cells, it is not readily detected on the cell surface (Graber *et al.*, 1998). However surface expression has recently been described in mouse and human Th17 polarised cells but not other T cell subsets (Newcomb *et al.*, 2009;Newcomb *et al.*, 2011). In lung specimens from asthmatic patients both IL-13Rα1 and IL-4Rα have been detected on bronchial smooth muscle cells, epithelial cells and fibroblasts (Kaur *et al.*, 2006;Heinzmann *et al.*, 2000;Ingram *et al.*, 2009). Thus numerous haematopoietic and non-haematopoietic cells implicated in asthma pathogenesis have the potential to respond to IL-13.

IL-13Rα2 has been detected intracellularly in monocytes, primary human epithelial cells and fibroblasts (Daines & Hershey, 2002;Yasunaga *et al.*, 2003;Konstantinidis *et al.*, 2008). In addition, surface expression of IL-13Rα2 is evident on fibroblasts, albeit at very low levels, and on bronchial epithelial cells (Daines & Hershey, 2002;Lordan *et al.*, 2002). IL-13Rα2 can be mobilised to the cell surface of monocytes, epithelial cells or fibroblasts by stimulation with IFNγ, though this does not up-regulate expression of IL-13Rα2 (Daines & Hershey, 2002;Andrews *et al.*, 2006). IL-13Rα2 expression can be up-regulated by exposure to IL-4 or IL-13 (Yasunaga *et al.*, 2003;Tanabe *et al.*, 2008). In mice both membrane bound IL-13Rα2 and sIL-13Rα2 have been demonstrated to be up-regulated in AAD, despite

differential regulation, however the effects of allergen exposure on IL-13Rα2 expression in humans are contentious (Yasunaga *et al.*, 2003;Tabata *et al.*, 2006;Daines *et al.*, 2007;O'Toole *et al.*, 2008).

1.2.4 Modulation of IL-13

The roles of IL-13 and it's receptors in the pathogenesis of AAD *in vivo* have previously been investigated using knock-out mice and by neutralising IL-13 activity with IL-13Rα2 fusion protein or anti-IL-13 antibodies (Table 1.2). However, much of this data is derived from experiments in which systemic sensitisation with antigen in the chemical adjuvant aluminium hydroxide (alum) is required to induce immunity to an otherwise innocuous protein such as ovalbumin (OVA). In these model systems the absence of IL-13 does not prevent development of a Th2 response; demonstrated by airway inflammation, the presence of antigen specific IgE and the production of IL-4 and IL-5 from draining lymph node cells following *ex vivo* stimulation in *Il13*$^{-/-}$ mice sensitised and challenged with OVA (Walter *et al.*, 2001). However, *Il13*$^{-/-}$ mice do exhibit reduced AAD pathophysiology. OVA induced changes in AHR, goblet cell frequency and collagen deposition are prevented in *Il13*$^{-/-}$ mice (Walter *et al.*, 2001;Leigh *et al.*, 2004b). In addition, allergen induced airway eosinophilia appears to be partially dependent upon IL-13.

	AHR	Eosinophilia	Mucus	Fibrosis	IgE	Reference
Il13$^{-/-}$	↓↓↓	↓↓	↓↓↓	↓↓↓	↓ specific	Walter 2001 Leigh 2004
sIL-13Rα2-Fc (T.O.C)	↓↓↓	↓↓	↓↓		- specific	Grunig 1998 Wills-Karp 1998
Anti-IL-13 (T.O.C)	↓↓↓	↓↓	↓↓↓	↓↓	-/↓↓ specific	Yang 2004 Yang 2005
Il13rα1$^{-/-}$	↓↓↓	↓	↓↓↓		↓↓ total	Munitz 2008 Ramalingam 2008
Il13rα2$^{-/-}$	-	-/↑	-			Zheng 2008 Wilson 2007
stat6$^{-/-}$	↓↓↓	↓↓/↓↓↓	↓↓↓		↓↓↓ total	Akimoto 1998 Kuperman 1998

Table 1.2 The effects of IL-13 signalling modulation. Table summarises the response to induction of AAD in mice deficient in IL-13, IL-13 receptors or signalling molecules and in mice in which IL-13 has been neutralised by fusion protein or mAb treatment at time of challenge (T.O.C). – No effect; ↓ <50% inhibition; ↓↓ >50% inhibition; ↓↓↓ >75% inhibition; ↑ elevation.

These effects have been recapitulated by IL-13 neutralisation by means of sIL-13Rα2-Fc fusion protein or anti-IL-13 polyclonal (pAb) or monoclonal antibodies (mAb) administered at time of allergen challenge. Initial studies utilised the high affinity of sIL-13Rα2 for IL-13 to generate fusion proteins that neutralise IL-13 *in vivo*. This approach abrogated the development of OVA induced AHR, goblet cell up-regulation and BAL eosinophilia (Grunig *et al.*, 1998;Wills-Karp *et al.*, 1998). Further investigation into allergen induced changes in lung function revealed treatment with sIL-13Rα2-Fc inhibited the late phase but not early phase response (Taube *et al.*, 2002). Moreover, sIL-13Rα2-Fc reduced BAL IL-5 concentration but had no affect on the generation of antigen specific antibodies (Taube *et al.*, 2002). Similarly, anti-IL-13 mAb treatment at time of allergen challenge inhibited AHR, goblet cell up-regulation and BAL eosinophilia in OVA sensitised and challenged mice (Yang *et al.*, 2004). Longer term studies have demonstrated that anti-IL-13 mAb treatment inhibits airway remodelling (Yang *et al.*, 2005) and furthermore can reduce eosinophilia, goblet cell hyperplasia, AHR and collagen deposition after the development of AAD (Kumar *et al.*, 2004). In an alternative model of AAD driven by *Aspergillus fumigatus* sensitisation, treatment with anti-IL-13 pAb after airway challenge also ameliorated AHR, collagen deposition and goblet cell hyperplasia (Blease *et al.*, 2001). In addition, anti-IL-13 treatment has been demonstrated to inhibit OVA induced IL-4, IL-5, TNFα, macrophage inflammatory protein (MIP)-1α, eotaxin, monocyte chemotactic protein (MCP)-1 and KC in lung tissue (Yang *et al.*, 2004;Yang *et al.*, 2005). However, the reduction in OVA induced IL-5 and eotaxin and the associated inhibition of eosinophilia has not always been reproduced (Eum *et al.*, 2005). Furthermore, there is some discrepancy in the effects of IL-13 neutralisation on the generation of antigen specific IgE. OVA specific IgE titres are partially reduced in *Il13*$^{-/-}$ mice and mice treated with anti-IL-13 mAb at time of allergen challenge however, no effects on OVA specific IgE were observed with sIL-13Rα2-Fc treatment or anti-IL-13 pAb treatment at time of challenge in equivalent models (Walter *et al.*, 2001;Yang *et al.*, 2004;Wills-Karp *et al.*, 1998;Wang & McCusker, 2005). These inconsistencies are likely to result from subtle differences in the experimental models, the IL-13 neutralising entity used and associated dosing regime. However, since murine B cells do not express IL-13Rα1, effects of IL-13 neutralisation on allergen specific antibody generation must be indirect (Punnonen *et*

al., 1993;Zurawski & de Vries, 1994). Thus, inhibition of antibody production in *Il13*$^{-/-}$ mice or by anti-IL-13 mAb treatment may be a reflection of reduced IL-4 production in these mice. Taken together these data demonstrate that IL-13 neutralisation after sensitisation, at the time of allergen challenge, replicates the effects observed in *Il13*$^{-/-}$ mice. Hence indicating IL-13 is not required for the initiation of Th2 immunity, but is a key effector cytokine in the development of airway responses.

Consistent with IL-13Rα1 being a component of the principal signalling receptor for IL-13, *Il13rα1*$^{-/-}$ mice exhibit pathophysiology comparable to *Il13*$^{-/-}$ mice and mice treated with sIL-13Rα2-Fc or anti-IL-13 antibodies following induction of AAD. Upon OVA sensitisation and challenge AHR and goblet cell hyperplasia were completely abrogated in *Il13rα1*$^{-/-}$ mice (Munitz *et al.*, 2008). Furthermore, eosinophilia, MCP-1, TARC, eotaxin-1, eotaxin-2 and TGFβ were reduced in BAL from *Il13rα1*$^{-/-}$ mice compared to wild type. However, the absence of IL-13Rα1 did not affect OVA induced IL-4 or IL-5 in BAL and IL-13 and IL-10 concentrations were actually elevated in BAL. Interestingly, although OVA sensitisation elevated serum IgE levels in wild type and *Il13rα1*$^{-/-}$ mice, *Il13rα1*$^{-/-}$ mice displayed lower titres compared to wild type controls in both sensitised and non-sensitised groups. This has also been observed in a *Schistosoma mansoni* egg antigen (SEA) model of AAD in *Il13rα1*$^{-/-}$ mice (Ramalingam *et al.*, 2008). *Il13rα1*$^{-/-}$ mice were also protected from SEA induced AHR and mucus hypersecretion. Furthermore, eotaxin-1 mRNA up-regulation in the lung tissue was prevented in SEA sensitised *Il13rα1*$^{-/-}$ mice and the corresponding BAL eosinophilia modestly reduced. However, SEA induced IL-4, IL-5 and IL-13 mRNA expression was heightened in *Il13rα1*$^{-/-}$ mice. Collectively, these data from *Il13rα1*$^{-/-}$ mice confirm IL-13Rα1 and therefore IL-13, is not required for the development of a Th2 response, but is essential for airway specific effector responses. These studies also reveal a novel role for IL-13Rα1 in the regulation of basal, natural IgE expression. Moreover, the observation that IL-13, amongst other Th2 cytokines, may be elevated in *Il13rα1*$^{-/-}$ mice with AAD indicates IL-13Rα1 could also play a role in negatively regulating Th2 responses. In addition, these two studies suggest that while the type II IL-4 receptor may be dispensable for alternative activation of macrophages, alternative activation marker genes are

differentially regulated by the type I and II IL-4 receptors and hence full differentiation may require IL-13Rα1 (Ramalingam *et al.*, 2008;Munitz *et al.*, 2008).

Deficiency in STAT6, the primary transcription factor for type II IL-4 receptor mediated signalling, also resulted in protection from allergen induced AHR and goblet cell up-regulation (Kuperman *et al.*, 1998;Akimoto *et al.*, 1998). However, since *stat6*$^{-/-}$ mice are also incapable of responding to IL-4 (via the type I or II IL-4 receptor) they cannot mount Th2 responses and therefore display a more profound reduction in AAD than that observed in *Il13rα1*$^{-/-}$ mice. Specifically, OVA induced eosinophilia and BAL IL-4 and IL-5 concentrations were severely impaired in *stat6*$^{-/-}$ mice (Kuperman *et al.*, 1998). Furthermore, serum IgE was undetectable in *stat6*$^{-/-}$ mice, even after OVA sensitisation and challenge indicating the generation of both antigen specific IgE and basal, natural IgE is STAT6 dependent (Kuperman *et al.*, 1998;Akimoto *et al.*, 1998).

In contrast to *Il13*$^{-/-}$ and *Il13rα1*$^{-/-}$ mice, *Il13rα2*$^{-/-}$ mice exhibit an exaggerated response to allergen. Total BAL cells, eosinophils and lymphocytes were significantly increased in *Il13rα2*$^{-/-}$ mice compared to wild type following OVA sensitisation and challenge (Zheng *et al.*, 2008). Furthermore, IL-13 (but not IL-4) induced airway inflammation, goblet cell up-regulation and fibrosis were elevated in *Il13rα2*$^{-/-}$ mice. However, OVA induced BAL IL-13, IL-4 and IL-5 levels were comparable in *Il13rα2*$^{-/-}$ and wild type mice, indicating IL-13Rα2 negatively regulates IL-13 effector functions in the lung without altering the underlying Th2 response. This is consistent with the hypothesis that IL-13Rα2 acts primarily as an IL-13 decoy receptor in this model. Conversely, in an SEA driven model of AAD airway inflammation, mucus hypersecretion and AHR were unaltered in *Il13rα2*$^{-/-}$ mice compared to wild type, however *Il13rα2*$^{-/-}$ mice developed a stronger IL-10 response which may be regulating AAD in the absence of IL-13Rα2 (Wilson *et al.*, 2007). Interestingly, the phenotype of naive *Il13rα2*$^{-/-}$ mice presents with reduced serum IL-13, increased IL-13 in the lung tissue and increased serum IgE titres, even in the absence of allergen exposure (Wood *et al.*, 2003). These observations indicate that IL-13Rα2 may play a homeostatic role in regulating IL-13 distribution and tissue clearance, perhaps by acting as a chaperone for IL-13; prolonging its plasma half-life.

Furthermore, they demonstrate IL-13Rα2 and therefore IL-13 regulates natural IgE production.

Based on the reported functions of IL-13, its up-regulation in asthma and its role in the pathogenesis of AAD in mice, neutralisation of IL-13 activity is being pursued as a novel therapeutic for the treatment of asthma. Further investigation into the effects of disrupting IL-13 signalling has been conducted in cynomolgus monkeys naturally sensitised to *Ascaris suum*. In this pre-clinical model of AAD treatment with the anti-human IL-13 mAb IMA-638, 24 hours prior to antigen challenge reduced total BAL cells, eosinophils, neutrophils and monocytes (Bree *et al.*, 2007). In addition, anti-IL-13 mAb treatment inhibited allergen induced eotaxin and RANTES (CCL5) production in BAL. In a subsequent study the same anti-IL-13 mAb was shown to reduce allergen specific IgE titre and allergen induced histamine release from basophils 8 weeks after allergen challenge (Kasaian *et al.*, 2008). In addition, another anti-human IL-13 mAb, CAT-345, has demonstrated inhibition of *A. suum* induced AHR, BAL eosinophilia and total IgE titres in an equivalent cynomolgus monkey model (Walsh, 2010). However, in *A. suum* sensitised macaques yet another anti-human IL-13 mAb inhibited allergen induced eotaxin production, but had no effect on lung function, BAL eosinophilia or BAL IgE concentrations (Martin *et al.*, 2008). Thus, variable results have been attained with IL-13 neutralising mAbs in pre-clinical, non-human primate models of AAD.

At present, multiple clinical trials are ongoing to evaluate the safety and efficacy of anti-IL-13 mAb treatment in asthma. An acceptable safety profile and linear pharmacokinetics in patients with mild to moderate asthma have been reported for the anti-IL-13 mAb CAT-354 (Singh *et al.*, 2010). A phase II study with this mAb, now termed "Tralokinumab", in adults with uncontrolled, moderate to severe asthma has recently completed. The primary endpoint for this study was asthma control, with secondary endpoints of time to asthma control; time to first exacerbation; exacerbation rates and severity and variable airflow obstruction, amongst others, however no data from this study is currently available (Walsh, 2010).

In patients with seasonal allergic rhinitis IL-13 neutralisation has been reported to have limited effects on the late phase reaction following allergen challenge despite

significant attenuation of free IL-13 (Nicholson *et al.*, 2011). Administration of QAX576, another anti-human IL-13 mAb, showed a trend towards reduced eotaxin production however no effects on nasal eosinophilia or symptom score were demonstrated.

IMA-638, "Anrukinzumab", demonstrated inhibition of the EAR and LAR post-allergen challenge in mild, atopic asthmatics however anrukinzumab treatment did not affect allergen induced AHR to methacholine (Gauvreau *et al.*, 2008). A subsequent phase II study with anrukinzumab in patients with persistent asthma did not reach its clinical efficacy endpoint, leading to termination of the development of this mAb (Oh *et al.*, 2010). IMA-638 was superseded by IMA-026; another anti-IL-13 mAb binding a different epitope. In a phase II trial directly comparing the two antibodies in mild atopic asthmatic patients the reduction in allergen induced EAR and LAR seen previously was reproduced in the IMA-638 arm (Gauvreau *et al.*, 2011). However IMA-026 failed to significantly affect allergen induced EAR or LAR. No significant effects on AHR, sputum eosinophilia or total IgE titres were observed with either mAb. Interestingly, a greater elevation in circulating IL-13 levels was observed in IMA-026 compared to IMA-638 treated patients. Further investigation revealed this IMA-026 induced accumulation of serum IL-13 was due to impaired IL-13 clearance via IL-13Rα2 dependent internalisation (Kasaian *et al.*, 2011). Since IMA-026 blocks the interaction between IL-13 and IL-13Rα2, but IMA-638 does not, this is proposed to account for the diminished efficacy of IMA-026.

Perhaps the furthest advanced anti-IL-13 mAb in the clinic is lebrikizumab (MILR1444A) which has recently completed two phase II studies assessing efficacy in patients with asthma not taking inhaled corticosteroids (ICS) and patients with asthma inadequately controlled by ICS (clinicaltrials.gov). The primary outcome for both studies was change in forced expiratory volume in 1s (FEV_1). Lebrikizumab treatment significantly improved FEV_1 in patients with inadequately controlled asthma (Corren *et al.*, 2011). In addition, lebrikizumab reduced fractional expiratory NO (F_ENO), serum MCP-4 (CCL13), TARC (CCL17) and IgE levels however, peripheral blood eosinophil counts were elevated. Furthermore, patients receiving lebrikizumab exhibited a trend towards reduced rate of exacerbations. Patient stratification based on serum periostin levels (a biomarker of IL-13 activity

(Woodruff *et al.*, 2007)) indicated patients with high periostin were more responsive to lebrikizumab treatment. Based on these positive phase II results lebrikizumab is to progress into phase III studies (Roche half-year results 2011).

An alternative approach to neutralising IL-13 activity has been investigated using pitrakinra, an IL-4 mutant protein (mutein) that binds IL-4Rα thus antagonising the effects of both IL-4 and IL-13. Pitrakinra has been formulated for both inhaled and subcutaneous (s.c.) administration. In *A.suum* sensitised cynomolgus monkeys both inhaled and s.c. formulations significantly attenuated allergen induced AHR and reduced airway eosinophilia (Tomkinson *et al.*, 2010). Both formulations were subsequently investigated in a phase II study of allergic asthmatic patients. Inhaled and s.c. pitrakinra inhibited the decline in FEV_1 associated with the LAR post-allergen challenge (Wenzel *et al.*, 2007). Furthermore, inhaled pitrakinra exhibited superior efficacy to s.c. administration. In addition, inhaled pitrakinra reduced basal F_ENO, but not post-challenge F_ENO. However, neither formulation significantly affected the EAR or AHR. Preliminary data from additional studies with inhaled pitrakinra in uncontrolled moderate to severe asthma indicated treatment failed to improve the primary endpoint, incidence of asthma exacerbation (Antoniu, 2010). However, incidence of exacerbation, time to exacerbation and asthma symptom scores were improved in a subset of patients with eosinophilic asthma. Thus, direct delivery of an IL-13 antagonist into the lungs may be beneficial in the treatment of a subpopulation of asthma patients.

In summary, there is evidence IL-13 plays a role in allergen induced airway responses and basal lung function in man. However, the limited data available from current trials is insufficient to establish whether anti-IL-13 therapy could be beneficial in asthma. It is likely that only a subpopulation of asthmatic patients may be responsive to anti-IL-13 therapy as indicated by trials with pitrakinra and lebrikizumab (Corren *et al.*, 2011;Antoniu, 2010). Therefore the key to demonstrating efficacy and subsequent patient treatment may be patient stratification into groups of potential responders. Woodruff *et al.* has identified two subpopulations of asthmatic patients; Th2-high and Th2-low asthma (Woodruff *et al.*, 2009). In the Th2-high subset IL-13 expression in bronchial biopsies, and hence potential susceptibility to IL-13 inhibition, was significantly elevated above controls and Th2-low asthma (Woodruff

et al., 2009). Furthermore, identification of serum periostin as a biomarker of IL-13 activity facilitates patient stratification (Woodruff *et al.*, 2007;Corren *et al.*, 2011). In addition, genetic analysis of asthma subpopulations and their subsequent division into clusters has been conducted however it is not yet known how these clusters relate to treatment susceptibility (Moore *et al.*, 2010;Haldar *et al.*, 2008). These early clinical studies with IL-13 neutralising entities highlight some discrepancies between data generated in mouse models of AAD and man. Mouse studies demonstrate IL-13 is instrumental in airway eosinophilia and AHR however IL-13 neutralisation in man had no effect on eosinophilia or AHR (Gauvreau *et al.*, 2011;Gauvreau *et al.*, 2008). This indicates that the mouse models currently used are inappropriate approximations of human asthma.

1.3 HDM induced AAD

As previously illustrated, models of AAD in mice commonly use the model antigen OVA. However, airway exposure to OVA is generally well tolerated and does not, in itself induce inflammation. Therefore mice are sensitised to OVA, often twice prior to airway exposure, by peritoneal injection of OVA adsorbed onto the adjuvant aluminium hydroxide (alum). This elicits a strong, systemic Th2 response which is subsequently directed to the lungs by a series of airway challenges with OVA. Clearly the induction of this immune response is quite dissimilar to the likely routes of allergen sensitisation in man. Furthermore, the period of airway challenge is often limited by a waning of the response and even induction of tolerance to OVA following prolonged periods of airway challenge (Van Hove *et al.*, 2007). Thus OVA induced models of AAD are typically of an acute nature and hence fail to replicate the chronic airway inflammation and associated airway remodelling that is characteristic of asthma. In addition, comparisons between OVA studies can be complicated by the varying levels of contaminating endotoxin in OVA preparations. A further disparity between asthma and OVA induced AAD is resolution after cessation of allergen challenge.

In order to circumvent some of these issues, a relatively novel model of AAD, elicited by the environmentally relevant aeroallergen HDM, has been developed (Johnson *et al.*, 2004). HDM extract (from *Dermatophagoides pteronyssinus* or *D.farinae*) is a complex allergen with numerous components that promote allergic sensitisation and

therefore negates the need for systemic sensitisation and chemical adjuvants. Thus, continuous airway exposure to HDM, via intranasal administration, evokes chronic airway inflammation. Furthermore, prolonged exposure elicits structural changes in the airway wall akin to those present in asthma. In addition, this remodelling and to an extent, AHR does not resolve following cessation of allergen challenge. Importantly, allergen exposure is only via the respiratory tract in this model and therefore the response to HDM is initiated by lung epithelial cells and pulmonary DCs; a mechanism likely to be relevant to aeroallergen exposure and sensitisation in man.

HDM extract is a cocktail of allergens and additional components that posses multiple intrinsic properties that activate innate immunity and promote allergen sensitisation (Figure 1.4). Detection of danger signals is paramount for the initiation of an immune response and relies heavily on pattern recognition receptors (PRR). PRRs can sense pathogen associated molecular patterns (PAMP) via toll-like receptors (TLR), C-type lectin receptors (CLR), nucleotide-binding oligomerization domain (NOD)-like receptors (NLR) and protease activated receptors (PAR) (Willart & Hammad, 2010). In addition, PRRs can recognise damage associated molecular patterns (DAMP) via complement receptors, purinergic receptors and heat shock protein receptors, amongst others. Many of these PAMP and DAMP receptors are expressed on lung epithelial cells and DCs where constituents of HDM, but not OVA, activate them upon inhalation.

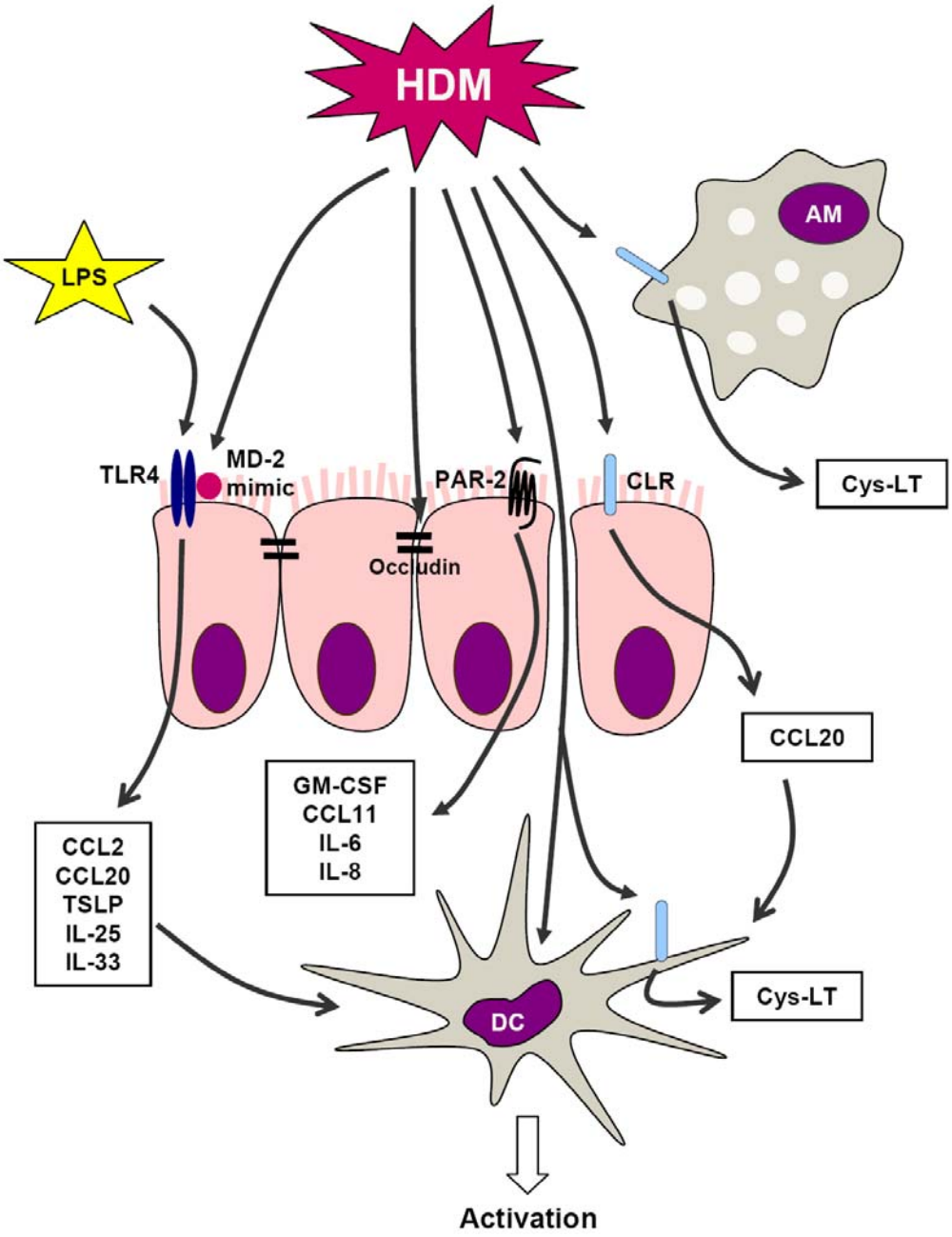


Figure 1.4 Allergeneic properties of HDM. Figure depicts multiple mechanisms by which HDM extract may promote allergic sensitisation by inducing the release of mediators: Toll-like receptor 4 (TLR4) activation on airway epithelial cells in the presence of lipopolysaccharide (LPS) and MD-2 mimic stimulates the release of CCL2, CCL20, thymic stromal lymphopoietin (TSLP), interleukin (IL)-25 and IL-33; occludin cleavage reduces epithelial barrier integrity and permits HDM exposure to underlying dendritic cells (DC) resulting in DC activation; activation of protease activated receptor (PAR)-2 on epithelial cells stimulates the production of granulocyte-macrophage colony-stimulating factor (GM-CSF), CCL11, IL-6 and IL-8; ligation of C-type lectin receptors (CLR) on airway epithelial cells, DC and alveolar macrophages (AM) induced production of CCL20 and cysteinyl leukotrienes (Cys-LT), respectively.

The development of HDM induced AAD has been demonstrated to be dependent upon the activation of TLR4 on airway epithelial cells (Hammad *et al.*, 2009). TLR4 is activated by LPS binding in conjunction with the accessory proteins MD-2 and CD14. Invariably, HDM preparations contain a degree of LPS from contaminating Gram-negative bacteria, furthermore, the major group 2 allergens of HDM (e.g. Der p 2) exhibit structural and functional homology to MD-2 (Trompette *et al.*, 2009). Ordinarily, the low level of MD-2 expression on airway epithelial cells renders them relatively unresponsive to LPS stimulation; hence administration of Der p 2 heightens LPS sensitivity (Jia *et al.*, 2004). Thus, HDM administration provides the TLR4 ligand LPS and furthermore, facilitates TLR4 signalling in epithelial cells by providing the MD-2 mimic, Der p 2. TLR4 signalling in epithelial cells stimulates the release of DC chemo-attractants such as CCL2 (MCP-1) and CCL20 (MIP-3α) and the epithelial derived cytokines TSLP, IL-25 and IL-33 which promote allergen sensitisation and Th2 immunity (Hammad *et al.*, 2009;Lloyd, 2009).

In addition to TLR4 ligands, HDM extract also contains TLR2 ligands such as chitins and TLR9 ligands such as mite and bacterial DNA. The roles of these TLRs in HDM induced AAD are currently unknown. Administration of chitin into the lungs has previously been demonstrated to induce accumulation of innate effector cells associated with AAD, however the role of chitins in Th2 responses is ambiguous (Reese *et al.*, 2007;Lee *et al.*, 2008).

Another characteristic property of HDM fundamental to its allergenicity is the protease activity of many of the main allergens. Der p 1, 3, 6 and 9 are all cysteine and/or serine proteases (John *et al.*, 2000;Wan *et al.*, 1999). This protease activity has numerous effects that are likely to contribute to allergen sensitisation; indeed administration of proteolytically active Der p 1 into the lungs of pre-sensitised mice induces a significantly greater response than that of inactive Der p 1 (Gough *et al.*, 2003). Importantly, Der p 1 is capable of disrupting epithelial tight junctions by cleaving occludin, and disrupting ZO-1 distribution thus increasing epithelial permeability (Wan *et al.*, 1999). This in turn enables allergens (together with other PAMPs that may be present in the airway lumen) to cross the epithelial barrier, therefore increasing the accessibility to DCs. In addition, Der p 1, 3 and 9 have been demonstrated to induce pro-inflammatory cytokine release from epithelial cells, in

part via PAR-2 activation (Asokananthan *et al.*, 2002;Sun *et al.*, 2001). Furthermore, HDM proteases have been reported to cleave a multitude of endogenous proteins that may influence the pathogenesis of AAD: Group 3 allergens (Der f 3 in this case) can cleave C3 and C5 to generate the anaphylatoxins C3a and C5a, respectively, (Maruo *et al.*, 1997). These active complement components have a range of actions including increasing vascular permeability, smooth muscle contraction and stimulating histamine release from mast cells. Der p 1 activity promotes the generation of Th2 responses and IgE production by cleaving various molecules involved in the development and regulation of B and T cell differentiation. Cleavage of CD40 and DC-specific intercellular adhesion molecule-3-grabbing non-integrin (DC-SIGN) from DCs, CD25 from T cells and CD23 from B cells has all been reported (Furmonaviciene *et al.*, 2007;Ghaemmaghami *et al.*, 2002;Schulz *et al.*, 1998;Schulz *et al.*, 1995). Der p 1 also degrades lung surfactant proteins A and D (SP-A and SP-D, respectively) which have previously been shown to be protective in AAD (Deb *et al.*, 2007). In addition, HDM has been demonstrated to cleave IL-13Rα2 from the cell surface and subsequently degrade sIL-13Rα2; potentially rendering cells more sensitive to IL-13 stimulation (Daines *et al.*, 2007).

HDM also contains glycans that are recognised by various CLRs. Indeed Der p 1 itself is taken up into DCs via mannose receptor mediated endocytosis (Deslee *et al.*, 2002). HDM derived β-glucan moieties interacting with an as yet unidentified dectin-like receptor have been reported to be the stimulus driving CCL20 release from airway epithelial cells (Nathan *et al.*, 2009). CCL20 is a chemoattractant for immature DCs which may subsequently take up allergen and initiate sensitisation. Furthermore, glycans present in HDM have been demonstrated to activate Dectin-2 on DCs to induce cys-LT production via activation of the arachidonic acid pathway (Barrett *et al.*, 2009). In addition, the glycan chitin can alternatively activate pulmonary macrophages, via an as yet unknown mechanism, to produce LTB_4 (Reese *et al.*, 2007).

These adjuvant properties intrinsic to HDM render this allergen capable of directly and indirectly (via stimulating the airway epithelium) activating DCs. DCs have been demonstrated to be crucial in both the initiation and maintenance of allergic responses (van Rijt *et al.*, 2005). Collectively, these data illustrate how HDM can be such a

potent inducer of allergic sensitisation in mice and men, and hence demonstrate why HDM is a preferred allergen for studying AAD in animal models.

1.4 Hypothesis

IL-13 is required for the initiation, development and maintenance of pulmonary inflammation, airway remodelling and AHR in mice chronically exposed to inhaled HDM allergen.

1.5 Aims

1. To establish the HDM induced model of AAD described by Johnson *et al.* with respect to expression of IL-13 (Johnson *et al.*, 2004).

2. To define the effects of IL-13 neutralisation in mice chronically exposed to inhaled HDM allergen on inflammation, lung function and airway remodelling.

3. To determine the distribution of IL-13 receptors in naïve and inflamed airways. The key cell types expressing IL-13Rα1 and IL-13Rα2 will be identified.

4. Use the appropriate cell type identified in aim 3 to characterise the underlying mechanisms of IL-13 inhibition *in vivo* by specific cell depletion.

2. MATERIALS AND METHODS

2.1 Animals

Male BALB/c mice (6-8 weeks old) were purchased from Harlan (Loughborough, UK). All mice were housed in specific pathogen free conditions and provided with food and water *ad libitum*. All experiments were performed in accordance with the UK Animals (Scientific Procedures) Act 1986.

2.2 HDM exposure

HDM used was whole milled *Dermatophagoides pteronyssinus* (Greer, Lenoir, USA; XPB82D3A2.5). Mice were exposed to 25µg HDM protein in 25µl saline via intra-nasal (i.n.) administration under light isoflurane anaesthesia for 4 consecutive days per week for 1-8 weeks. Sham exposed mice received 25µl saline alone i.n., 4 times per week for the duration of the study. Mice were killed by cervical dislocation 4 or 24 hours after the final HDM exposure.

2.3 Anti-IL-13 mAbs and treatment

Murinised anti-mouse IL-13 mAbs, CA154_582 (582) and CA154_587 (587) were generated by UCB and *in vitro* activities were characterised as reported previously (Berry *et al.*, 2009). 582 prevents the interaction between IL-13 and IL-13Rα1 and hence the subsequent association with IL-4Rα (K_D 11pM). In addition, 582 prevents IL-13 binding to IL-13Rα2. 587 blocks the interaction between the IL-13-IL-13Rα1 complex and IL-4Rα (K_D 8pM), but does not prohibit IL-13 binding IL-13Rα2. Both mAbs 582 and 587 disrupt assembly of the IL-13 receptor signalling complex and hence prevent STAT6 activation. The isotype control mAb, 101.4, was also generated by UCB.

Mice were dosed with 582, 587, 101.4 or vehicle (phosphate buffered saline (PBS)) s.c. weekly at 0.3, 3, 10 or 30mg/kg, as indicated, in 100µl injection volume. Anti-IL-13 treatment commenced prior to HDM exposure (prophylactically) or after 5 weeks of HDM exposure (therapeutically). Once initiated IL-13 treatment continued for the course of the experiment during concomitant HDM exposure.

2.4 Assessment of AHR

AHR was determined by direct measurement of lung resistance (R_L) and dynamic compliance (C_{dyn}) in anaesthetised, ventilated mice using FinePoint apparatus (Buxco,

Wilmington, USA). Twenty-four hours post HDM exposure mice were terminally anaesthetised with ketamine (200mg/kg i.m., Vetalar V, Pfizer, Sandwich, UK) and pentobarbital (35mg/kg i.p., Sigma-Aldrich, Dorset, UK; P3761), tracheostomised and ventilated via a tracheal cannula at 160 breaths/min, tidal volume 200µl. After a short period of acclimatisation mice were exposed to aerosolised PBS followed by increasing concentrations of aerosolised methacholine (3, 10, 30 and 100mg/ml MCh; Sigma-Aldrich, Dorset, UK; A2251) via the tracheal cannula. MCh was aerosolised for 30s and mean R_L and C_{dyn} recorded for the following 3min with a 2min recovery period between doses.

In addition AHR was determined as enhanced pause (Penh) using unrestrained whole body plethysmography (WBP; Buxco, Wilmington, USA) during the fourth week of HDM sensitisation (Hamelmann *et al.*, 1997). Changes in Penh were measured in response to PBS followed by doubling concentrations of MCh (3.125-50mg/ml) aerosolised into the chambers for 2 minute periods. The average Penh was taken over a 4 minute period from the start of aerosolisation. Mice were allowed time to recover and Penh stabilise between each MCh exposure.

2.5 Collection of samples

Blood samples were collected via cardiac puncture under terminal anaesthesia prior to cervical dislocation. Blood samples were allowed to clot for several hours at room temperature prior to centrifugation (10,000g, 10min). Serum was taken and stored at -20°C for future analysis. Where blood was required for analysis of cells by flow cytometry, blood was taken via cardiac puncture, into heparinised syringes. BAL was performed post mortem via tracheal cannula with 3 x 0.4ml PBS (containing 0.4%w/v bovine serum albumin (BSA; Sigma-Aldrich, Dorset, UK; A7906) and 12mM HEPES (Sigma-Aldrich, Dorset, UK; H0887)). Lungs were excised post mortem and processed accordingly (unless otherwise stated): Left lobe preserved in 10% formalin (Surgipath, Peterborough, UK; 3800754) for histological analysis; caudal lobe digested for analysis by flow cytometry; medial lobe preserved in RNAlater (Ambion, Applied Biosystems, Warrington, UK; 7021) for RNA extraction and subsequent real-time polymerase chain reaction (PCR); cranial lobe snap frozen in liquid nitrogen for future cytokine analysis.

2.6 Lung digest

Lung tissue cells were liberated from the caudal lobe by digestion. Prior to digestion lung lobes were finely chopped with a mechanical tissue chopper. Tissues were incubated in media (RPMI 1640 (GIBCO, Invitrogen, Paisley, UK) + 10% FCS, 100U/ml penicillin/streptomycin) containing 150µg/ml Collagenase D (Roche Applied Science, Burgess Hill, UK; 11088858001) and 25µg/ml DNAse (Roche Applied Science, Burgess Hill, UK; 10104159001) for one hour at 37ºC in a shaking water bath. Single cell suspensions were generated by pushing the resultant digest through 70µm nylon sieves. Cells were centrifuged at 700g for 5min, supernatants discarded and cells resuspended in 10ml media. Cells were washed in media twice more (450g, 5min) then finally resuspended in 1-5ml media.

2.7 Flow cytometry

BAL, lung digest (LD) and blood cells were phenotyped and quantified by flow cytometry. Prior to staining blood samples (500µl) were subjected to red cell lysis (Sigma-Aldrich, Dorset, UK; R7757; 3ml for 5 minutes), washed and resuspended in 500µl FACS buffer (PBS + 0.4% BSA, 12mM HEPES, 500mM EDTA). 50-100µl BAL, LD or blood cells were stained with combinations of antibodies listed in Table 2.1. Where stimulation of cells was required for intracellular cytokine staining BAL, LD and blood cells were incubated with 1 in 500 BD Activation cocktail (BD Biosciences, Oxford, UK; 550583) containing phorbol 12-myristate 13-acetate (PMA), ionomycin and brefeldin A for 4 hours at 37°C. After stimulation cells were washed and resuspended in FACS buffer for staining. Prior to addition of staining antibody cocktails cells were incubated with 1 in 100 Fc block (BD Biosciences, Oxford, UK; 553142) for 5min. Antibody cocktails were then added to the cells and incubated for 20 minutes at 4°C in the presence of Fc block. Cells were washed by addition of 2ml FACS buffer and centrifugation (450g, 5min). Samples were fixed with Cytofix (BD Biosciences, Oxford, UK; 554655), Cytofix/Cytoperm (BD Biosciences, Oxford, UK; 554722) or FACSLyse (BD Biosciences, Oxford, UK; 349202) for 10min, RT, then washed as above. Samples requiring intracellular staining that were not fixed with Cytofix/Cytoperm were permeabilised with 1ml Perm/Wash buffer (BD Biosciences, Oxford, UK; 554723) for 15min, RT or with 500µl 0.1% nonidet-P40 (Fluka, Sigma-Aldrich, Dorset, UK; 74385) for 3min for

FoxP3 staining. Samples were then centrifuged and supernatants discarded. Cells were resuspended in intracellular staining antibody cocktails prepared in Perm/Wash buffer and incubated for 20min, 4°C, then washed by addition of 2ml Perm/Wash buffer and centrifugation (450g, 5min).

Prior to acquisition samples were resuspended in a know concentration of reference microbeads for quantification of events acquired. Each sample was resuspended in 300µl PKH26 reference microbeads (Sigma-Aldrich, Dorset, UK; P7458) at 22 000 beads/ml. Samples were acquired on a FACScan or FACSCanto II (BD Biosciences, Oxford, UK) and analysed offline using Flowjo v8.8.4 (Tree Star, Ashland, USA). Where population comparisons were made, the Overton cumulative histogram comparison algorithm was used to determine the percentage of stained cells (Overton, 1988).

Antibody specificity	Conjugation	Dilution used (1 in X)	Supplier	Catalogue no.
CD3e	APC-Cy7	100	BD Biosciences	557596
CD3e	FITC	200	BD Biosciences	553061
CD3e	PE-Cy7	100	BD Biosciences	552774
CD4	APC	200	BD Biosciences	553051
CD4	PE	100, 200	BD Biosciences	553048
CD4	PerCP-Cy5.5	100, 200, 400	BD Biosciences	550954
CD8	APC-Cy7	100	BD Biosciences	557654
CD8	PE	200	BD Biosciences	553033
CD8	FITC	200	BD Biosciences	553030
CD11b	APC-Cy7	100	BD Biosciences	557657
CD11b	PE	200	BD Biosciences	553311
CD11c	APC-Cy7	100	BD Biosciences	561241
CD11c	PE	200	BD Biosciences	553802
CD11c	PerCP-Cy5.5	100	BD Biosciences	560584
CD16/CD32 (Fc block)	purified	100	BD Biosciences	553142
CD19	FITC	100	BD Biosciences	557398
CD25	APC-Cy7	400	BD Biosciences	557658
CD44	FITC	1000	BD Biosciences	553133
CD45	APC-Cy7	200	BD Biosciences	557659
CD45	PE	1000	BD Biosciences	553081
CD45	PE-Cy5	1000	BD Biosciences	553082
CD45	PE-Cy7	200	BD Biosciences	552848
CD45	PerCP-Cy5.5	200	BD Biosciences	550994
CD62L	PE-Cy7	200	BD Biosciences	560516
CD68	RPE	neat	AbD Serotec	MCA1957PEB
CD205	PE-Cy7	20	eBioscience	25-2051-42
CD206	PE	neat	AbD Serotec	MCA2235PE
Dectin-1	Alexa-647	neat	AbD Serotec	MCA2289A647
F4/80	PE-Cy7	40	eBioscience	25-4801-82
FoxP3	PE	200	eBioscience	12-5773-82
Gr-1	PE	500	BD Biosciences	553128
Gr-1	PerCP-Cy5.5	200	BD Biosciences	552093
IFNγ	PE-Cy7	100, 500	BD Biosciences	557649
IL-10	PerCP-Cy5.5	100	eBioscience	45-7101-82
IL-13	Alexa-647	100	eBioscience	51-7133-80
IL-13	PE	100	eBioscience	12-7133-82
IL-13Rα1	purified	20	Santa Cruz Biotechnology	sc-27861
IL-17	PE	100, 500	BD Biosciences	559502
MOMA2	FITC	100	AbD Serotec	MCA519F
Siglec F	PE	200	BD Biosciences	552126
T1ST2	FITC	200, 400	MD Biosciences	101001F
TGFβ	PE	neat	R&D Systems	IC1835P
Secondaries				
Goat	Cy5	100, 200	Jackson ImmunoResearch	705-176-147
Goat	Dy-light 649	200	Jackson ImmunoResearch	705-496-147

Table 2.1 Antibodies used for flow cytometry. Suppliers: BD Biosciences, Oxford, UK; AbD Serotec, Kidlington, UK; eBioscience, Hatfield, UK; Santa Cruz Biotechnology, Santa Cruz, USA; MD Biosciences, St. Paul, USA; Jackson ImmunoResearch, West Grove, USA.

2.8 Cytokine analysis

BAL samples were centrifuged (450g, 5min), supernatants taken and stored at -80ºC until required for assay. Cranial lobes were also stored at -80ºC prior to homogenisation. Lobes were thawed, weighed and homogenised in Hank's balanced salt solution (HBSS; GIBCO, Invitrogen, Paisley, UK) containing complete protease inhibitor (Roche Applied Science, Burgess Hill, UK; 11697498001) at 50mg tissue per ml HBSS. Homogenates were centrifuged (20820g, 25min, +4 ºC), supernatants taken and stored at -80 ºC until required for assay.

BAL and lung homogenate (LH) supernatants were analysed for cytokine and chemokine content by sandwich enzyme-linked immunosorbent assay (ELISA) or multiplex MSD assay. IL-4, IL-5, IFNγ, IL-12, IL-10 and KC were quantified using mouse Th1/Th2 9-plex ultra-sensitive kits (Meso Scale Discovery (MSD), Gaithersburg, USA; K11013C-2) according to the manufacturer's instructions. IL-17 (R&D Systems, Abingdon, UK; DY421), eotaxin (R&D Systems, Abingdon, UK; DY420), IL-25 (R&D Systems, Abingdon, UK; DY1399), IL-33 (R&D Systems, Abingdon, UK; DY3626) and TSLP (R&D Systems, Abingdon, UK; DY555) were quantified using the appropriate DuoSet kit according to the manufacturer's recommendations.

2.9 Detection of serum immunoglobulins

Total serum IgE was assessed by sandwich ELISA. 96 well polystyrene plates (MaxiSorp, Nunc, Thermo Fisher Scientific, Rochester, USA) were coated with 4μg/ml anti-mouse IgE (BD Biosciences, Oxford, UK; 553413) in PBS (100μl/well) at +4ºC, overnight. Plates were washed twice with wash buffer (PBS + 0.05% Tween), blocked for 1 hour with 200μl assay diluent (PBS + 1% BSA) then washed twice. Samples were loaded in the plates in duplicate, 100μl/well, and incubated for 2 hours at RT. Samples were diluted 1 in 100 or 1 in 500 in assay diluent. Plates were then washed four times in wash buffer before addition of 100μl horseradish peroxidise (HRP) conjugated rat anti-mouse IgE (AbD Serotec, Kidlington, UK; MCA419P) at 1 in 1000. Plates were incubated for a further hour prior to washing four times. 100μl 3,3',5,5'-tetramethylbenzidine (TMB) substrate (Sigma-Aldrich, Dorset, UK; T8665) was added and colour allowed to develop for 5-10min. The

reaction was stopped with 50µl 1N H_2SO_4 and read at 450-650nm. Data are presented as mean optical density (OD) from duplicate wells, for each mouse.

HDM specific IgE, IgG1, IgG2a and IgG2b antibodies in the serum were detected by ELISA. Plates were coated with 4µg/ml HDM in PBS (100µl/well) at +4ºC, overnight. The following day plates were washed twice with wash buffer, blocked for 1 hour with 200µl assay diluent then washed twice more. Samples were loaded in the plates in duplicate, 100µl/well, and incubated for 2 hours at RT. Samples were diluted in assay diluent according to Table 2.2. Plates were then washed four times in wash buffer before addition of 100µl of detection antibody (see Table 2.2 for details) and incubated for a further hour prior to washing four times. For the detection of HDM specific IgE an additional step was required; addition of 100µl HRP conjugate for 30min followed by 4 washes. 100µl TMB was added and colour allowed to develop for 5-10min. The reaction was stopped with 50µl 1N H_2SO_4 and read at 450-650nm. Data are presented as mean OD from duplicate wells, for each mouse.

Assay	Sample Dilution (1 in X)	Detection Antibody		
		Specificity	Supplier (Catalogue number)	Dilution (1 in X)
IgE	100, 300	Rat anti-mouse IgE	BD Biosciences (553413)	1 000
		Goat anti-rat Fc-HRP	Jackson ImmunoResearch (112-036-071)	10 000
IgG1	1 000, 2 000	Rat anti-mouse IgG1-HRP	AbD Serotec (MCA336P)	5 000
IgG2a	100	Rat anti-mouse IgG2a-HRP	AbD Serotec (MCA421P)	5 000
IgG2b	100	Goat anti-mouse IgG2b-HRP	AbD Serotec (STAR83P)	5 000

Table 2.2 Antibodies used for immunoglobulin ELISAs. Suppliers: BD Biosciences, Oxford, UK; AbD Serotec, Kidlington, UK; Jackson ImmunoResearch, West Grove, USA.

2.10 Histology

2.10.1 Paraffin sections

Left lobes (unless stated) were excised post mortem and preserved in 10% formalin (Surgipath, Peterborough, UK), embedded in paraffin and sectioned for staining with Alcian blue periodic acid Schiff's stain (AB/PAS) for mucin or Masson's Trichrome for collagen visualisation. The frequency of goblet cells was assessed by scoring bronchioles according to the extent of mucin staining within the airway epithelia (Figure 2.1). A score of 0 indicated no positive staining, bronchioles with few stained

cells (<5%) scored 1, moderate numbers of stained cells scored 2 and bronchioles scoring 3 exhibited high numbers of positively stained cells (>95%). All visible bronchioles were scored in each section; one section was analysed per mouse and data represented as median score from each mouse. Peribronchial collagen thickness was measured using Image-Pro Plus (v5, Media Cybernetics, Bethesda, USA) or AxioVision (release 4.7.2, Carl Zeiss MicroImaging, Göttingen, Germany) software. Three bronchioles were selected at random from each section and the mean depth of collagen from the basement membrane determined from five measurements around the bronchiole (Figure 2.2). Peribronchial collagen associated with adjacent blood vessels was disregarded. One section was analysed per mouse and data presented as mean collagen depth for each mouse.

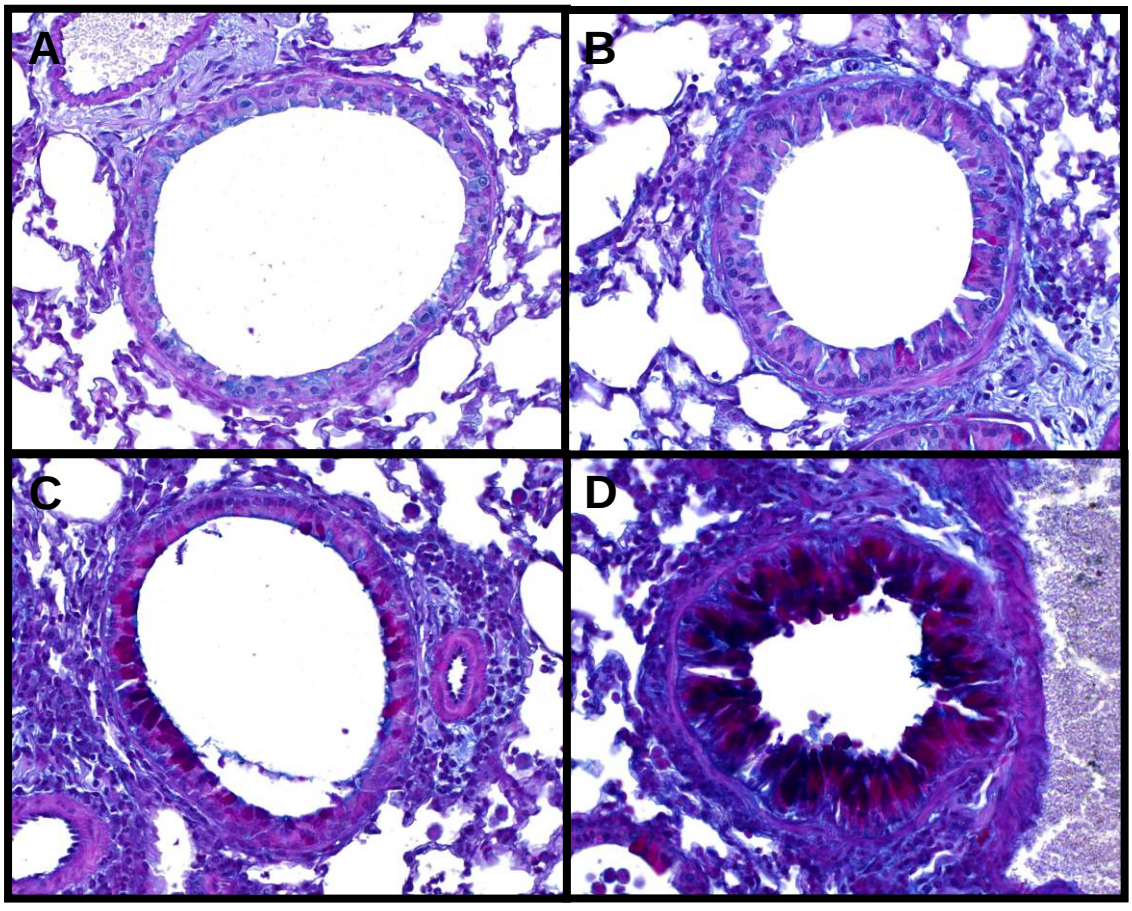


Figure 2.1 Goblet cell scoring. Representative images of bronchioles scoring 0 (A), 1 (B), 2 (C) and 3 (D); original magnification x400.

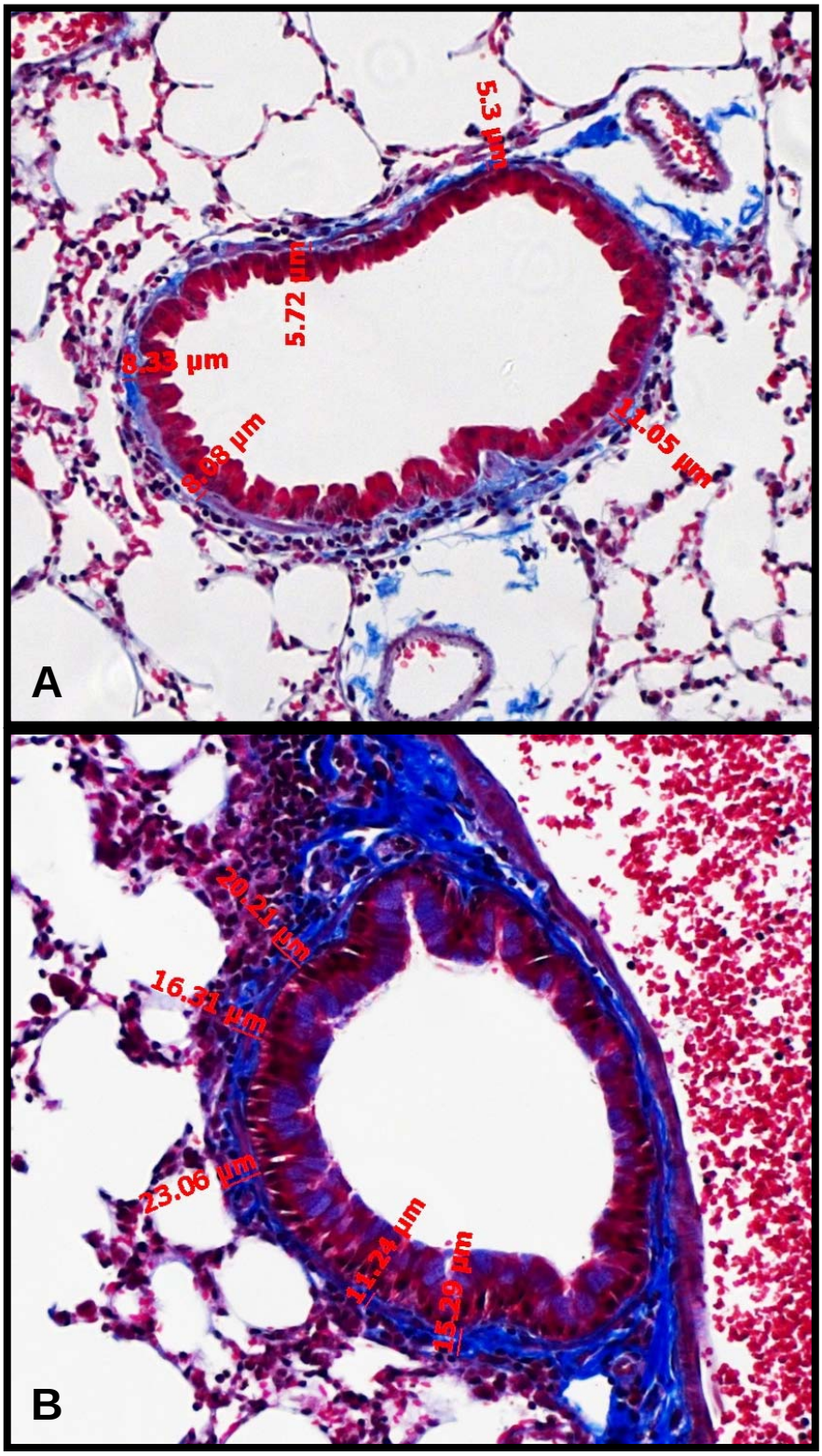


Figure 2.2 Measurement of peribronchial collagen. Representative of bronchioles from sham (A) and HDM mice (B), showing collagen depth measurements; original magnification x200.

2.10.2 Frozen sections

Left lobes were inflated with 1:1 optimum cutting temperature formulation (OCT):PBS via a tracheal cannula, excised, mounted on a cork bed and frozen in isopentane over liquid nitrogen. Blocks were stored at -80ºC until required for staining. 6µm sections were cut and stained according to the immunofluorescence staining protocol below (2.10.4).

2.10.3 BAL cytospins

50-100µl BAL was loaded into disposable cassettes and spun onto slides by cytocentrifugation (190g, 1min). Slides were air-dried for 30min, fixed with 2-3 drops of ICC fixative (BD Biosciences, Oxford, UK; 550010) then washed in tris-buffered saline (TBS; 2 x 5min). After air-drying over night slides were foil wrapped and stored at -80ºC until required for staining.

2.10.4 Immunofluorescence

Lung sections were fixed with 4% paraformaldehyde for 10min, rinsed in PBS and permeabilised in blocking buffer (TBS + 0.3% Triton X100 (Sigma-Aldrich, Dorset, UK; X100) + 10% normal donkey serum (Jackson ImmunoResearch, West Grove, USA; 017-000-121) + 1% BSA (Jackson ImmunoResearch, West Grove, USA; 001-000-162) + 1% normal mouse serum) for 1 hour, RT. After tipping off the buffer, primary antibodies or controls (Table 2.3) were added onto the slides and incubated overnight, 4 ºC. All antibodies were diluted in blocking buffer. Slides were washed 3 times in wash buffer (TBS + 0.3% Triton X100) followed by 2 washes in TBS (3min/wash) then incubated in fluorochrome conjugated secondary antibodies (Table 2.3) for 1 hour in the dark, RT. Slides were washed in wash buffer and TBS as above, incubated in 600nM 4',6-diamidino-2-phenylindole dilactate (DAPI; Invitrogen, Paisley, UK; D3571) for 5min then rinsed twice in PBS. Slides were mounted using ProLong Gold antifade reagent (Invitrogen, Paisley, UK; P36930) for imaging on a Leica SP5 (10x oil/0.4NA).

Antibody specificity	Format	Working concentration	Supplier	Catalogue no.
IL-13Rα1	Goat pAb	2μg/ml	Santa Cruz Biotechnology	sc-27861
control	Goat pAb	2μg/ml	R&D Systems	AB-108-C
IL-13Rα2	Goat pAb	1 - 4μg/ml	R&D Systems	AF539
control	Goat pAb	1 - 4μg/ml	R&D Systems	AB-108-C
MOMA-2	Rat mAb	2 - 10μg/ml	AbD Serotec	MCA519G
control	Rat mAb	2 - 10μg/ml	R&D Systems	MAB006
CD68	Rat mAb	1 - 4μg/ml	AbD Serotec	MCA1957
control	Rat mAb	1 - 4μg/ml	R&D Systems	MAB006
Secondaries				
Rat	Cy3 F(ab')$_2$	1 in 250	Jackson ImmunoResearch	712-166-153
Goat	Cy5 F(ab')$_2$	1 in 250	Jackson ImmunoResearch	705-176-147

Table 2.3 Antibodies used for immunofluorescence. Suppliers: Santa Cruz Biotechnology, Santa Cruz, USA; R&D Systems, Abingdon, UK; AbD Serotec, Kidlington, UK; Jackson ImmunoResearch, West Grove, USA.

2.11 cDNA Synthesis and real-time PCR

Real-time PCR was used to quantify expression of muc5ac, IL-13, IL-13Rα1, IL-13Rα2 and IL-4Rα mRNA in lung tissue. The medial lobe, preserved in RNAlater, was homogenised and total RNA isolated using RNeasy Plus Mini Kits (Qiagen, Crawley, UK; 74104) according to the manufacturer's instructions. Genomic DNA was eliminated using gDNA eliminator columns included in the kit. 1μg of total RNA (quantified by spectrophotometry) was reverse transcribed using TaqMan Reverse Transcription Reagents (Applied Biosystems, Warrington, UK; N8080234) containing MultiScribe Reverse Transcriptase and random hexamers as primers. The samples were incubated at 25ºC for 10 minutes to allow hexamer binding, 37ºC for 60 minutes for the reverse transcription followed by 95ºC for enzyme inactivation. Specific cDNA was detected by pre-designed probes from Applied Biosystems (Warrington, UK; Table 2.4). TaqMan Eukaryotic 18S rRNA Endogenous Control (Applied Biosystems, Warrington, UK; 4333760F) was used as an internal calibrator. 10μl real-time PCR reactions were performed in a 7900HT Fast Real-Time PCR System (Applied Biosystems, Warrington, UK) using TaqMan Universal PCR Master Mix (Applied Biosystems, Warrington, UK; 4304437). Relative gene expression levels were calculated using the Comparative C_T ($\Delta\Delta C_T$) method (Livak & Schmittgen, 2001) and results expressed as fold change in expression relative to sham mice ($2^{-\Delta\Delta C_T}$).

mRNA	TaqMan Gene Expression Assay I.D. Number
muc5ac	Mm01276725_g1
IL-13	Mm00434204_m1
IL-13Rα1	Mm00446729_m1
IL-13Rα2	Mm00515166_m1
IL-4Rα	Mm00439634_m1

Table 2.4 Probes used for real-time PCR. All probes were sourced from Applied Biosystems, Warrington, UK.

2.12 Statistical Analysis

3-11 mice per group were used in all experiments. Experiments were performed once only, unless otherwise stated. Data are expressed as single data points with bars representing group medians, unless otherwise stated. Statistical significance was determined by Mann Whitney test where 2 groups are compared or non-parametric one-way analysis of variance (Kruskal-Wallis ANOVA) with Dunn's post test where analysis of more than two groups was required. Statistically significant differences are denoted by asterisks whereby * $p<0.05$, ** $p<0.01$ and *** $p<0.001$. Graph generation and statistical analyses were performed using GraphPad Prism (version 5, USA).

3. CHARACTERISATION OF HDM INDUCED AAD

3.1 Introduction

Animal models used to replicate the features of asthma have focussed on inducing a Th2 response and AHR in the lungs, but rarely recapitulate the frequency of allergen exposure and hence chronicity of airway inflammation seen in patients. The most commonly used animal model of AAD uses the relatively innocuous protein OVA as an antigen. Exposure of the airways to OVA alone in naïve mice does not induce inflammation. Therefore to stimulate an immune response animals must first be sensitised to OVA by peripheral injection (usually i.p.) of OVA in the adjuvant alum prior to airway challenge with OVA. Although this induces a strong Th2 response, it does not reflect the likely allergen sensitisation pathway in man. Furthermore, continuous OVA challenge in sensitised mice can induce tolerance (Van Hove *et al.*, 2007). To mimic sensitisation to aeroallergens it is important that the first exposure to allergen is via the respiratory tract where local pulmonary antigen presenting cells (APC), rather than peritoneal APCs, will process the allergen and initiate a response accordingly. For this reason a relatively novel model of AAD induced by HDM was chosen in which to study mechanisms of allergic inflammation.

This mouse model of experimental asthma aims to replicate the persistence and chronicity of pulmonary inflammation in asthma by continuous exposure to a relevant aeroallergen, HDM (Johnson *et al.*, 2004). The allergenic properties of HDM negate the requirement for powerful chemical adjuvants such as alum. Chronic exposure of the airways to HDM elicits strong Th2 driven inflammation accompanied by airway remodelling, goblet cell hyperplasia and AHR. And importantly, this allergic response is stimulated by activation of lung epithelial cells and pulmonary dendritic cells; a mechanism that may be applicable to the provocation of asthma and hence may share subsequent mechanisms of pathophysiology (Hammad & Lambrecht, 2008).

HDM extract possesses multiple properties that promote allergic sensitisation, primarily via activation of airway epithelial cells and DCs. The proteolytic activity of Der p 1 and Der p 9 disrupts epithelial integrity by cleavage of tight junction proteins, thus allowing increased access between allergen and sub-epithelial DCs (Wan *et al.*, 1999). In addition these proteases can directly activate DCs and epithelial cells via PARs which polarise DCs to induced Th2 responses and stimulate the production of

Th2 cytokines and chemokines (Hammad & Lambrecht, 2008). Der p enzymes also cleave of various cell surface molecules such as DC-SIGN, CD40, CD25 and CD23 which further tilts the balance in favour of Th2 sensitisation. C-type lectins within the HDM cocktail attract DCs, via the production of CCL20 from epithelial cells, and induce production of cysteinyl leukotrienes (Nathan *et al.*, 2009;Barrett *et al.*, 2009). HDM extract also induces TLR4 signalling by containing contaminating LPS. Airway exposure to low level LPS promotes Th2, rather than Th1 responses (Eisenbarth *et al.*, 2002). In addition TLR4 expression may be stabilised by Der p 2, a functional homolog of MD-2 (Trompette *et al.*, 2009). Taken together, these observations demonstrate HDM is a potent inducer of Th2 immunity.

3.1.1 Aim

1. To establish the HDM induced model of AAD described by Johnson *et al.* with respect to expression of IL-13 (Johnson *et al.*, 2004).

The aim of this chapter was to establish the HDM induced model of AAD described by Johnson *et al.* with respect to IL-13 and draw parallels to the pathophysiology of clinical asthma (Johnson *et al.*, 2004). Furthermore, to assess the suitability of the model for investigating the role of IL-13 in AAD.

3.2 Methods

3.2.1 HDM exposure.

Male balb/c mice were exposed to 25μg intranasal HDM extract, 4 consecutive days per week for 1, 3 or 5 weeks according to Figure 3.1.

3.2.2 IL-13 Immunofluorescence staining.

Staining was conducted on BAL cytospins and frozen lung sections as Kim *et al.* with anti-IL-13 from R&D Systems (BAF413) and tyramide signal amplification (TSA) kit (Invitrogen T20933) (Kim *et al.*, 2008). Briefly, lung sections were fixed with 4% paraformaldehyde for 10min, rinsed in PBS and endogenous peroxidise activity quenched with peroxidise-blocking solution (Dako S2023) for 10min followed by a rinse in H_20 then TBS (5min). Endogenous biotin was blocked by sequential incubations with avidin solution (15min), TBS wash (5min) then biotin solution (15min; Vector, SP-2001) followed by two TBS washes (5min/wash). Sections were blocked with 2% gelatin (Sigma G7765) in blocking buffer (TBS + 0.1% saponin (Sigma S4521) + 5% normal goat serum (Jackson ImmunoResearch 005-000-121)) for 1 hour, RT. After tipping off the buffer, biotinylated goat anti-mouse IL-13 (BAF413) or biotinylated normal goat IgG control (BAF108, R&D Systems) were added onto the slides at 0.5-2μg/ml in blocking solution D and incubated overnight, 4ºC. Slides were washed 3 times in wash buffer (PBS + 0.1% saponin; 3min/wash) followed by incubation with HRP conjugate at 1 in 100 in blocking solution D for 45min in the dark, RT. Slides were washed in wash buffer as above, and incubated in tyramide solution at 1 in 100 in amplification buffer for 10min. Finally, slides were washed in wash buffer as above and incubated in 600nM DAPI (Invitrogen D3571) for 5min then rinsed twice in PBS. Slides were mounted using Prolong Gold Antifade (Invitrogen P3693) for imaging.

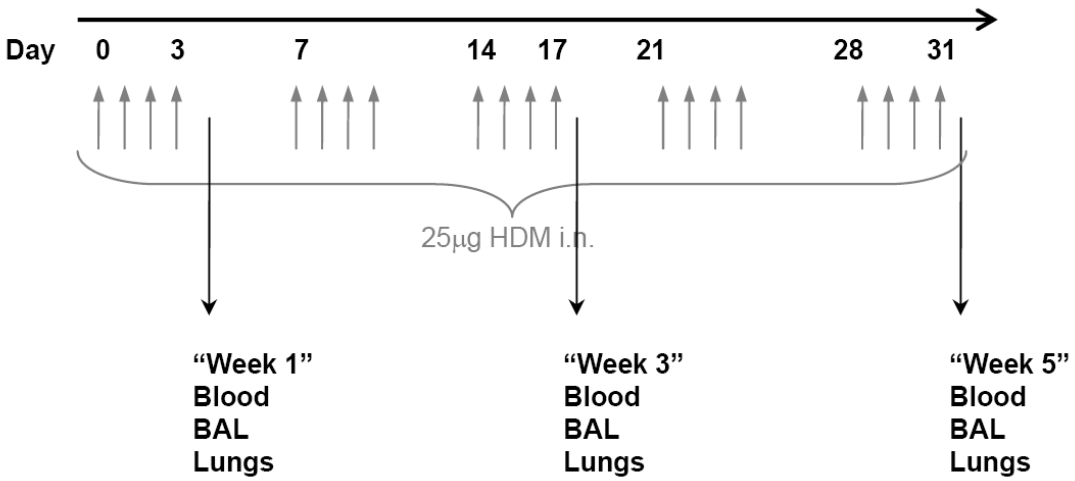


Figure 3.1 Experimental protocol for exposure to HDM. Mice were exposed to intranasal HDM on 4 consecutive days per week for 1, 3 or 5 weeks. Sham treated mice received intranasal saline alone. Mice were culled 4 or 24 hours after the final HDM exposure for collection of blood, BAL and lung samples.

3.3 Results

3.3.1 Chronic exposure to HDM induces AHR

As previously reported chronic exposure of the airways to HDM extract administered 5 times per week induces AHR to inhaled spasmogens such as MCh (Gregory *et al.*, 2009;Johnson *et al.*, 2004). The current exposure regime of 25μg HDM i.n. for 4 consecutive days per week did not induce AHR to MCh challenge after just one week of exposure (Figure 3.2 A-B). After 3 weeks of HDM exposure the decline in C_{dyn} in response to MCh challenge was enhanced compared to sham exposed control mice; however no changes in R_L were observed (Figure 3.2 C-D). Five weeks of HDM exposure provoked an exacerbated response to MCh challenge observed as elevated R_L and reduced C_{dyn} (Figure 3.2 E-F). Moreover, baseline lung function prior to methacholine exposure was impaired in mice exposed to HDM for 5 weeks compared to sham exposed mice (Figure 3.2 G-H). Changes in basal lung function were not observed after one or 3 weeks of HDM exposure (data not shown).

3.3.2 Chronic exposure to HDM induces pulmonary inflammation

Accumulation of eosinophils, neutrophils, CD4+ T cells and CD8+ T cells in BAL and lung tissue were quantified following repeated intranasal exposure to HDM. HDM induced eosinophilia was apparent after 3 and 5 weeks in both lung tissue and BAL however there was no change number of eosinophils compared to sham mice after just one week of exposure (Figure 3.3 A-B). Significant infiltration of neutrophils was detected in BAL at week 1 and continued to increase throughout the 5 week time-course with increased HDM exposure. Tissue neutrophilia was not apparent after one week of HDM; however 3 weeks of exposure induced significant neutrophilia which was further elevated at 5 weeks (Figure 3.3 C-D). HDM exposure induced accumulation of CD4+ and CD8+ T cells in BAL from week 1. The number of BAL CD4+ and CD8+ T cells was further elevated at weeks 3 and 5. Conversely, the number of tissue CD4+ and CD8+ T cells appeared slightly reduced at week 1 compared to sham treated mice however 5 weeks of HDM exposure induced significant CD4+ and CD8+ T cell accumulation in the lung tissue (Figure 3.3 E-H).

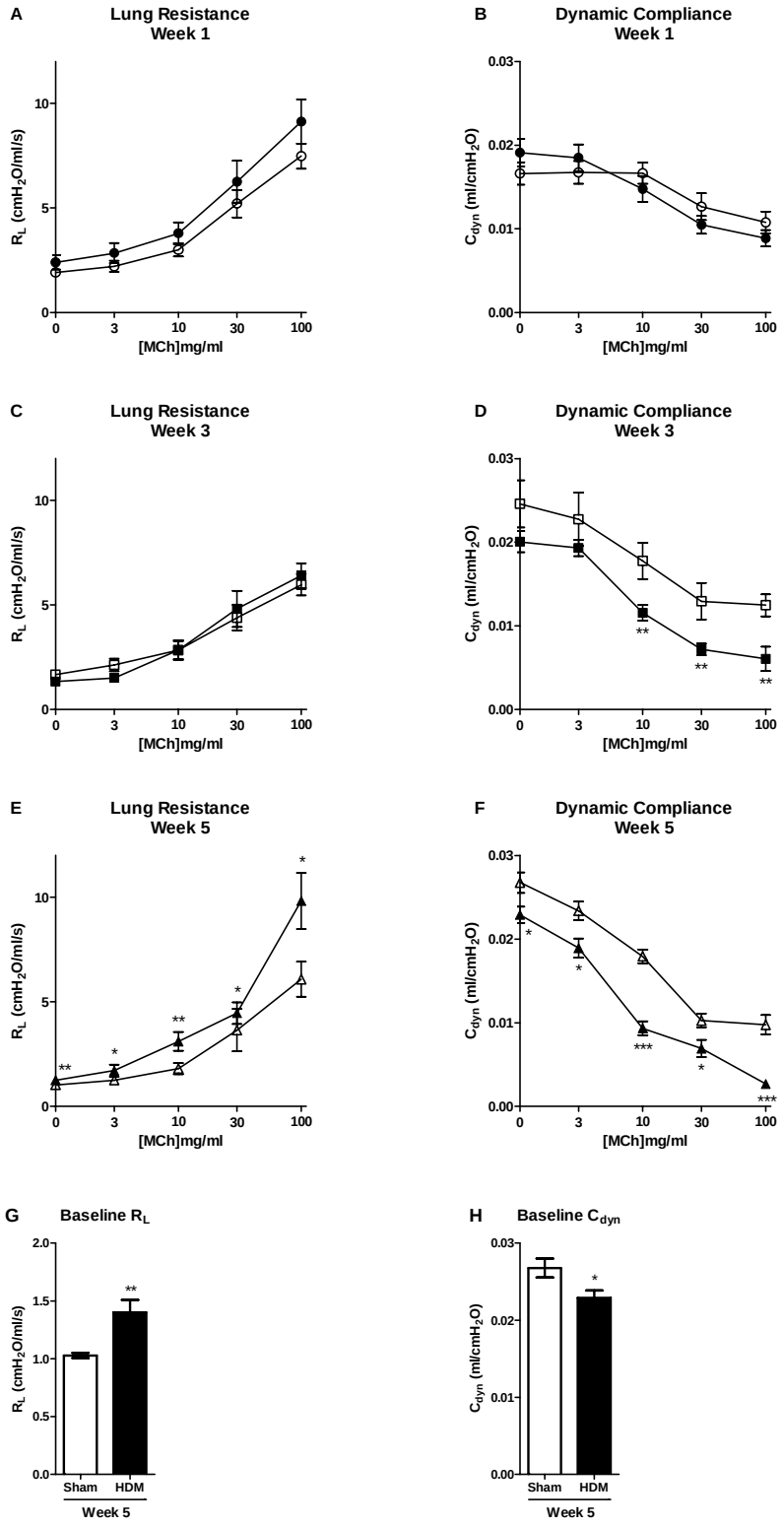


Figure 3.2 Chronic exposure to HDM induces AHR. AHR to MCh was determined as changes in lung resistance (R_L) (A, C, E and G) and dynamic compliance (C_{dyn}) (B, D, F and H) measured 24 hours post HDM. AHR was assessed after 1 (A-B), 3 (C-D) or 5 (E-H) weeks of HDM exposure. Open symbols represent saline exposed mice and closed symbols HDM exposed mice. (G-H) Baseline R_L (G) and C_{dyn} (H) after 5 weeks of HDM exposure. Data are shown as mean ± SEM, n = 6-8 mice/group. * p<0.05, ** p<0.01 and *** p<0.001 relative to saline group by Mann Whitney test.

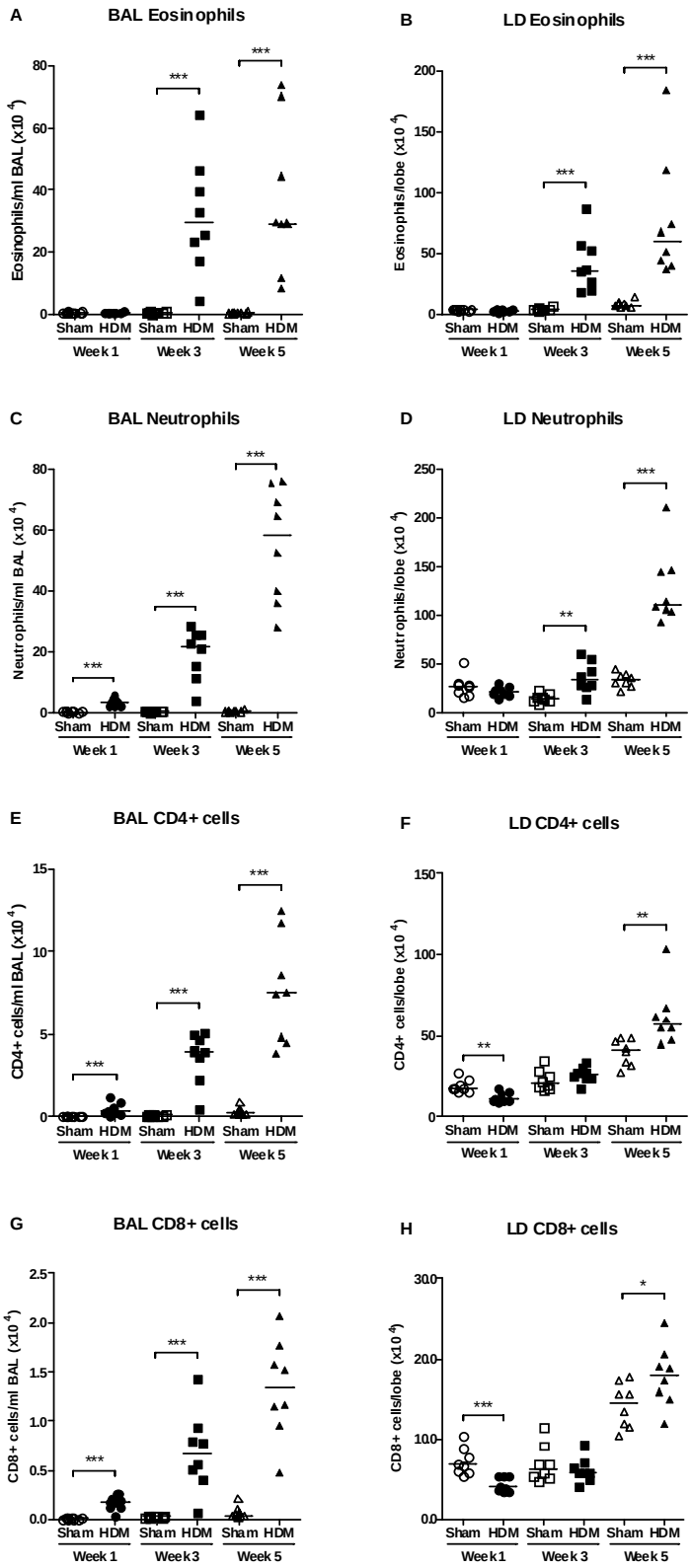


Figure 3.3 Chronic exposure to HDM induced pulmonary inflammation. BAL and lungs (caudal lobe) were taken after 1, 3 or 5 weeks of HDM exposure, 4 hours after the last HDM instillation. Eosinophils (A-B), neutrophils (C-D), CD4+ T cells (E-F) and CD8+ T cells (G-H) in BAL (A, C, E and G) and lung tissue digest (LD) (B, D, F and H) were identified and quantified by flow cytometry. n = 8 mice/group, bar represents median. * $p<0.05$, ** $p<0.01$ and *** $p<0.001$ relative to sham group by Mann Whitney test.

3.3.3 HDM induced pulmonary inflammation is Th2 biased

To further characterise HDM induced inflammation T-helper subsets within the BAL and tissue CD4+ T cell populations were identified and quantified. Th2 cells were defined by T1ST2 expression (Xu *et al.*, 1998;Lohning *et al.*, 1998); Th1 cells by intracellular IFNγ and Th17 cells by intracellular IL-17 expression. HDM exposure stimulated accumulation of all three T-helper subsets in BAL from week 1 which increased further with continued HDM exposure (Figure 3.4). However, the number of Th2 cells in BAL at weeks 3 and 5 were at least 2-fold greater than the number of Th1 or Th17 cells present. In lung tissue the number of Th2 cells was elevated above sham after 3 weeks of HDM exposure and further increased after 5 weeks. Contrary to the BAL, there were no significant changes in the number of Th1 cells in the lung tissue over the 5 week time-course. Accumulation of Th17 cells in lung tissue was modestly increased above sham after 3 weeks of exposure and further increased at week 5. In the lung tissue, as in BAL, the number of Th2 cells exceeds that of Th1 or Th17 cells indicating a predominant but not exclusively Th2 biased response to HDM exposure.

3.3.4 HDM induced cytokine profile

The cytokine milieu in the lung tissue was assessed to corroborate the inflammation observed after HDM exposure. Cytokine and chemokine concentrations in lung homogenate supernatants were measured by ELISA or MSD multiplex assay. In accordance with the predominant presence of Th2 cells identified above, the Th2 cytokines IL-4 and IL-5 were elevated above sham levels after 3 and 5 weeks of HDM exposure (Figure 3.5 A-B). Similarly, modest increases in IL-17 were detected after 3 and 5 weeks of HDM exposure which are likely to reflect the accumulation of Th17 cells at the same time points (Figure 3.5 C). Low levels of IFNγ were measured above sham at week 5 which may be linked with the low level presence of Th1 cells at this time point (Figure 3.5 D). However, high concentrations of IL-12 were measured in the tissue after one week of HDM exposure. HDM induced IL-12 concentrations diminish slightly after week 1 but remain elevated at weeks 3 and 5 (Figure 3.5 E). Interestingly, the regulatory cytokine IL-10 was induced by HDM, but not before 5 weeks of exposure (Figure 3.5 F).

The eosinophil chemoattractant eotaxin was elevated in LH after 3 and 5 weeks of HDM exposure (Figure 3.6 A), corresponding to the presence of eosinophils in the lungs at the same time points. However, in BAL a significant increase in eotaxin above sham was only observed at 3 weeks of HDM exposure (Figure 3.6 B). The neutrophil chemoattractant KC was elevated in LH at 3 and 5 weeks (Figure 3.6 C) indicative of the tissue neutrophilia observed after 3 and 5 weeks of HDM exposure. In BAL, significant increases in KC were observed at weeks 1, 3 and 5 (Figure 3.6 D).

No changes were observed in concentrations of the epithelial derived cytokines IL-25 or TSLP after HDM exposure; however IL-33 was significantly elevated at week one and further increased at each time point (Figure 3.7).

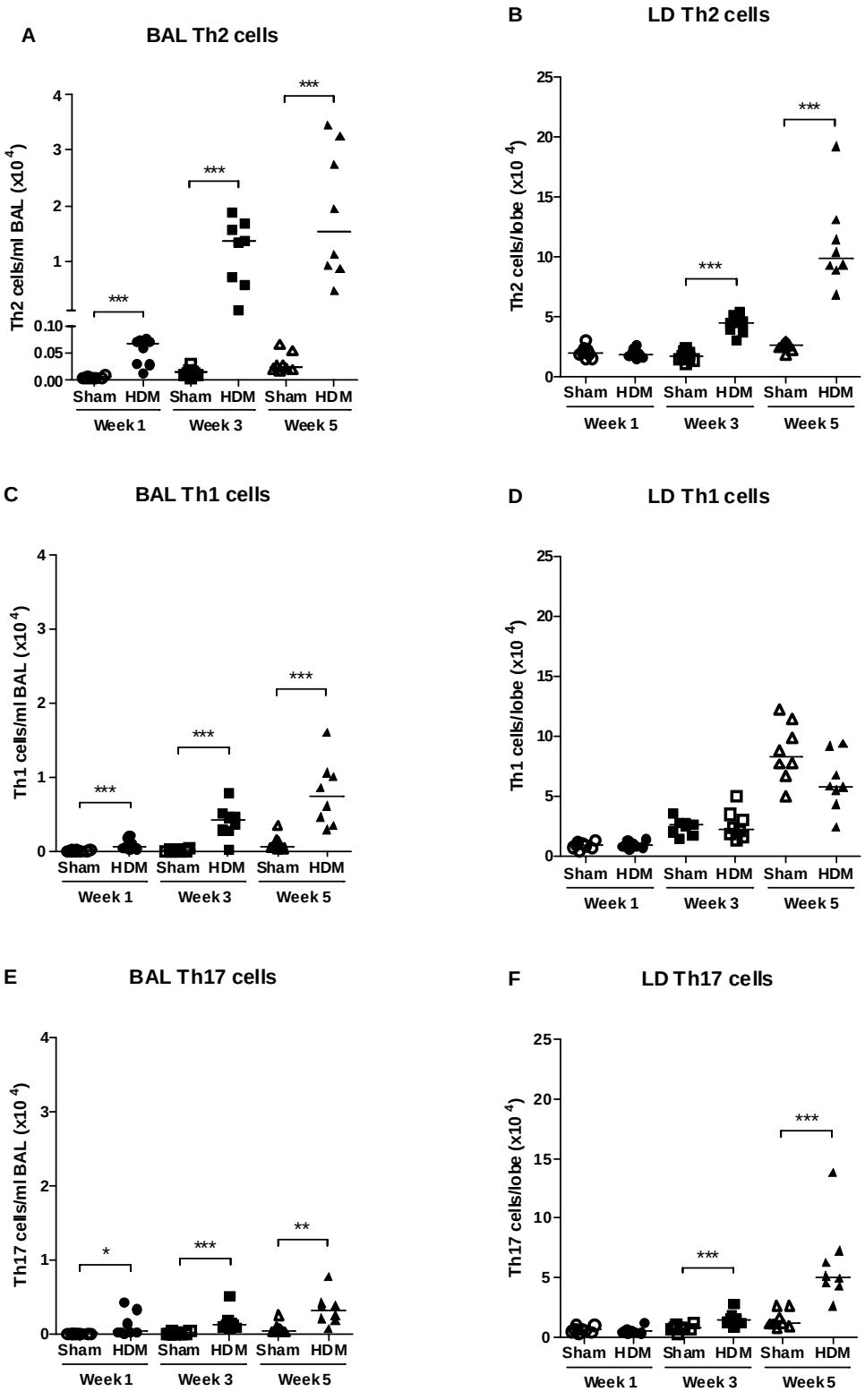


Figure 3.4 Chronic exposure to HDM induces a predominant Th2 response. BAL and lungs (caudal lobe) were taken after 1, 3 or 5 weeks of HDM exposure, 4 hours after the last HDM instillation. Th2 (A, B), Th1 (C, D) and Th17 cells (E, F) in BAL (A, C and E) and lung tissue digest (LD) (B, D and F) were identified and quantified by flow cytometry. n = 8 mice/group, bar represents median. * $p<0.05$, ** $p<0.01$ and *** $p<0.001$ relative to sham group by Mann Whitney test.

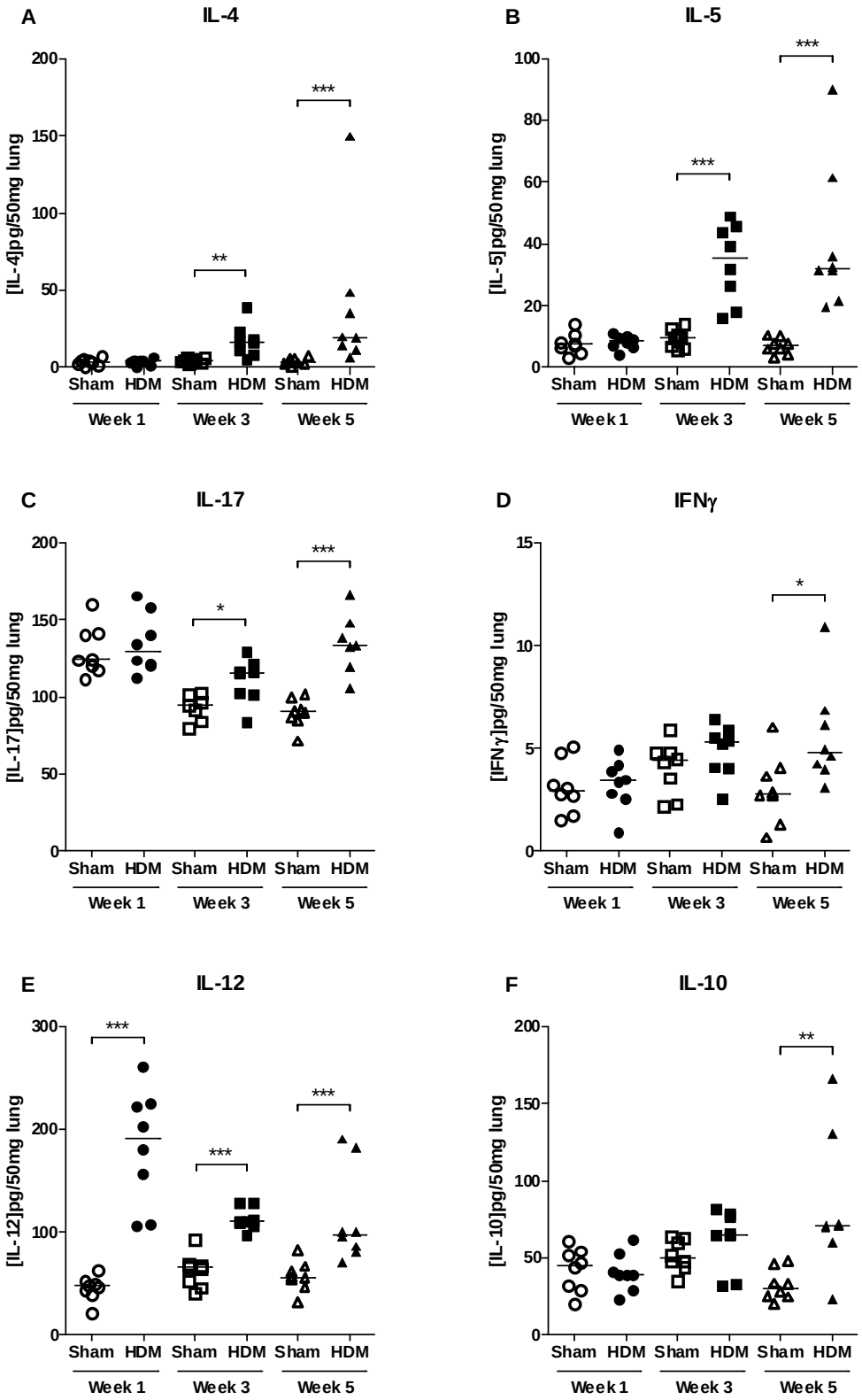


Figure 3.5 Induction of T cell cytokines following HDM exposure. Lungs (cranial lobe) were taken after 1, 3 or 5 weeks of HDM exposure, 4 hours after the last HDM instillation. Cytokines were quantified in lung homogenate supernatant by MSD assay (A-B, D-F) or ELISA (C). n = 7-8 mice/group, bar represents median. * $p<0.05$, ** $p<0.01$ and *** $p<0.001$ relative to sham group by Mann Whitney test.

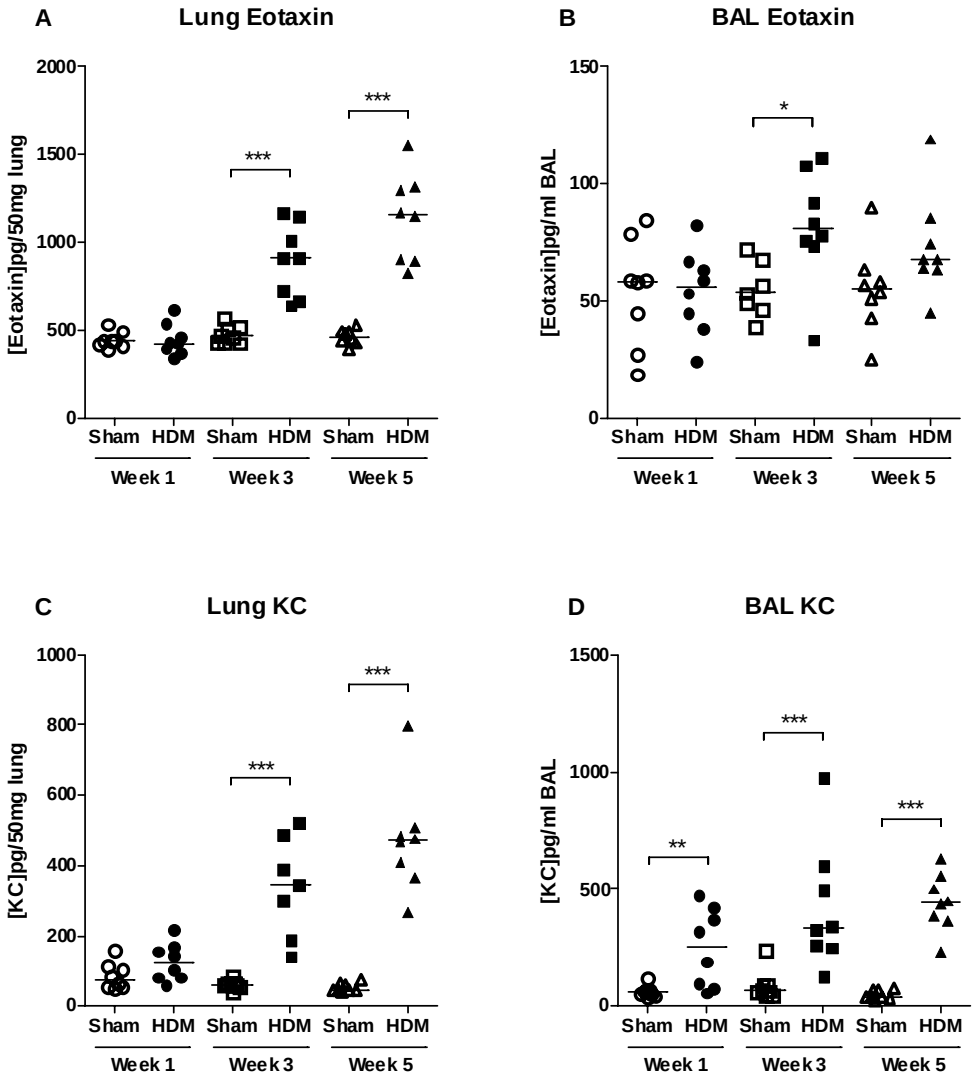


Figure 3.6 HDM induced chemokine expression. Lungs (cranial lobe) and BAL were taken after 1, 3 or 5 weeks of HDM exposure, 4 hours after the last HDM instillation. Chemokines were quantified in lung homogenate and BAL supernatant by ELISA (A-B) or MSD assay (C-D). n = 7-8 mice/group, bar represents median. * $p<0.05$, ** $p<0.01$ and *** $p<0.001$ relative to sham group by Mann Whitney test.

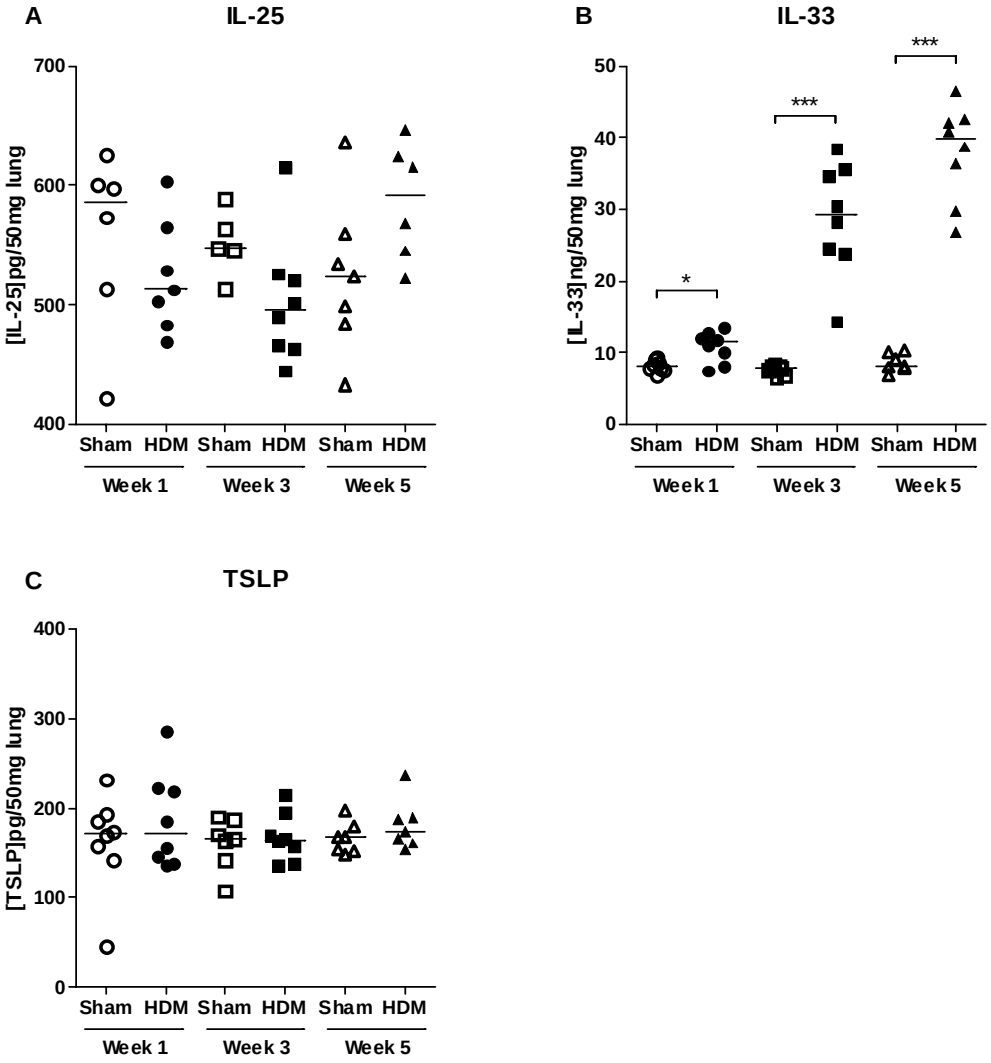


Figure 3.7 Expression of epithelial derived cytokines following HDM exposure. Lungs (cranial lobe) were taken after 1, 3 or 5 weeks of HDM exposure, 4 hours after the last HDM instillation. Cytokines were quantified in lung homogenate supernatant by ELISA. n = 5-8 mice/group, bar represents median. * $p<0.05$ and *** $p<0.001$ relative to sham group by Mann Whitney test.

3.3.5 HDM induced antibody production

Total serum IgE was assessed by ELISA to indicate the presence of an allergic response. Total serum IgE titres were elevated after 5 weeks of HDM exposure (Figure 3.8 A). In addition HDM specific antibodies in the serum were measured by ELISA to gauge antigen specificity of the HDM induced inflammatory response. HDM specific IgE, IgG1, IgG2a and IgG2b were detected after 3 weeks of HDM exposure and titres further increased after 5 weeks of HDM exposure (Figure 3.8 B-E). This confirms the presence of an antigen specific, adaptive immune response after 3 weeks of chronic exposure to HDM.

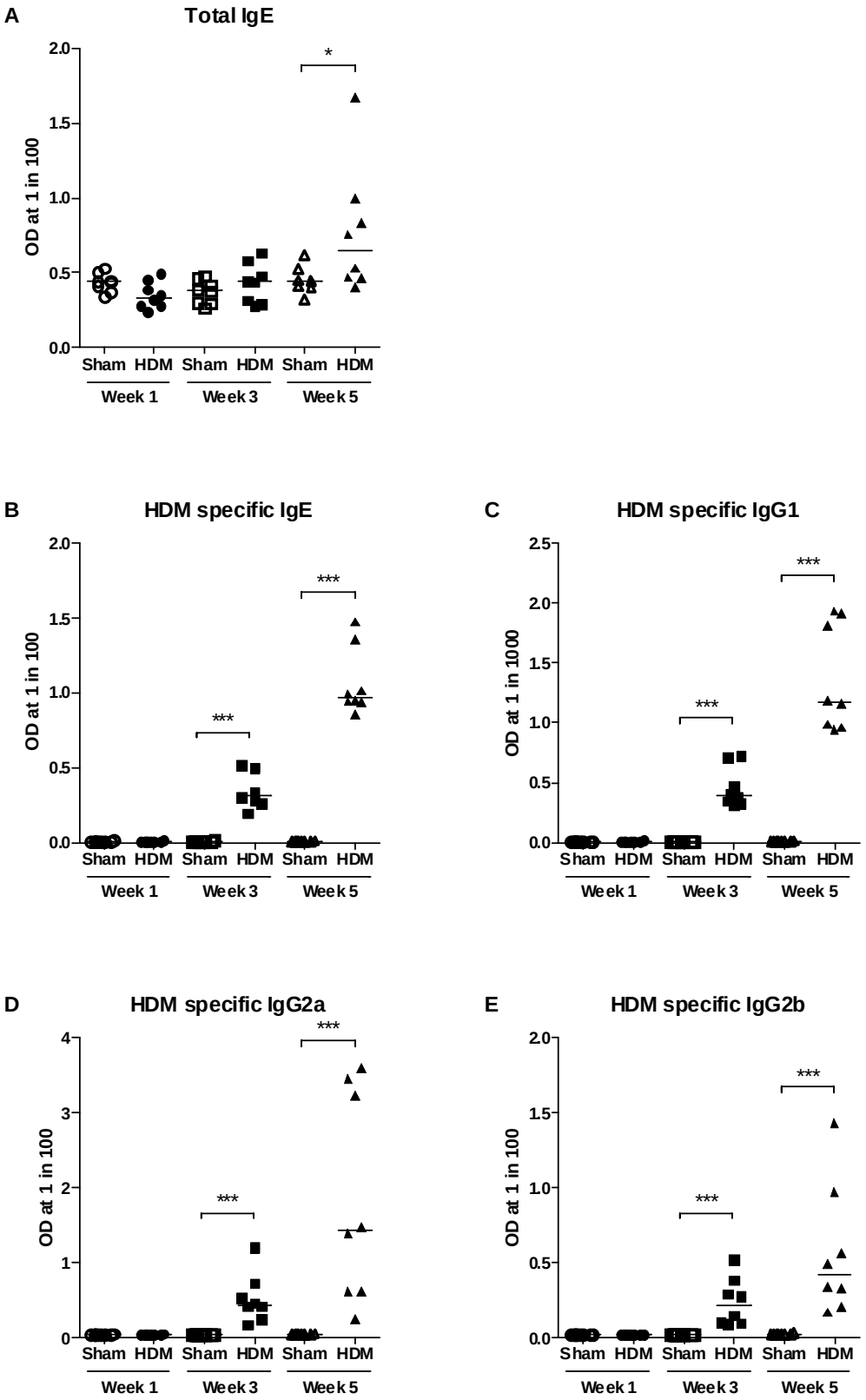


Figure 3.8 Generation of IgE and HDM specific antibodies following HDM exposure. Blood was taken via cardiac puncture after 1, 3 or 5 weeks of HDM exposure, 4 hours after the last HDM instillation. Total IgE (A) and HDM specific IgE (B), IgG1 (C), IgG2a (D) and IgG2b (E) were assessed in serum by ELISA. n = 8 mice/group, bar represents median. * $p<0.05$ and *** $p<0.001$ relative to sham group by Mann Whitney test.

3.3.6 HDM induced airway remodelling

Prolonged airway inflammation is proposed to lead to structural changes in the airways such as goblet cell hyperplasia/metaplasia and increased collagen deposition. Goblet cell frequency was assessed histologically in AB/PAS stained sections and scored accordingly. Increased goblet cell frequency was apparent after 3 and 5 weeks of HDM exposure (Figure 3.9 A-E). In addition, muc5ac mRNA expression in lung tissue was determined by real time PCR. Muc5ac expression was significantly elevated at weeks 3 and 5 after HDM exposure corroborating goblet cell up-regulation at these time points (Figure 3.9 F).

Peribronchial collagen depth was measured in Masson's trichrome stained sections. Significant collagen deposition was detected as early as one week after HDM exposure. This was further elevated at week 3 and 5 following HDM exposure (Figure 3.10).

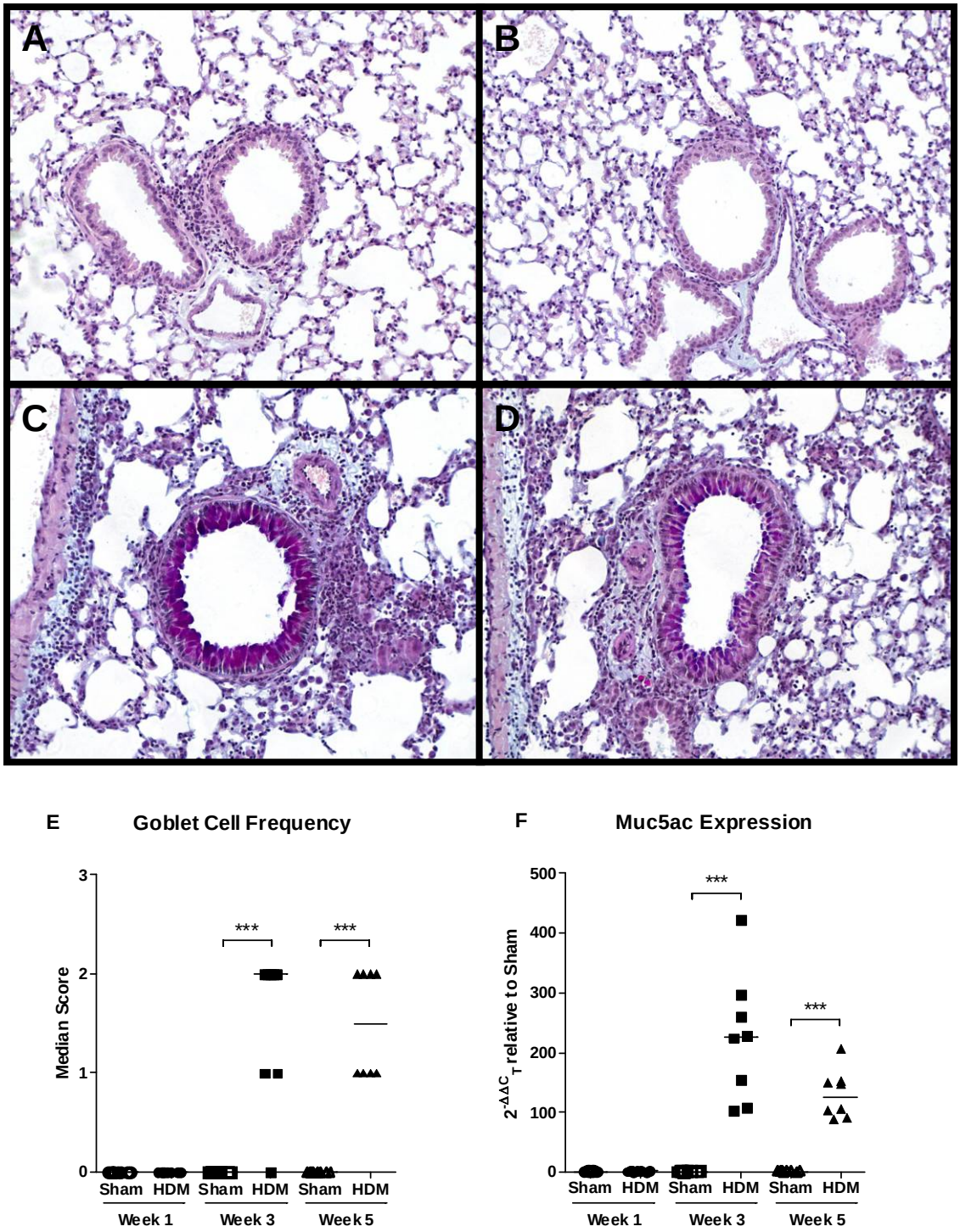


Figure 3.9 Up-regulation of mucus production following HDM exposure. Lungs were taken after 1, 3 or 5 weeks of HDM exposure, 4 hours after the last HDM instillation. (A-D) representative photomicrographs of airway sections stained with AB/PAS from mice exposed to saline (A) or HDM for 1 (B), 3 (C) or 5 (D) weeks; original magnification x200. (E) Goblet cell frequency was scored in AB/PAS stained sections. (F) Muc5ac mRNA in lung tissue was quantified by RT-PCR and normalised to sham. n = 7-8 mice/group, bar represents median. *** $p<0.001$ relative to sham group by Mann Whitney test.

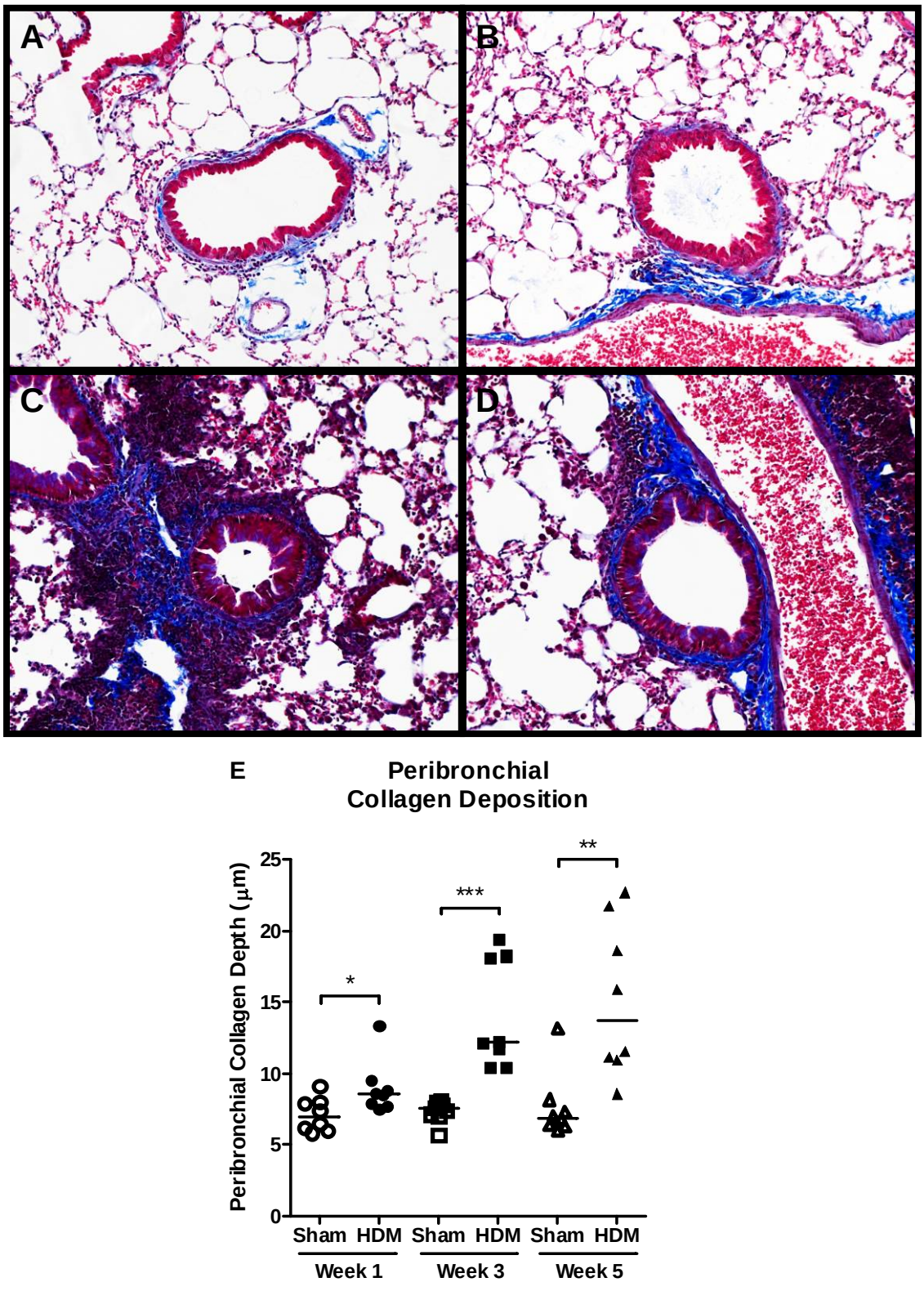


Figure 3.10 Chronic exposure to HDM induces peribronchial collagen deposition. Lungs were taken after 1, 3 or 5 weeks of HDM exposure, 4 hours after the last HDM instillation. (A-D) representative photomicrographs of airway sections stained with Masson's trichrome from mice exposed to saline (A) or HDM for 1 (B), 3 (C) or 5 (D) weeks; original magnification x200. (E) Peribronchial collagen depth was measured in Masson's trichrome stained sections. n = 8 mice/group, bar represents median. * $p<0.05$, ** $p<0.01$ and *** $p<0.001$ relative to sham group by Mann Whitney test.

3.3.7 HDM exposure up-regulates IL-13

Repeated exposure of the airways to HDM induced significant IL-13 mRNA up-regulation in the lung tissue evident from week 1 of exposure. IL-13 mRNA was 5.4 fold greater than sham treated mice after one week of HDM exposure and further elevated to over 500-fold greater than sham at weeks 3 and 5 (Figure 3.11 A). In addition elevated concentrations of IL-13 protein were detected in lung tissue after 3 and 5 weeks of HDM exposure. However no significant increases in IL-13 were detected in BAL supernatants from HDM exposed mice compared to sham at the time points assessed in this study.

Immunofluorescence (IF) staining of the lung tissue and BAL cells was employed to reveal potential sources of IL-13 in the lungs. No specific IL-13 signal could be detected in the tissue or BAL. High background staining was observed in epithelial cells and subsets of lung parenchyma cells (Figure 3.12) and in BAL cells (Figure 3.13). This was observed even in the absence of primary control antibodies and hence is likely to result from the signal amplification kit used. A variety of anti-IL-13 antibodies, in the presence or absence of signal amplification, were tested however no specific IL-13 signal could be detected.

Alternatively, intracellular IL-13 staining of inflammatory cells in the lung digest was conducted in order to identify IL-13 expressing cells after HDM exposure. IL-13 was detected in CD4+ T cells following *ex vivo* stimulation; shown as a shift in fluorescence compared to isotype control (Figure 3.14 A-C). Following one week of HDM exposure there was no differences in the mean fluorescence intensity (MFI) of IL-13 staining in CD4+ cells, or the frequency of IL-13+ cells within the CD4+ population. However, the number of IL-13+ CD4+ T cells was slightly diminished in HDM exposed mice compared to sham. At week 3, the intensity of IL-13 staining was greater in CD4+ cells from HDM exposed mice than sham mice, although the percentage of IL-13+ cells within the CD4+ population was higher in sham mice. No differences were observed in the number of IL-13+ CD4+ T cells after 3 weeks of HDM exposure compared to sham. After 5 weeks of HDM exposure, IL-13 MFI and the number of IL-13+ CD4+ T cells were equivalent to sham, however the frequency of IL-13+ cells within the CD4+ population was greater in sham mice compared to HDM exposed (Figure 3.14 D-F).

Low levels of IL-13 staining were also detected in CD8+ T cells following *ex vivo* stimulation (Figure 3.15 A). One week of HDM exposure had no effect on the MFI of IL-13 staining, proportion of IL-13+ CD8+ cells or the number of IL-13+ CD8+ T cells. Following 3 weeks of HDM exposure the intensity of IL-13 staining in CD8+ cells was elevated however, both the percentage of IL-13+ CD8+ cells and the number of IL-13+ CD8+ cells was diminished compared to sham. At week 5, no differences in IL-13 MFI or the number of IL-13+ CD8+ T cells were observed between sham and HDM exposures, although the proportion of IL-13+ cells within the CD8+ population was greater in sham than HDM exposed mice (Figure 3.15 B-D).

Analysis of IL-13 expression specifically in Th2 cells revealed the intensity of IL-13 staining was significantly higher in HDM mice than sham mice after 3 and 5 weeks of exposure (Figure 3.16 A-B). Due to the very low levels of Th2 cells in LD from sham mice, calculation of the percentage and number of IL-13 expressing cells within this population was not deemed valid. However, IL-13+ Th2 cells were present in LD from HDM exposed mice and increased in both proportion and number with length of HDM exposure (Figure 3.16 C-D).

In addition to T cells, IL-13 was detected in neutrophils and eosinophils in the lungs. After 5 weeks of HDM exposure, the numbers of IL-13+ neutrophils and eosinophils were significantly greater in the lungs of HDM exposed mice compared to sham exposed mice (Figure 3.17).

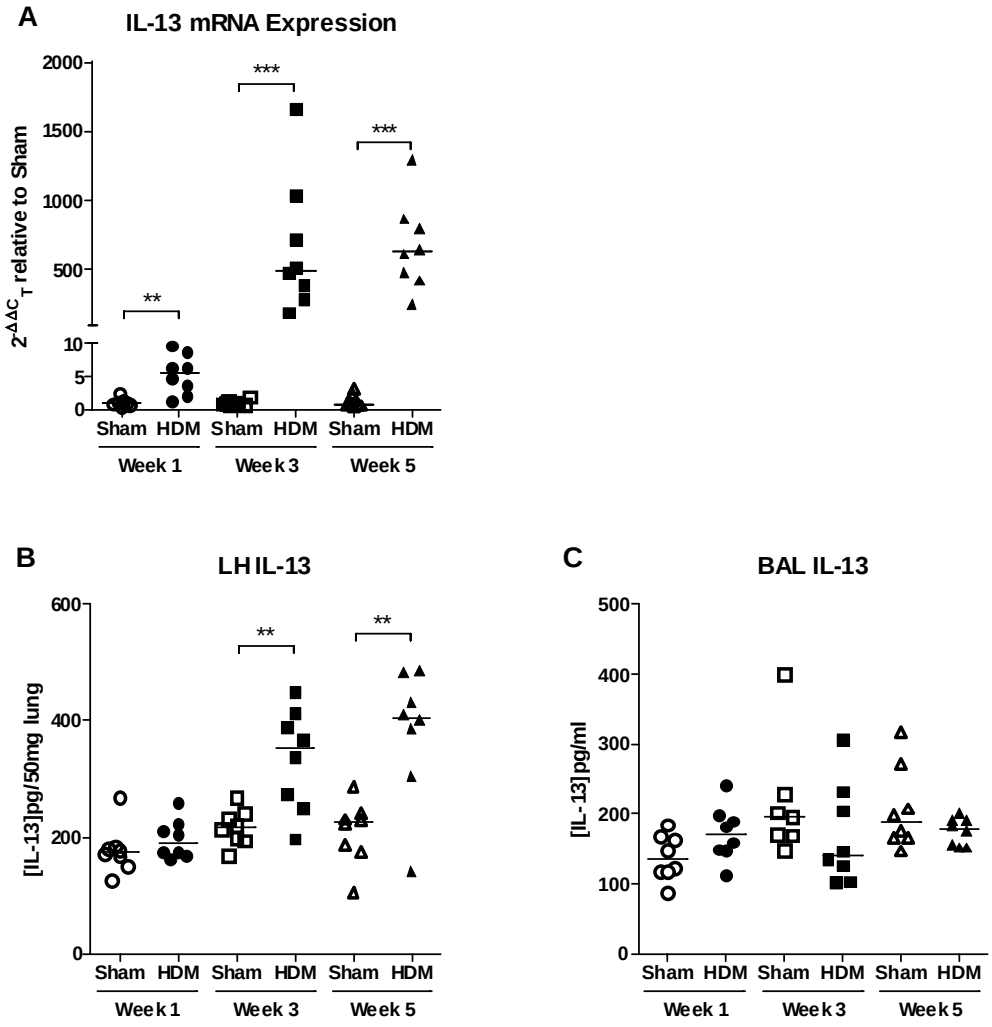


Figure 3.11 IL-13 expression following chronic HDM exposure. Lungs were taken after 1, 3 or 5 weeks of HDM exposure, 4 hours after the last HDM instillation. (A) IL-13 mRNA in lung tissue was quantified by real time PCR and normalised to sham. IL-13 protein was quantified in lung homogenate supernatant (B) and BAL (C) by ELISA. n = 7-8 mice/group, bar represents median. ** p<0.01 and *** p<0.001 relative to sham group by Mann Whitney test.

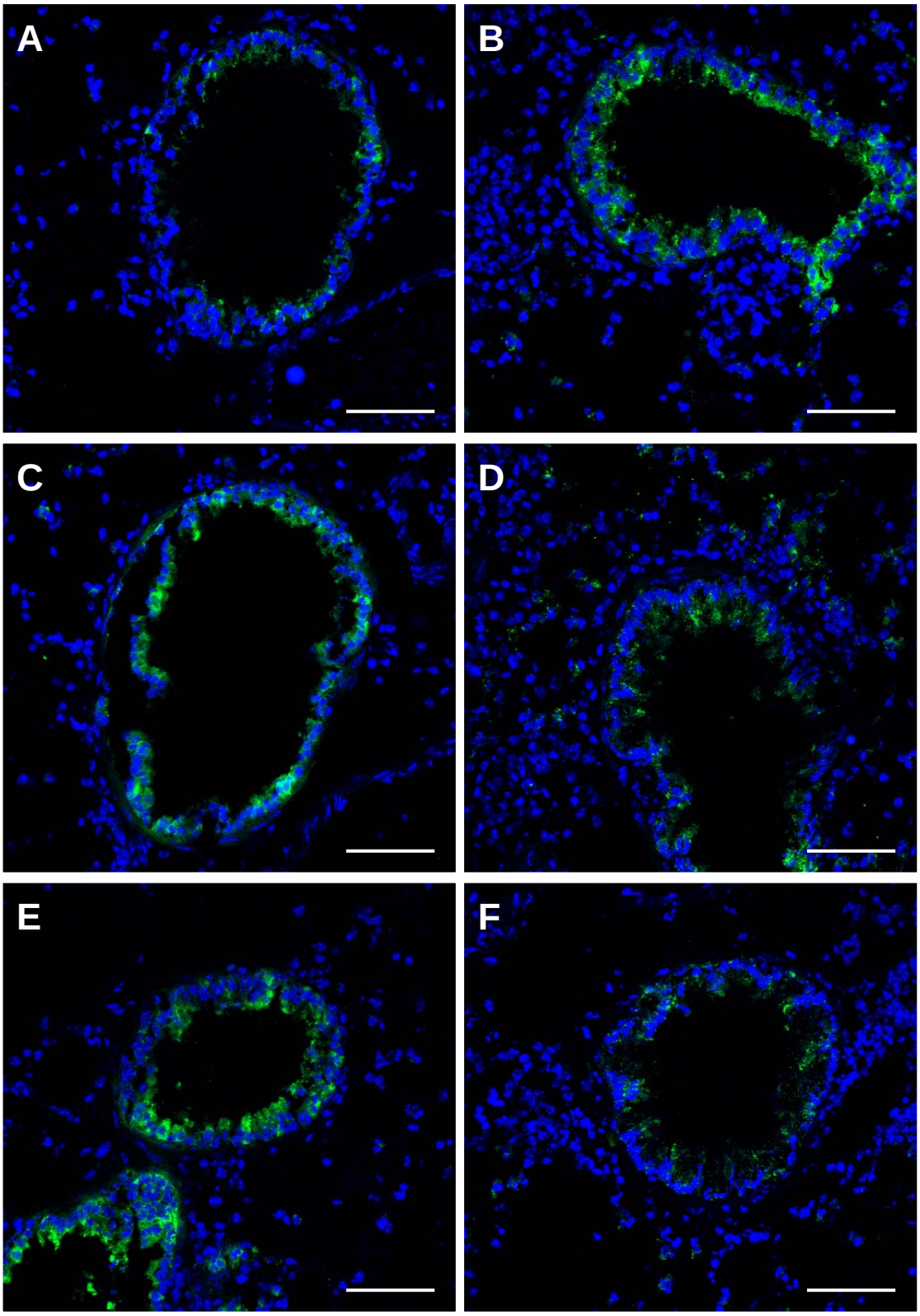


Figure 3.12 Non-specific IL-13 staining in the lungs following exposure to HDM. Lungs were taken after 5 weeks of HDM exposure, 24 hours after the last HDM instillation. Green indicates IL-13 staining and blue is DAPI. Representative images of lungs stained with IL-13 (A, B), isotype control (C, D) or no primary antibody (E, F) from sham (A, C, E) and HDM (B, D, F) exposed mice. Scale bar represents 75μm.

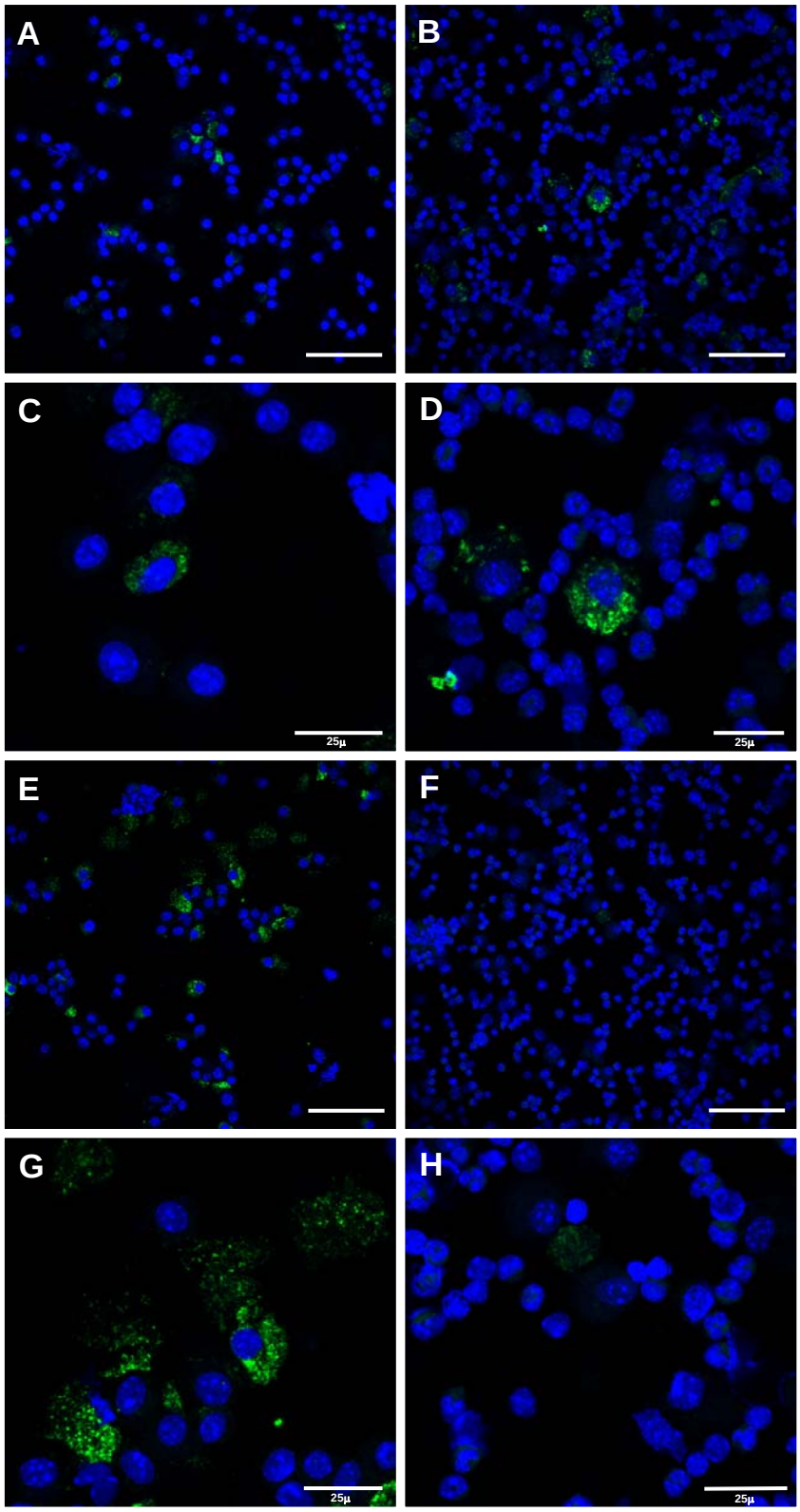


Figure 3.13 Non-specific IL-13 staining in BAL following exposure to HDM. Cytospin slides were generated from BAL. BAL was taken after 5 weeks of HDM exposure, 24 hours after the last HDM instillation. Green indicates IL-13 staining and blue is DAPI. Representative images of BAL from sham (A, C, E, G) and HDM (B, D, F, H) exposed mice. BAL was stained with IL-13 (A-D) or isotype control (E-H). (C), (D), (G) and (H) depict further magnified images of (A), (B), (E) and (F), respectively. Scale bar represents 75µm, unless stated.

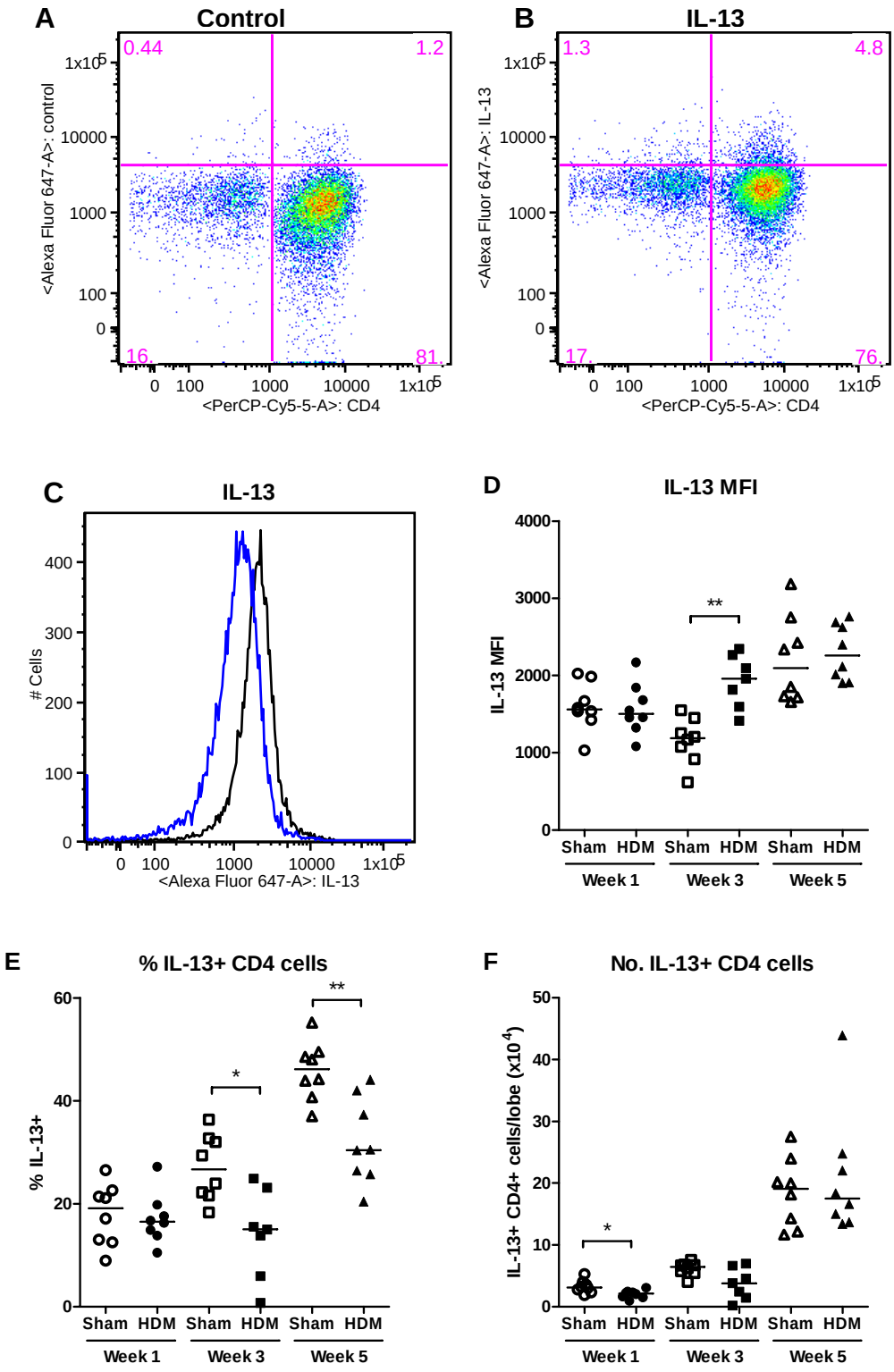


Figure 3.14 IL-13 expression in CD4+ cells following chronic HDM exposure. Lungs were taken 4 hours after the last HDM instillation. (A-B) Representative plots of CD4+ T cells stained with anti-CD4 and intracellular IL-13 (B) or isotype control (A) at week 5. (C) Representative histogram of intracellular IL-13 staining (black line) and isotype control (blue line) in CD4+ T cells at week 5. MFI (D), % (E) and number (F) of IL-13+ CD4+ T cells, identified and quantified by flow cytometry. n = 7-8 mice/group, bar represents median. * $p<0.05$ and ** $p<0.01$ relative to sham group by Mann Whitney test.

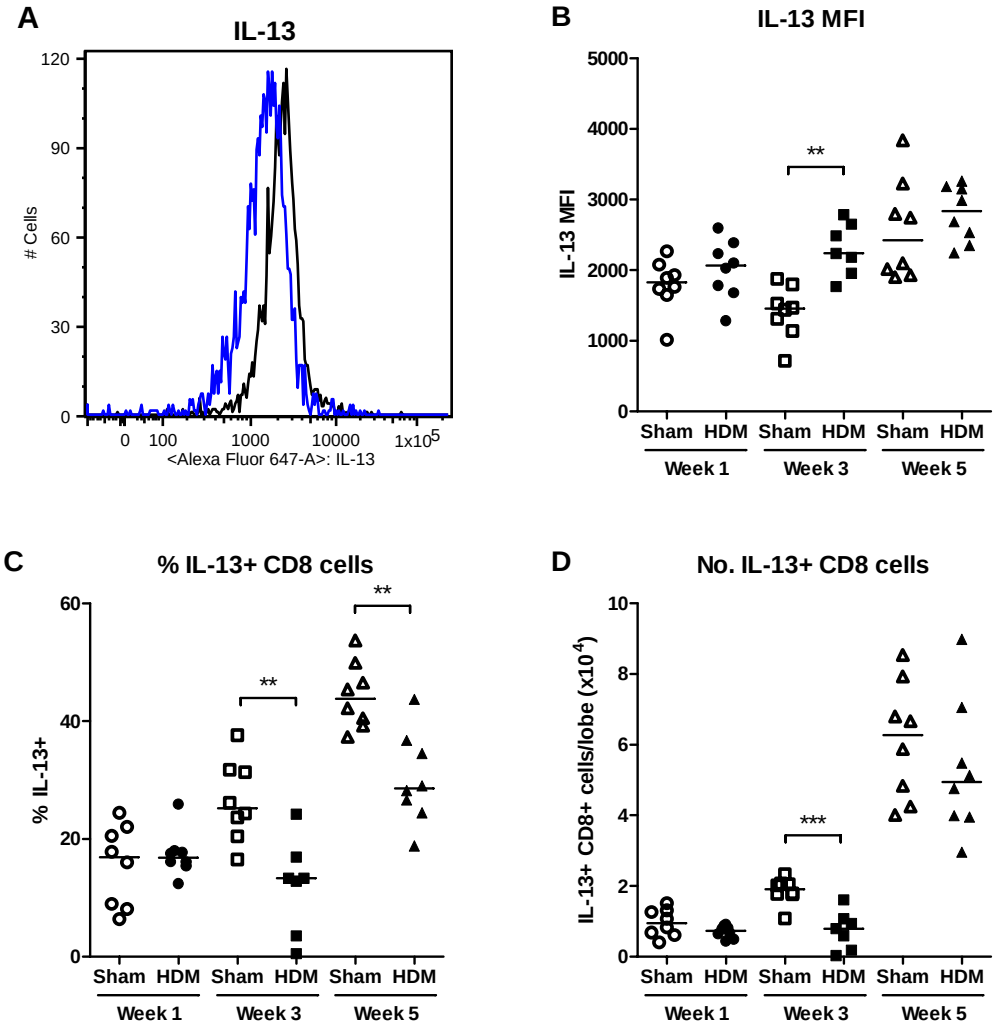


Figure 3.15 IL-13 expression in CD8+ cells following chronic HDM exposure. Lungs were taken 4 hours after the last HDM instillation. (A) Representative histogram of intracellular IL-13 staining (black line) and isotype control (blue line) in CD8+ T cells at week 5. MFI (B), % (C) and number (D) of IL-13+ CD8+ T cells, identified and quantified by flow cytometry. n = 7-8 mice/group, bar represents median. ** $p<0.01$ and *** $p<0.001$ by Mann Whitney test.

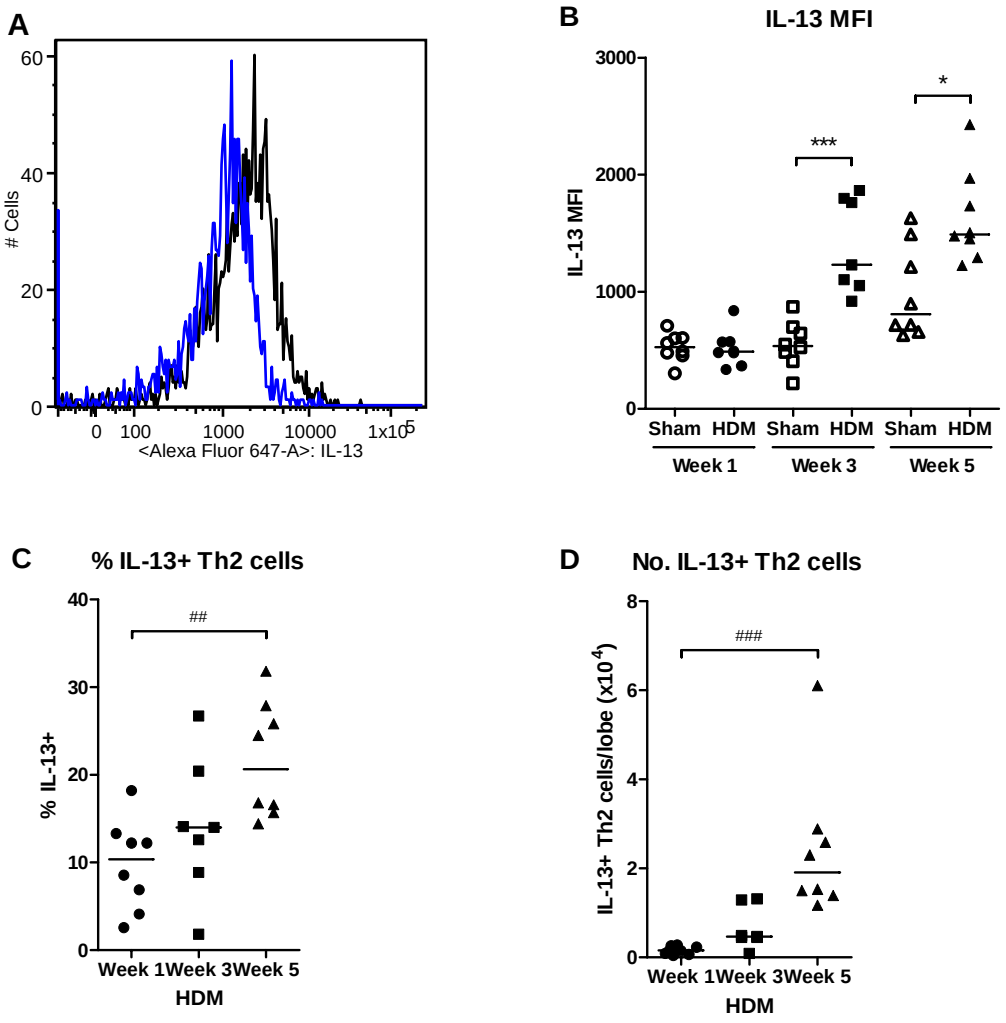


Figure 3.16 IL-13 expression in Th2 cells following chronic HDM exposure. Lungs were taken 4 hours after the last HDM instillation. (A) Representative histogram of intracellular IL-13 staining (black line) and isotype control (blue line) in Th2 cells at week 5. MFI (B), % (C) and number (D) of IL-13+ Th2 cells, identified and quantified by flow cytometry. n = 7-8 mice/group, bar represents median. * $p<0.05$ and *** $p<0.001$ relative to sham group by Mann Whitney test or ## $p<0.01$ and ### $p<0.001$ by Kruskal-Wallis test with Dunn's post test.

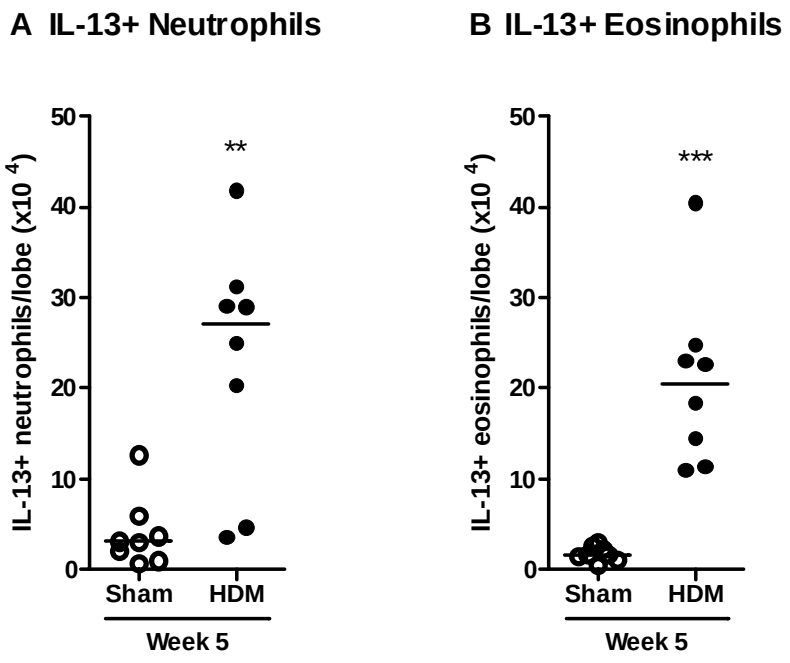


Figure 3.17 IL-13 expression in neutrophils and eosinophils following chronic HDM exposure. Lungs were taken after 5 weeks of HDM exposure, 4 hours after the last HDM instillation and stained for intracellular IL-13 or isotype control. Numbers of IL-13+ neutrophils (A) and eosinophils (B) were identified and quantified by flow cytometry. n = 8 mice/group, bar represents median. ** $p<0.01$ and *** $p<0.001$ relative to sham group by Mann Whitney test.

3.4 Discussion

The induction of airway pathophysiology by chronic intranasal exposure to HDM was first described by Johnson *et al.* (Johnson *et al.*, 2004). Allergic airways disease (AAD) with similarities to asthma was induced in the absence of prior systemic sensitisation and without the use of chemical adjuvants. The primary aim of this chapter was to establish this model of AAD and further characterise the allergic response. This will allow identification of an appropriate HDM exposure regime to be used in subsequent studies analysing the role of specific mediators and cell types in AAD pathophysiology. In addition this chapter aimed to confirm the up-regulation of IL-13 previously observed in lungs from mice chronically exposed to HDM and identify potential sources of IL-13 in the lungs during AAD (Gregory *et al.*, 2009).

3.4.1 HDM exposure induces allergic airways disease

The use of relevant animal models to study the mechanisms and molecules involved in the pathogenesis of allergic asthma is paramount. HDM is a complex cocktail of antigens, proteases and TLR agonists, e.g. endotoxin. This is much more akin to the array of substances people are regularly exposed to via their airways and hence provides a more relevant experimental allergen than previously used surrogate antigens, such as ovalbumin. Importantly, the nature of HDM as an allergen mitigates the requirement for systemic sensitisation with chemical adjuvants, such as alum, prior to airway exposure. Therefore the first contact with allergen is via the airways and hence the allergic response is initiated by airway resident APCs; providing a much more appropriate means of studying the pathogenesis of allergic asthma. Furthermore, this allergenic property of HDM allows repeated exposure of the airways to HDM without the induction of tolerance. The ability to chronically expose the airways in this way permits the induction of persistent inflammation and hence investigation into the subsequent structural changes in the airways.

As previously reported, chronic exposure to i.n. HDM induced AHR, inflammation and airway remodelling (Johnson *et al.*, 2004). AHR was assessed 24 hours post-HDM; the optimal time point for observing changes in R_L in HDM exposed mice (Gregory *et al.*, 2009). In the current study, hyper-reactivity was apparent after 3 weeks of HDM exposure as an exaggerated decline in C_{dyn} in response to MCh challenge. However, this was not accompanied by increased R_L at the same time

point. By week 5 AHR was evident as both increased R_L and reduced C_{dyn} in response to MCh. Moreover a decline in basal lung function was also observed at week 5 prior to MCh challenge. These observations at week 5 are in agreement with those previously reported however, Gregory *et al.* demonstrated significant changes in R_L from week 3 of HDM exposure (Johnson *et al.*, 2004;Gregory *et al.*, 2009). This apparent disparity may be attributable to variation between batches of HDM or subtle differences in the HDM exposure regime and techniques used for assessing lung function.

Analyses of cellular inflammation and inflammatory mediators were conducted 4 hours post-HDM to capture peak cytokine production in the lungs and encompass significant cell infiltration (Gregory *et al.*, 2009). Infiltration of all the cell subsets investigated in this study increased throughout the 5 week time course of HDM exposure. One week of HDM exposure induced an early, low level, accumulation of neutrophils and T cells (CD4+ and CD8+) in BAL. In contrast to the BAL, T cells (CD4+ and CD8+) in the tissue appear to dip at the same time point. This was unexpected but may be due to migration of cells from the circulation and/or lung parenchyma into the airway lumen as a result of HDM exposure. Neutrophils however, did not exhibit a corresponding dip in the tissue, perhaps because they are more readily mobilised into the circulation from bone marrow. On further analysis of BAL CD4+ T cells Th1, Th2 and Th17 cells were present at week 1 although none of the cytokines or chemokines investigated were detected in the tissue at this early time point, with the exception of IL-12 and IL-33. This suggests the immune response at this early time point is not yet adaptive and is perhaps initiated by an innate response to HDM. The induction of IL-12 at week 1 suggests exposure of airway APCs to LPS with in the HDM extract and may indicate DC activation (Eisenbarth *et al.*, 2002). This LPS component of HDM can also activate the airway epithelium via pattern recognition receptors leading to release of epithelial derived cytokines such as IL-33 (Hammad *et al.*, 2009). IL-33, in turn, acts as an alarmin and is capable of promoting innate and allergic inflammation by multiple mechanisms (Lloyd, 2010). IL-33 has been reported to recruit Th2 cells; activate mast cells, eosinophils, basophils, polarised Th2 cells, natural killer (NK) cells, iNKT cells and DCs; amplify the polarisation of alternatively activated macrophages and activate innate lymphoid cells (Komai-Koma *et al.*, 2007;Allakhverdi *et al.*, 2007;Cherry *et al.*, 2008;Stolarski *et al.*,

2010;Smithgall *et al.*, 2008;Hammad & Lambrecht, 2008;Kurowska-Stolarska *et al.*, 2009;Neill *et al.*, 2010;Price *et al.*, 2010;Chang *et al.*, 2011). In addition, direct administration of IL-33 into the airways, or transgenic over-expression of IL-33, induces airway inflammation, goblet cell hyperplasia, up-regulation of Th2 cytokines and eosinophilia (Kurowska-Stolarska *et al.*, 2009).

After 3 weeks of HDM exposure the profound eosinophilia and accumulation of Th2 cells in both BAL and lung tissue indicates a strong Th2 response. This was supported by the presence of Th2 cytokines IL-4 and IL-5, the eosinophil chemo-attractant eotaxin and the Th2 amplifying cytokine IL-33 in the lung tissue and corresponds with the development of AHR. Gregory *et al.* observed a similar profile of AHR, eosinophilia, accumulation of Th2 cells and up-regulation of Th2 cytokines at this time point (Gregory *et al.*, 2009).

In addition to this dominant Th2 response, low levels of Th1 and Th17 cells were present in BAL after 3 weeks of HDM exposure. This was accompanied by low levels of tissue IL-17 but not IFNγ. Interestingly the accumulation of Th17 cells in BAL following HDM exposure, but not the corresponding tissue IL-17, has been previously reported by Gregory *et al.* (Gregory *et al.*, 2009). In addition, Gregory *et al.* also detected significant levels of IFNγ in the tissue, in contrast to the data presented here at this time point. IL-12 concentrations in the tissue of HDM exposed mice at week 3 remain significantly greater than sham exposed, though are reduced compared to week 1. The presence of IL-4 at this time point may be down-regulating the production of IL-12 (Koch *et al.*, 1996). Taken together, HDM exposure appears to stimulate weak Th1 and Th17 responses in conjunction with a dominant Th2 response.

BAL neutrophilia is further elevated at week 3 and coupled to a significant tissue neutrophilia. The neutrophil chemo-attractant KC was also elevated in the tissue. This strong neutrophilic response may be driven directly by HDM exposure, via endotoxin stimulation of TLR4, although the ensuing adaptive immune response may also play a role in driving neutrophilia. For example both IL-13 and IL-17 are capable of recruiting neutrophils via KC generation (Grunig *et al.*, 1998;Witowski *et*

al., 2000). HDM induced KC and neutrophilia have been previously reported (Gregory *et al.*, 2009).

After 5 weeks of HDM exposure the inflammatory profile was comparable to week 3 but heightened. Significant numbers of eosinophils, neutrophils, CD4+ T cells and CD8+ T cells were detected in both BAL and tissue. Further analysis of CD4+ T cell phenotype revealed a dominant presence of Th2 cells in BAL and tissue. Th1 cells were detected in the BAL but not tissue while Th17 where present in BAL and tissue. IL-4, IL-5, IL-17, IFNγ, IL-12, IL-10, eotaxin, KC and IL-33 were all elevated in the lung tissue.

Further evidence to support the development of a HDM specific Th2 response is provided by the analysis of total IgE and HDM specific serum antibodies. Total serum IgE was elevated after 5 weeks of HDM exposure and HDM specific IgE, IgG1, IgG2a and IgG2b were detected in the serum of mice exposed to HDM for 3 weeks and further elevated after 5 weeks of exposure. The presence of these isotypes indicates the coexistence of multiple T cell responses however the abundance of HDM specific IgG1 indicates a predominant Th2 response. The induction of the Th2 associated antibodies IgE and IgG1 by HDM exposure has been shown previously and confirms allergic sensitisation of the mice from 3 weeks of exposure to HDM (Johnson *et al.*, 2004;Gregory *et al.*, 2009).

Chronic inflammatory insult of the airways leads to structural changes within the airway wall such as goblet cell hyperplasia and peribronchial collagen deposition (McMillan & Lloyd, 2004;Johnson *et al.*, 2004;Southam *et al.*, 2007). Histological assessment of the lungs revealed goblet cell hyperplasia after 3 weeks of HDM exposure which was accompanied by a robust up-regulation of muc5ac mRNA expression. Interestingly neither goblet cell frequency nor muc5ac expression increased with further exposure to HDM. Significant peribronchial collagen deposition was evident as early as week 1 of HDM exposure, but more robust after 3 and 5 weeks of HDM exposure. Peribronchial collagen depth was greatest at week 5, which was coincident with peak AHR and deterioration of basal lung function, the latter of which may be in part attributable to collagen deposition (Southam *et al.*, 2007).

Chronic exposure to HDM induces allergic airways disease which shares many of the hallmarks of allergic asthma. AHR, airway inflammation with eosinophilia and a strong Th2 component, elevated IgE titres and airway remodelling are cardinal features of asthma that have been demonstrated in mice after 3-5 weeks of HDM exposure (O'Byrne & Inman, 2003;Bousquet *et al.*, 1990;Robinson *et al.*, 1992;Brightling *et al.*, 2002;Vignola *et al.*, 2000;Bergeron *et al.*, 2009). However, while exposure to HDM induces a dominant Th2 response, other, weaker T cell responses are also evident. In light of recent observations that T cells may be more plastic than originally suggested and the identification of alternative T cell subsets in the lungs of asthmatic patients, the heterogeneous inflammation induced by HDM exposure may be more relevant to clinical disease (Lloyd & Hessel, 2010). Accumulation of both Th1 and Th17 subsets was observed in BAL after HDM exposure. Th1 cells have been detected in BAL from asthmatic patients, including during exacerbation, however their presence is controversial, thus their role remains unknown (Krug *et al.*, 1996;Mamessier *et al.*, 2008;Brightling *et al.*, 2002;Vock *et al.*, 2010). The presence of Th17 cells and IL-17 expression in asthma have also been demonstrated, although the source of IL-17 is not solely Th17 cells (Pene *et al.*, 2008;Molet *et al.*, 2001;Bullens *et al.*, 2006). Interestingly, IL-17 appears to correlate with disease severity (Al-Ramli *et al.*, 2009).

3.4.2 HDM exposure up-regulates IL-13

IL-13 is proposed to be a central mediator of asthma (Wills-Karp, 2004). It is elevated in both asthma and models of AAD (Berry *et al.*, 2004;Gregory *et al.*, 2009). It was important to confirm the up-regulation of IL-13 in HDM exposed mice and thus validate this mouse model as appropriate for determining the role of IL-13 in driving airway pathophysiology in future studies. IL-13 mRNA expression was up-regulated from week 1 of HDM exposure and subsequently vigorously up-regulated at weeks 3 and 5. This was detected as an increase in the tissue concentration of IL-13 protein at weeks 3 and 5, but not 1. In contrast to the findings of Gregory *et al.*, significant changes in IL-13 were not observed in the BAL (Gregory *et al.*, 2009). Again, this may be due to subtle differences in the HDM exposure regime or HDM batch variations or different assay sensitivities for measuring IL-13. However, HDM induced up-regulation of IL-13 mRNA in the lung tissue, in the absence of detectable

IL-13 protein in the BAL has previously been reported at week 5 in an equivalent mouse model (Ulrich *et al.*, 2008).

On establishing the up-regulation of IL-13 in lung tissue following HDM exposure, IF staining was conducted in order to identify potential sources of IL-13 within the lungs. Initial IF stains using a series of different anti-IL-13 reagents in the protocol described in 2.10.4 failed to produce a positive signal, therefore a signal amplification system was employed as used by Kim *et al.* for IL-13 detection in lung tissue (Kim 2008). This protocol generated a positive signal in airway epithelial cells and a subset of parenchymal cells and BAL cells, possibly alveolar macrophages; a similar staining pattern to that reported by Kim *et al.* in mice with virally induced chronic lung inflammation. However, in the present studies these cells also stained positive in sections incubated with control primary antibody or with no primary at all demonstrating this signal was not specific to IL-13. Furthermore, this indicated that the amplification system employed was responsible for this non-specific staining, and is therefore inappropriate for the detection of IL-13 in this case.

In the absence of an effective IF protocol, flow cytometry was used to determine whether any of the leukocytes assessed in these studies were responsible, in part, for the observed increase in IL-13 production. Intracellular IL-13 was detected in CD4+ T cells, including but not exclusively Th2 cells, and in CD8+ T cells. However, the number of IL-13+ CD4+ and IL-13+ CD8+ T cells was not elevated after HDM exposed when compared to sham exposure. Following one week of HDM exposure there was little deviation from sham with respect to the intensity of IL-13 staining, percentage of IL-13+ cells and number of IL-13+ cells in both CD4+ and CD8+ T cell populations. At week 3 the intensity of IL-13 staining in CD4+ and CD8+ cells was greater in HDM than sham mice. However, the proportion of IL-13+ cells within these populations was reduced in the HDM group compared to sham. The actual number of IL-13+ CD4+ T cells was comparable in sham and HDM mice, while the number of IL-13+ CD8+ T cells was slightly less in HDM compared to sham mice. This indicated the majority of T cells accumulating in the lungs following HDM exposure did not express IL-13 and were therefore having a dilution effect on the existing IL-13+ T cells present. Coupled with the increase in MFI this also suggested that these existing IL-13+ cells express more IL-13 per cell upon exposure to HDM,

rather than the number of IL-13 expressing cells increasing. After 5 weeks of HDM exposure the percentage of IL-13+ CD4+ and CD8+ T cells remained lower than sham while the numbers of IL-13+ T cells were equivalent in sham and HDM groups; again indicating that the majority of T cells accumulating in the lungs do not express IL-13. Furthermore, no differences in IL-13 MFI were apparent between sham and HDM T cells at this time point. Interestingly, the numbers of IL-13+ CD4+ and IL-13+ CD8+ T cells in sham exposed mice appear to increase over time. This may be an age related effect or might be a result of repeated anaesthetic events and i.n. instillations.

Specific analysis of Th2 cells demonstrated IL-13 staining was more intense following 3 or 5 weeks of HDM exposure compared to sham. This was accompanied by an increase in both the percentage of Th2 cells expressing IL-13 and the number of IL-13+ Th2 cells compare to week one of HDM exposure. Thus, Th2 cells were identified as a potential source of IL-13 in the lungs during HDM exposure. In addition, neutrophils and eosinophils also represented sources of IL-13 in the lungs of HDM exposed mice.

Many cell types, both haematopoietic and stromal, are reported to be potential sources of IL-13 in the lung. IL-13 was first discovered in activated T cells and although subsequently characterised as a Th2 cytokine, its production has also been demonstrated in Th1, CD8+ T cells, memory T cells, naïve T cells and NKT cells (Minty *et al.*, 1993;de Waal *et al.*, 1995;Jung *et al.*, 1996;Kim *et al.*, 2008). Mast cells, eosinophils and basophils are all competent IL-13 producing cells present in asthmatic airways (Jaffe *et al.*, 1996;Brightling *et al.*, 2003;Schmid-Grendelmeier *et al.*, 2002;Spencer *et al.*, 2009;Spencer *et al.*, 2009;Gibbs *et al.*, 1996;Ochensberger *et al.*, 1996;Schroeder *et al.*, 2010). Resident cells such as airway smooth muscle, airway epithelium, macrophages and DCs are also capable of IL-13 production under certain conditions (Grunstein *et al.*, 2002;Freishtat *et al.*, 2010;Prieto *et al.*, 2000;de Saint-Vis *et al.*, 1998). The recent characterisation of innate lymphoid cells/nuocytes as key IL-13 producing cells could be of significant importance in the pathogenesis of allergic inflammation although, as yet these cells have not been identified in the lungs of mice with AAD (Saenz *et al.*, 2010;Moro *et al.*, 2010;Neill *et al.*, 2010;Chang *et al.*, 2011). However, contrary to the observations in this study, there have been no

reports in the literature of neutrophils producing IL-13. In fact Reglier *et al.* reported human neutrophils from healthy volunteers unable to produce or release IL-13 (Reglier *et al.*, 1998). This discrepancy may lie in species differences between mouse and human, or the allergic status of the subjects. Nonetheless, this observation warrants further investigation to confirm or disprove neutrophils as a source of IL-13 during allergic inflammation. Taken together, the present study verifies T cells and eosinophils are sources of IL-13 in allergic lungs and that neutrophils may represent an addition source of IL-13. However, a multitude of other cell types, both stromal and haematopoietic, are also likely to be contributing the increased production of IL-13 in HDM induced AAD.

In summary, a mouse model of HDM induced AAD has been reproduced from the literature and further characterised. AAD with similarities to asthma was observed after 3-5 weeks of exposure. In addition IL-13 was up-regulated throughout the HDM exposure period. Thus this animal model was considered appropriate for the subsequent investigation into the role of IL-13 in AAD.

4. THE ROLE OF IL-13 IN HDM INDUCED AAD

4.1 Introduction

Multiple pathophysiological features of AAD have been demonstrated to be IL-13 dependent in various animal models. Previous reports have assessed the role of IL-13 by use of sIL-13Rα2-Fc, *Il13*$^{-/-}$ mice, *Il13ra1*$^{-/-}$ mice and anti-IL-13 monoclonal and polyclonal antibodies in mice, sheep or non-human primates (NHP). However, much of the mouse data is derived from OVA induced models of lung inflammation, dependent on peripheral sensitisation prior to airways exposure and there are no reports of the effects of IL-13 neutralisation in HDM induced AAD. Furthermore, very few studies have investigated the role of IL-13 in established AAD. In addition, there are a number of discrepancies between reports of IL-13 depletion, depending upon the animal model employed and the method of IL-13 depletion. Therefore, the present series of experiments were conducted to determine the role of IL-13, using an anti-IL-13 monoclonal antibody, in the HDM induced mouse model of AAD described in chapter 3. Prophylactic and therapeutic dosing regimes with anti-IL-13 mAb were employed in this mouse model to investigate the role of IL-13 in both the development and maintenance of AAD.

Due to the sequential nature of type II IL-4 receptor assembly (Figure 4.1A), there are at least two distinct axes of intervention for IL-13 specific neutralising mAbs; blocking IL-13 binding IL-13Rα1 (Figure 4.1 B) or preventing the subsequent association of IL-13 with IL-4Rα (Figure 4.1 C). Both of these approaches prevent receptor assembly and hence IL-13 induced STAT6 activation. However blocking the interaction between IL-13 and IL-13Rα1 also prevents IL-13 binding IL-13Rα2. MAbs 582 and 587 are murinised anti-mouse IL-13 mAbs which bind these distinct functional epitopes; previously identified and characterised *in vitro* and *in vivo* (Berry *et al.*, 2009). These mAbs both bind IL-13 with high affinity (K_D 11pM and 8pM, respectively) and prevent IL-13 signalling via the type II IL-4 receptor. Upon binding IL-13 mAb 582 blocks the initial association between IL-13 and IL-13Rα1 and hence prevents recruitment of the IL-4Rα subunit. In addition 582 blocks IL-13 binding IL-13Rα2 (Figure 4.1 B). Conversely, mAb 587 binds IL-13 but does not prevent binding to IL-13Rα1 or IL-13Rα2. 587 blocks the ensuing interaction between the IL-13-IL-13Rα1 complex and IL-4Rα subunit (Figure 4.1 C). Thus one of the key differentiating factors between these mAbs is their ability to block IL-13 binding IL-

13Rα2. In mice, IL-13Rα2 may be membrane bound or soluble and has at least three potential functions which may play a role in the pathogenesis of AAD. Membrane bound IL-13Rα2 has been reported to deliver a pro-fibrotic signal and hence may contribute to IL-13 dependent pathology in AAD (Fichtner-Feigl *et al.*, 2006). Conversely, sIL-13Rα2 is proposed to act as a decoy receptor, sequestering IL-13 thus potentially reducing IL-13 dependent pathology (Andrews *et al.*, 2006;Yasunaga *et al.*, 2003). Furthermore, membrane bound IL-13Rα2 may negatively regulate type II IL-4 receptor dependent pathology by sequestering IL-4Rα (Andrews *et al.*, 2006). Thus, the additional effects of blocking IL-13Rα2 are unpredictable and depend upon the relative contributions of the mechanisms described above. Both blocking mechanisms elicited equivalent inhibition of OVA induced mucin gene up-regulation in OVA sensitised mice (Berry *et al.*, 2009). Similarly, using different mAbs with corresponding binding properties, comparable inhibition of antigen induced IgE and pulmonary inflammation has been demonstrated in an NHP model of AAD (Kasaian *et al.*, 2008). However, neither of these studies examined the effects of both blocking approaches on chronic features of asthma, such as airway remodelling, in which IL-13Rα2 may be implicated. Therefore, prior to in depth analysis of anti-IL-13 efficacy, a direct comparison between 582 and 587 was conducted in order to elucidate whether these distinct binding specificities confer any differences in efficacy. The most appropriate anti-IL-13 mAb was then selected to elucidate the effects of IL-13 neutralisation on the development of AAD.

The effects of IL-13 neutralisation in established AAD is of greater clinical relevance than neutralising IL-13 during the development of AAD. Prophylactic treatment of asthma is impractical since diagnosis is made upon presentation of symptoms which occur after the disease is established (GINA, 2006). Hence, current treatment of asthma is therapeutic. Therefore it is important to ascertain the role of IL-13 in maintaining established AAD and whether features of airway pathophysiology are reversible. To address this, a therapeutic protocol was devised in which anti-IL-13 mAb treatment was not commenced until significant airway hyperreactivity, inflammation and remodelling had developed. Based on the time-course of pathophysiology characterised in chapter 3 dosing began after 5 weeks of HDM exposure and proceeded for a further 3 weeks during continued HDM exposure.

4.1.1 Aim

2. To define the effects of IL-13 neutralisation in mice chronically exposed to inhaled HDM allergen on inflammation, lung function and airway remodelling.

The initial aims of this chapter were to determine a suitable dose and mAb for IL-13 neutralisation *in vivo* and subsequently define the effects of IL-13 neutralisation on the development of HDM induced AAD. In addition, to elucidate the effects of therapeutic IL-13 neutralisation on established HDM induced AAD.

.

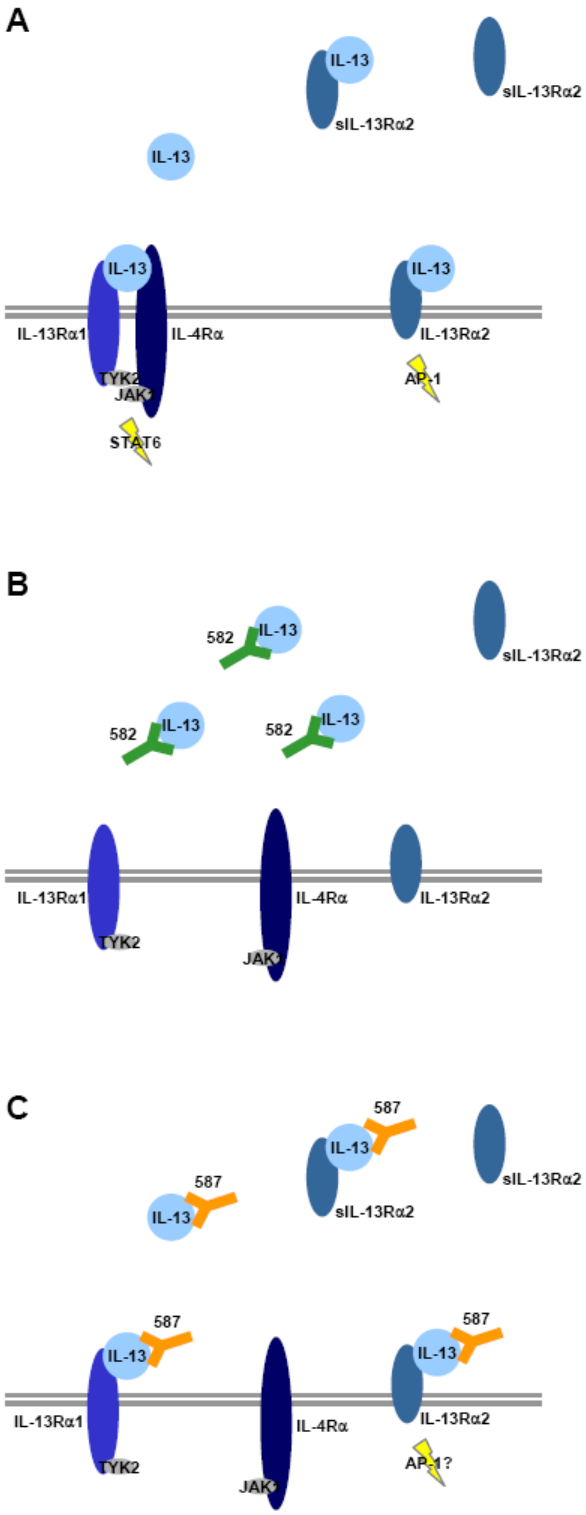


Figure 4.1 Type II IL-4 receptor formation and mAb specificity.
IL-13 has two receptors; the type II IL-4 receptor and IL-13Rα2. The type II IL-4 receptor comprises of IL-13Rα1 and IL-4Rα subunits which activate STAT6 in the presence of IL-13. Membrane associated IL-13Rα2 signals via an AP-1-like molecule in the presence of IL-13. IL-13 also binds sIL-13Rα2 (A). MAb 582 binds IL-13 and prevents IL-13 binding IL-13Rα1 or IL-13Rα2 (B). MAb 587 binds IL-13 and permits binding of IL-13Rα1 and IL-13Rα2 but prevents binding to IL-4Rα (C).

4.2 Methods

4.2.1 Mice and HDM sensitisation.

Male balb/c mice were exposed HDM for 5 or 8 weeks. For prophylactic anti-IL-13 mAb treatment mice were exposed to HDM for 5 weeks and dosed with 0.3, 3, 10 or 30mg/kg 582, 587, 101.4 mAb (isotype control) or vehicle (PBS) s.c., weekly throughout the exposure period from 1 hour prior to the first HDM exposure (Figure 4.2 A). Unrestrained WBP, where used, was conducted during the fourth week of HDM exposure, 24 hours post HDM. Mice were killed after 5 weeks for collection of samples, 24 hours after the last HDM exposure, or 4 hours post HDM exposure for cytokine and chemokine readouts.

For therapeutic anti-IL-13 mAb treatment mice were exposed to HDM for 8 weeks and dosed with 10mg/kg 582 or 101.4 s.c., weekly from the beginning of week 6 (day 35) (Figure 4.2 B). Mice were killed after 8 weeks for collection of samples 24 hours post HDM. An additional group of HDM exposed mice was killed after 5 weeks, immediately before the start of therapeutic anti-IL-13 dosing, to assess histological changes in the lung prior to treatment ("pre-dose").

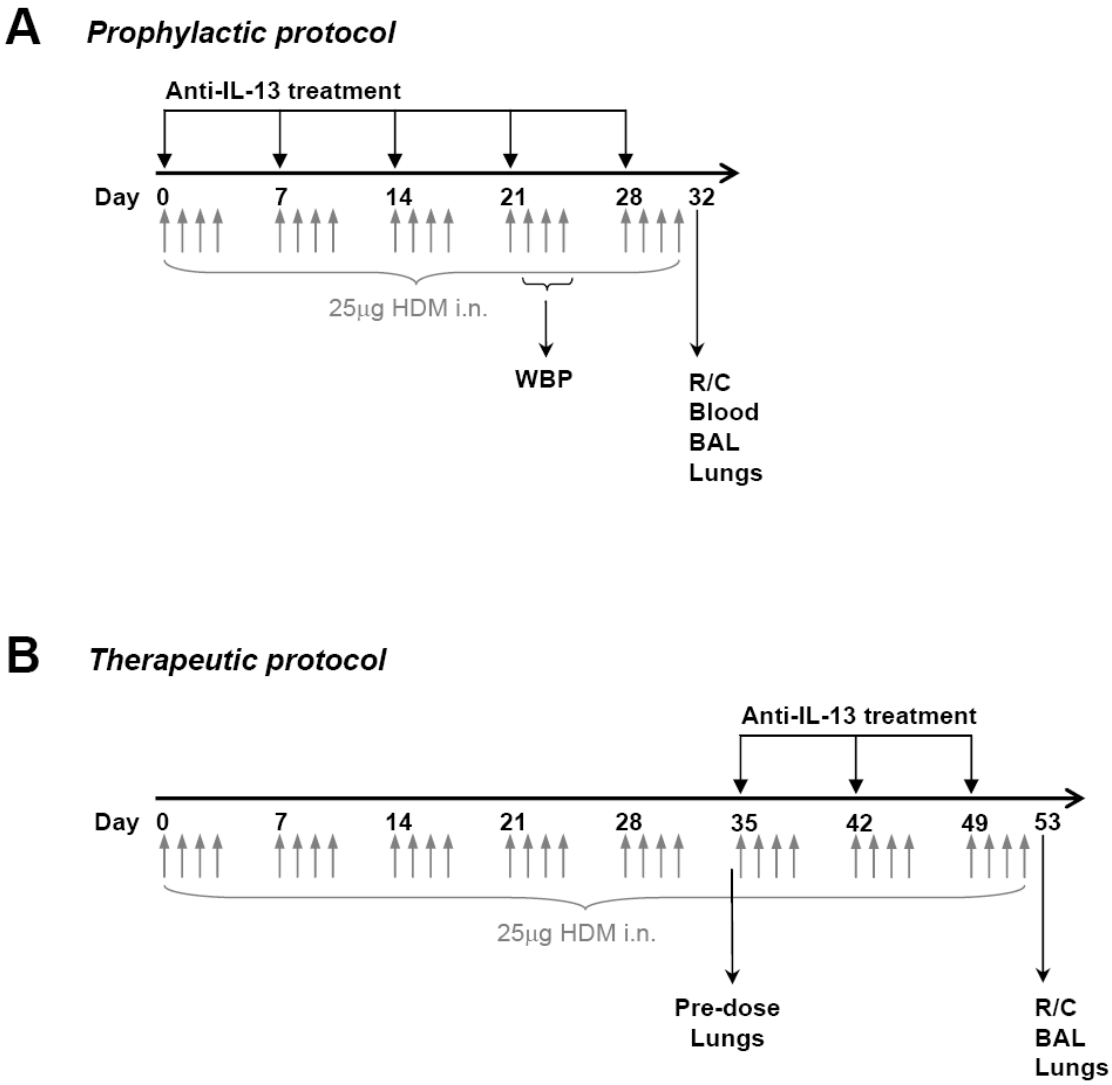


Figure 4.2 Experimental protocols for exposure to HDM. Mice were exposed to intranasal HDM on 4 consecutive days per week for 5 or 8 weeks. Sham treated mice received intranasal saline alone. Mice were dosed with anti-IL-13 mAb s.c., weekly, throughout HDM exposure (A; prophylactic protocol) or after AAD had established from day 35 (B; therapeutic protocol). AHR was assessed by WBP during week 4 or by direct measurement of R_L and C_{dyn} (R/C) at the end of the study. Mice were culled 4 or 24 hours after the final HDM exposure for collection of blood, BAL and lung samples.

4.3 Results

4.3.1 Dose response to anti-IL-13 mAb

To determine the effects of neutralising IL-13 in HDM induced AAD an initial dose finding study was conducted with 0.3, 3 and 30mg/kg 582. The effects of 582 on BAL inflammatory infiltrate, goblet cells and collagen deposition were assessed after 5 weeks of HDM exposure with prophylactic 582 treatment.

Treatment with 582 had comparable effects on BAL cellularity at 0.3, 3 and 30mg/kg thus no dose response relationship was observed over these doses. 3mg/kg 582 significantly reduced the total number of BAL leukocytes, with 0.3 and 30mg/kg exhibiting a similar, but non-significant effect (Figure 4.3 A). All three doses of 582 elicited robust inhibition of BAL eosinophilia, but had no significant effect on BAL neutrophilia (Figure 4.3 B-C). A non-significant trend towards inhibition of T cell accumulation in BAL was observed with each dose of 582 (Figure 4.3 D).

Prophylactic 582 treatment dose-dependently inhibited HDM induced goblet cell hyperplasia. 0.3mg/kg 582 partially reduced the frequency of goblet cells but did not affect the expression of muc5ac mRNA. However 3 and 30mg/kg 582 had comparable effects in completely reducing goblet cell frequency and significantly attenuating muc5ac expression (Figure 4.4 A-B). A non-significant trend towards dose related inhibition of peribronchial collagen deposition was observed with the three doses of 582 tested in this study (Figure 4.3 C). Since 3mg/kg 582 induced equivalent efficacy to 30mg/kg, 3mg/kg was presumed to be at the top of the dose-response curve. Therefore, 10mg/kg 582 was selected as a super-maximally efficacious dose for subsequent studies.

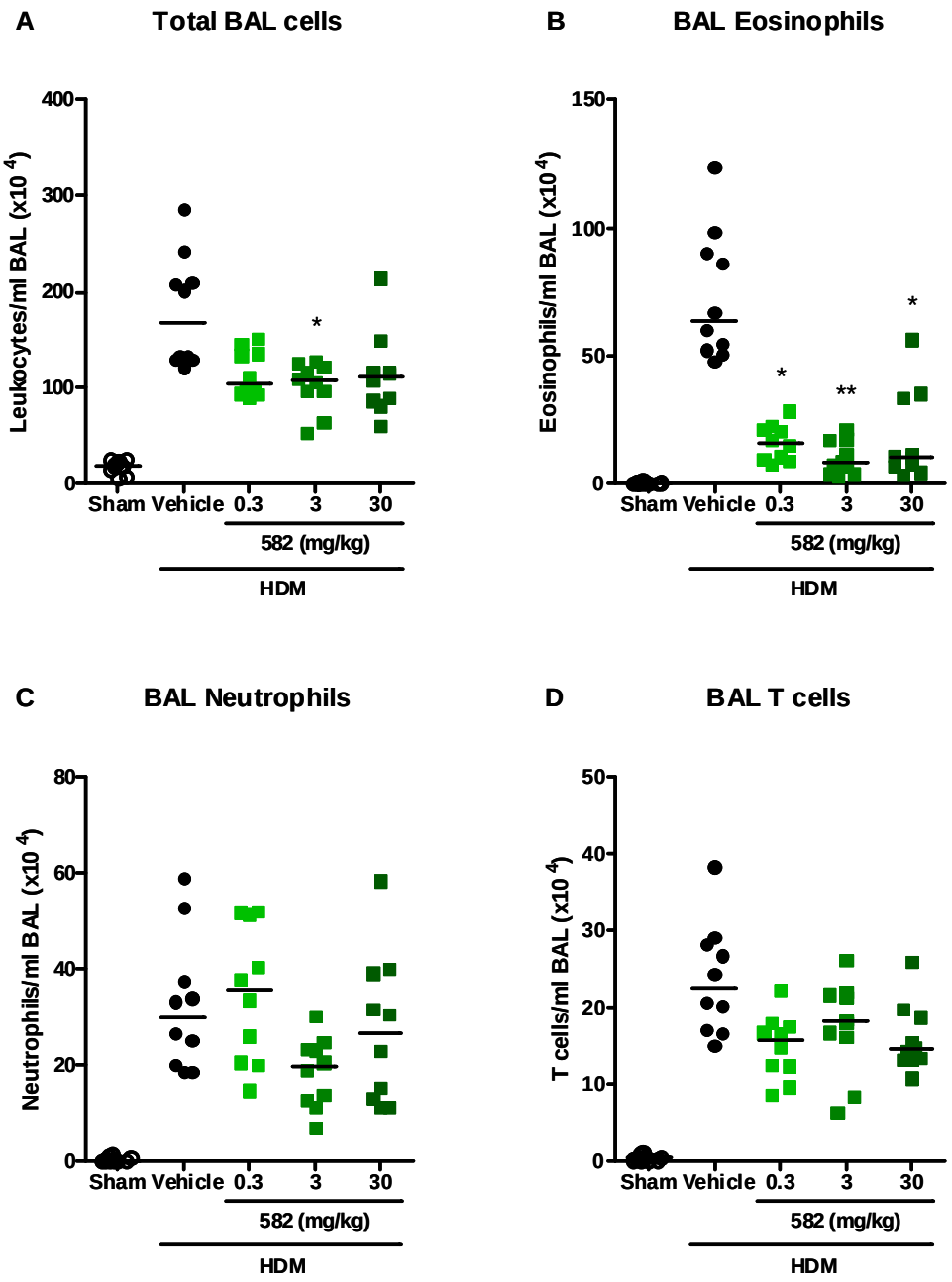


Figure 4.3 Effects of IL-13 neutralisation on BAL cells. BAL was taken after 5 weeks of HDM exposure, 24 hours after the last HDM instillation. Mice were dosed with 0.3, 3 or 30mg/kg 582 s.c., weekly, throughout the HDM exposure period. Total leukocytes (A), eosinophils (B), neutrophils (C) and T cells (D) in BAL were identified and quantified by flow cytometry. n = 10 mice/group, bar represents median. * $p<0.05$ and ** $p<0.01$ relative to vehicle group by Kruskal-Wallis test with Dunn's post test.

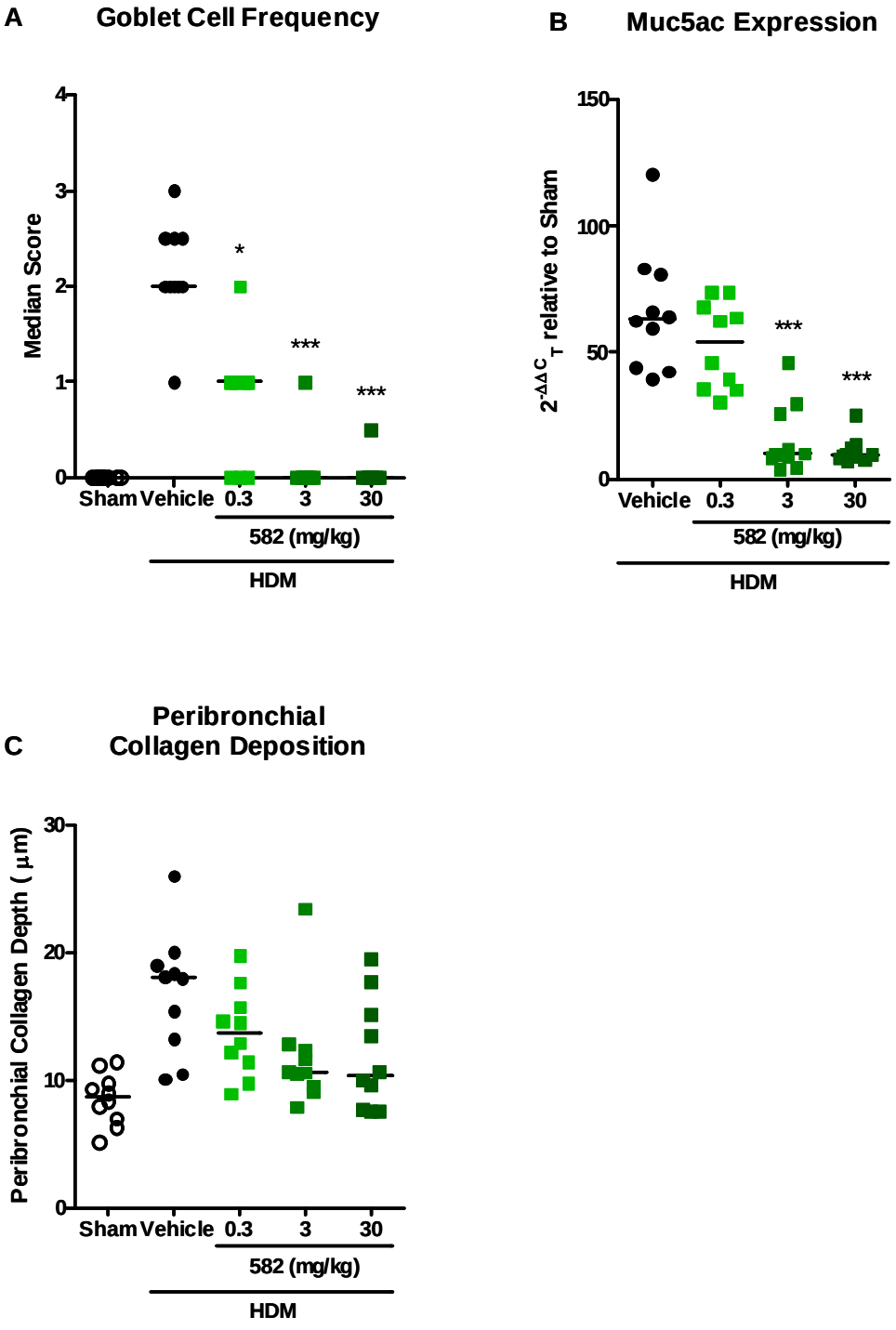


Figure 4.4 Effects of IL-13 neutralisation on airway remodelling. Lungs were taken after 5 weeks of HDM exposure, 24 hours after the last HDM instillation. Mice were dosed with 0.3, 3 or 30mg/kg 582 s.c., weekly, throughout the HDM exposure period. (A) Goblet cell frequency was scored in AB/PAS stained sections. (B) Muc5ac mRNA in lung tissue was quantified by real-time PCR and normalised to sham. (C) Peribronchial collagen depth was measured in Masson's trichrome stained sections. n = 10 mice/group, bar represents median. * $p<0.05$ and *** $p<0.001$ relative to vehicle group by Kruskal-Wallis test with Dunn's post test.

4.3.2 Direct comparison of anti-IL-13 mAbs with distinct functional epitopes.

582 and 587 are affinity matched IL-13 neutralising mAbs which recognise distinct functional epitopes on IL-13 and thus disrupt assembly of the type II IL-4 receptor signalling complex at different stages of assembly. Importantly, 582 also prevents IL-13 binding IL-13Rα2 whereas 587 does not (Berry *et al.*, 2009). In order to determine whether these differences in binding specificities conferred any functional consequence, a study was conduced in which 582 and 587 were directly compared at single dose levels. Mice were dosed with 10mg/kg anti-IL-13 mAb, weekly, throughout the 5 week HDM exposure period, after which BAL cellularity, AHR, goblet cell hyperplasia and collagen deposition were assessed.

Both anti-IL-13 mAbs elicited equivalent, reproducible effects on AAD pathophysiology. 582 and 587 profoundly reduced the number of BAL eosinophils whilst having no significant effects on neutrophil or T cell accumulation in BAL (Figure 4.5 A-C). Both antibodies completely prevented the development of AHR, determined by WBP (Figure 4.6), and goblet cell hyperplasia, assessed histologically (Figure 4.7 A-E). Similarly, both 582 and 587 inhibited peribronchial collagen deposition to the same degree (Figure 4.8 A-E). No significant differences were observed between the effects of 582 and 587 at 10mg/kg with respect to any of the parameters assessed in this study, therefore 582 was selected for further investigation into the effects of IL-13 neutralisation in this mouse model.

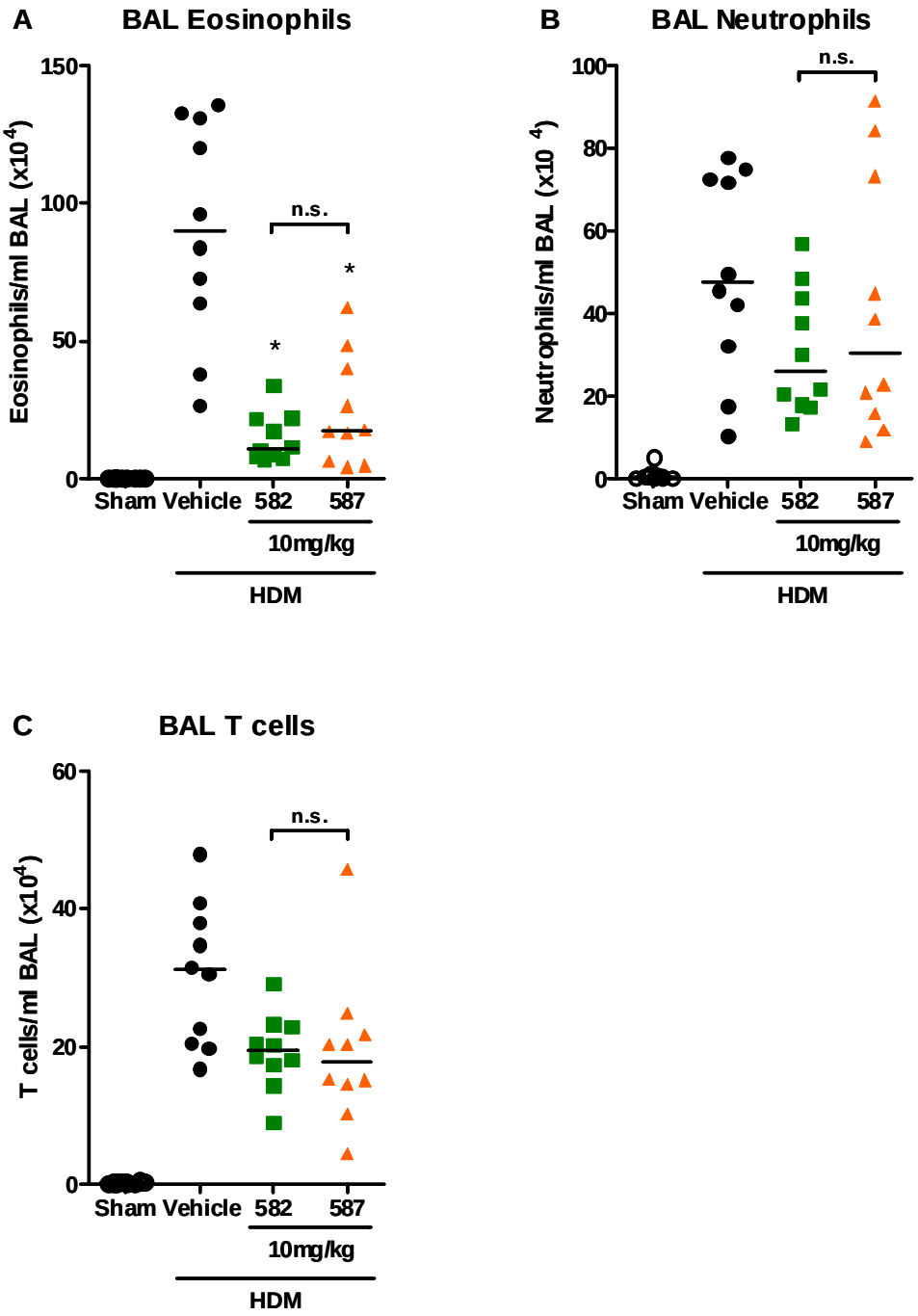


Figure 4.5 Effects of 582 and 587 treatment on BAL cells. BAL was taken after 5 weeks of HDM exposure, 24 hours after the last HDM instillation. Mice were dosed with 10mg/kg 582 or 587 s.c., weekly, throughout the HDM exposure period. Eosinophils (A), neutrophils (B) and T cells (C) in BAL were identified and quantified by flow cytometry. n = 10 mice/group, bar represents median. * $p<0.05$ relative to vehicle group by Kruskal-Wallis test with Dunn's post test. n.s.: no significant difference.

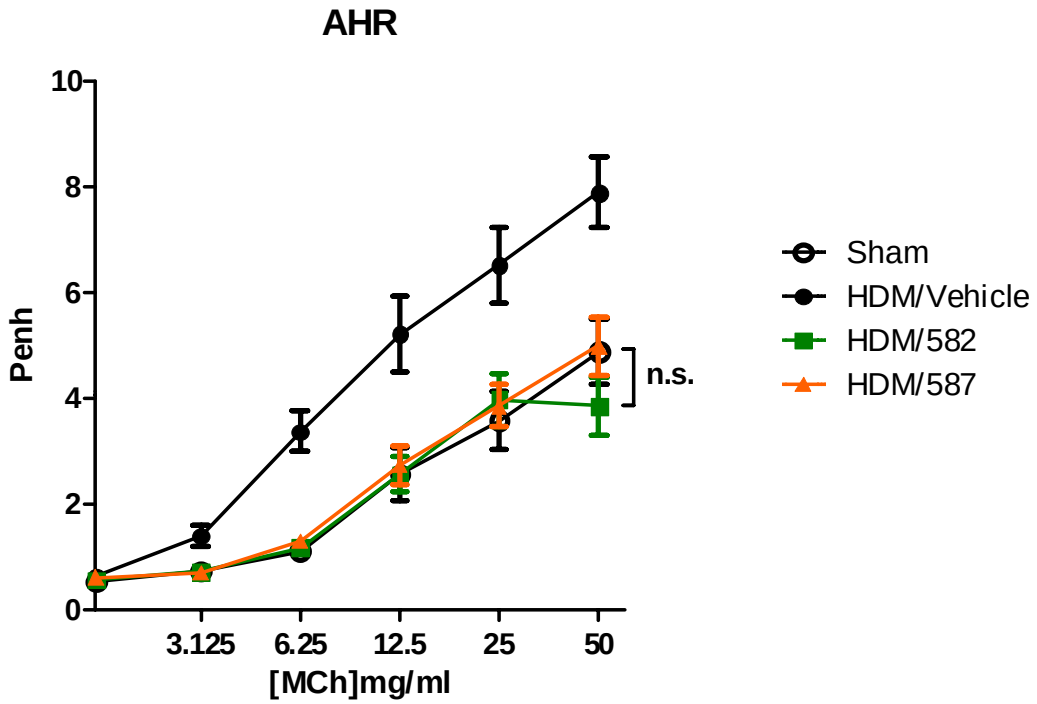


Figure 4.6 Effects of 582 and 587 treatment on AHR. AHR to MCh was determined as changes Penh measured by WBP during the fourth week of HDM exposure, 24 hours post HDM exposure. Mice were dosed with 10mg/kg 582 or 587 s.c., weekly, throughout the HDM exposure period. Data are shown as mean ± SEM, n = 10 mice/group. n.s.: no significant difference by Kruskal-Wallis test with Dunn's post test.

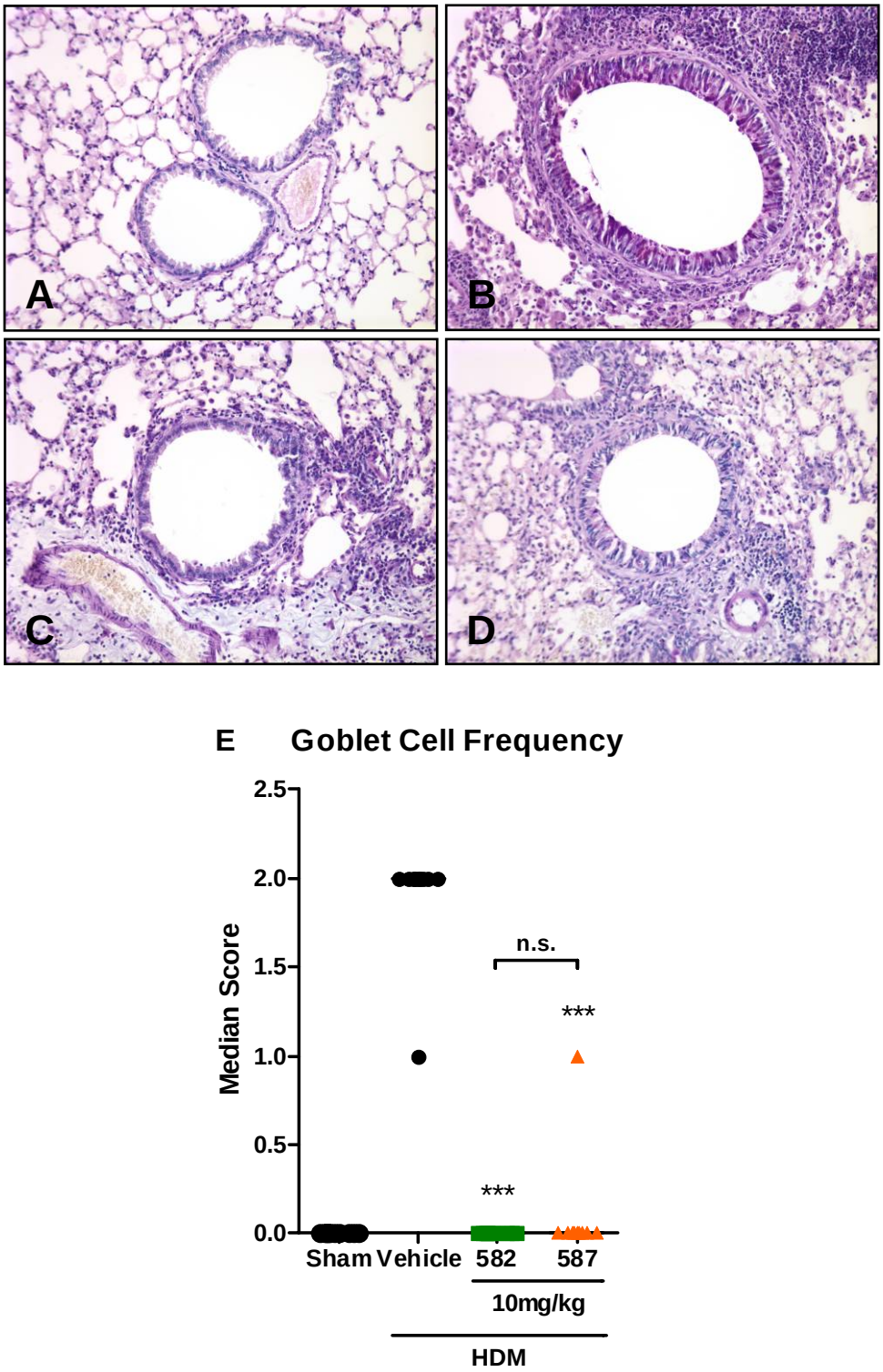


Figure 4.7 Effects of 582 and 587 treatment on goblet cell frequency. Lungs were taken after 5 weeks of HDM exposure, 24 hours after the last HDM instillation. Mice were dosed with 10mg/kg 582 or 587 s.c., weekly, throughout the HDM exposure period. (A-D) Representative AB/PAS stained sections from sham exposed (A), HDM exposed vehicle dosed (B), HDM exposed 582 dosed (C) and HDM exposed 587 dosed (D) mice; original magnification x200. (E) Goblet cell frequency was scored in AB/PAS stained sections. n = 10 mice/group, bar represents median. *** $p<0.001$ relative to vehicle group by Kruskal-Wallis test with Dunn's post test. n.s.: no significant difference.

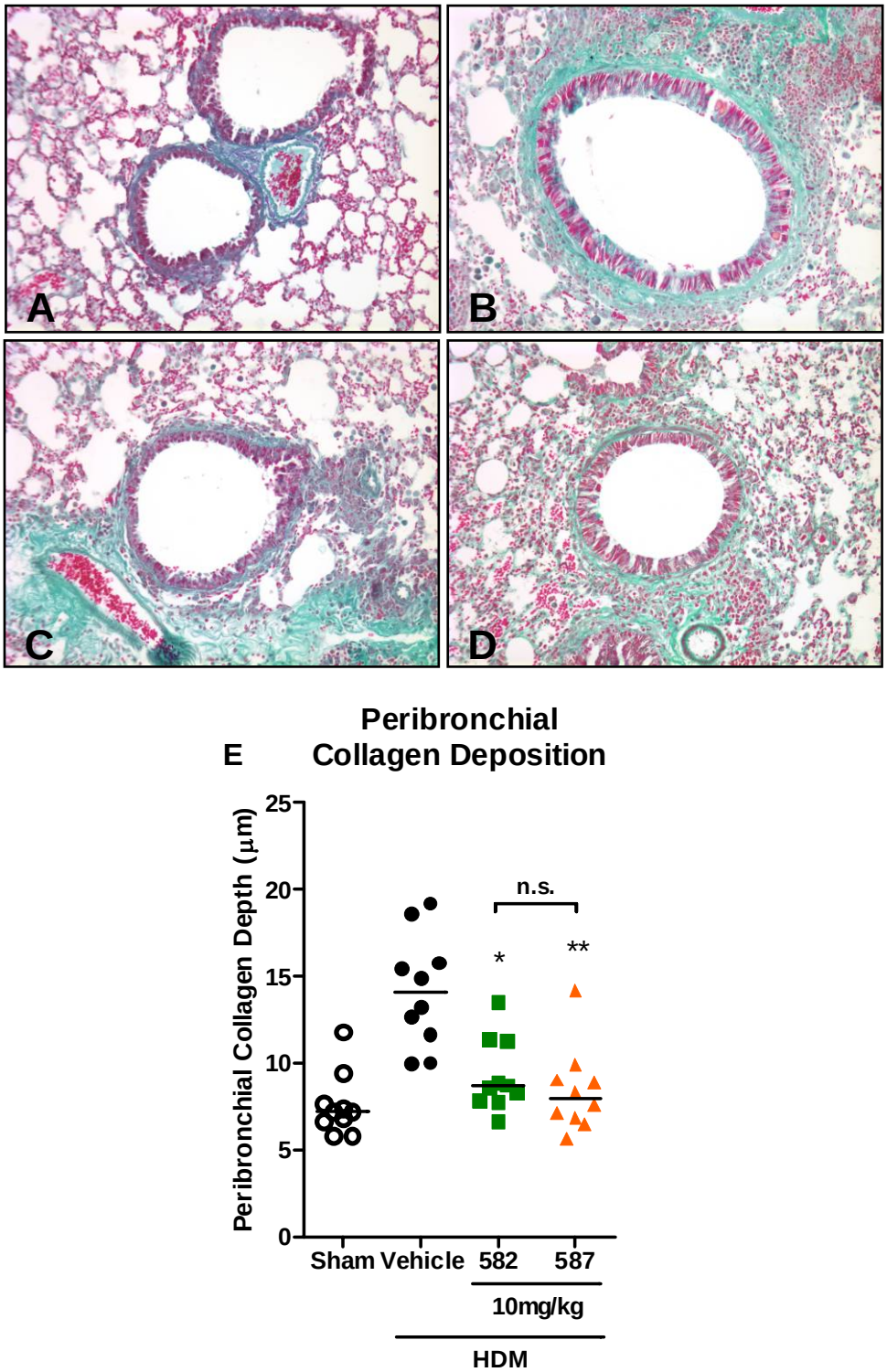


Figure 4.8 Effects of 582 and 587 treatment on peribronchial collagen deposition. Lungs were taken after 5 weeks of HDM exposure, 24 hours after the last HDM instillation. Mice were dosed with 10mg/kg 582 or 587 s.c., weekly, throughout the HDM exposure period. (A-D) Representative Masson's trichrome stained sections from sham exposed (A), HDM exposed vehicle dosed (B), HDM exposed 582 dosed (C) and HDM exposed 587 dosed (D) mice; original magnification x200. (E) Peribronchial collagen depth was measured in Masson's trichrome stained sections. n = 10 mice/group, bar represents median. * $p<0.05$ and ** $p<0.01$ relative to vehicle group by Kruskal-Wallis test with Dunn's post test. n.s.: no significant difference.

4.3.3 IL-13 neutralisation inhibits AHR

AHR is a defining feature of asthma and AAD in which IL-13 is proposed to play a key role. The previous study alluded to a role for IL-13 in the development of AHR by assessment of Penh by WBP. In order to confirm these observations AHR to MCh was assessed by direct measurement of lung resistance (R_L) and dynamic compliance (C_{dyn}) in terminally anaesthetised, ventilated mice previously exposed to HDM for 5 weeks and dosed prophylactically with 10mg/kg 582. Prophylactic IL-13 neutralisation inhibited MCh stimulated changes in R_L and C_{dyn} at each MCh concentration (Figure 4.9 A, C), thus confirming prior results obtained by WBP. In addition, anti-IL-13 mAb treatment prevented HDM induced changes in baseline R_L and C_{dyn} (Figure 4.9 B, D).

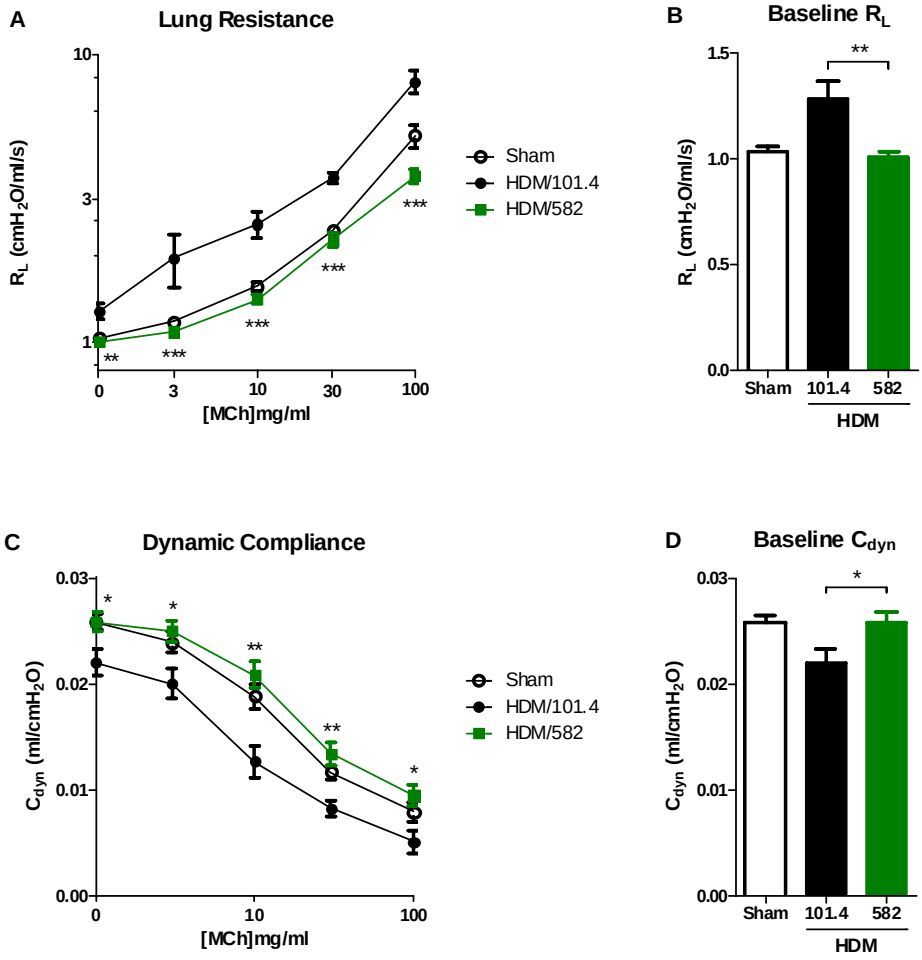


Figure 4.9 Effects of IL-13 neutralisation on AHR. AHR to MCh was determined as changes in lung resistance (R_L) (A, B) and dynamic compliance (C_{dyn}) (B, C) measured 24 hours post HDM, after 5 weeks of HDM exposure. Mice were dosed with 10mg/kg 582 or isotype control (101.4) s.c., weekly, throughout the HDM exposure period. Data are shown as mean ± SEM, n = 6-8 mice/group. * p<0.05, ** p<0.01 and *** p<0.001 relative to HDM/101.4 group by Mann Whitney test.

4.3.4 Effects of IL-13 neutralisation on pulmonary inflammation

The effects of anti-IL-13 mAb treatment on pulmonary inflammation have previously been alluded to by assessment of BAL cells; however it is important to establish the inflammatory infiltrate within the lung tissue itself since this is likely to have a greater impact on lung physiology. Thus, lung digest (LD) cells were phenotyped and quantified by flow cytometry in addition to BAL cells. Furthermore, a greater diversity of inflammatory cell types implicated in the allergic response was assessed in BAL and LD.

IL-13 neutralisation reduced the total number of leukocytes in both BAL and LD, but not to levels seen in non-allergic mice (Figure 4.10 A-B). As previously observed, anti-IL-13 mAb treatment profoundly reduced the number of BAL eosinophils; this effect was also evident in LD (Figure 4.10 C-D). In addition, IL-13 neutralisation partially inhibited neutrophilia in BAL and LD; an effect not seen in earlier studies (Figure 4.10 E-F). Interestingly, anti-IL-13 mAb treatment induced a modest increase in BAL and LD macrophages (Figure 4.11 A-B). In the BAL this was attributable to an increase in alveolar macrophages (AM; Figure 4.11 C) whereas both alveolar and interstitial macrophages (IM) were elevated in the lung tissue (Figure 4.11 D and F). Anti-IL-13 mAb treatment had no significant effects on the number of CD4+ or CD8+ T cells in BAL or LD after exposure to HDM (Figure 4.12 A-D). However, 582 did reduce the number of B cells present in BAL following HDM exposure, although this effect was not evident in LD (Figure 4.12 E-F). When the phenotype of infiltrating CD4+ T cells was further investigated after anti-IL-13 mAb treatment, no significant effects were observed on the accumulation of Th2, Th1 or Th17 cells in BAL or LD, although there was a trend towards reduced Th2 cells in BAL (Figure 4.13 A-F).

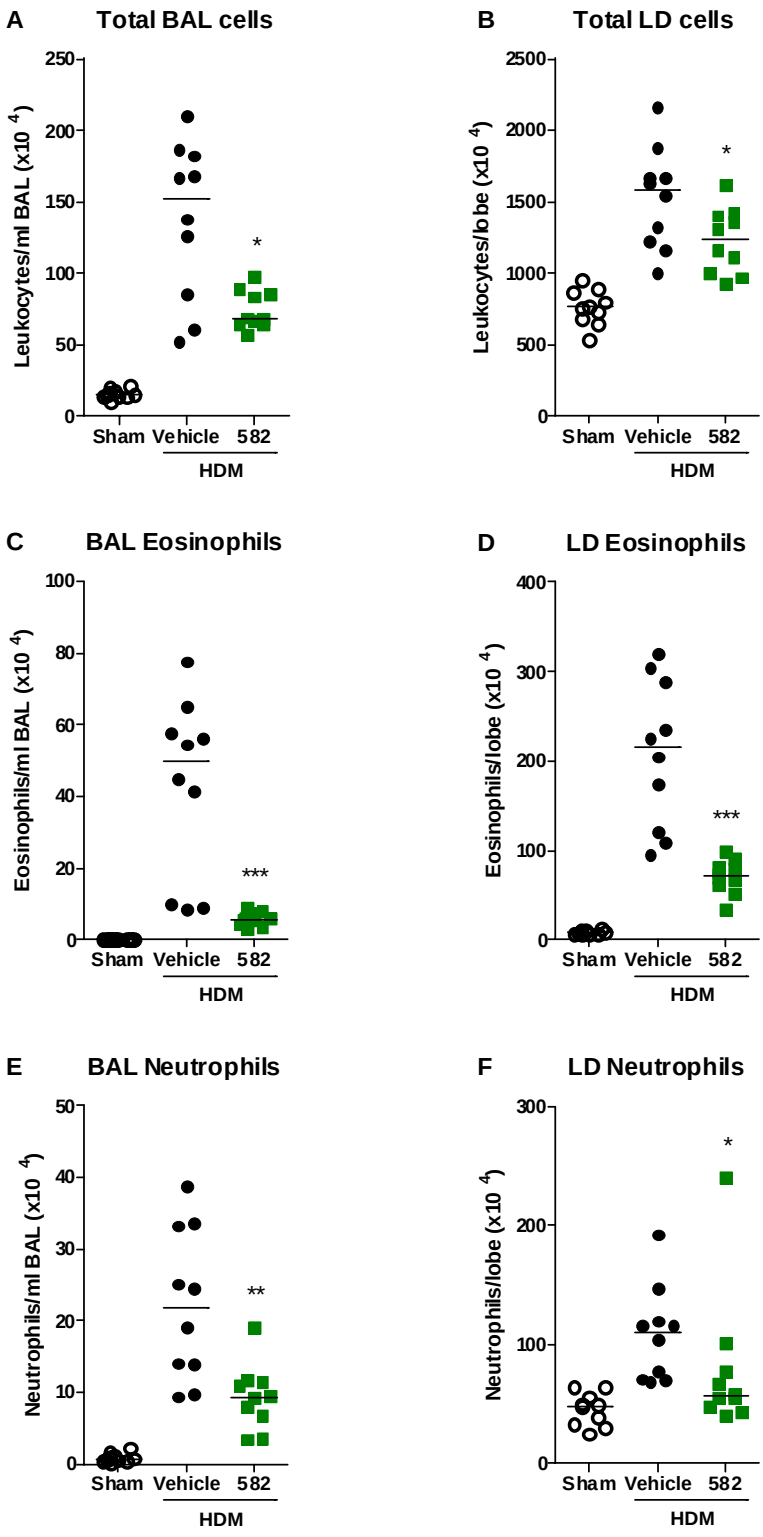


Figure 4.10 Effects of IL-13 neutralisation on HDM induced pulmonary inflammation. BAL and lungs (caudal lobe) were taken after 5 weeks of HDM exposure, 24 hours after the last HDM instillation. Mice were dosed with 10mg/kg 582 (or vehicle) s.c., weekly, throughout the HDM exposure period. Total leukocytes (A-B), eosinophils (C-D) and neutrophils (E-F) in BAL (A, C and E) and lung tissue digest (LD) (B, D and F) were identified and quantified by flow cytometry. n = 10 mice/group, bar represents median. Data represents of one of two experiments. * $p<0.05$, ** $p<0.01$ and *** $p<0.001$ relative to vehicle group by Mann Whitney test.

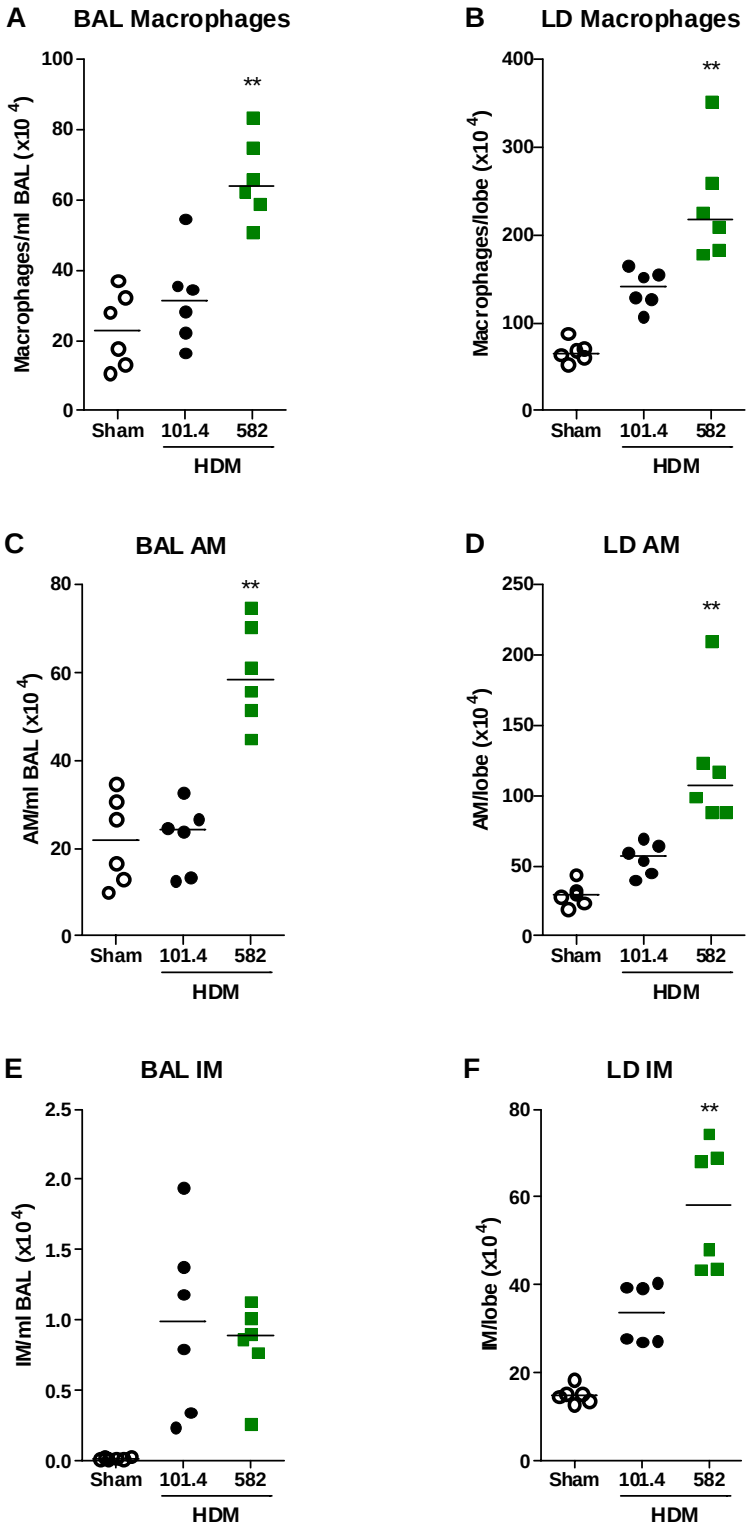


Figure 4.11 Effects of IL-13 neutralisation on macrophage accumulation. BAL and lungs (left lobe) were taken after 5 weeks of HDM exposure, 4 hours after the last HDM instillation. Mice were dosed with 10mg/kg 582 or isotype control (101.4) s.c., weekly, throughout the HDM exposure period. Total macrophages (A-B), alveolar macrophages (AM) (C-D) and interstitial macrophages (IM) (E-F) in BAL (A, C and E) and lung tissue digest (LD) (B, D and F) were identified and quantified by flow cytometry. n = 6 mice/group, bar represents median. Data represents one of two experiments. ** $p<0.01$ relative to 101.4 group by Mann Whitney test.

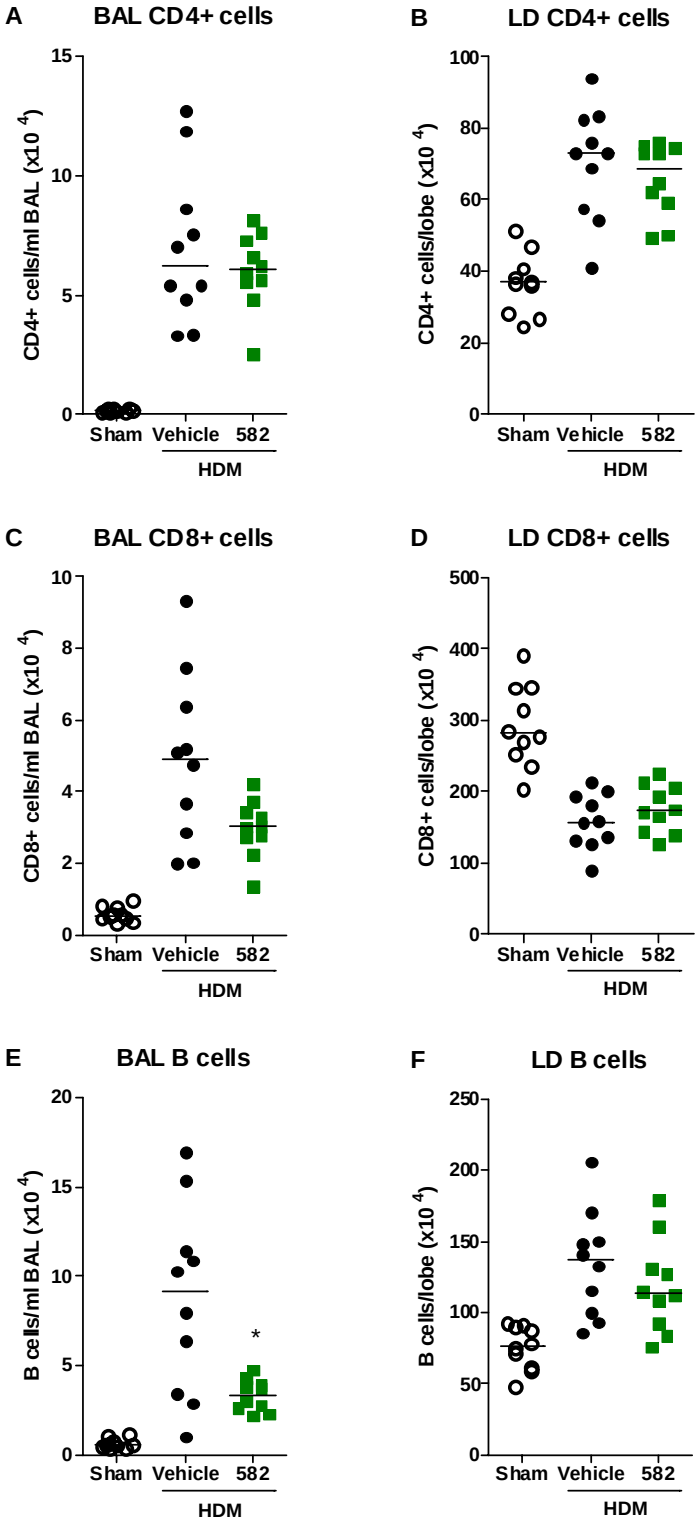


Figure 4.12 Effects of IL-13 neutralisation on HDM induced T and B cell accumulation. BAL and lungs (caudal lobe) were taken after 5 weeks of HDM exposure, 24 hours after the last HDM instillation. Mice were dosed with 10mg/kg 582 (or vehicle) s.c., weekly, throughout the HDM exposure period. CD4+ T cells (A-B), CD8+ T cells (C-D) and B cells (E-F) in BAL (A, C and E) and lung tissue digest (LD) (B, D and F) were identified and quantified by flow cytometry. n = 10 mice/group, bar represents median. * $p<0.05$ relative to vehicle group by Mann Whitney test.

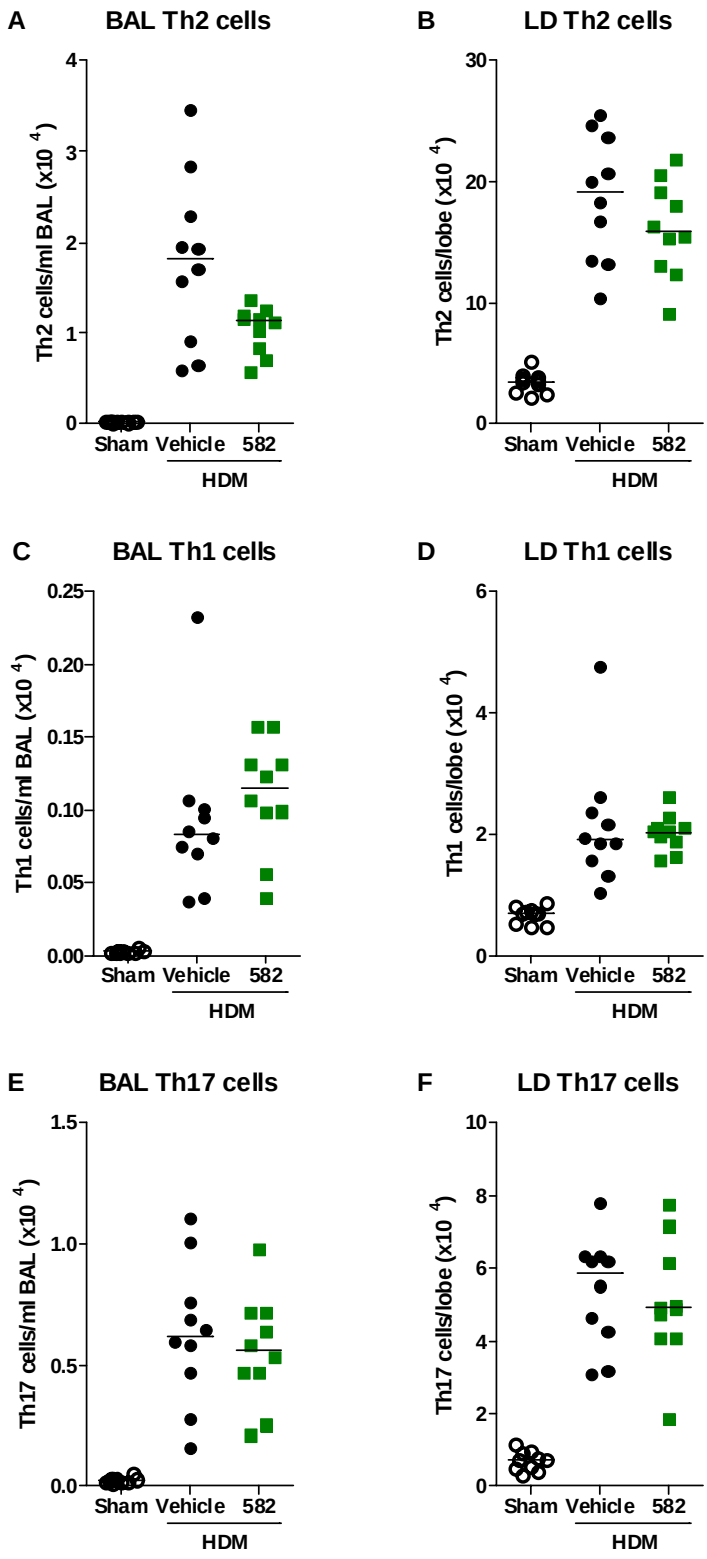


Figure 4.13 Effects of IL-13 neutralisation on T helper cell phenotype. BAL and lungs (caudal lobe) were taken after 5 weeks of HDM exposure, 24 hours after the last HDM instillation. Mice were dosed with 10mg/kg 582 (or vehicle) s.c., weekly, throughout the HDM exposure period. Th2 cells (A-B), Th1 cells (C-D) and Th17 cells (E-F) in BAL (A, C and E) and lung tissue digest (LD) (B, D and F) were identified and quantified by flow cytometry. n = 10 mice/group, bar represents median. Data represents one of two experiments.

4.3.5 Effects of IL-13 neutralisation on the cytokine milieu

Cytokine and chemokine concentrations were measured in BAL and lung homogenate (LH) supernatants by multiplex and ELISA assays 4 hours post HDM exposure after 5 weeks of concomitant HDM and anti-IL-13 mAb treatment. IL-13 neutralisation reduced IL-4 concentration in BAL, but not LH, and had no effect on the level of IL-5 in BAL or LH (Figure 4.14 A-D). BAL IL-10 was reduced by anti-IL-13 mAb treatment, although this was not observed in LH (Figure 4.14 E-F). Treatment with 582 had no effect on the levels of IFNγ, IL-12 or IL-17 in BAL or LH after HDM exposure (Figure 4.15 A-F). However IL-13 neutralisation profoundly inhibited HDM induced eotaxin in both BAL and LH and reduced BAL and LH KC concentrations (Figure 4.16 A-D). Upon analysis of the epithelial derived cytokines, anti-IL-13 mAb treatment induced a modest reduction in LH IL-25 and TSLP concentrations. No effects were seen on HDM induced IL-33 levels in LH (Figure 4.17 A-C).

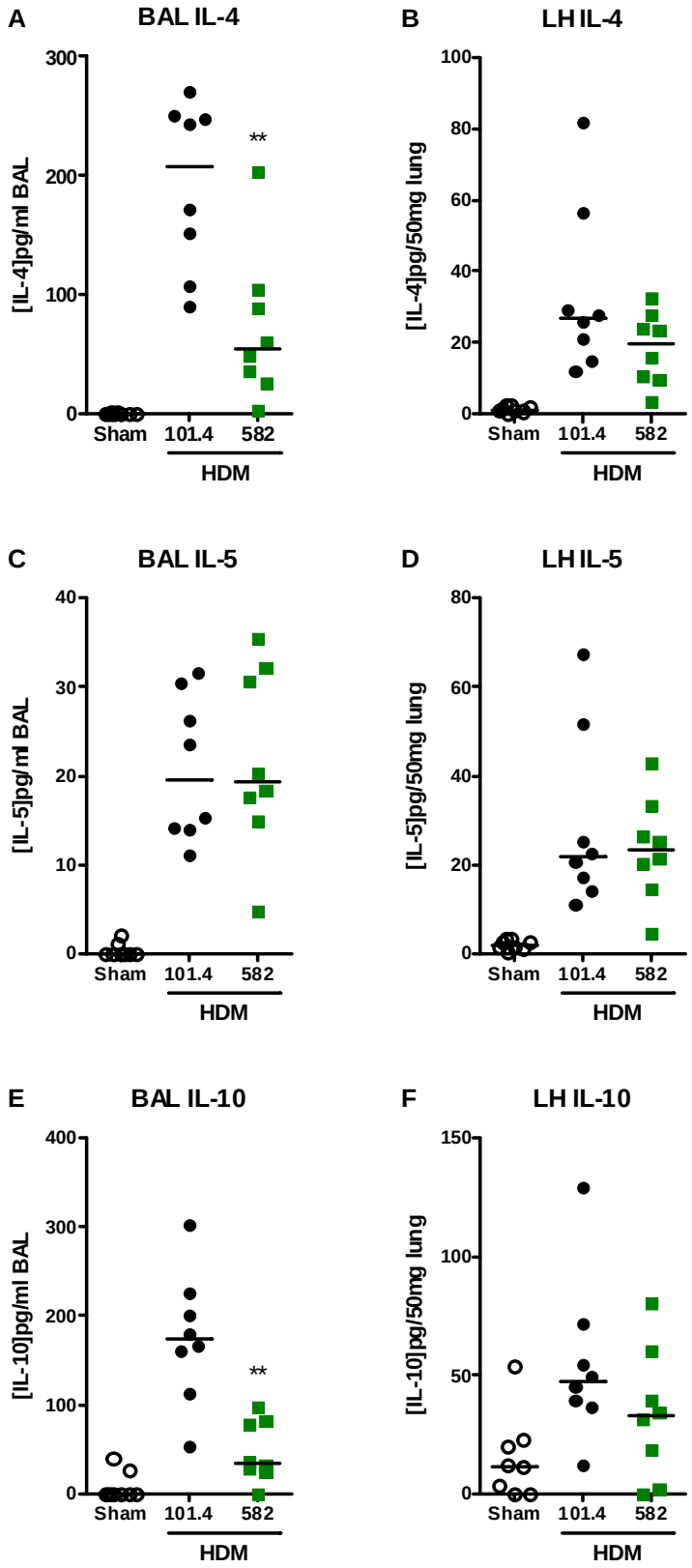


Figure 4.14 Effects of IL-13 neutralisation on IL-4, IL-5 and IL-10 production. Lungs (cranial lobe) and BAL were taken after 5 weeks of HDM exposure, 4 hours after the last HDM instillation. Mice were dosed with 10mg/kg 582 or isotype control (101.4) s.c., weekly, throughout the HDM exposure period. Cytokines were quantified in BAL and lung homogenate supernatant by MSD assay. n = 8 mice/group, bar represents median. ** $p<0.01$ relative to 101.4 group by Mann Whitney test.

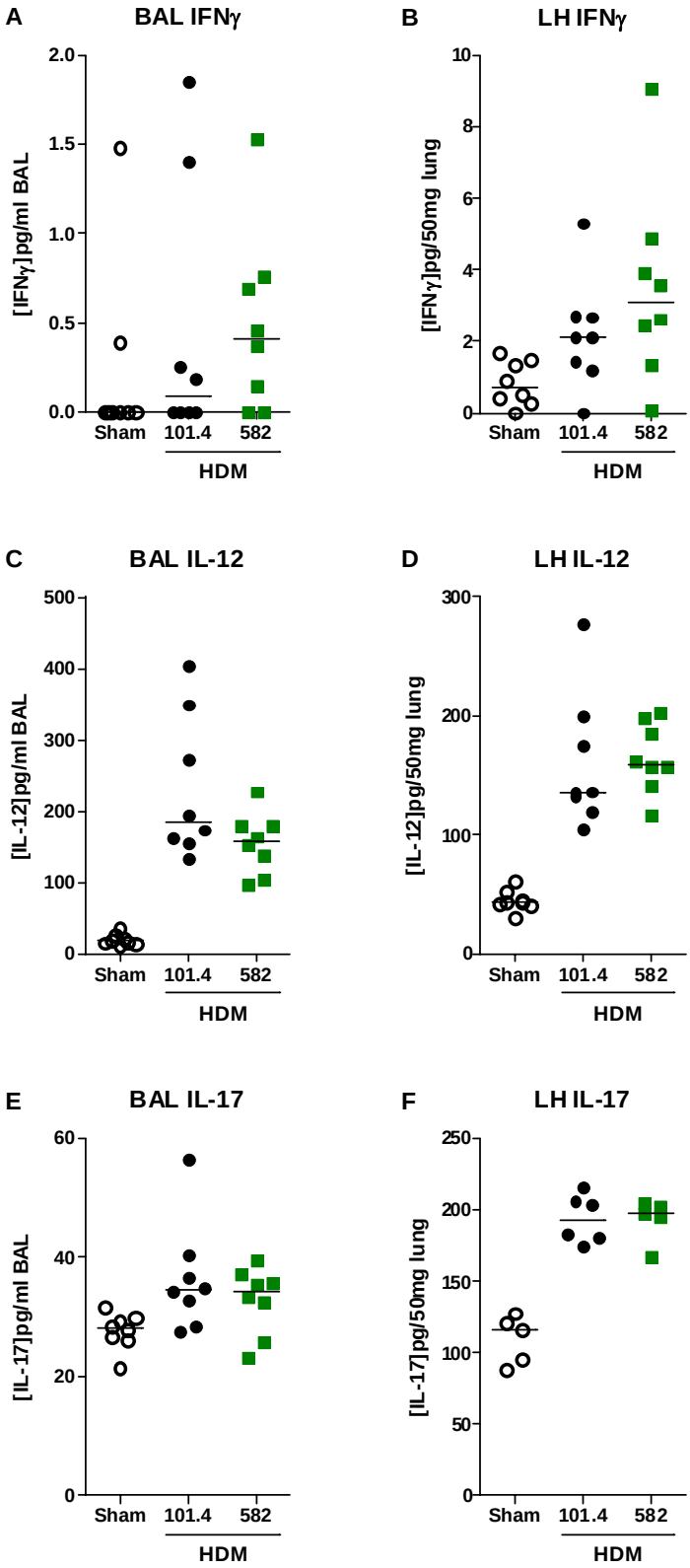


Figure 4.15 Effects of IL-13 neutralisation on IFNγ, IL-12 and IL-17 production. Lungs (cranial lobe) and BAL were taken after 5 weeks of HDM exposure, 4 hours after the last HDM instillation. Mice were dosed with 10mg/kg 582 or isotype control (101.4) s.c., weekly, throughout the HDM exposure period. Cytokines were quantified in BAL and lung homogenate supernatant by MSD assay (A-D) or ELISA (E-F). n = 5-8 mice/group, bar represents median.

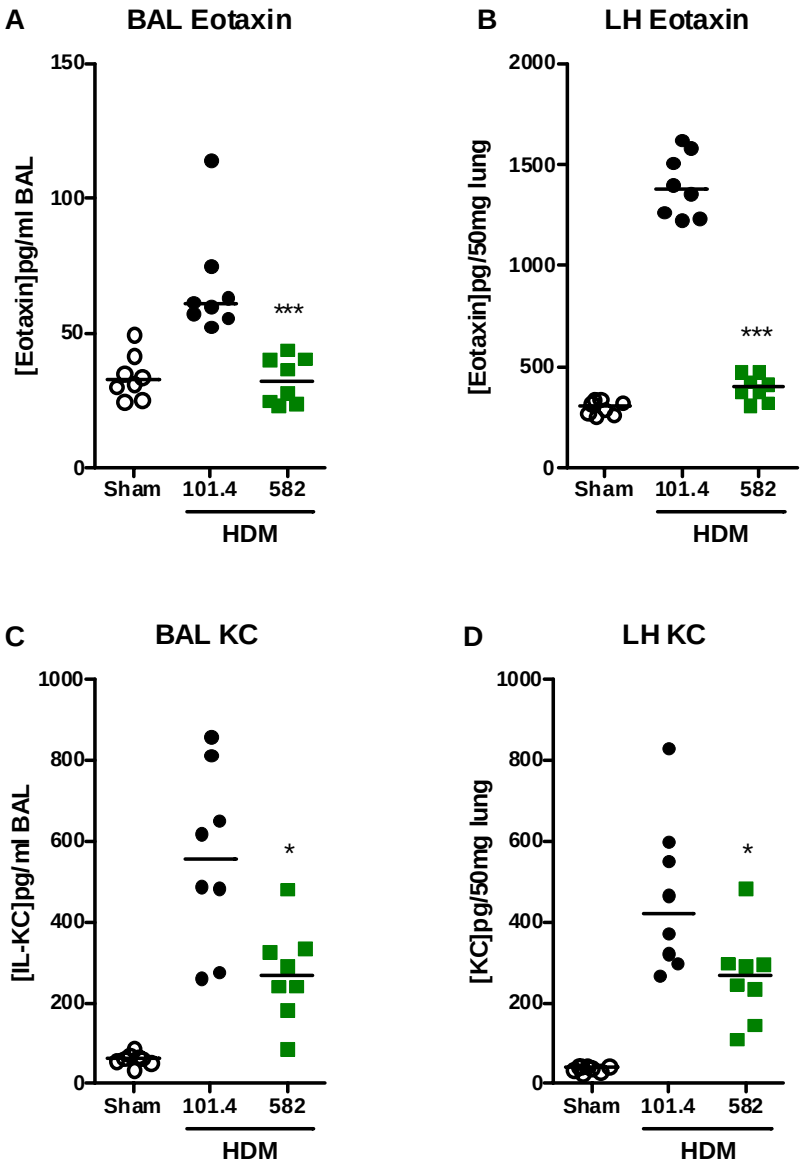


Figure 4.16 Effects of IL-13 neutralisation on chemokines. Lungs (cranial lobe) and BAL were taken after 5 weeks of HDM exposure, 4 hours after the last HDM instillation. Mice were dosed with 10mg/kg 582 or isotype control (101.4) s.c., weekly, throughout the HDM exposure period. Chemokines were quantified in BAL and lung homogenate supernatant by ELISA (A-B) or MSD assay (C-D). n = 8 mice/group, bar represents median. * $p<0.05$ and *** $p<0.001$ relative to 101.4 group by Mann Whitney test

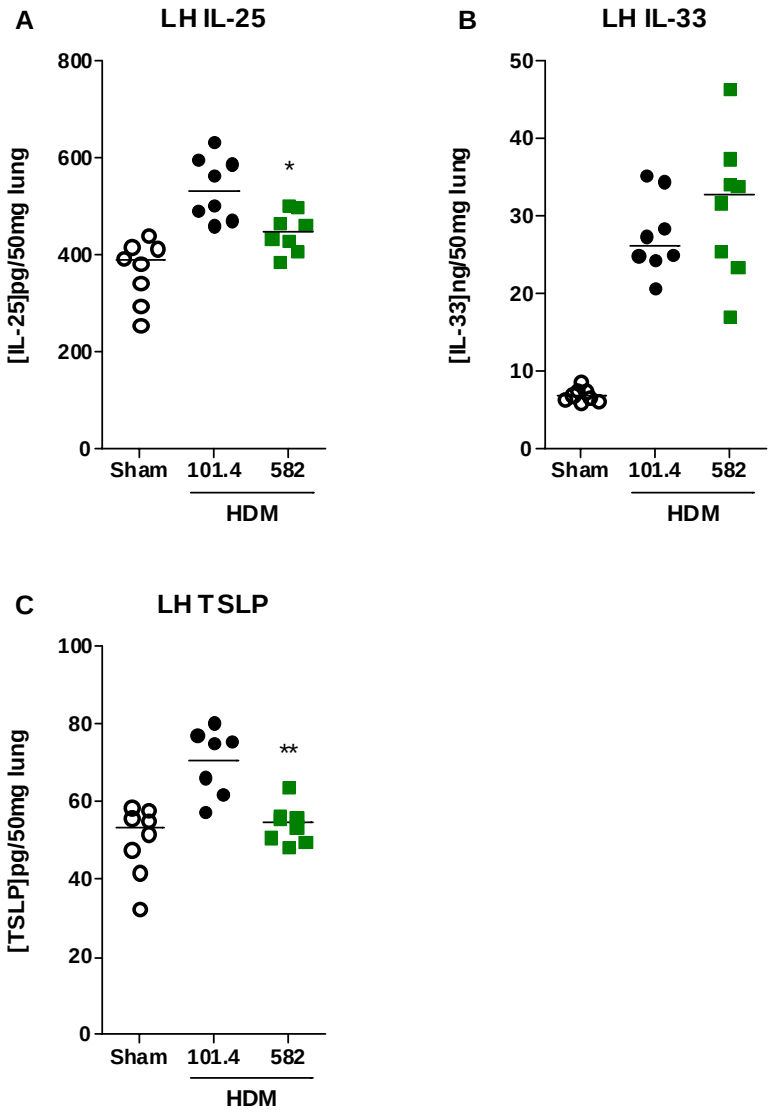


Figure 4.17 Effects of IL-13 neutralisation on epithelial derived cytokines. Lungs (cranial lobe) were taken after 5 weeks of HDM exposure, 4 hours after the last HDM instillation. Mice were dosed with 10mg/kg 582 or isotype control (101.4) s.c., weekly, throughout the HDM exposure period. Cytokines were quantified in lung homogenate supernatant by ELISA. n = 7-8 mice/group, bar represents median. * $p<0.05$ and ** $p<0.01$ relative to 101.4 group by Mann Whitney test

4.3.6 Effects of IL-13 neutralisation on antibody generation

Serum levels of total IgE and HDM specific IgE, IgG1, IgG2a and IgG2b were determined by ELISA after 5 weeks of HDM exposure and prophylactic anti-IL-13 mAb treatment. IL-13 neutralisation significantly reduced total serum IgE (Figure 4.18 A) however, no effects were observed on the generation of HDM specific IgE, IgG1, IgG2a and IgG2b in HDM exposed mice (Figure 4.18 B-E).

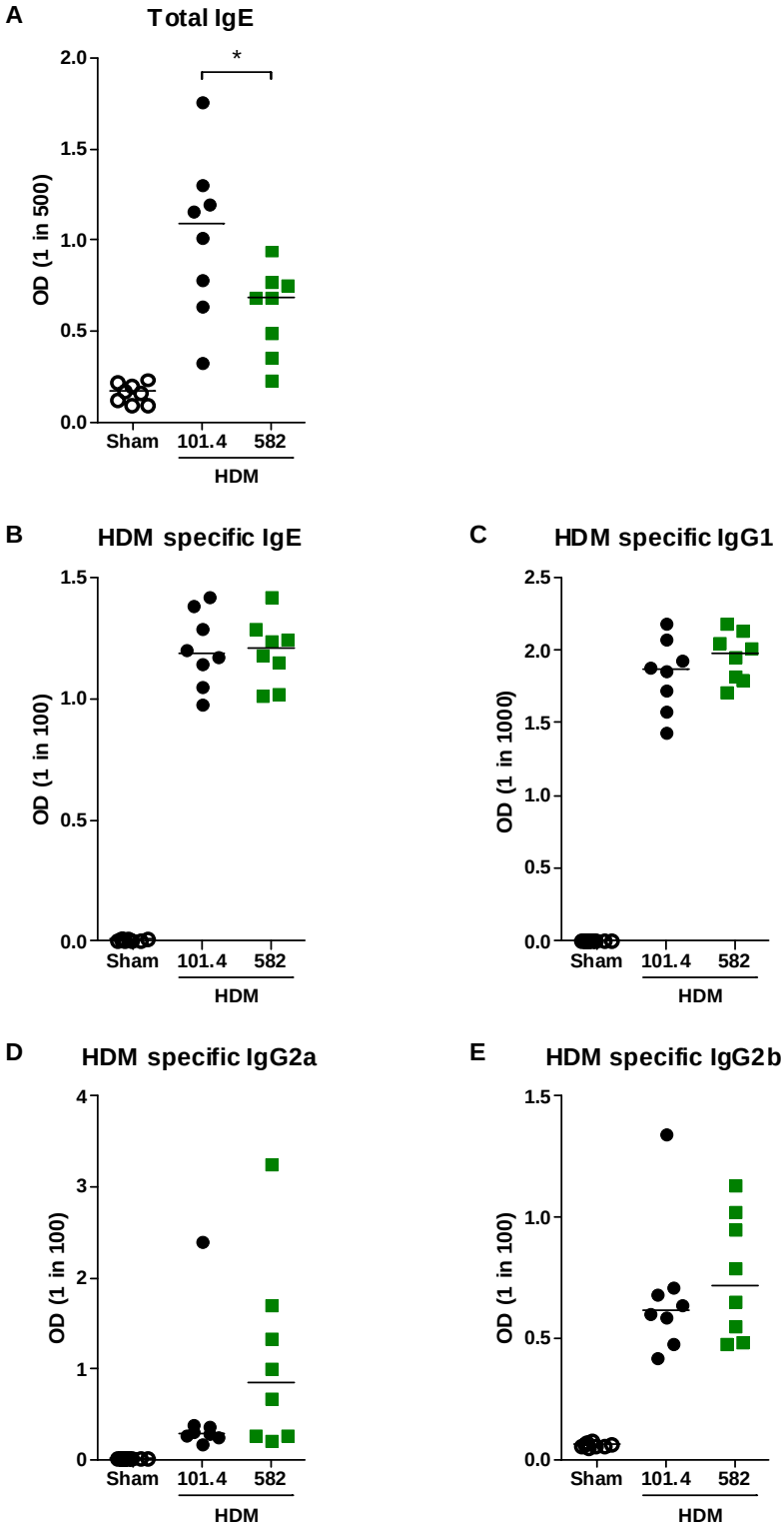


Figure 4.18 Effects of IL-13 neutralisation on antibody generation following HDM exposure. Blood was taken via cardiac puncture after 5 weeks of HDM exposure, 24 hours after the last HDM instillation. Mice were dosed with 10mg/kg 582 or isotype control (101.4) s.c., weekly, throughout the HDM exposure period. HDM specific antibodies were assessed in serum by ELISA. n = 8 mice/group, bar represents median. * $p<0.05$ by Mann Whitney test.

4.3.7 Effects of therapeutic IL-13 neutralisation

Having characterised the effects of IL-13 neutralisation during the initiation of the allergic response it was important, and more clinically relevant, to determine the effects of neutralising IL-13 after the allergic response has been established. To address this, mice were dosed with anti-IL-13 mAb therapeutically. Mice were exposed to HDM for 5 weeks to provoke airway hyperreactivity, inflammation and remodelling prior to anti-IL-13 mAb treatment. After 5 weeks mice were dosed with 10mg/kg 582 s.c. weekly for 3 additional weeks, during continued HDM exposure. For assessment of the histological parameters an additional group of HDM exposed mice was terminated immediately prior to the first anti-IL-13 mAb dose ("pre-dose"). This was to assess the degree of goblet cell frequency and peribronchial collagen deposition prior to therapeutic intervention.

Therapeutic IL-13 neutralisation partially reversed AHR to MCh. Anti-IL-13 mAb treatment returned baseline lung function to that seen in sham sensitised mice however, the inhibition of AHR in response to MCh was incomplete (Figure 4.19). Analysis of BAL cell infiltrate revealed therapeutic administration of anti-IL-13 mAb fractionally reduced the total number of BAL leukocytes. Significant reductions in the numbers of eosinophils, CD4+ T cells and specifically Th2 cells were also observed although there were no effects on the numbers of BAL neutrophils or CD8+ cells (Figure 4.20). Therapeutic anti-IL-13 mAb treatment profoundly inhibited HDM induced goblet cell up-regulation, shown by both goblet cell score and muc5ac mRNA expression (Figure 4.21 A-B). In addition, therapeutic anti-IL-13 mAb appeared to prevent collagen deposition during the dose period, but did not reduced existing peribronchial collagen. Hence collagen depth at 8 weeks, following 3 weeks of 582 treatment, was equivalent to that seen after 5 weeks of HDM exposure and significantly less than that observed after 8 weeks of HDM exposure (Figure 4.21 C).

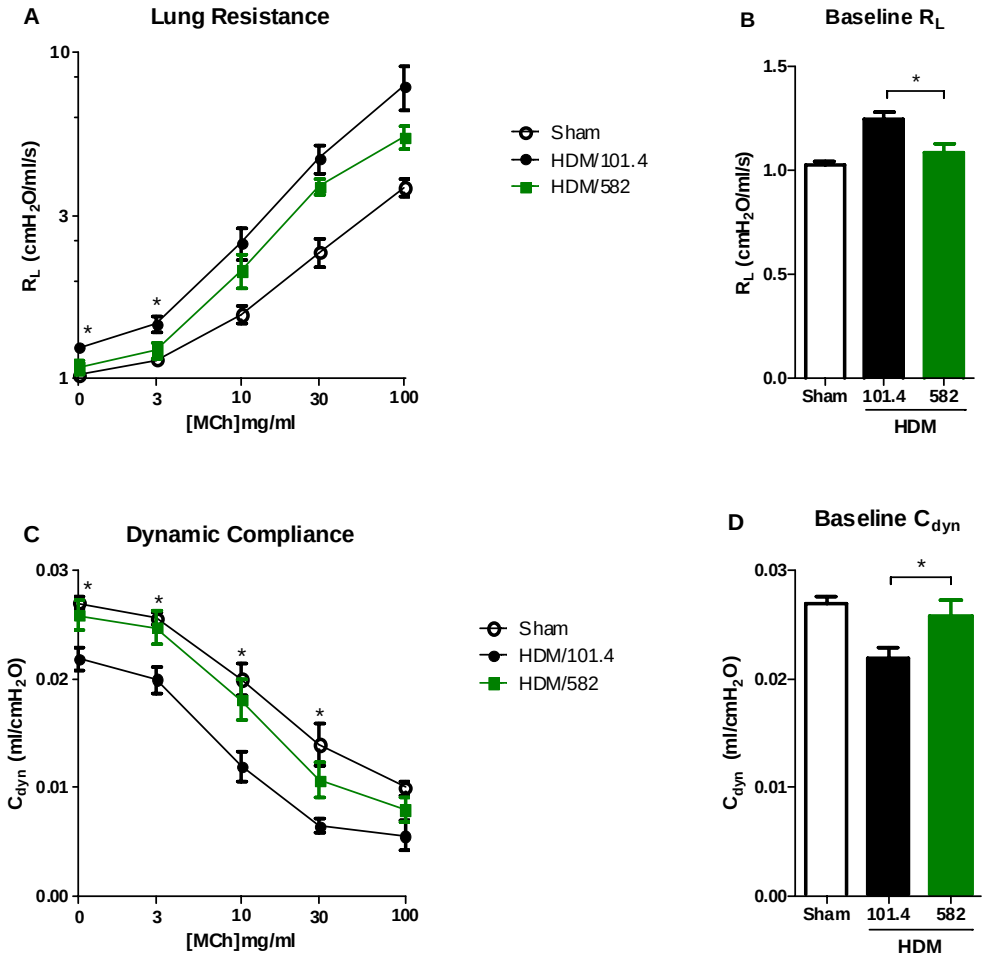


Figure 4.19 Effects of therapeutic IL-13 neutralisation on AHR. AHR to MCh was determined as changes in lung resistance (R_L) (A, C) and dynamic compliance (C_{dyn}) (B, D) measured 24 hours post HDM, after 8 weeks of HDM exposure. Mice were dosed with 10mg/kg 582 or isotype control (101.4) s.c., weekly, from week 6. Data are shown as mean ± SEM, n = 7-8 mice/group. * p<0.05 relative to HDM/101.4 group by Mann Whitney test.

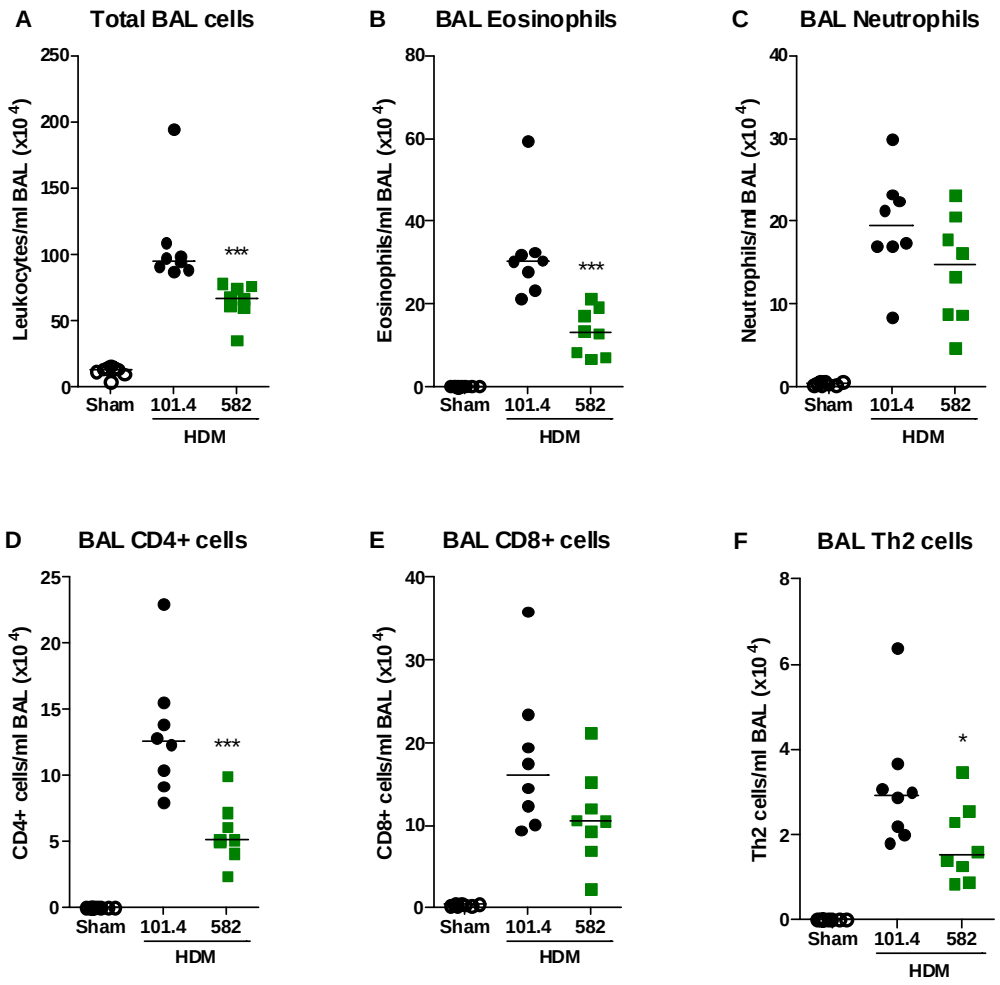


Figure 4.20 Effects of therapeutic IL-13 neutralisation on pulmonary inflammation. BAL was taken after 8 weeks of HDM exposure, 24 hours after the last HDM instillation. Mice were dosed with 10mg/kg 582 or isotype control (101.4) s.c., weekly, from week 6. Total leukocytes (A), eosinophils (B), neutrophils (C), CD4+ T cells (D), CD8+ T cells (E) and Th2 cells (F) in BAL were identified and quantified by flow cytometry. n = 8 mice/group, bar represents median. * $p<0.05$ and *** $p<0.001$ relative to HDM/101.4 group by Mann Whitney test.

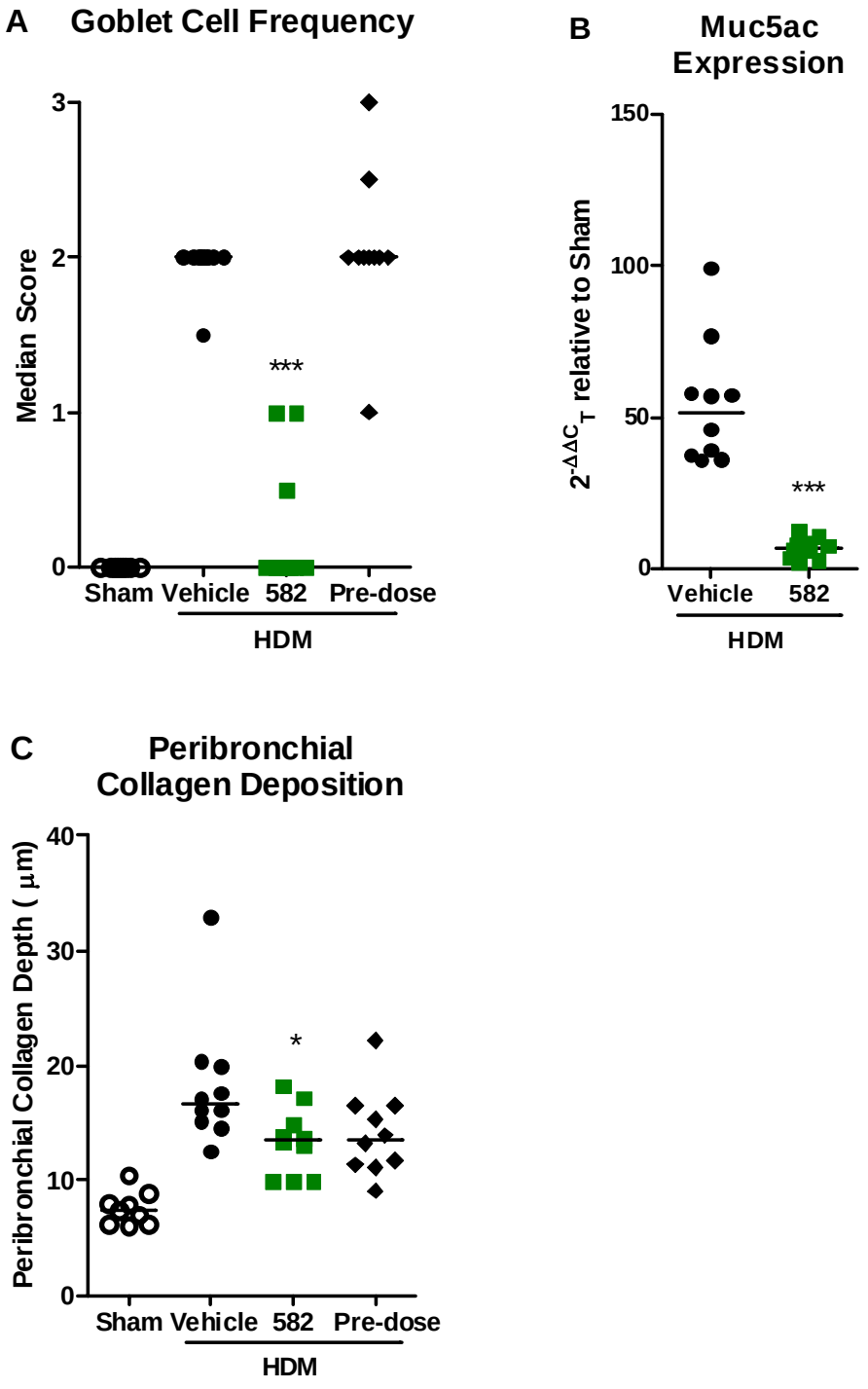


Figure 4.21 Effects of therapeutic IL-13 neutralisation on airway remodelling. Lungs were taken after 5 (pre-dose) or 8 weeks of HDM exposure, 24 hours after the last HDM instillation. Mice were dosed with 10mg/kg 582 (or vehicle) s.c., weekly, from week 6. (A) Goblet cell frequency was scored in AB/PAS stained sections. (B) Muc5ac mRNA in lung tissue was quantified by real time PCR and normalised to sham. (C) Peribronchial collagen depth was measured in Masson's trichrome stained sections. n = 9-10 mice/group, bar represents median. * $p<0.05$ and *** $p<0.001$ relative to vehicle group by Mann Whitney test.

4.4 Discussion

The objective of this chapter was to determine the effects of IL-13 neutralisation in HDM induced AAD. Prior to in depth analysis of the effects of IL-13 neutralisation in this model a preliminary dose finding study was conducted. Furthermore it was necessary to select a suitable IL-13 neutralising antibody. Once an appropriate dose and antibody was chosen the effects of both prophylactic and therapeutic IL-13 neutralisation were assessed.

4.4.1 Anti-IL-13 mAb dose selection

Prophylactic anti-IL-13 mAb treatment with mAb 582 reduced lung inflammation, specifically BAL eosinophils, although no dose-response relationship was observed over the dose range studied (0.3, 3 and 30mg/kg). Dose proportionality was apparent on analysis of airway remodelling; 3mg/kg and 30mg/kg 582 elicited comparable inhibition of goblet cell frequency and muc5ac mRNA expression, whereas 0.3mg/kg only partially reduced goblet cell frequency and had no significant effects on muc5ac mRNA expression. A similar dose-response relationship was noted in peribronchial collagen deposition although no significance reached in this study. Berry *et al.* previously reported dose dependent effects of 582 (denoted mAb A) on muc5ac mRNA up-regulation in the lungs of mice sensitised and challenged with OVA (Berry *et al.*, 2009). In this study Berry *et al.* observed significant inhibition of muc5ac expression at 10, 1 and 0.1mg/kg 582 indicating mucin expression in this model may be more sensitive to IL-13 inhibition than in HDM induced AAD.

In the current study maximal efficacy was observed at 3mg/kg 582, with no additional efficacy apparent at 30mg/kg, thus revealing the top of the dose-response curve to 582. However, in order to ensure the dose used for future studies was super-maximal, a dose of 10mg/kg was selected with which to proceed.

4.4.2 Anti-IL-13 mAb selection

Two anti-IL-13 mAbs binding distinct functional epitopes were available for use in *in vivo* neutralisation studies. 582 and 587 both bind IL-13 with high affinity (K_D 11pM and 8pM, respectively) and prevent assembly of the type II IL-4 receptor, and hence signalling (characterised by (Berry *et al.*, 2009). MAb 582 prevents IL-13 binding IL-13Rα1 and IL-13Rα2 whereas 587 permits these interactions but blocks the ensuing

association of the IL-13-IL-13Rα1 complex with IL-4Rα. Due to these differences in binding specificity a study was conducted to directly compare 582 and 587 in HDM induced AAD. Since 582 and 587 are affinity matched and previous studies have demonstrated equivalent potency both *in vitro* and *in vivo*, a single dose level of 10mg/kg was used in this study to distinguish any discrepancies in activity (Berry *et al.*, 2009).

Analysis of HDM induced inflammatory BAL cell infiltrate, AHR and airway remodelling at 5 weeks after prophylactic, weekly treatment with 10mg/kg 582 or 587 did not reveal any significant differences between the effects of 582 and 587. Both mAbs significantly reduced BAL eosinophilia, completely prevented the development of AHR assessed by WBP, blocked goblet cell up-regulation determined by histological score and inhibited peribronchial collagen deposition. Using the same mAbs Berry *et al.* demonstrated equivalent efficacy in basic models of IL-13 stimulated eotaxin release and muc5ac mRNA up-regulation in OVA sensitised and challenged mice (Berry *et al.*, 2009). Taken together these data demonstrate complete or partial disruption of the type II IL-4R is sufficient for anti-IL-13 mAb efficacy. In addition, since equivalent efficacy was observed whether IL-13Rα2 binding was blocked or permitted this indicates HDM induced AAD may be independent of IL-13Rα2 signalling. However, although IL-13 can bind IL-13Rα2 in the presence of 587, it is not known whether the IL-13-587 complex can still induce signalling via IL-13Rα2. It is possible both 582 and 587 prevent IL-13Rα2 signalling and hence both inhibit IL-13 dependent fibrosis. With respect to the role of sIL-13α2 as a decoy receptor it might be expected that preventing IL-13 binding sIL-13Rα2 would lead to reduced anti-IL-13 mAb efficacy. This was not observed with 582 in this study most likely due to the use of super-maximal anti-IL-13 mAb doses. However, even at very low doses of mAb Berry *et al.* did not observe any differences in efficacy between 582 and 587, albeit in more simplistic, acute models of IL-13 driven pathology (Berry *et al.*, 2009). These data indicate IL-13Rα2 does not play a role in driving AAD pathology or as a negative regulator of IL-13 in this mouse model.

Kasaian *et al.* evaluated the effects of two corresponding anti-human IL-13 mAbs, with receptor blocking mechanisms comparable to 582 and 587, in a cynomolgus monkey model of allergic lung inflammation driven by *Ascaris suum* (Kasaian *et al.*,

2008). The two antibodies were compared at a single dose, 10mg/kg, and elicited equivalent inhibition of BAL infiltrate, antigen specific IgE titres and histamine release from *ex vivo* stimulated basophils. This supports the present observation that anti-IL-13 mAbs with distinct receptor blocking mechanisms do not confer any functional differences in efficacy. However, the same mAbs did show some discrepancies in efficacy in a small clinical trial in mild atopic asthma (Gauvreau *et al.*, 2011). Blockade of the IL-13-IL-13Rα1 complex binding IL-4Rα significantly reduced both the early and late phase declines in lung function following allergen challenge whereas blockade of the initial interaction between IL-13 and IL-13Rα1 (and IL-13 with IL-13Rα2) had no significant effects. This may have been due to elevated levels of IL-13 detected after the latter but not former mAb therapy. In a subsequent study the authors demonstrate IL-13Rα2 plays a role in IL-13 clearance, hence blockade of IL-13Rα2 lead to accumulation of IL-13 (Kasaian *et al.*, 2011). Since IL-13 was not assessed in the present studies due to the potential for 582 and 587 to interfere with IL-13 detection it is not know whether the same mechanism of IL-13Rα2 mediated IL-13 clearance occurs in mice. The equivalent efficacy observed between 582 and 587 indicates IL-13 is not elevated when IL-13Rα2 binding is prohibited and hence that this mechanism may not occur in mice. However, the effects of IL-13 accumulation may not have been seen in the present studies due to the use of super-maximal doses of anti-IL-13 mAb. In addition, Cuff *et al.* reported that a mAb blocking IL-13 binding both IL-13Rα1 and IL-13Rα2 conferred greater efficacy than an affinity matched anti-IL-13 mAb that permitted IL-13Rα2 binding in a murine model of OVA induced lung inflammation (Cuff *et al.*, 2008). It is likely that anti-IL-13 mAb efficacy is dictated by the specific epitope for each mAb and that these differences in epitopes give rise to variations in efficacy. Furthermore, the altered distribution of soluble and membrane IL-13Rα2 in humans compared to mice further complicates these potential mechanisms of action. Of note, none of the studies discussed above assessed airway remodelling; a potential axis in which IL-13Rα2 may play a role and hence potentially a key differentiating feature between the two mAbs.

In summary, no differences in efficacy were observed between 582 and 587 in HDM induced AAD in mice. 582 was selected for use in future studies investigating the

mechanisms of IL-13 inhibition in AAD due to it's ability to block IL-13 binding both IL-13Rα1 and IL-13Rα2 and hence inhibit all potential components of IL-13 induced pathology.

4.4.3 Effects of prophylactic IL-13 neutralisation in HDM induced AAD

The effects of IL-13 neutralisation have previously been reported in mouse models of lung inflammation driven by OVA and fungal antigens and in sensitised sheep and NHP models. However the role of IL-13 in HDM induced AAD in mice has not been reported, hence the current series of experiments was conducted to determine the effects of prophylactic IL-13 neutralisation in mice chronically exposed to HDM for 5 weeks. As established in previous studies, IL-13 was neutralised with 10mg/kg 582 weekly. See Table 4.1 for a summary of IL-13 dependent effects observed in the present series of experiments.

4.4.3.1 AHR

Prophylactic administration of anti-IL-13 mAb prevented the development of HDM induced AHR to MCh, assessed by direct measurement of R_L and C_{dyn}. This confirmed previous assessments of AHR determined by WBP after prophylactic 582 treatment. In addition, assessment of R_L and C_{dyn} revealed anti-IL-13 mAb treatment prevented the HDM induced decline in basal lung function measured prior to MCh exposure. A role for IL-13 in the development of AHR has previously been demonstrated in acute OVA induced models of lung inflammation using IL-13 deficient mice, *Il13ra1*$^{-/-}$ mice, sIL-13Rα2-Fc fusion protein, polyclonal anti-IL-13 and monoclonal anti-IL-13 antibodies (Walter *et al.*, 2001;Leigh *et al.*, 2004b;Grunig *et al.*, 1998;Wills-Karp *et al.*, 1998;Leigh *et al.*, 2004a;Wang & McCusker, 2005;Yang *et al.*, 2004;Eum *et al.*, 2005). However, the use of alum in these models to induce a Th2 response may be biasing the system towards IL-13 dependency. Blease *et al.* assessed the role of IL-13 in the development of AHR in fungal induced AAD using a polyclonal anti-IL-13 antibody (Blease *et al.*, 2001). This model does not use alum although peripheral sensitisation with antigen in incomplete freunds adjuvant is still required to sensitise the mice. Neutralisation of IL-13 in this model also abrogated AHR. Furthermore, this study demonstrated that inhibition of AHR can be achieved by neutralisation of IL-13 during antigen challenge and that IL-13 neutralisation during sensitisation is not required for ablation of AHR. However,

there is also evidence that IL-13 neutralisation does not effect AHR when anti-IL-13 treatment is commenced after chronic allergen challenge at a time-point when inflammation has resolved but airway remodelling persists (Leigh *et al.*, 2004a). Importantly, this indicates aspects of AHR are independent of IL-13 and are instead attributable to the persistence of airway remodelling. Taken together with the present study, these data prove the presence of IL-13 during allergen exposure in the lung is critical for the development of AHR, irrespective of the allergen or adjuvant used.

The development of AHR is multi-factorial. Inflammatory processes play a key role however, other factors such as airway wall remodelling (as illustrated by Leigh *et al.*) and neuronal control of airway tone also play a role in AHR. In addition, airway wall oedema and epithelial desquamation can influence AHR. Direct mediators of AHR include cytokines such as IL-13, IL-25 and IL-33 derived from T cells and epithelial cells, amongst others, and lipid mediators such as leukotrienes, prostaglandins and histamine released from mast cells and eosinophils. The mechanisms by which IL-13 drives AHR in HDM induced AAD are unknown; it may be via direct action of IL-13 on ASM, via the activation and degranulation of mast cells and eosinophils, via remodelling of the airway wall or most likely a combination of these factors. IL-13 neutralisation prevented airway remodelling and inhibited various aspects of inflammation in the present study, which may contribute to the inhibition of AHR. However, IL-13 neutralisation does not alter the generation of antigen specific IgE and the effects of IL-13 neutralisation on the production of lipid mediators in HDM induced AAD is unknown. Thus the precise mechanisms by which anti-IL-13 mAb treatment prevents AHR in this model are unknown.

4.4.3.2 Inflammation

In the present study anti-IL-13 mAb treatment inhibited the total number of leukocytes infiltrating the BAL and lung tissue. This was primarily accounted for by the profound reduction in BAL and tissue eosinophilia induced by anti-IL-13 mAb. The role of IL-13 in allergen induced eosinophilia has been well established however relatively limited analysis of BAL and lung tissue inflammatory infiltrates has been conducted in previous studies reporting the effects of IL-13 neutralisation *in vivo*. As observed in HDM exposed mice, total BAL cells were reduced after IL-13 neutralisation with sIL-13Rα2-Fc in an acute model of OVA induced lung

inflammation (Leigh *et al.*, 2004a). Lung and BAL eosinophilia have also been demonstrated to be IL-13 dependent in acute OVA models by the employment of *Il13*$^{-/-}$ mice, *Il13ra1*$^{-/-}$ mice, sIL-13Rα2-Fc and anti-IL-13 mAb (Leigh *et al.*, 2004b;Munitz *et al.*, 2008;Grunig *et al.*, 1998;Yang *et al.*, 2004). However, not all studies observed reduced eosinophilia with sIL-13Rα2-Fc or anti-IL-13 intervention (Wills-Karp *et al.*, 1998;Leigh *et al.*, 2004a;Eum *et al.*, 2005). This may be due to subtle differences in the dosing regimes employed, sensitisation and challenge protocols or, in some cases the strain of mice used. Where reduced eosinophilia was apparent, lack of IL-13 or IL-13 neutralisation did not completely abrogate lung eosinophilia. In the present study, BAL eosinophilia was almost completely dependent upon IL-13 mediated effector pathways. However, a small degree of eosinophilia persisted in the tissue after IL-13 neutralisation indicating some IL-13 independent factors contribute to the accumulation of eosinophils in the lung tissue.

In the current study, anti-IL-13 mAb treatment prevented elevation of the eosinophil chemo-attractant eotaxin in the BAL and tissue of HDM exposed mice. This corresponds with reduced eosinophilia following anti-IL-13 mAb treatment. Profound inhibition of allergen induced eotaxin and the consequent reduction in eosinophilia has previously been demonstrated in OVA sensitised and challenged *Il13ra1*$^{-/-}$ mice and anti-IL-13 mAb treated mice (Yang *et al.*, 2004;Munitz *et al.*, 2008). In addition, eotaxin mRNA expression was significantly reduced in *Il13ra1*$^{-/-}$ mice compared to wild type mice following SEA sensitisation and challenge (Ramalingam *et al.*, 2008). These data indicate that the primary mechanism driving eosinophilia in HDM exposed mice is via IL-13 dependent production of eotaxin. However, IL-13 and eotaxin independent pathways as identified by Munitz *et al.* may also be contributing to tissue eosinophilia (Munitz *et al.*, 2008).

The Th2 cytokine IL-5 can also induce eosinophilia and is up-regulated in both BAL and lungs following HDM exposure. However, IL-5 production is not dependent upon IL-13 in this mouse model. In OVA models IL-5 generation has also been demonstrated to be IL-13 independent using an anti-IL-13 mAb and *Il13ra1*$^{-/-}$ mice however, Yang *et al.* observed reduced LH IL-5 following anti-IL-13 mAb treatment (Yang *et al.*, 2005;Eum *et al.*, 2005;Munitz *et al.*, 2008). Furthermore, IL-5 mRNA was actually increased in lung tissue from *Il13ra1*$^{-/-}$ mice compared to wild type in an

SEA driven model of lung inflammation although protein concentrations are not reported (Ramalingam *et al.*, 2008). In human ASM there is evidence IL-13 stimulates IL-5 production (Grunstein *et al.*, 2002), thus the requisite of IL-13 for IL-5 generation may be species dependent. The IL-13 independent production of IL-5 in the present study may account for the low level of lung eosinophilia still present after anti-IL-13 mAb treatment.

Partial inhibition of neutrophilia was noted in BAL and lung tissue of 582 treated HDM exposed mice, however this effect was not consistently observed across all experiments (Figures 4.3 C, 4.5 B and 4.10 E). Accordingly, anti-IL-13 mAb treatment also partially reduced levels of the neutrophil chemoattractant KC in BAL and lung tissue. In the literature, no significant reduction of BAL neutrophils has been demonstrated following IL-13 neutralisation despite Yang *et al.* reporting a reduction in KC in the lung tissue in an acute OVA model (Grunig *et al.*, 1998;Yang *et al.*, 2004). Munitz *et al.* reported an increase in BAL neutrophils in OVA sensitised and challenged *Il13ra1*$^{-/-}$ mice (Munitz *et al.*, 2008). The present data suggest a component of HDM induced neutrophilia is dependent upon IL-13 induced KC however, KC production and neutrophilia is also driven by IL-13 independent events. One such pathway might be IL-17 stimulated KC production (Witowski *et al.*, 2000); IL-17 is up-regulated in HDM exposed mice and not affected by IL-13 neutralisation. The balance between these IL-13 dependent and independent pathways in eliciting neutrophilia may account for the differences observed in OVA and HDM driven models of lung inflammation.

Interestingly, IL-13 neutralisation in HDM exposed mice appeared to increase the number of macrophages in BAL and LD. Classification of these macrophages into alveolar (AM) and interstitial (IM) macrophage phenotypes revealed the elevation in BAL macrophages to be attributable to an increase in AM, whereas both AM and IM sub-populations were increased in the tissue (Bedoret *et al.*, 2009). Administration of anti-IL-13 mAb to sham exposed mice had no effect on the number of lung macrophages (data not shown). Ramalingham *et al.* also reported an increase in macrophages in the lungs of *Il13ra1*$^{-/-}$ mice in an SEA induced model of allergic lung inflammation, thus corroborating observations in the present HDM study (Ramalingam *et al.*, 2008). Taken together these data suggest the IL-13/IL-13Rα1

axis may play a role in regulating the number of macrophages in the lungs during AAD. The functional consequences of increased accumulation of macrophages with respect to AAD pathogenesis is unknown and therefore warrants further investigation.

IL-13 neutralisation had no significant effects on accumulation of CD4+ or CD8+ T cells in BAL and lung tissue of HDM exposed mice. Detailed analysis of the effects of IL-13 neutralisation on T cells in the lung and BAL has not previously been reported, although no effects on the total numbers of BAL lymphocytes or mononuclear cells were demonstrated with sIL-13Rα2-Fc or anti-IL-13 mAb treatment in acute OVA models (Wills-Karp *et al.*, 1998;Yang *et al.*, 2004). Upon further analysis of T cell phenotypes in the present study, a non-significant trend towards reduced BAL Th2 cells was observed, although not evident in the tissue. This reduction in BAL Th2 cells did reach significance in repeat studies (Tomlinson *et al.*, 2010). Analysis of the key Th2 differentiating cytokine IL-4 revealed IL-13 neutralisation reduced BAL IL-4. Inhibition of IL-4 secretion in the absence of IL-13 has previously been observed *ex vivo*, in stimulated lymph node cells from SEA sensitised *Il13*$^{-/-}$ mice (McKenzie *et al.*, 1998). However *in vivo*, BAL IL-4 levels in mice sensitised and challenged with OVA were equivalent in *Il13ra1*$^{-/-}$ and wild type mice (Munitz *et al.*, 2008). Furthermore, IL-4 mRNA expression in an SEA model of lung inflammation in was actually increased in *Il13ra1*$^{-/-}$ compared to wild type mice (Ramalingam *et al.*, 2008). Hence, Munitz and Ramalingam propose the development of Th2 responses is IL-13Rα1 independent. Data from the present study supports this hypothesis. IL-13 neutralisation had no effect on the generation of HDM specific antibodies, specifically IgE and IgG1, suggesting a competent Th2 response is mounted in the absence of IL-13 stimulation. Since Th2 cells (and naïve T cells) do not express IL-13Rα1, the contribution of IL-13 to Th2 responses must be indirect (Zurawski & de Vries, 1994;de Waal *et al.*, 1995;Graber *et al.*, 1998). Hence, the modest effect on accumulation of BAL Th2 cells is likely to be downstream of the development of Th2 immunity, such as inhibition of Th2 cell trafficking to the lungs by reduced TARC expression or down-regulation of adhesion molecules. TARC is a specific chemotactic factor for Th2 cells which selectively express the TARC receptor CCR4 (Bonecchi *et al.*, 1998;Imai *et al.*, 1999). IL-13 neutralisation reduced BAL IL-4. This may be due in part to the reduction in BAL Th2 cells however; IL-13 may also be modulating IL-4 expression in cells such as DC, macrophages, basophils and

innate lymphoid cells present in the lungs. In summary, contrary to early reports from McKenzie *et al.* of *Il13*$^{-/-}$ mice, the present data demonstrate Th2 differentiation occurs independently of IL-13 (McKenzie *et al.*, 1998). Thus, the role of IL-13 in AAD is in modulating events downstream of Th2 cell development.

IL-13 neutralisation in the current study had no significant effects on HDM induced accumulation of Th1 or Th17 cells in BAL or tissue. Accordingly, no significant modulation of the Th1 cytokines IL-12 and IFNγ or the Th17 cytokine IL-17 was observed following anti-IL-13 mAb treatment. IL-13 has previously been reported to negatively regulate Th17 cells *in vitro*; however no changes in the frequency of Th17 cells, or IL-17 production were observed in the absence of IL-13 in the present study indicating this phenomenon may not be applicable *in vivo* (Newcomb *et al.*, 2009). Thus, IL-13 neutralisation suppresses functions of Th2 immunity, without altering opposing Th1 or Th17 responses.

Anti-IL-13 mAb treatment reduced the number of B cells in BAL although this effect was not seen in the tissue. Unlike human B cells, mouse B cells do not express IL-13 receptors and hence IL-13 has no direct effects on mouse B cells (Punnonen *et al.*, 1993;Gauchat *et al.*, 1997;Graber *et al.*, 1998). Hence, as with Th2 cells, this reduction in BAL infiltrate is likely to be a reflection of IL-13 dependent modulation of factors controlling cell recruitment; however there are no previous reports of tissue infiltration of B cells following IL-13 depletion or neutralisation. In accordance with the lack of IL-13 receptor expression on mouse B cells, isotype switching and the subsequent production of HDM specific antibodies in the present study were IL-13 independent. This has previously been demonstrated in mice sensitised and challenged with OVA in which IL-13 neutralisation had no affect on OVA specific IgE titres (Wills-Karp *et al.*, 1998;Taube *et al.*, 2002;Wang & McCusker, 2005). Contrary to this, Yang *et al.* reported anti-IL-13 mAb intervention reduced OVA specific IgE titres, but not OVA specific IgG1 and IgG2a titres, in an acute OVA model (Yang *et al.*, 2004). This latter study indicates IL-13 may play an indirect role in IgE production. Of note, IL-13 neutralisation does reduce allergen specific IgE in NHPs (Kasaian *et al.*, 2008) and would be predicted to affect IgE production in man due to the expression of IL-13Rα1 on human B cells (Punnonen *et al.*, 1993;Zurawski & de Vries, 1994). Interestingly, anti-IL-13 mAb treatment does reduce total serum

IgE in the current study. This has previously been demonstrated in *Il13*$^{-/-}$ and *Il13ra1*$^{-/-}$ mice, both naïve and sensitised, and implicates IL-13 in the homeostatic control of IgE levels (McKenzie *et al.*, 1998;Munitz *et al.*, 2008;Ramalingam *et al.*, 2008). In addition, transgenic over-expression of IL-13 in mice results in increased serum titres of total IgE (Emson *et al.*, 1998). It has been proposed that IL-13 controls the spontaneous production of natural IgE by a subpopulation of B2 cells (Munitz *et al.*, 2008;McCoy *et al.*, 2006). Thus, IL-13 does not play a role in the production of antigen specific antibodies in mice, possibly because this process is dependent on T cell help, the generation of which is IL-13 independent. However, IL-13 is required for the modulation of total IgE titres.

Cytokine analysis of BAL in the present study revealed IL-13 neutralisation reduced levels of the regulatory cytokine IL-10. This appears contrary to the general reduction in inflammation observed with anti-IL-13 mAb treatment however, IL-13 has previously been reported to inhibit IL-10 production from LPS stimulated monocytes (de Waal *et al.*, 1993). Furthermore, HDM extract contains endotoxin thus providing a potential mechanism for the IL-13 dependent down-regulation of IL-10 in HDM induced AAD. However, *Il13ra1*$^{-/-}$ mice sensitised and challenged with OVA exhibit elevated BAL IL-10 (Munitz *et al.*, 2008). These discrepancies may be due to the added effects of inhibiting IL-4 signalling in *Il13ra1*$^{-/-}$ mice, not affected during IL-13 specific inhibition.

HDM induced IL-25 and TSLP levels in the lung were also inhibited by anti-IL-13 mAb treatment in the present study. The effects of IL-13 neutralisation on IL-25 and TSLP have not previously been reported in models of AAD. The primary function of these epithelial derived cytokines is to promote the initiation of Th2 immunity upon insult to the airway epithelium i.e. upon activation of pattern recognition receptors such as TLRs and protease-activated receptors (Paul & Zhu, 2010;Ziegler & Artis, 2010). However, TSLP mRNA expression has previously been reported to be up-regulated in human bronchial epithelial cells following IL-13 stimulation *in vitro* (Kato *et al.*, 2007), indicating a TSLP-IL-13 loop may play a role inTh2 amplification (Paul & Zhu, 2010). Conversely, there is no evidence suggesting IL-25 can act downstream of IL-13, thus the effects of IL-13 neutralisation on IL-25 production may be indirect (Barlow & McKenzie, 2009;Fort *et al.*, 2001).

4.4.3.3 Remodelling

IL-13 is proposed to be a key mediator of airway remodelling in AAD and asthma. Its role in the pathogenesis of airway remodelling is in part via direct action on epithelial cells, fibroblasts and ASM. In addition, IL-13 may promote airway remodelling indirectly by stimulating the release of pro-fibrotic mediators such as TGFβ and growth factors e.g. PDGF (Malavia *et al.*, 2008;Ingram *et al.*, 2004). In the present studies HDM induced structural changes within the airway wall were shown to be IL-13 dependent. Increased goblet cell frequency and muc5ac mRNA expression were completely abrogated by IL-13 neutralisation, despite the persistence of some inflammatory components such as neutrophilia. The role of IL-13 in goblet cell up-regulation has previously been established in OVA driven models of AAD. Allergen induced goblet cell hyperplasia is absent in *Il13*$^{-/-}$ mice (Walter *et al.*, 2001;Leigh *et al.*, 2004b) and profoundly reduced in wild type mice treated with sIL-13Rα2-Fc or anti-IL-13 mAb (Grunig *et al.*, 1998;Wills-Karp *et al.*, 1998;Yang *et al.*, 2004). In an alternative model of AAD driven by fungal antigen Blease *et al.* also demonstrated goblet cell hyperplasia was sensitive to IL-13 inhibition, using a polyclonal anti-IL-13 antibody (Blease *et al.*, 2001). Thus, IL-13 is essential for goblet cell metaplasia/hyperplasia and muc5ac mRNA up-regulation in AAD, apparently irrespective of allergen.

In the current study peribronchial collagen deposition was prevented by prophylactic administration of anti-IL-13 mAb to HDM exposed mice. Accordingly, OVA induced subepithelial fibrosis has been shown to be completely abrogated in *Il13*$^{-/-}$ mice and mice treated with anti-IL-13 mAb (Leigh *et al.*, 2004b;Yang *et al.*, 2004). Similarly, subepithelial fibrosis is dependent upon IL-13 in AAD driven by exposure to fungal antigen (Blease *et al.*, 2001). These data demonstrate IL-13 is critical for the excessive deposition of collagen along the basement membrane during AAD. Furthermore, the prevention of airway remodeling in the present study may, in part, contribute to anti-IL-13 mAb induced inhibition of AHR.

4.4.4 Effects of therapeutic IL-13 neutralisation in HDM induced AAD

Having defined the effects of prophylactic IL-13 neutralisation in HDM induced AAD a therapeutic dosing protocol was employed to evaluate the effects of IL-13 neutralisation in established AAD. In these studies anti-IL-13 mAb treatment was not

commenced until significant airway hyperreactivity, inflammation and remodelling were present, thus, based on the time-course of pathophysiology characterised in chapter 3 dosing began after 5 weeks of HDM exposure. After which administration of anti-IL-13 mAb continued for a further 3 weeks during concomitant HDM exposure. As in previous studies, IL-13 was neutralised with 10mg/kg 582 s.c. weekly. It is of greater clinical relevance to understand the role of IL-13 in maintaining established AAD and whether features of airway pathophysiology are reversible because prophylactic therapy of asthma is not feasible. See Table 4.1 for a summary of therapeutic anti-IL-13 mAb effects compared to prophylactic anti-IL-13 mAb treatment.

4.4.4.1 AHR

AHR was partially reversed by therapeutic IL-13 neutralisation in HDM exposed mice. Specifically, anti-IL-13 mAb treatment reversed the HDM induced changes in basal lung function and attenuated changes in C_{dyn}, however inhibition of R_L was incomplete with anti-IL-13 mAb treatment. Thus, HDM induced changes in basal lung function and MCh induced decline in C_{dyn} are dependent on the continued presence of IL-13, while MCh induced increases in R_L are in part IL-13 independent. This is contrary to the effects of prophylactic anti-IL-13 mAb treatment in which HDM induced changes in basal lung function, MCh induced C_{dyn} and R_L are completely IL-13 dependent. Hence, IL-13 is required for the development of AHR but not for the persistence of particular aspects of AHR. These data demonstrate that HDM induced AHR is not driven solely by the direct actions of IL-13 on ASM. Furthermore, this may be indicative of the IL-13 independent AHR associated with airway remodelling observed by Leigh *et al.*, particularly in light of the effects of therapeutic anti-IL-13 mAb on collagen deposition in the present study (Leigh *et al.*, 2004a); therapeutic IL-13 neutralisation inhibited collagen deposition, but did not affect the level of collagen deposited prior to treatment.

Changes in basal lung function may be attributable to a combination of airway remodelling, mucus hyper-secretion, airway wall oedema (and therefore inflammation) and changes in airway tone. Since therapeutic IL-13 neutralisation completely reversed the decline in basal lung function, the predominant determinants of basal lung function must also require the continued presence of IL-13. The effects

of anti-IL-13 mAb on airway tone are unknown however goblet cell up-regulation was completely dependent on the presence of IL-13 whilst only partial inhibition of inflammation and collagen deposition was achieved with therapeutic anti-IL-13 mAb treatment. Thus linking mucus over-production with HDM induced changes in basal lung function.

The effects of therapeutic IL-13 neutralisation observed on MCh induced AHR were greater with respect to C_{dyn} than R_L demonstrating anti-IL-13 mAb treatment has differential effects on the compliance and resistance aspects of MCh induced AHR. Increases in R_L are predominantly determined by ASM contraction, i.e. bronchoconstriction, and accumulation of mucus in large, conducting airways whereas the decline in C_{dyn} is governed by changes in the small airways such as oedema in addition to ASM contraction. Hence the present results suggest therapeutic neutralisation of IL-13 reverses changes in the small airways such as oedema. In the conducting airways, therapeutic anti-IL-13 mAb treatment reversed goblet cell up-regulation indicating the residual deficit in R_L following IL-13 neutralisation may be attributable to incomplete inhibition of bronchoconstriction. In addition, this irreversible component of AHR may be attributable to airway remodelling, as previously suggested.

In the literature the extent to which IL-13 neutralisation can inhibit established AHR is variable and is likely to depend heavily on the antigen exposure protocol and the relative length of the anti-IL-13 treatment period. In mice sensitised to OVA anti-IL-13 mAb treatment during the last 17 days of a 31 day challenge period completely reversed AHR assessed by WBP however anti-IL-13 treatment for the last 14 days of a 42 day challenge period in a comparable model only partially reduced Penh at the top MCh concentration (Yang *et al.*, 2005;Kumar *et al.*, 2004). Furthermore, IL-13 neutralisation in OVA sensitised mice 4 weeks after cessation of chronic OVA challenge had no effect on AHR (Leigh *et al.*, 2004a). Similarly IL-13 neutralisation after chronic challenge with multiple, combined allergens did not reduce AHR (Goplen *et al.*, 2009), although IL-13 neutralisation after antigen challenge in a fungal model of AAD did inhibit AHR (Blease *et al.*, 2001). Parallels may be drawn between therapeutic treatment in chronically sensitised mice and experimental models of asthma in larger mammals in which animals are naturally sensitised to allergen and

are likely to experience multiple challenges prior to therapeutic intervention. Antigen induced AHR in sheep naturally sensitised to *Ascaris suum* is completely abrogated by pre-challenge anti-IL-13 treatment (Kasaian *et al.*, 2007). However, this efficacy is not supported by recent clinical data investigating the activity of IL-13 neutralisation in patients with atopic asthma. Neither anti-IL-13 mAb treatment, nor administration of a dual IL-4/IL-13 inhibitor pitrakinra, had any significant effects on AHR (Gauvreau *et al.*, 2010;Wenzel *et al.*, 2007). These studies did demonstrate that IL-13 neutralisation improved lung function during the allergen induced late phase response or during both the early and late phase responses (Wenzel *et al.*, 2007;Gauvreau *et al.*, 2010). In addition, IL-13 neutralisation with lebrikizumab in patients with uncontrolled asthma has been demonstrated to improve basal lung function (Corren *et al.*, 2011). Thus, the effects of therapeutic IL-13 neutralisation on AHR observed in HDM exposed mice more accurately reflect data emerging from the clinic than data derived from prophylactic studies. The improvement in basal lung function elicited by therapeutic administration of anti-IL-13 mAb in HDM exposed mice could be indicative of the diminished late phase response or improved lung function observed in anti-IL-13 mAb clinical trials.

4.4.4.2 Inflammation

As with prophylactic treatment, therapeutic anti-IL-13 mAb treatment significantly reduced the total number of BAL cells and eosinophils. Therapeutic IL-13 neutralisation also reduced the numbers of BAL CD4+ T cells and Th2 cells; an effect not consistently seen with prophylactic IL-13 neutralisation. No significant effects on the numbers of BAL neutrophils or CD8+ T cells were observed. A reduction in total BAL cells and reduced eosinophilia following therapeutic IL-13 neutralisation has previously been described in OVA induced AAD (Taube *et al.*, 2002;Kumar *et al.*, 2004;Yang *et al.*, 2005). Although there are no reports of effects on specific T cell subsets, Yang *et al.* demonstrated therapeutic anti-IL-13 mAb treatment elicited a modest reduction in the number of BAL mononuclear cells whilst Taube *et al.* showed no significant effects on the number of BAL lymphocytes (Yang *et al.*, 2005;Taube *et al.*, 2002). In agreement with the current study, no effects on the accumulation of BAL neutrophils were observed by Yang or Taube (Yang *et al.*, 2005;Taube *et al.*, 2002). Interestingly, IL-13 neutralisation in an NHP model of AAD also demonstrated reduced accumulation of total cells and eosinophils post-allergen

challenge (Bree *et al.*, 2007), although these effects were not consistently significant (Kasaian *et al.*, 2008). Bree *et al.* also noted anti-IL-13 mAb treatment reduced BAL neutrophilia (Bree *et al.*, 2007). Significantly, IL-13 neutralisation with anti-IL-13 mAb or pitrakinra in patients with atopic asthma showed no changes in the number of sputum eosinophils post allergen challenge compared to placebo, highlighting inconsistencies between animal models of asthma and clinical disease (Wenzel *et al.*, 2007;Gauvreau *et al.*, 2010). In summary, the present study demonstrates IL-13 is required for the perpetuation of certain aspects of airway inflammation in HDM induced AAD such as eosinophilia and accumulation of Th2 cells however, this may not hold true in man.

4.4.4.3 Remodelling

Therapeutic administration of anti-IL-13 mAb reversed HDM induced goblet cell hyperplasia and the corresponding up-regulation of muc5ac mRNA. In accordance with the current study therapeutic IL-13 neutralisation consistently abrogated goblet cell up-regulation in OVA and *Aspergillus* induced AAD (Taube *et al.*, 2002;Kumar *et al.*, 2004;Yang *et al.*, 2005;Blease *et al.*, 2001). IL-13 neutralisation after the allergen challenge period did not affect goblet cell frequency (Leigh *et al.*, 2004a). These data indicate the maintenance of goblet cells during allergen exposure requires IL-13, whereas the frequency of goblet cells after cessation of allergen exposure is independent of IL-13. In addition, the reduction in goblet cells and therefore mucin production in the current study may contribute to the improvement of basal lung function by prohibiting the formation of mucus plugs in the airways.

In the present study therapeutic IL-13 neutralisation prevented peribronchial collagen deposition although treatment did not reverse existing subepithelial fibrosis. Comparable results have been obtained in OVA and *Aspergillus* induced AAD (Yang *et al.*, 2005;Blease *et al.*, 2001) and accordingly IL-13 neutralisation after allergen challenge does not reduce established collagen deposition (Leigh *et al.*, 2004a). Due to the invasive nature of assessing airway remodelling, no data is available on the effects of IL-13 neutralisation in NHP models or early clinical trials. Thus, IL-13 is required for the deposition of collagen within the airway wall during allergen exposure, but once laid down the maintenance of subepithelial collagen is independent of IL-13. This persistence of airway remodelling independently of IL-13

is proposed to account for IL-13 independent aspects of AHR, observed in the present study as a residual deficit in MCh induced changes in R_L following anti-IL-13 mAb treatment (Leigh *et al.*, 2004a).

Therapeutic IL-13 neutralisation has been demonstrated to reduce HDM induced changes in lung function, eosinophilia, goblet cell frequency and collagen deposition in the present study. By comparison, treatment with current asthma therapies in a similar mouse model of AAD has demonstrated HDM induced inflammation to be highly sensitive to therapeutic administration of oral or inhaled corticosteroids (Ulrich *et al.*, 2008). Oral prednisolone and i.n. fluticasone both dose-dependently inhibited the accumulation of eosinophils, neutrophils and lymphocytes in BAL. Furthermore, prednisolone reduced mRNA expression of various pro-inflammatory mediators in the lung tissue. However, corticosteroid treatment only partially inhibited HDM induced expression of Th2 cytokine mRNAs, including IL-13, and as a likely consequence inhibition of muc5ac mRNA only reached 64% at the top dose of corticosteroid used. Although the effects of corticosteroid therapy on HDM induced changes in lung function and airway remodelling have not been reported, these data suggest that IL-13 and hence IL-13 induced airway pathology may be relatively resistant to corticosteroid therapy. Indeed, airway disease induced by adenoviral expression of IL-13 has been demonstrated to be corticosteroid resistant (Therien *et al.*, 2008). If this also holds true for clinical asthma, novel IL-13 neutralising therapies could provide added efficacy in combination with corticosteroid therapy.

In summary, after selection of an appropriate dose and anti-IL-13 antibody, the effects of both prophylactic and therapeutic IL-13 neutralisation in HDM induced AAD have been characterised. Lung function, eosinophilia, goblet cell hyperplasia and subepithelial fibrosis have been identified as dependent upon IL-13 in this model. In addition, preliminary data obtained using two different anti-IL-13 mAbs recognising distinct functional epitopes demonstrate that prevention of IL-13 signalling through partial or full disruption of the type II IL-4 receptor complex is sufficient for efficacy, irrespective of IL-13Rα2 binding.

		Prophylactic		Therapeutic	
Lung function	Baseline R_L	↓↓↓		↓↓	
	Baseline C_{dyn}	↓↓↓		↓↓↓	
	AHR (R_L)	↓↓↓		↓	
	AHR (C_{dyn})	↓↓↓		↓↓	
Inflammatory cells		**BAL**	**Tissue**	**BAL**	**Tissue**
	Total cells	↓↓	↓	↓	ND
	Eosinophils	↓↓↓	↓↓	↓↓	ND
	Neutrophils	↓↓	↓↓↓	-	ND
	Total macrophages	↑	↑	ND	ND
	AM	↑	↑	ND	ND
	IM	-	↑	ND	ND
	CD4+ T cells	-	-	↓↓	ND
	CD8+ T cells	-	-	-	ND
	B cells	↓↓	-	ND	ND
	Th2	-	-	↓	ND
	Th1	-	-	ND	ND
	Th17	-	-	ND	ND
Mediators	IL-4	↓↓	-	ND	ND
	IL-5	-	-	ND	ND
	IL-10	↓↓↓	-	ND	ND
	IFNγ	-	-	ND	ND
	IL-12	-	-	ND	ND
	IL-17	-	-	ND	ND
	Eotaxin	↓↓↓	↓↓↓	ND	ND
	KC	↓↓	↓	ND	ND
	IL-25	ND	↓↓	ND	ND
	IL-33	ND	-	ND	ND
	TSLP	ND	↓↓↓	ND	ND
Antibodies	Total IgE	↓		ND	
	HDM specific IgE	-		ND	
	HDM specific IgG1	-		ND	
	HDM specific IgG2a	-		ND	
	HDM specific IgG2b	-		ND	
Remodelling	Goblet cells	↓↓↓		↓↓↓	
	Muc5ac mRNA	↓↓↓		↓↓↓	
	Peribronchial Collagen	↓↓↓		↓↓↓	

Table 4.1 Summary of IL-13 effects. Table summarises the significant effects of prophylactic or therapeutic treatment with anti-IL-13 mAb in HDM induced AAD. – No effect; ↓ <50% inhibition; ↓↓ >50% inhibition; ↓↓↓ >75% inhibition; ↑ elevation; ND not determined.

5. IL-13 RECEPTOR DISTRIBUTION

5.1 Introduction

Multiple cells types have been reported to be responsive to IL-13, many of which are present in the lungs during AAD such as monocytes, macrophages, DC, eosinophils, mast cells, epithelial cells, fibroblasts, ASM and endothelial cells. However, much of this data is derived from *in vitro* systems which do not reflect the complexity of the lung microenvironment or the cocktail of mediators that cells are likely to be exposed to *in vivo* and hence may not accurately represent pathways involved in the allergic response *in vivo*. Furthermore, few studies have substantiated IL-13 responsiveness with analysis of IL-13 receptor expression on the cell surface. In addition, data on the expression of IL-13 receptors in tissues is limited and has not yet been conducted in the context of AAD.

The previous chapter established many pathophysiological features of HDM induced AAD were dependent upon IL-13, including airway eosinophilia, AHR, goblet cell hyperplasia and peribronchial collagen deposition. To further elucidate the mechanisms involved in IL-13 driven pathology the present studies were conducted to investigate IL-13 receptor expression by cells within the lung tissue and circulation. Determination of the phenotype of IL-13 receptor expressing cells could then indicate IL-13 responsive cells that may be involved in driving AAD. Furthermore, modulation of receptor expression during the course of HDM exposure, compared to sham, could be relevant to IL-13 dependent pathways involved in AAD. Since both IL-13Rα1 and IL-13Rα2 are capable of signalling, it was important to investigate expression of both receptor subunits in HDM induced AAD. Moreover, initial analysis of mRNA was followed up with determination of protein expression on the cell surface where possible, in order to verify that the receptor would be accessible to extracellular IL-13.

5.1.1 Aim

3. To determine the distribution of IL-13 receptors in naïve and inflamed airways. The key cell types expressing IL-13Rα1 and IL-13Rα2 will be identified.

The aim of this chapter was to identify IL-13 receptor expressing cells within the lungs and circulation of HDM exposed mice. And hence reveal the cell types implicated in IL-13 driven pathology to further elucidate the mechanisms involved in anti-IL-13 mAb inhibition of AAD.

5.2 Methods

5.2.1 IL-13Rα2 ELISA

IL-13Rα2 ELISA protocol was directly replicated from Tabata *et al.* (Tabata *et al.*, 2006). Briefly, plates were coated with 1μg/ml goat anti-mouse IL-13Rα2 pAb (R&D Systems, AF539) overnight, washed twice, blocked for 1 hour with 1% BSA then washed a further two times. Samples and standards (rmIL-13Rα2-Fc, R&D Systems, 539-1R) were loaded onto plates in duplicate and incubated for 2 hours and washed four times followed by incubation with biotinylated anti-mouse IL-13Rα2 (R&D Systems, BAF539) at 0.5μg/ml for 2 hours. After washing four times, streptavidin-HRP (R&D Systems, DY998) at 1 in 200 was loaded onto the plates, incubated for an hour then washed four times more. Peroxidase activity was revealed by addition of TMB and the reaction subsequently stopped with H_2SO_4 and read at 450-650nm.

5.2.2 IL-13Rα1 staining for flow cytometry

Goat anti-human IL-13Rα1 polyclonal with cross-reactivity to mouse (Santa Cruz Biotechnologies, sc-27861) was used to stain LD and BAL cells for analysis of receptor expression. Cells were stained with 10μg/ml anti-IL-13Rα1 primary or control goat IgG (R & D Systems, AB-108-C) for 20min at +4ºC then washed prior to incubation with additional extracellular staining antibodies. Donkey anti-goat IgG $F(ab')_2$-Cy5 or $F(ab')_2$-Dy-light 649 secondary (Jackson ImmunoResearch, 705-176-147 or 705-496-147, respectively) was added to the cells at a dilution of 1 in 200, together with the relevant extracellular staining cocktail. Cells were subsequently washed and treated according to the staining protocol in materials and methods.

For visualisation of cells stained for flow cytometry stained samples were spun onto slides by cytocentrifugation according to 2.10.3. After air-drying slides were mounted for imaging using ProLong Gold antifade reagent with DAPI (Invitrogen P36935).

5.3 Results

5.3.1 IL-13 receptor mRNA expression following HDM exposure

To determine whether the expression of IL-13 receptor subunits in the lungs was modulated during the development of HDM induced AAD the relative levels of IL-13Rα1, IL-13Rα2 and IL-4Rα specific mRNA were quantified by real-time PCR. No significant changes in IL-13Rα1 mRNA expression were observed after 1, 3 or 5 weeks of HDM exposure, compared to sham (Figure 5.1 A). IL-13Rα2 mRNA however, was significantly up-regulated by exposure to HDM. Increased expression, relative to sham, was apparent after just one week of HDM exposure and further elevated by over 100-fold by weeks 3 and 5 (Figure 5.1 B). Exposure to HDM induced a modest reduction in expression of IL-4Rα at week 1 compared to sham, followed by increased expression after weeks 3 and 5 weeks of HDM (Figure 5.1 C).

5.3.2 IL-13Rα2 expression following HDM exposure.

Soluble IL-13Rα2 (sIL-13Rα2) protein levels in BAL, lung homogenate (LH) and serum were determined over 5 weeks of HDM exposure to verify the increased expression of IL-13Rα2 mRNA described above. Compared to sham, no changes in BAL sIL-13Rα2 concentrations were observed following 1, 3 or 5 weeks of HDM exposure (Figure 5.2 A). Levels of sIL-13Rα2 protein in LH were increased above sham after 3 weeks of HDM exposure, and further elevated after 5 weeks (Figure 5.2 B). sIL-13Rα2 protein was also detected in the serum of HDM exposed mice, though only differed significantly from sham at week 3 (Figure 5.2 C).

The greatest expression of both IL-13Rα2 mRNA and protein in the lung tissue was observed after 5 weeks of HDM exposure. Therefore, lungs from this time point were used for IF staining to localise IL-13Rα2 within the tissue. IL-13Rα2 was detected in the airway epithelia of sham exposed mice (Figure 5.3 A-B). Following exposure to HDM the whole lung tissue stained positively for IL-13Rα2, with the airway epithelia remaining the brightest signal (Figure 5.3 D-E). This HDM induced up-regulation of IL-13Rα2 expression in the lung tissue confirmed the elevation of IL-13Rα2 mRNA and protein in HDM exposed mice previously detected by real time PCR and ELISA, respectively.

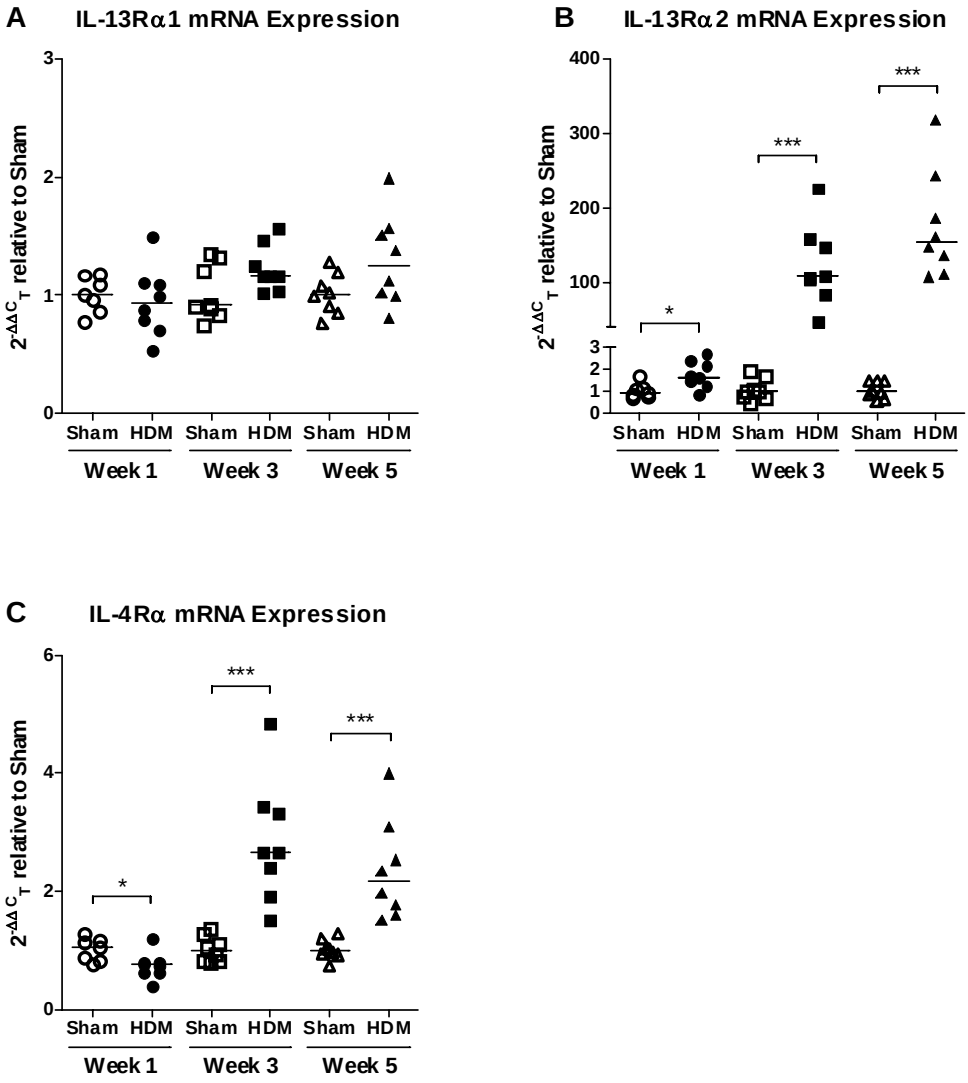


Figure 5.1 IL-13 receptor expression following exposure to HDM. Lungs were taken after 1, 3 or 5 weeks of HDM exposure, 4 hours after the last HDM instillation. mRNA in lung tissue was quantified by real time PCR and normalised to sham; (A) IL-13Rα1, (B) IL-13Rα2 and (C) IL-4Rα mRNA. n = 7-8 mice/group, bar represents median. * $p<0.05$ and *** $p<0.001$ by Mann Whitney test.

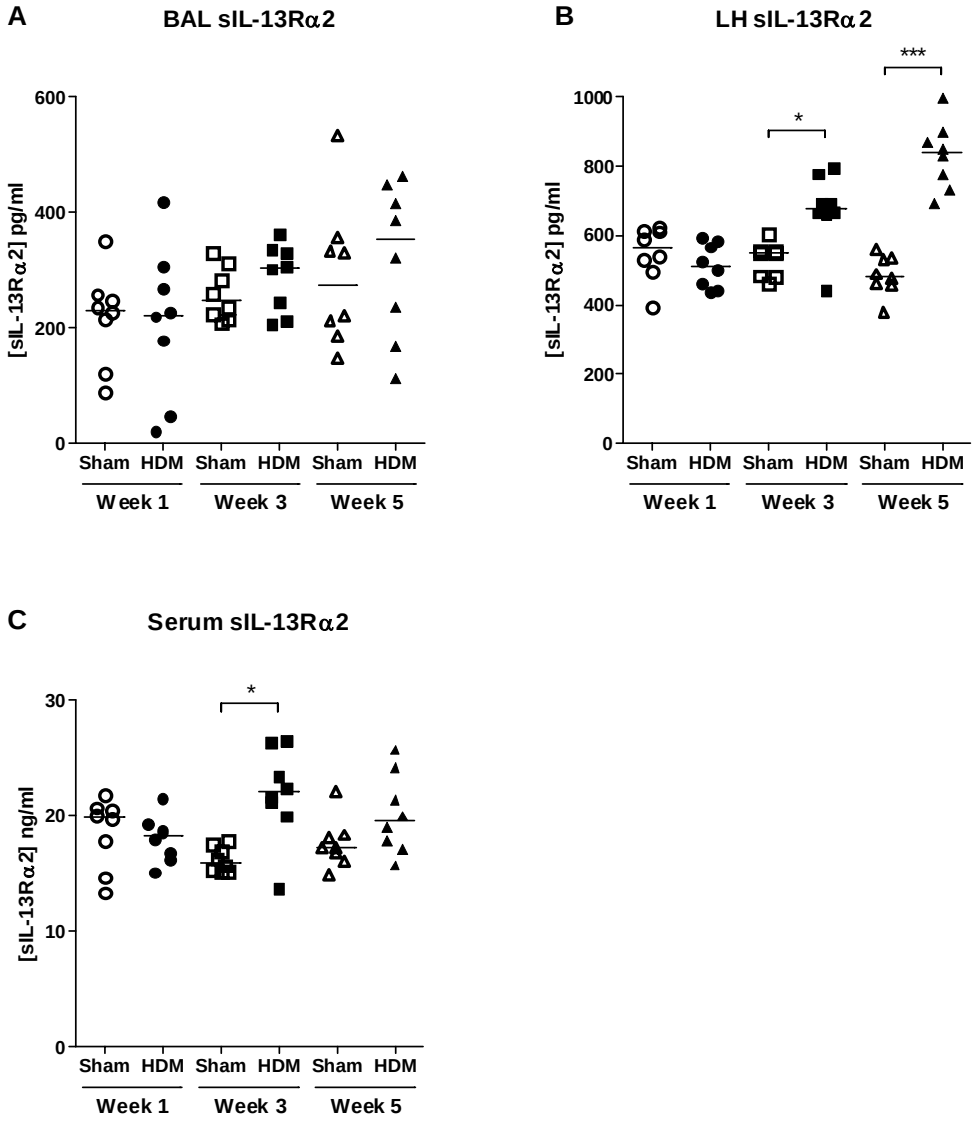


Figure 5.2 IL-13Rα2 concentrations following exposure to HDM. BAL, Lungs and serum were taken after 1, 3 or 5 weeks of HDM exposure, 4 hours after the last HDM instillation (serum was taken 24 hours after the last HDM instillation). IL-13Rα2 concentrations were quantified by ELISA in BAL (A), LH (B) and serum (C). n = 8 mice/group, bar represents median. * $p<0.05$ and *** $p<0.001$ by Mann Whitney test.

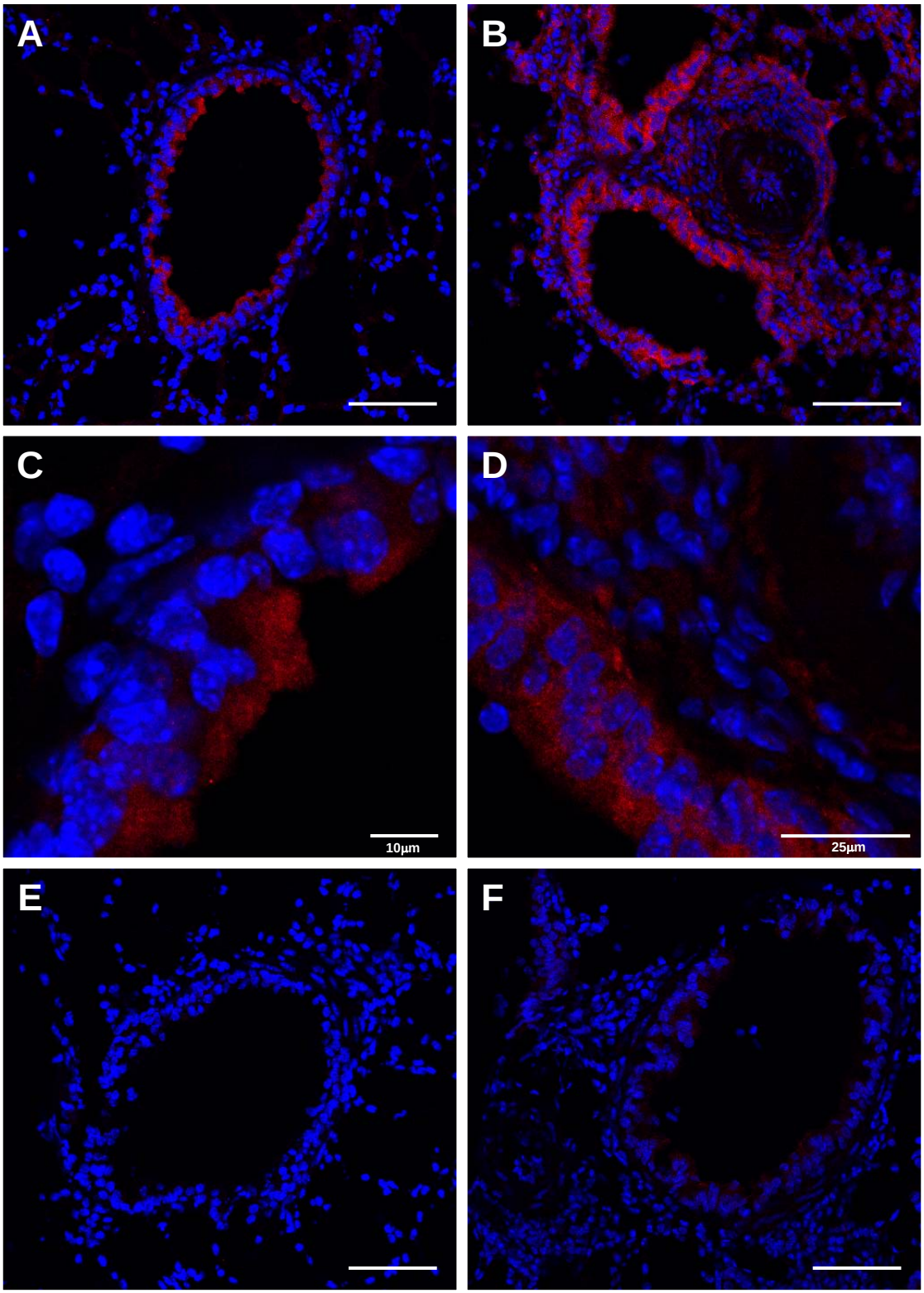


Figure 5.3 Localisation of IL-13Rα2 following exposure to HDM. Lungs were taken after 5 weeks of HDM exposure, 24 hours after the last HDM instillation. Red indicates IL-13Rα2 staining and blue is DAPI. Representative images of IL-13Rα2 staining in sham (A, C) and HDM lungs (B, D). (C) and (D) depict further magnified images of (A) and (B), respectively. (E-F) Control staining in sham (E) and HDM lungs (F). Scale bar represents 75µm, unless stated.

5.3.3 IL-13Rα1 expression in the lungs following HDM exposure.

The expression and localisation of IL-13Rα1 was assessed by IF in the lungs of mice exposed to HDM or saline (sham) for 5 weeks. IL-13Rα1+ cells were detected throughout the lung parenchyma of both sham and HDM exposed mice (Figure 5.4). Despite relatively high background staining in HDM mice, specific IL-13Rα1 staining was bright and punctate. IL-13Rα1+ cells appeared larger in HDM exposed mice than in sham mice.

Due to the size and location of IL-13Rα1+ cells, sections were stained with MOMA2 to determine whether IL-13Rα1+ cells were macrophages. In addition, cytospin slides of BAL cells from sham and HDM exposed mice were stained with the same antibody combination to determine whether IL-13Rα1+ cells were present in BAL. Unfortunately, MOMA2 staining was not sufficiently bright in the lung sections, to establish whether the staining co-localised (Figure 5.5). However, MOMA2 staining was detected in BAL cells. IL-13Rα1+ cells were present in BAL, the majority of which were also positive for MOMA2 indicating IL-13Rα1+ BAL cells were macrophages (Figure 5.6). Interestingly, an additional population of IL-13Rα1+ MOMA2- cells was identified in BAL from HDM exposed mice (Figure 5.6 D). These cells were small with a diffuse, membrane associated staining pattern, distinct from the punctate stain of larger cells.

To verify whether the large IL-13Rα1+ cells in lung tissue and BAL were macrophages, sections and cytospins were stained with IL-13Rα1 and CD68. IL-13Rα1 staining in sham and HDM lungs was closely associated with CD68 expression (Figure 5.7). Of note, while the majority of IL-13Rα1 staining co-localised to CD68+ cells, not all CD68+ cells were IL-13Rα1+. This was particularly evident in lungs from HDM exposed mice in which macrophages residing throughout the parenchyma were CD68+ IL-13Rα1+ whereas macrophages in the peribronchial inflammatory cuffs were CD68+ IL-13Rα1-. The majority of IL-13Rα1 staining in BAL cells from sham and HDM mice also co-localised to CD68 (Figure 5.8), although some of the IL-13Rα1 staining was masked by the intensity of CD68 staining in HDM BAL cells.

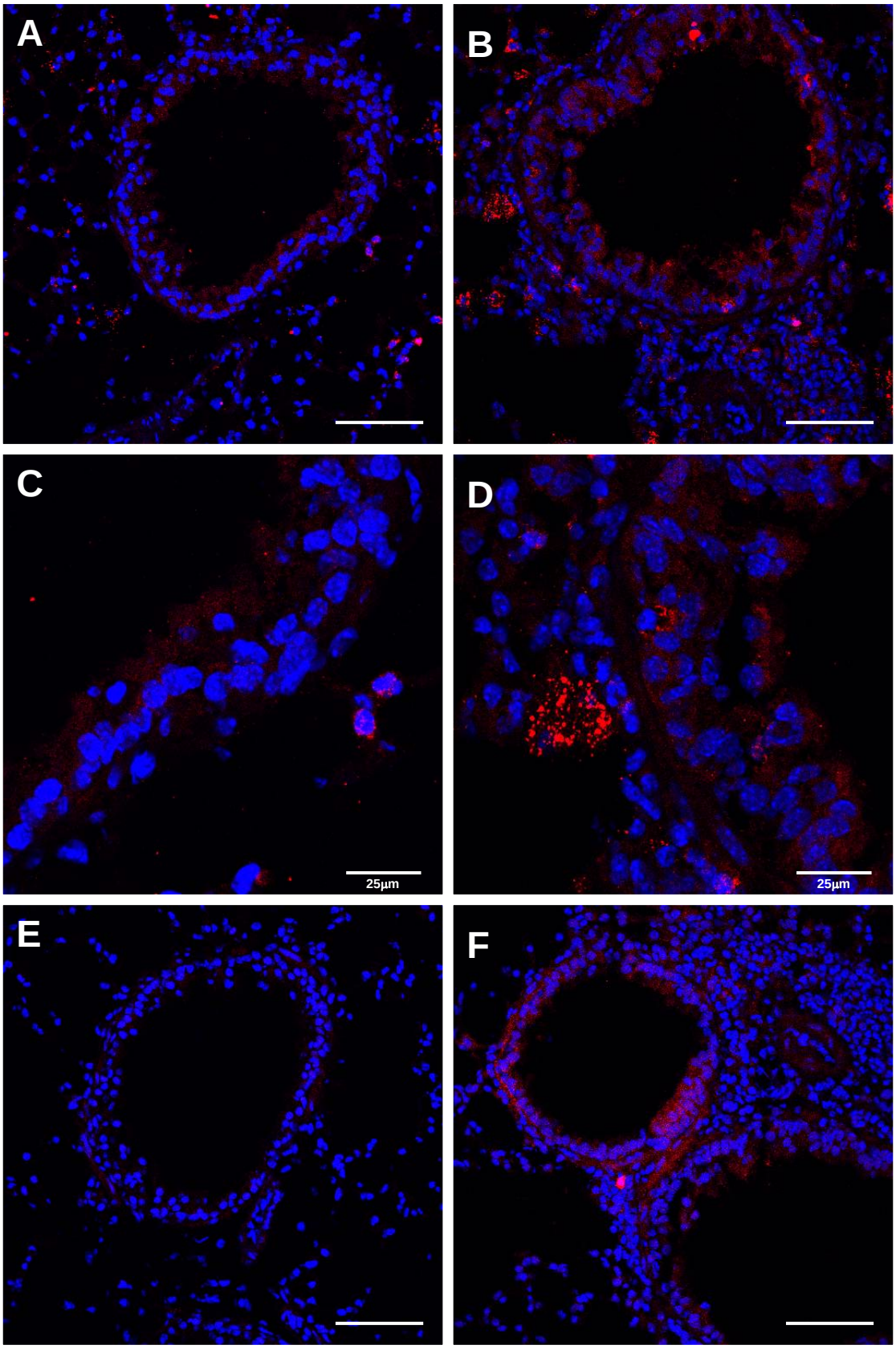


Figure 5.4 Localisation of IL-13Rα1 following exposure to HDM. Lungs were taken after 5 weeks of HDM exposure, 24 hours after the last HDM instillation. Red indicates IL-13Rα1 staining and blue is DAPI. Representative images of IL-13Rα1 staining in sham (A, C) and HDM lungs (B, D). (C) and (D) depict further magnified images of (A) and (B), respectively. (E-F) Control staining in sham (E) and HDM lungs (F). Scale bar represents 75µm, unless stated.

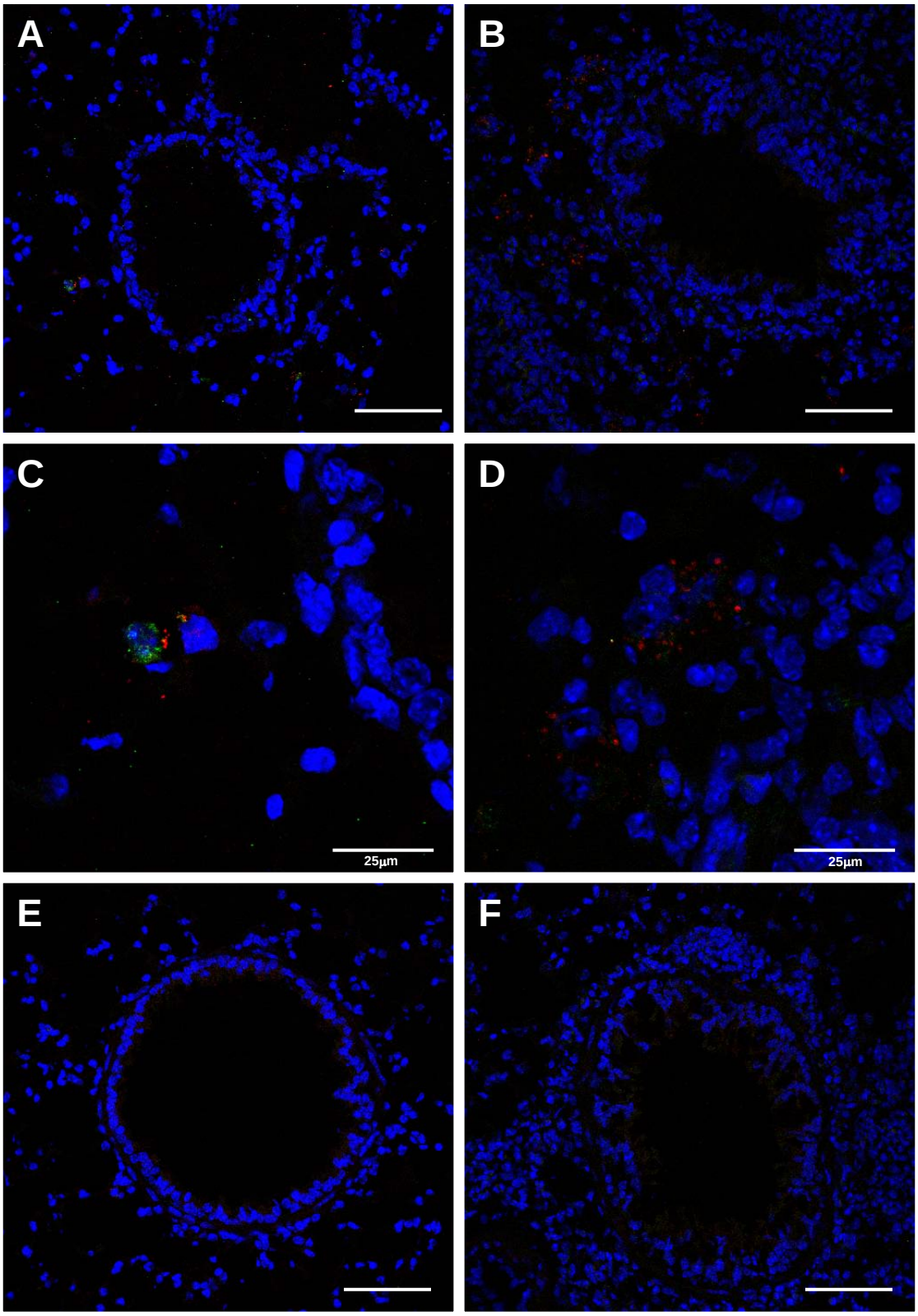


Figure 5.5 Co-localisation of IL-13Rα1 with MOMA2 in Lungs. Lungs were taken after 5 weeks of HDM exposure, 24 hours after the last HDM instillation. Red indicates IL-13Rα1 staining, green MOMA2 and blue DAPI. Representative images of IL-13Rα1 and MOMA2 staining in sham (A, C) and HDM lungs (B, D). (C) and (D) depict further magnified images of (A) and (B), respectively. (E-F) Control staining in sham (E) and HDM lungs (F). Scale bar represents 75µm, unless stated.

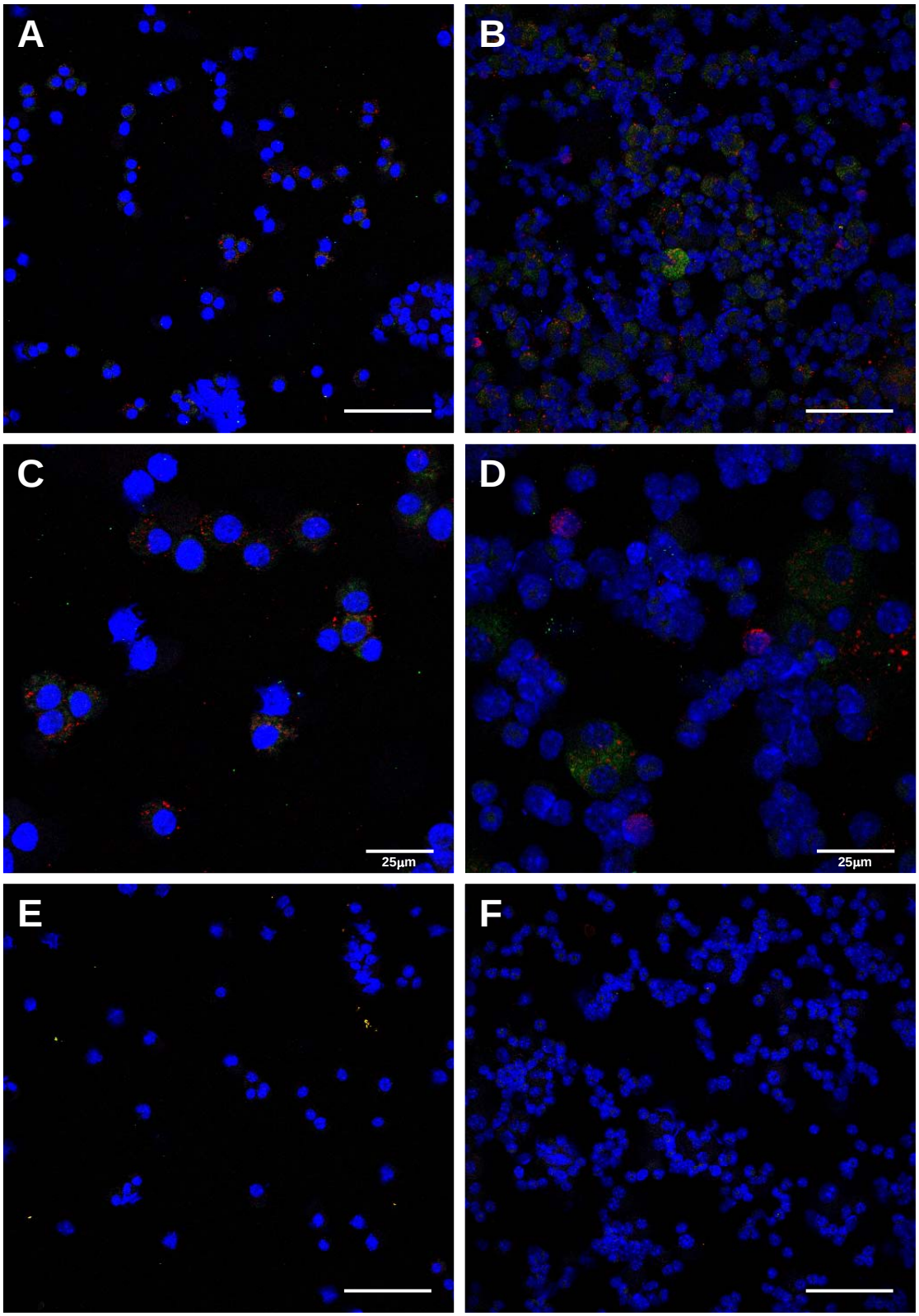


Figure 5.6 Co-localisation of IL-13Rα1 with MOMA2 in BAL. BAL was taken after 5 weeks of HDM exposure, 24 hours after the last HDM instillation. Red indicates IL-13Rα1 staining, green MOMA2 and blue DAPI. Representative images of IL-13Rα1 and MOMA2 staining in sham (A, C) and HDM BAL (B, D). (C) and (D) depict further magnified images of (A) and (B), respectively. (E-F) Control staining in sham (E) and HDM BAL (F). Scale bar represents 75µm, unless stated.

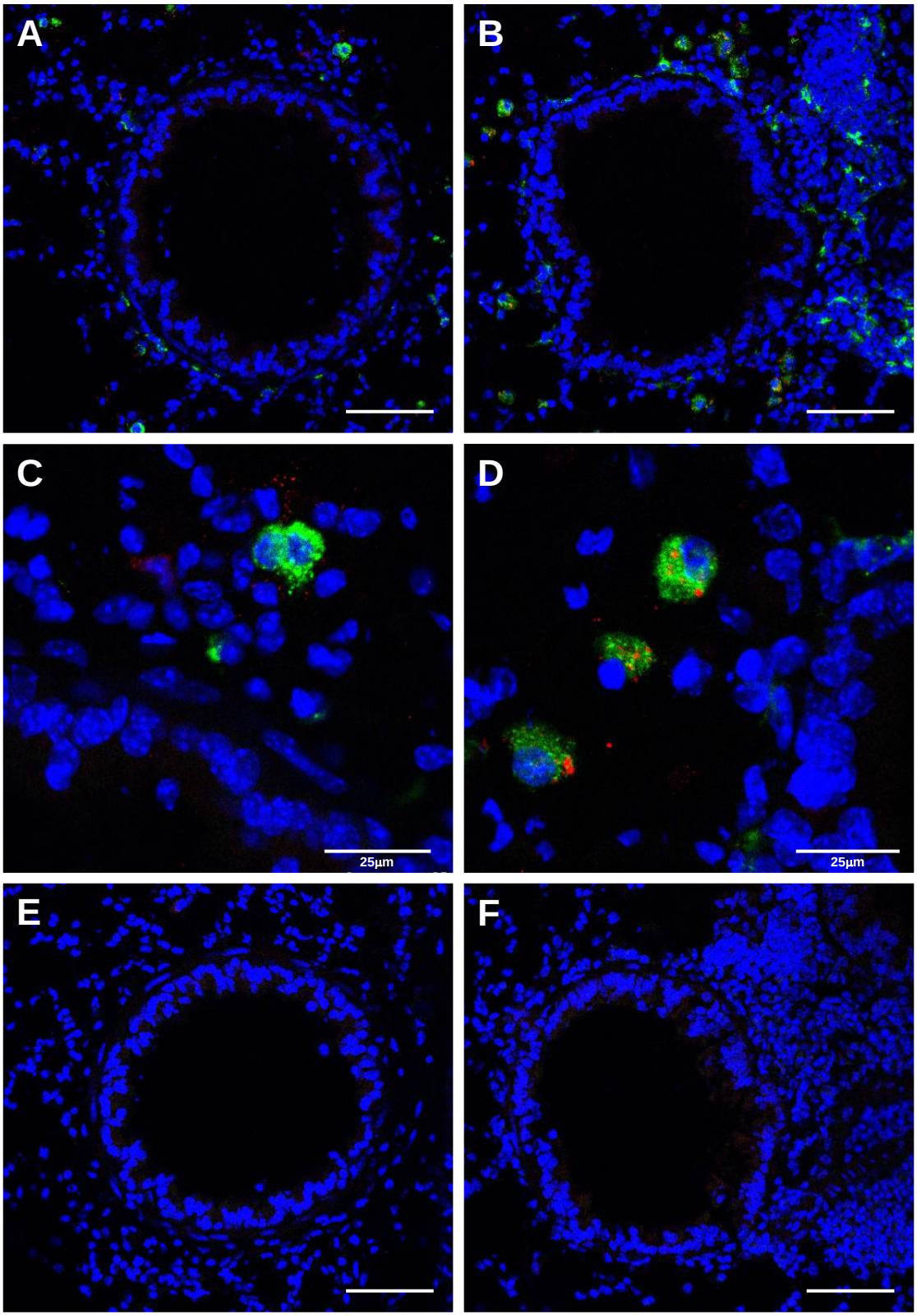


Figure 5.7 Co-localisation of IL-13Rα1 to CD68+ cells in lungs. Lungs were taken after 5 weeks of HDM exposure, 24 hours after the last HDM instillation. Red indicates IL-13Rα1 staining, green CD68 and blue DAPI. Representative images of IL-13Rα1 and CD68 staining in sham (A, C) and HDM lungs (B, D). (C) and (D) depict further magnified images of (A) and (B), respectively. (E-F) Control staining in sham (E) and HDM lungs (F). Scale bar represents 75µm, unless stated.

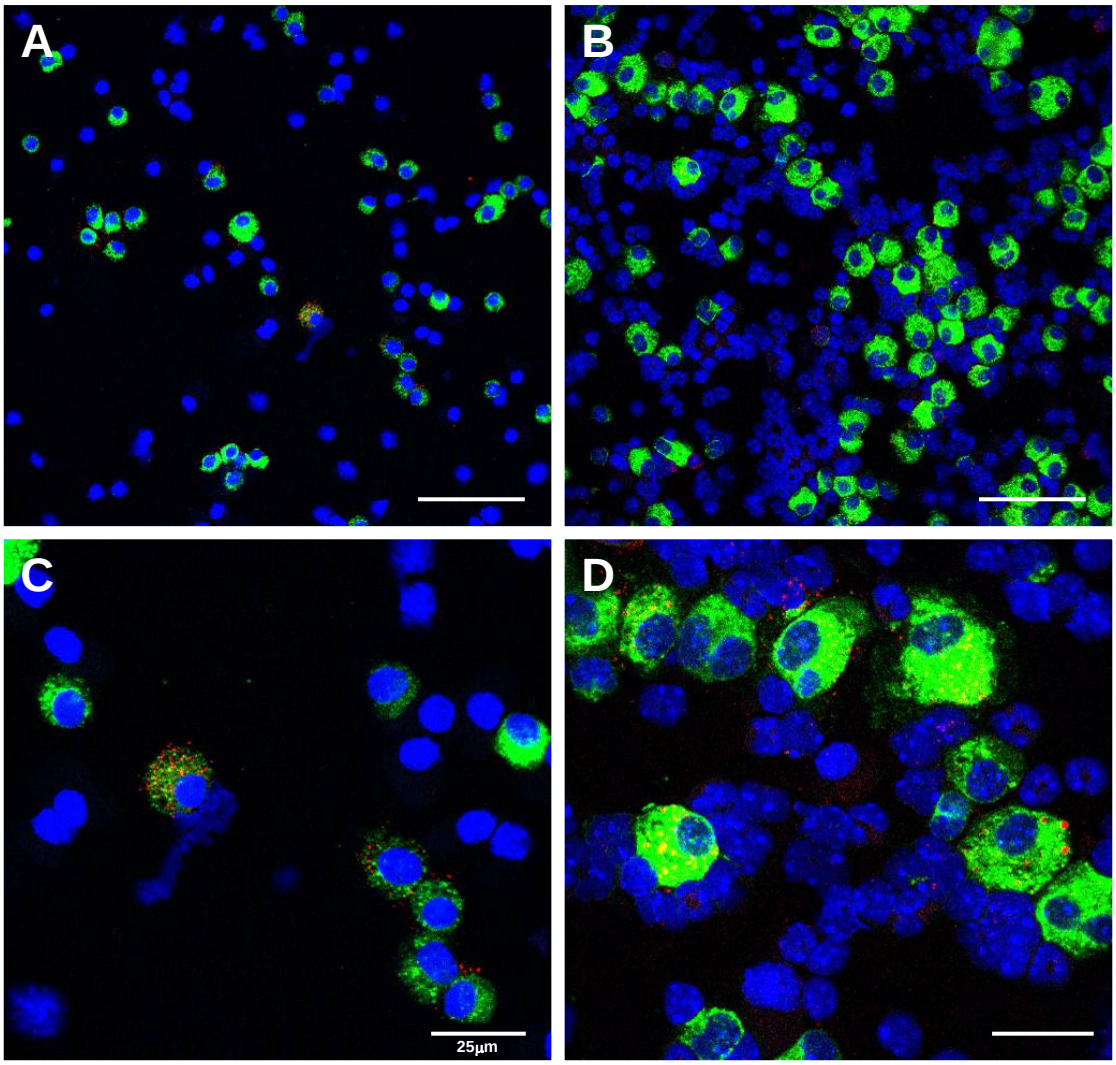


Figure 5.8 Co-localisation of IL-13Rα1 to CD68+ cells in BAL. BAL was taken after 5 weeks of HDM exposure, 24 hours after the last HDM instillation. Red indicates IL-13Rα1 staining, green CD68 and blue DAPI. Representative images of IL-13Rα1 and CD68 staining in sham BAL (A, C) and HDM BAL (B, D). (C) and (D) depict further magnified images of (A) and (B), respectively. Scale bar represents 75µm, unless stated.

5.3.4 Quantification of IL-13Rα1+ cells.

To further investigate the phenotype and quantify IL-13Rα1+ cells it was necessary to develop a protocol to stain cells for IL-13Rα1 for analysis by flow cytometry. A range of primary antibody concentrations were tested and IL-13Rα1 specific staining on BAL cells was detected in a concentration dependent manner (Figure 5.9). 10μg/ml anti-IL-13Rα1 produced optimal staining and thus, was selected for use in subsequent studies assessing IL-13Rα1 expression by flow cytometry.

IL-13Rα1+ cells in BAL from sham and HDM exposed mice were quantified by flow cytometry. The total number of IL-13Rα1+ cells was elevated in BAL after 5 weeks of HDM exposure, compared to sham (Figure 5.10 A). This was attributable in part, to an increase in the number of IL-13Rα1+ macrophages (Figure 5.10 B), but primarily due to a significant increase in the number of non-macrophage IL-13Rα1+ cells (Figure 5.10 C). The identity of this latter population is explored later in this chapter.

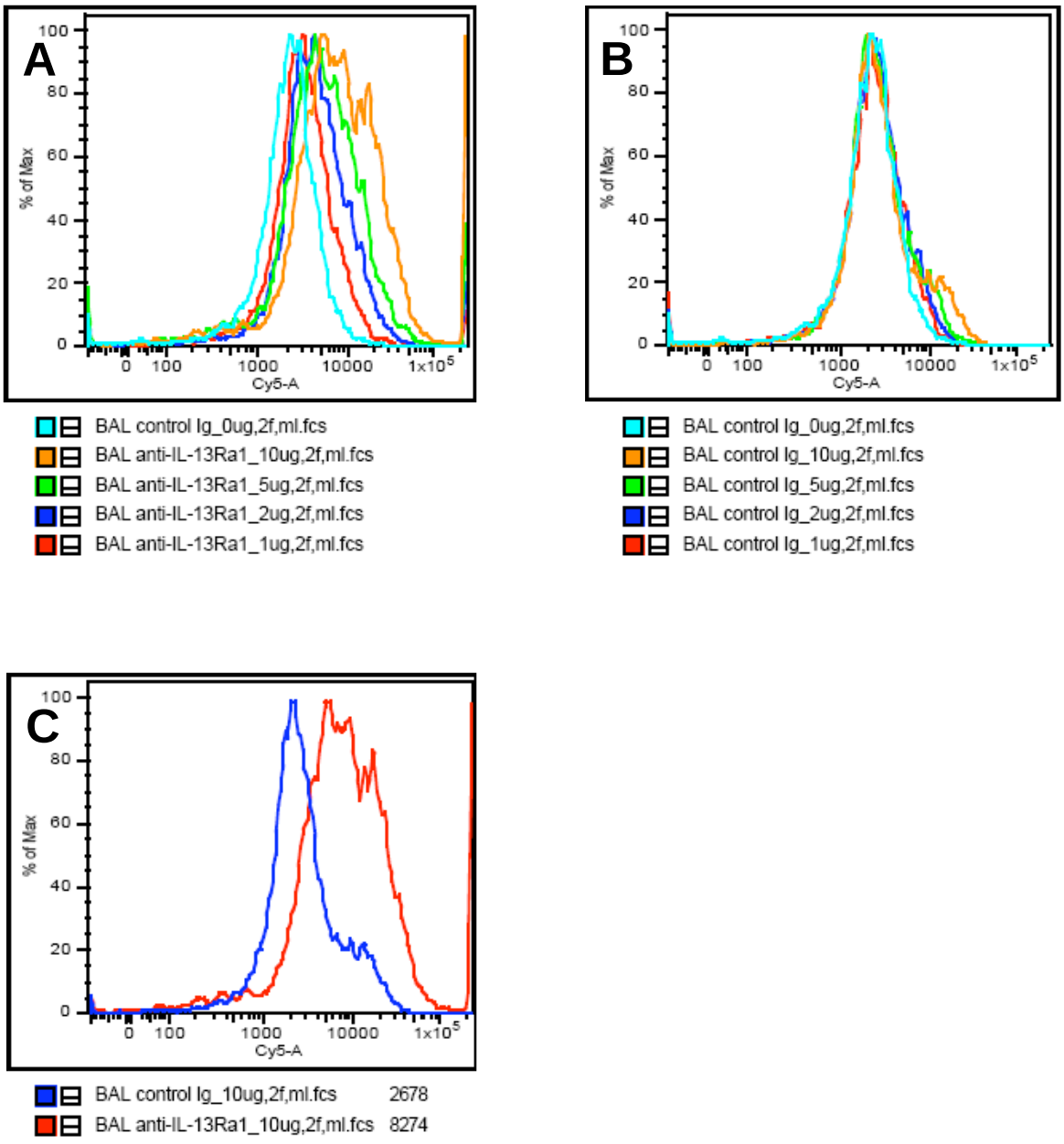


Figure 5.9 Development of a flow cytometry stain for IL-13Rα1. Naïve BAL cells were stained with 1-10μg/ml anti-IL-13Rα1 (A) or control Ig (B) followed by anti-goat-Cy5 secondary. (C) Overlay of 10μg/ml anti-IL-13Rα1 and control Ig.

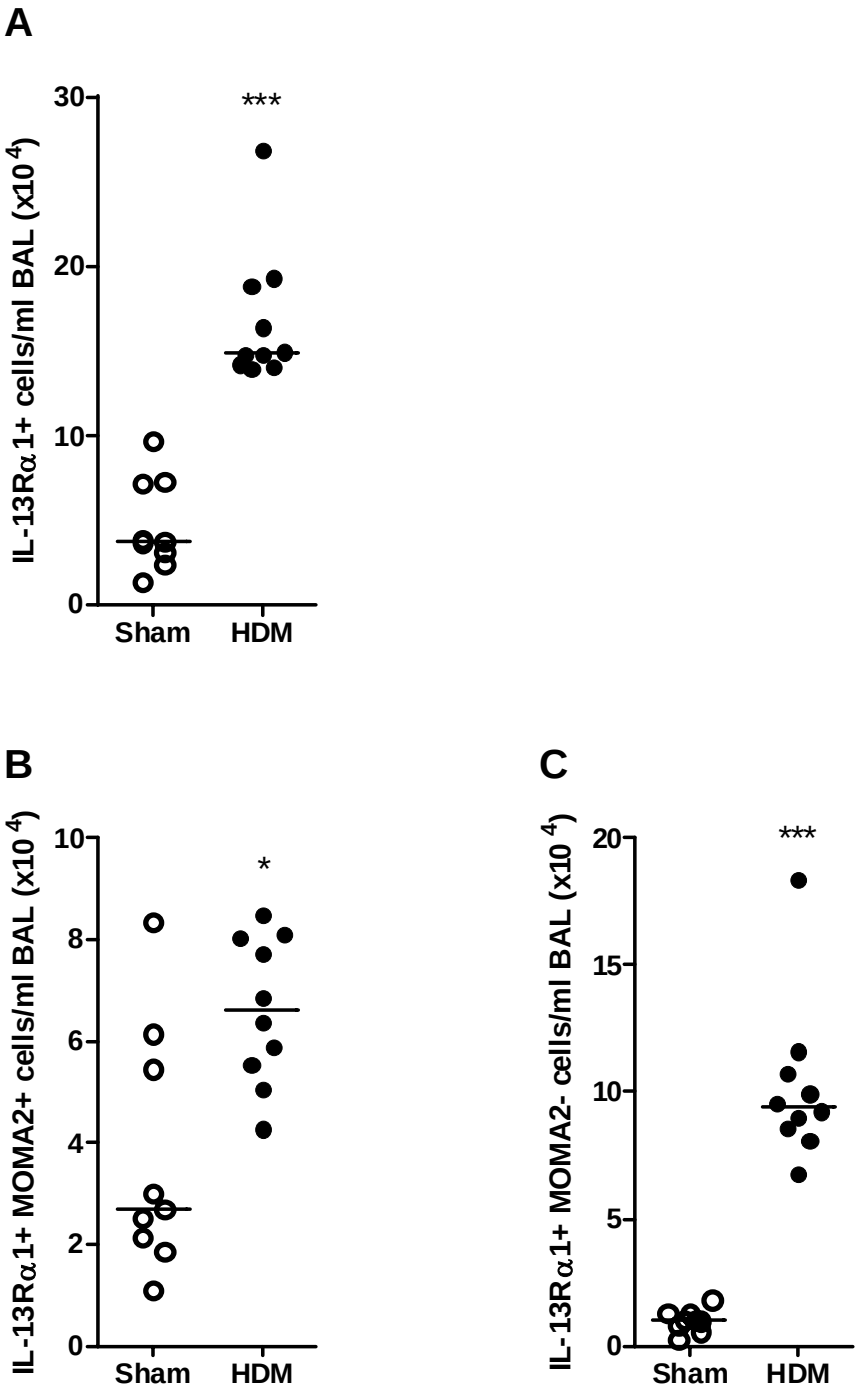


Figure 5.10 Quantification of IL-13Rα1+ BAL cells. BAL was taken after 5 weeks of HDM exposure, 24 hours after the last HDM instillation. The number of IL-13Rα1+ BAL cells was quantified by flow cytometry. (A) IL-13Rα1+ BAL cells, (B) IL-13Rα1+ MOMA2+ BAL cells and (C) IL-13Rα1+ MOMA2- BAL cells. n = 9-10 mice/group, bar represents median. Data represents one of two experiments. * $p<0.05$ and *** $p<0.001$ by Mann Whitney test.

5.3.5 IL-13Rα1+ macrophages

Characterisation of IL-13Rα1+ macrophages in BAL from sham and HDM exposed mice revealed a reduction in the intensity of IL-13Rα1 staining following HDM exposure compared to sham (Figure 5.11 A-C). This was associated with a fall in the proportion of IL-13Rα1+ cells within the macrophage population of HDM BAL (Figure 5.11 D); despite the actual number of IL-13Rα1+ macrophages in BAL increasing upon HDM exposure (Figure 5.11 E). This may be due to a dilution effect of infiltrating IL-13Rα1- macrophages during lung inflammation; however loss of receptor from the cell surface may also be a contributing factor since IL-13Rα1 is still readily detected by IF after HDM exposure. To gauge whether IL-13Rα1 may be internalised following HDM exposure BAL cells from sham and HDM exposed mice were stained for extracellular and intracellular IL-13Rα1 and analysed by flow cytometry. Cells from the same preparation were also assessed visually by fluorescence microscopy. The reduction in extracellular IL-13Rα1 staining intensity on macrophages from HDM mice was apparent by both flow cytometry and microscopy (Figure 5.12). Intracellular staining revealed intense IL-13Rα1 staining in both sham and HDM macrophages however the distribution of IL-13Rα1 was distinct in sham and HDM macrophages. Intracellular IL-13Rα1 in sham macrophages localised predominantly to the periphery of the cell, whereas IL-13Rα1 in HDM macrophages was apparent throughout the cells in a punctate, vesicular pattern (Figure 5.13).

To investigate the expression of IL-13Rα1 on macrophage subpopulations in the lung BAL and LD macrophages from sham and HDM exposed mice were subdivided into AM and IM populations based on F4/80 and CD11c expression. Subsequently, extracellular receptor expression and its modulation after HDM exposure were assessed on each population. The majority of BAL cells were AM in both sham and HDM exposed mice (Figure 5.14 A-B). Hence, as previously observed in total BAL macrophages, IL-13Rα1 expression was present on BAL AM in sham exposed mice (Figure 5.14 C). In addition, receptor expression on BAL AM was substantially reduced following HDM exposure (Figure 5.14 D). Analysis of IL-13Rα1 expression on BAL IM was not conducted due to the small size of this population. In LD IL-13Rα1 expression was detected on AM in sham mice and, as in BAL, this was

significantly reduced in HDM mice (Figure 5.15 C-D). LD IM from sham mice exhibited negligible IL-13Rα1 expression which appeared further diminished after exposure to HDM (Figure 5.15 E-F). Quantitatively, the proportion of BAL AM expressing IL-13Rα1 was approximately 52% in sham mice, which fell to 6% in HDM mice (Figure 5.16 A). Similarly, 22% of LD AM were IL-13Rα1+ in sham mice compared to 4% in HDM mice (Figure 5.16 B). Approximately 17% of LD IM in sham exposed mice expressed IL-13Rα1 which was non-significantly reduced to 6% after HDM exposure (Figure 5.16 C).

Since the largest population of IL-13Rα1 expressing cells in the lung was BAL AM, the phenotype of BAL AM in sham and HDM exposed mice was analysed. Sham BAL AM expressed minimal CD206 (mannose receptor) however expression was elevated by exposure to HDM (Figure 5.17 A and D). The DC and AM marker CD205 (DEC-205) was expressed by both sham and HDM AM, with AM from HDM exposed mice having greater expression than sham (Figure 5.17 B and E). Similarly, Dectin-1 (β-glucan receptor) was expressed by sham and HDM AM with higher expression on HDM AM compared to sham (Figure 5.17 C and F). Intracellular cytokine staining of AM stimulated *ex vivo* was employed to further characterise the phenotype of BAL AM from sham and HDM exposed mice. Minimal IL-13 was detected in HDM AM which was not present in sham AM (Figure 5.18 A, D). Both sham and HDM AM expressed IL-10 and TGFβ, however little difference was observed between AM from sham and HDM exposed mice (Figure 5.18 B-C and E-F).

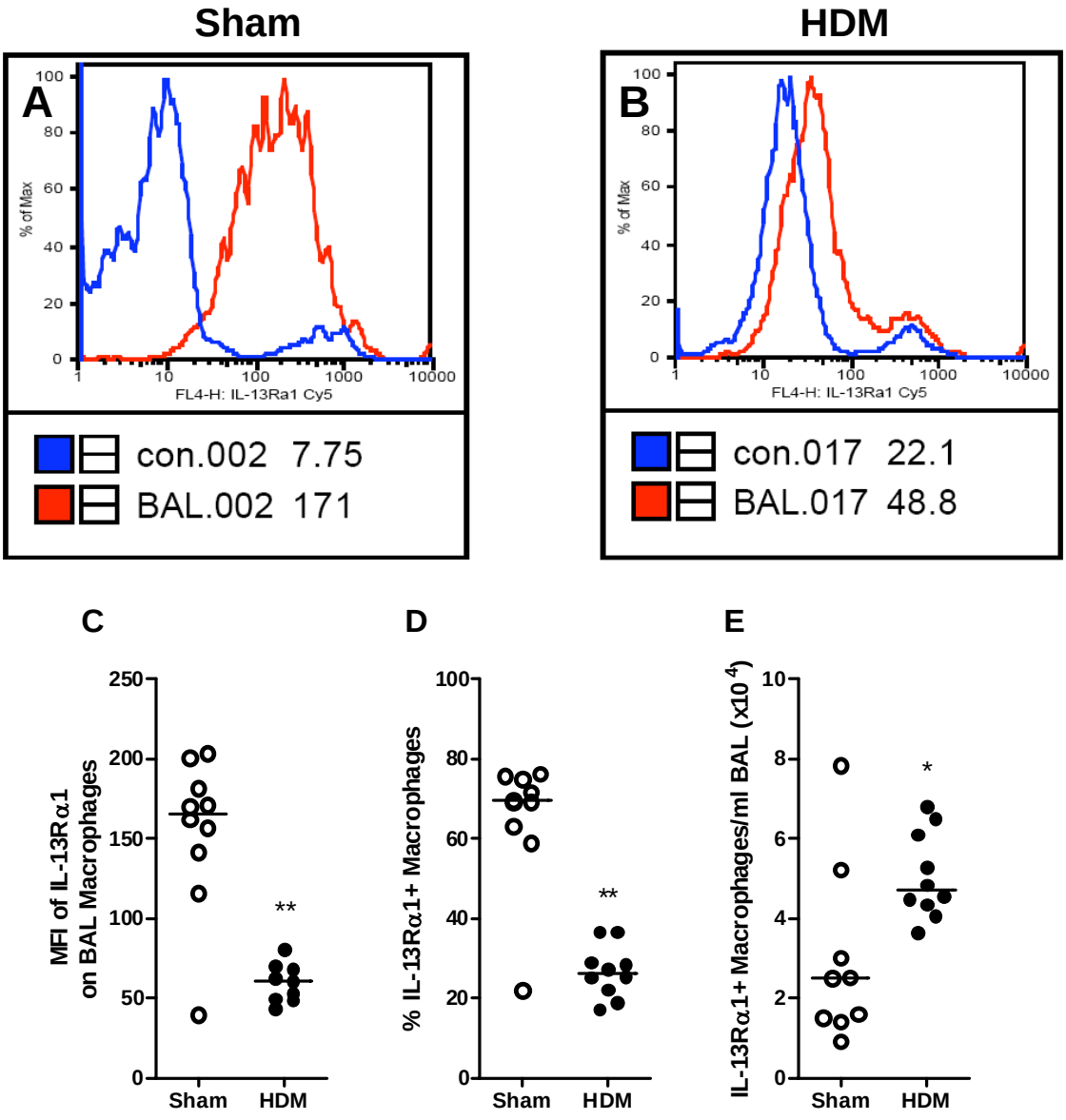


Figure 5.11 IL-13Rα1 expression on BAL macrophages is reduced following HDM exposure. BAL was taken after 5 weeks of HDM exposure, 24 hours after the last HDM instillation. The number of IL-13Rα1+ BAL cells was quantified by flow cytometry. (A-B) Representative histograms and MFI of IL-13Rα1 expression on sham BAL cells (A) and HDM BAL cells (B). (C) Mean fluorescence intensity (MFI) of IL-13Rα1 staining on BAL macrophages; (D) proportion of BAL macrophages staining positive for IL-13Rα1 and (E) number of IL-13Rα1+ BAL macrophages. n = 9-10 mice/group, bar represents median. Data represents one of two experiments. * $p<0.05$ and ** $p<0.01$ by Mann Whitney test.

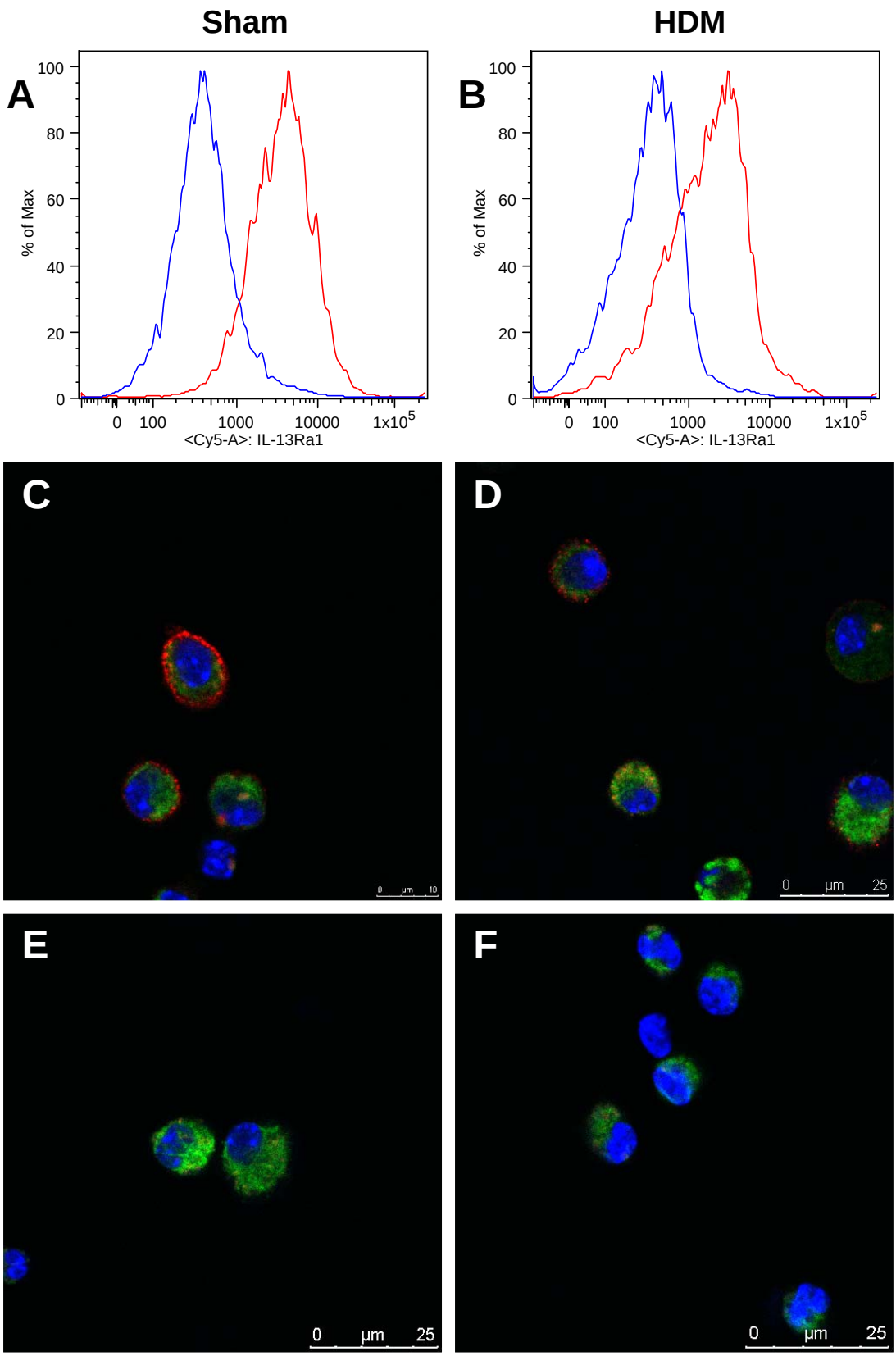


Figure 5.12 Extracellular IL-13Rα1 expression on BAL macrophages. BAL was taken from sham or HDM exposed mice, 24 hours after the last HDM exposure. (A-B) Representative histograms of extracellular IL-13Rα1 (red line) or control (blue line) staining on MOMA2+ BAL macrophages in sham (A) and HDM mice (B). (C-D) Representative images of BAL cells stained for IL-13Rα1 (red), MOMA2 (green) and DAPI (blue) for analysis by flow cytometry. n = 3 mice/group. (E-F) BAL cells stained with control (red), MOMA2 (green) and DAPI (blue).

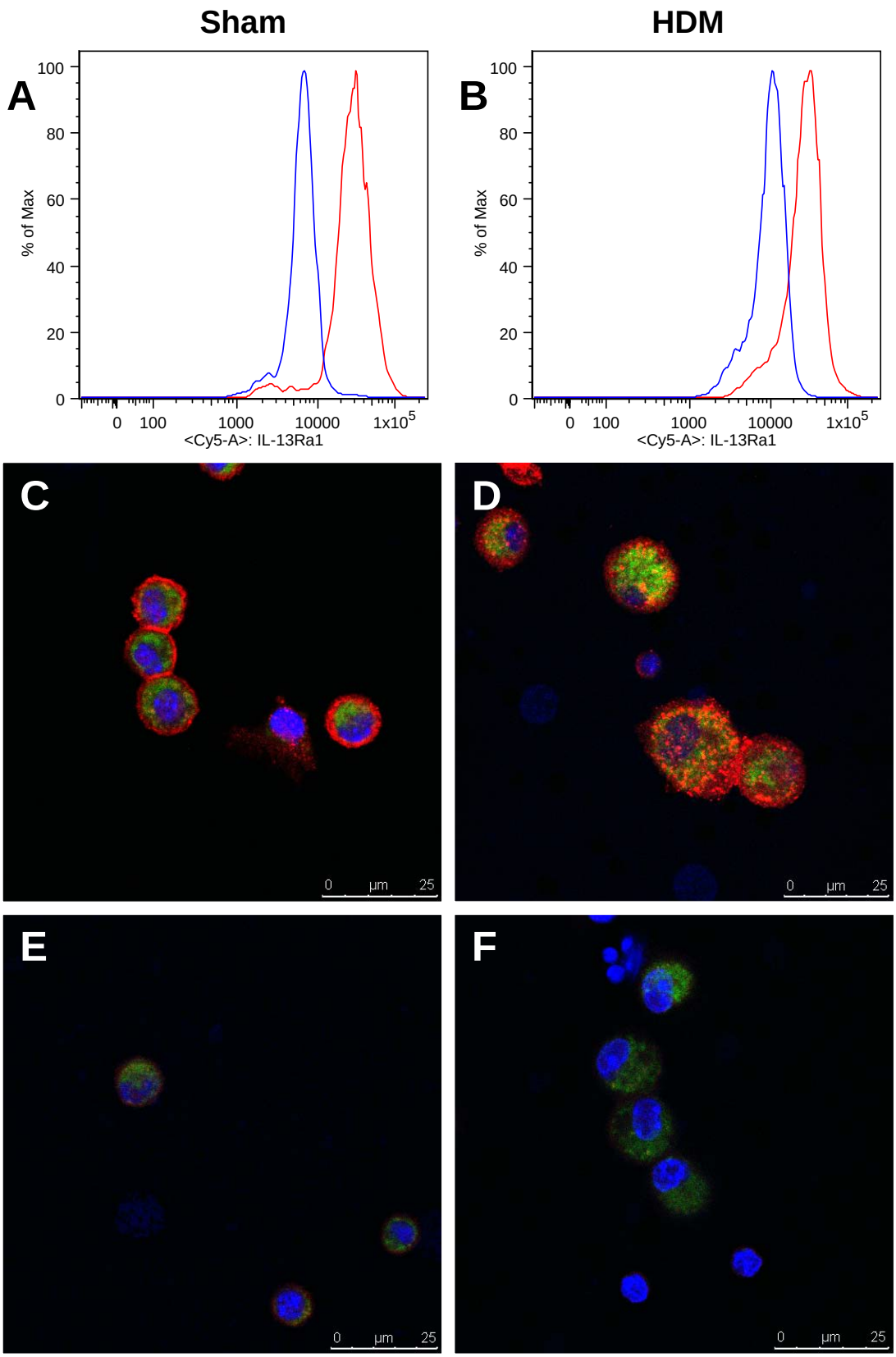


Figure 5.13 Intracellular IL-13Rα1 expression in BAL macrophages. BAL was taken from sham or HDM exposed mice, 24 hours after the last HDM exposure. (A-B) Representative histograms of intracellular IL-13Rα1 (red line) or control (blue line) staining on MOMA2+ BAL macrophages in sham (A) and HDM mice (B). (C-D) Representative images of BAL cells stained for intracellular IL-13Rα1 (red), MOMA2 (green) and DAPI (blue) for analysis by flow cytometry. n = 3 mice/group. (E-F) BAL cells stained with control (red), MOMA2 (green) and DAPI (blue).

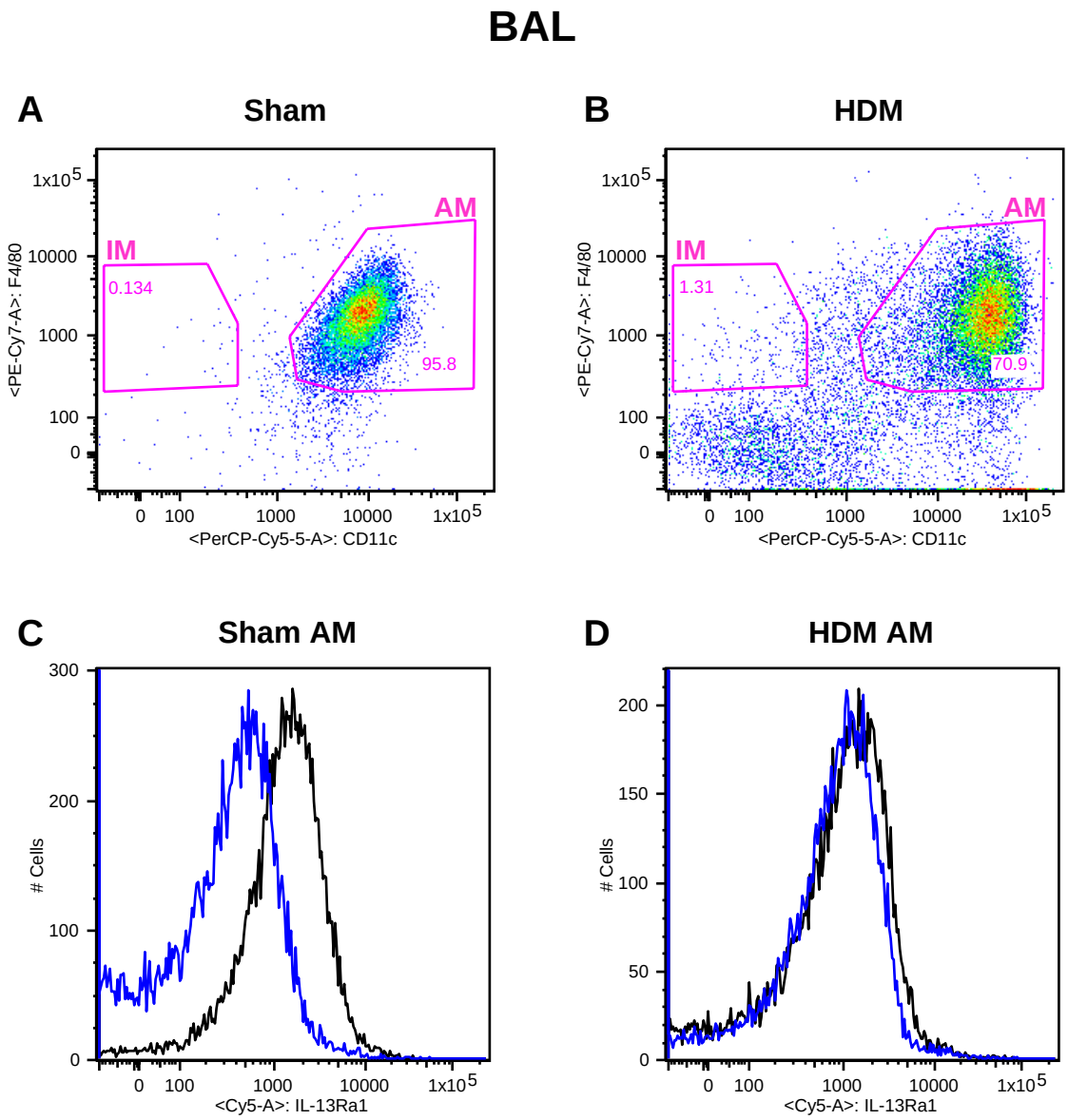


Figure 5.14 IL-13Rα1 expression on BAL AM. BAL was taken after 5 weeks of HDM exposure, 24 hours after the last HDM instillation. (A-B) Representative dot plots of BAL macrophages in sham exposed (A) and HDM exposed mice (B). (C-D) Representative histograms of IL-13Rα1 staining (black line) compared to control stain (blue line) on BAL AM from sham exposed (C) and HDM exposed mice (D). n = 6 mice/group, data represents one of two experiments.

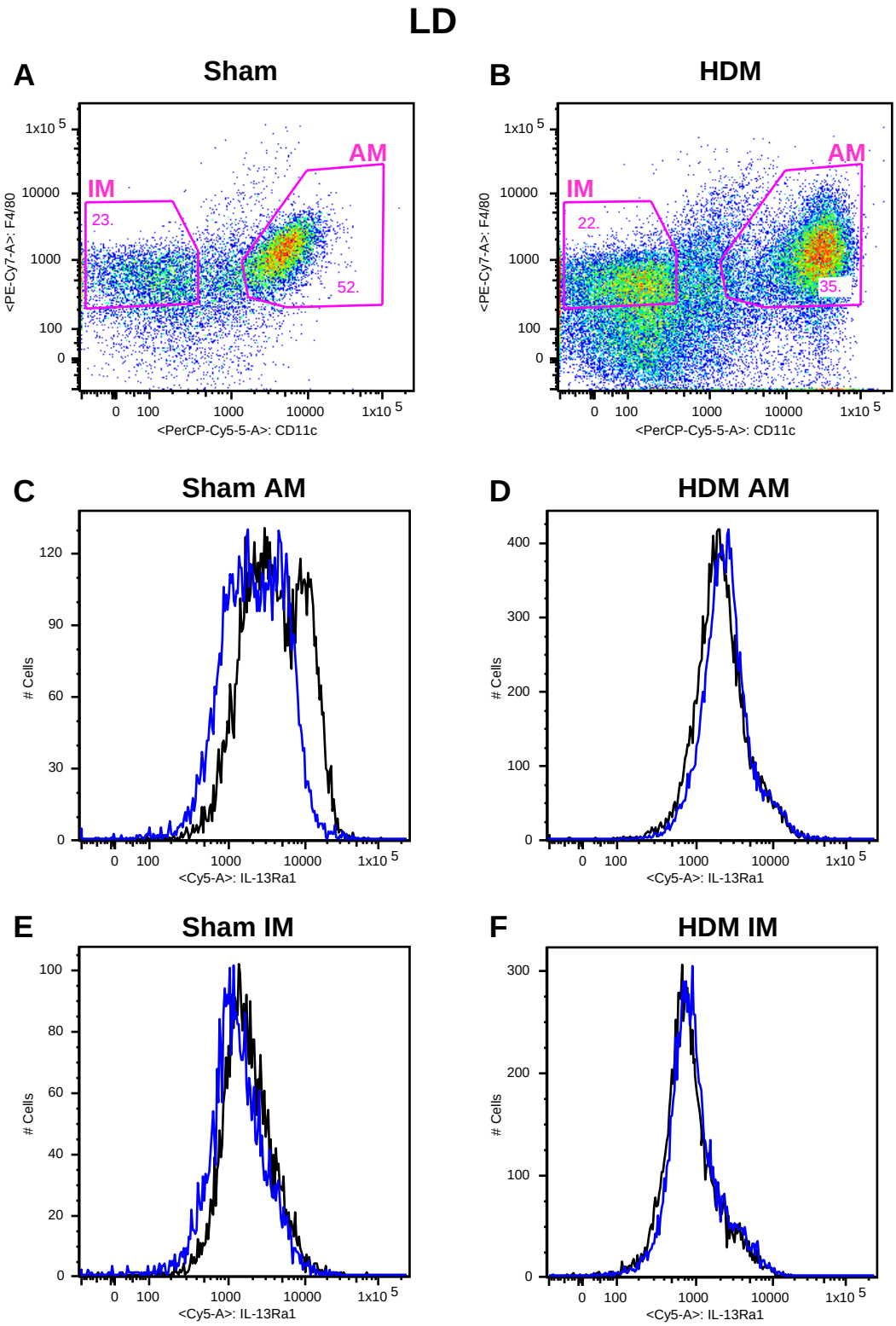


Figure 5.15 IL-13Rα1 expression on LD AM and IM. Lungs were taken after 5 weeks of HDM exposure, 24 hours after the last HDM instillation. (A-B) Representative dot plots of LD macrophages in sham exposed (A) and HDM exposed mice (B). (C-F) Representative histograms of IL-13Rα1 staining (black line) compared to control stain (blue line) on LD AM from sham exposed mice (C); LD AM from HDM exposed mice (D); LD IM from sham exposed mice (E) and LD IM from HDM exposed mice (F). n = 6 mice/group, data represents one of two experiments.

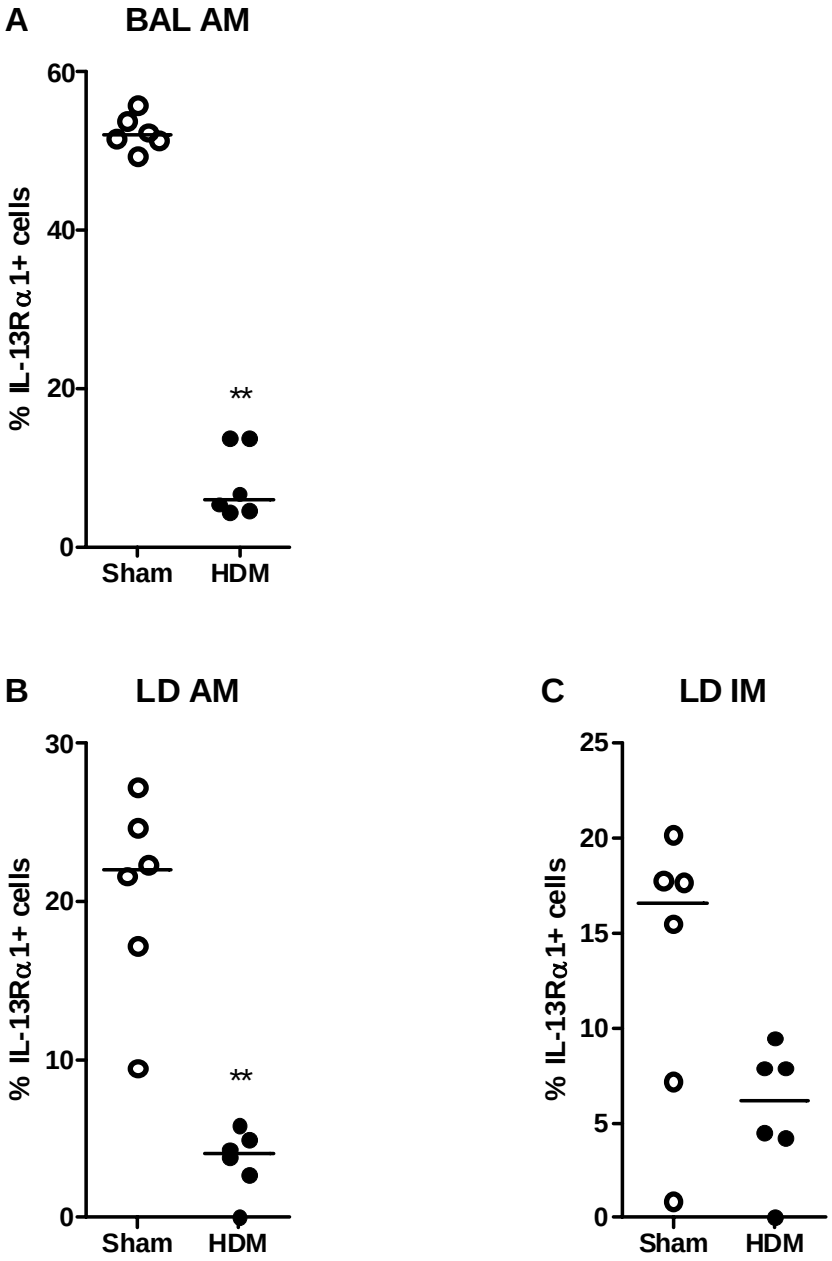


Figure 5.16 Proportion of IL-13Rα1+ AM and IM following HDM exposure. BAL and lungs were taken after 5 weeks of HDM exposure, 24 hours after the last HDM instillation. The proportions of IL-13Rα1+ cells were assessed by flow cytometry. (A) The proportion of IL-13Rα1+ AM in BAL; (B) the proportion of IL-13Rα1+ AM in LD; and (C) the proportion of IL-13Rα1+ IM in LD. n = 6 mice/group, bar represents median, data represents one of two experiments. ** $p<0.01$ by Mann Whitney test.

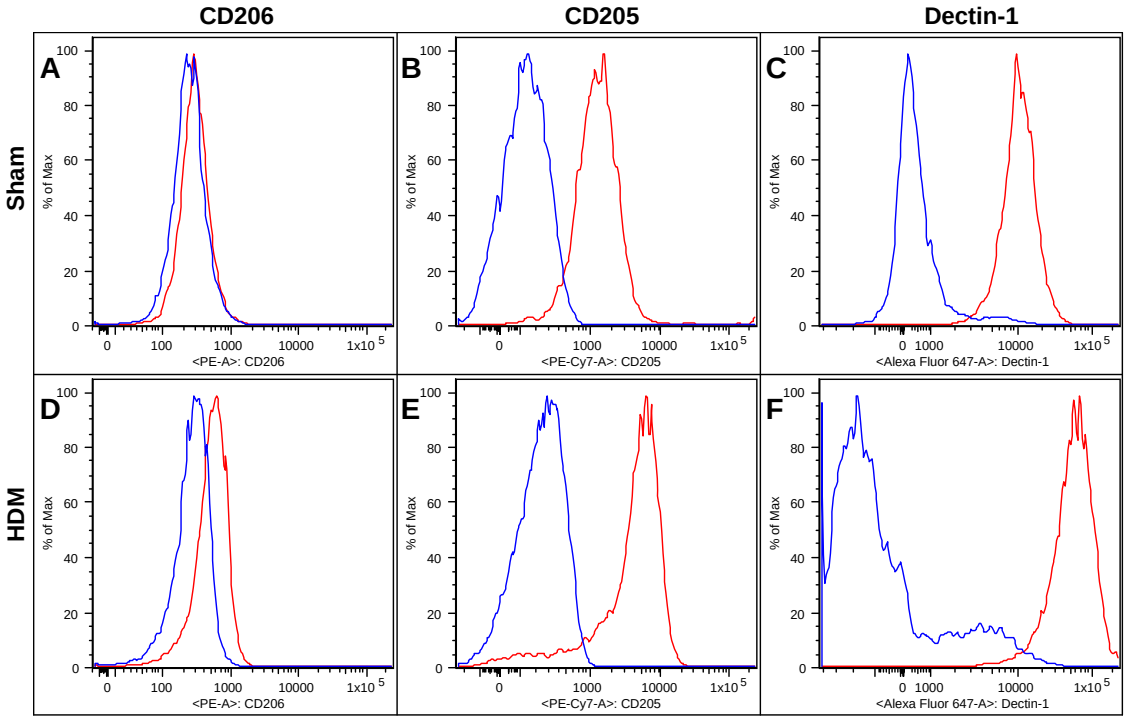


Figure 5.17 Phenotype of BAL AM. Representative histograms of BAL AM from sham (A-C) or HDM exposed mice (D-F) depicting expression of CD206 (A, D), CD205 (B, E) and Dectin-1 (C, F) in red or isotypes controls in blue. n = 5 mice/group, data represents one of two experiments.

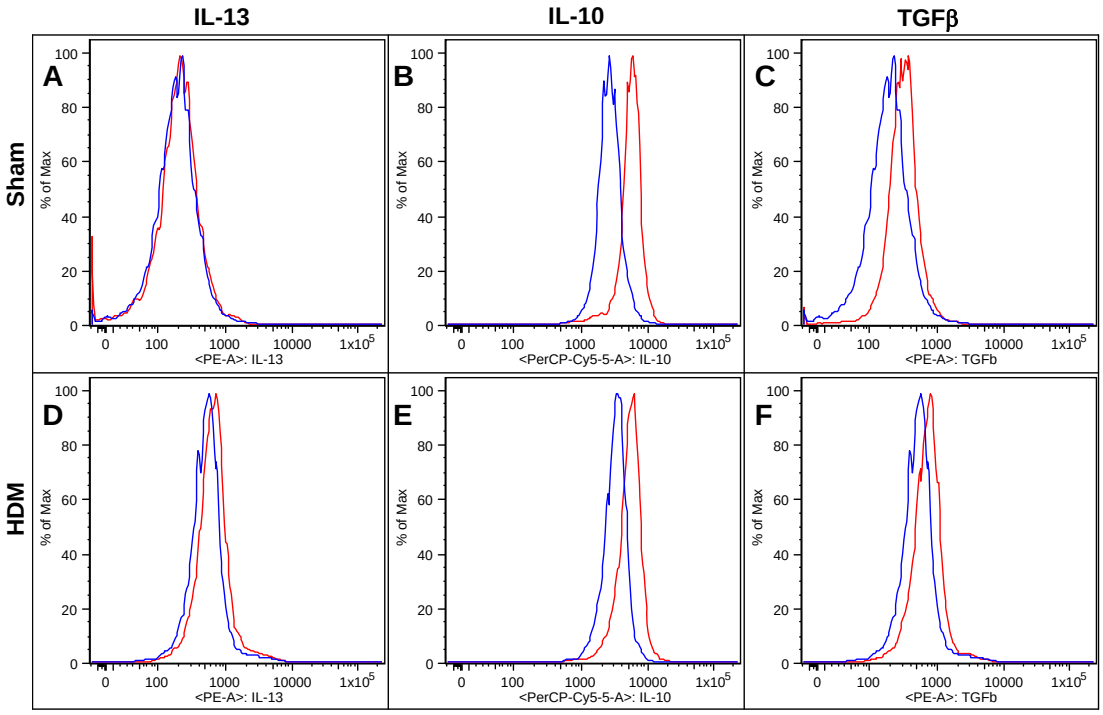


Figure 5.18 Intracellular cytokine staining of BAL AM. Representative histograms of BAL AM from sham (A-C) or HDM exposed mice (D-F) depicting expression of IL-13 (A, D), IL-10 (B, E) and TGFβ (C, F) in red or isotypes controls in blue. n = 5 mice/group.

5.3.6 IL-13Rα1 expression on non-macrophages

In addition to BAL and LD cells, IL-13Rα1 staining was also conducted in naïve blood to investigate whether any normal circulating cells have the potential to respond to IL-13. IL-13Rα1 was detected on both MOMA2+ and MOMA2- cells (Figure 5.19 A-B). IL-13Rα1+ MOMA2+ cells were also Gr-1+ and CD11b+ indicating this was a subpopulation of monocytes (Figure 5.19 C-D). IL-13Rα1+ MOMA2- cells however, were Gr-1- and CD11b- excluding granulocytic and monocytic phenotypes (Figure 5.19 E-F). Further analysis demonstrated the majority of IL-13Rα1+ MOMA2- cells in naïve blood to be CD3+ CD4+ lymphocytes (Figure 5.20 A). A small population, representing approximately 6% of CD4+ cells in naïve blood, were IL-13Rα1+ (Figure 5.20 B). Negligible IL-13Rα1 staining was detected in CD8+ lymphocytes (Figure 5.20 C).

Following induction of HDM induced AAD, IL-13Rα1+ CD4+ lymphocytes were also detected in BAL and LD (Figure 5.21 A and B, respectively). Quantification of these cells revealed HDM exposure significantly increased the numbers of IL-13Rα1+ CD4+ cells in BAL and LD, compared to sham (Figure 5.21 C and D, respectively). No changes were observed in the total number of IL-13Rα1+ CD4+ cells in the blood of HDM exposed mice compared to sham (data not shown).

A subsequent study was conducted to determine the phenotype of IL-13Rα1+ CD4+ cells in blood, BAL and LD from sham and HDM exposed mice. In the blood a naïve phenotype ($CD44^{lo}$) was the most common within the IL-13Rα1+ CD4+ population. However, IL-13Rα1+ $CD44^{lo}$ CD4+ cells represented only 3.3% of total $CD44^{lo}$ CD4+ cells in sham mice. Following HDM exposure the frequency of IL-13Rα1+ $CD44^{lo}$ CD4+ cells increased to 5.5% of total $CD44^{lo}$ CD4+ cells. Approximately 27% of central memory cells ($CD44^{hi}$ CD62L+) and 35% of effector memory cells ($CD44^{hi}$ CD62L-) in the blood expressed IL-13Rα1; the size of these populations appeared unaltered following HDM exposure (Figure 5.22). In BAL, the number of CD4+ T cells present in sham mice was negligible, however after exposure to HDM the majority of IL-13Rα1+ CD4+ cells were effector memory cells; representing 39% of total effector memory T cells. Significant populations of IL-13Rα1+ cells were also detected within the naïve and central memory T cell populations following HDM

exposure. 29% of naïve CD4+ T cells and 80% of central memory T cells expressed IL-13Rα1 (Figure 5.23). In LD, the numbers of IL-13Rα1+ naïve and memory T cells were elevated following HDM exposure. The proportion of IL-13Rα1+ cells within the naïve T cell population in the lungs increased from 4% to 10% with exposure to HDM. In addition, the proportion of IL-13Rα1+ cells within the central memory cell population increased from 57% to 67% with exposure to HDM. The majority of IL-13Rα1+ CD4+ T cells in LD were effector memory cells. IL-13Rα1+ effector memory cells represented 48% of the total effector memory cell population. The size of this population increase following exposure to HDM however the proportion of IL-13Rα1+ cells within the effector memory cell population remained relatively unaltered at 39% (Figure 5.24).

Since the largest populations of IL-13Rα1+ CD4+ cells in BAL and LD were effector cells, the phenotypes of these populations were further investigated. BAL and LD cells from HDM and sham mice were stained for IFNγ, T1ST2, IL-17, CD25 and FoxP3 expression, in conjunction with IL-13Rα1, CD4 and CD3, to define the phenotype of IL-13Rα1+ effector T cells. IL-13Rα1 expression was detected on subsets of Th0, Th1, Th2, Th17 and regulatory T cells (Tregs) in BAL and LD from HDM exposed mice. Furthermore, HDM exposure elevated the number of IL-13Rα1+ Th0, Th1, Th2, Th17 and Tregs in BAL and LD. In HDM BAL 17% of Th0 cells; 28% of Th1 cells; 29% of Th2 cells; 22% of Th17 cell and 57% of Tregs expressed IL-13Rα1 (Figure 5.25). In HDM LD 12% of Th0 cells; 19% of Th1 cells; 28% of Th2 cells; 21% of Th17 cell and 46% of Tregs expressed IL-13Rα1 (Figure 5.26).

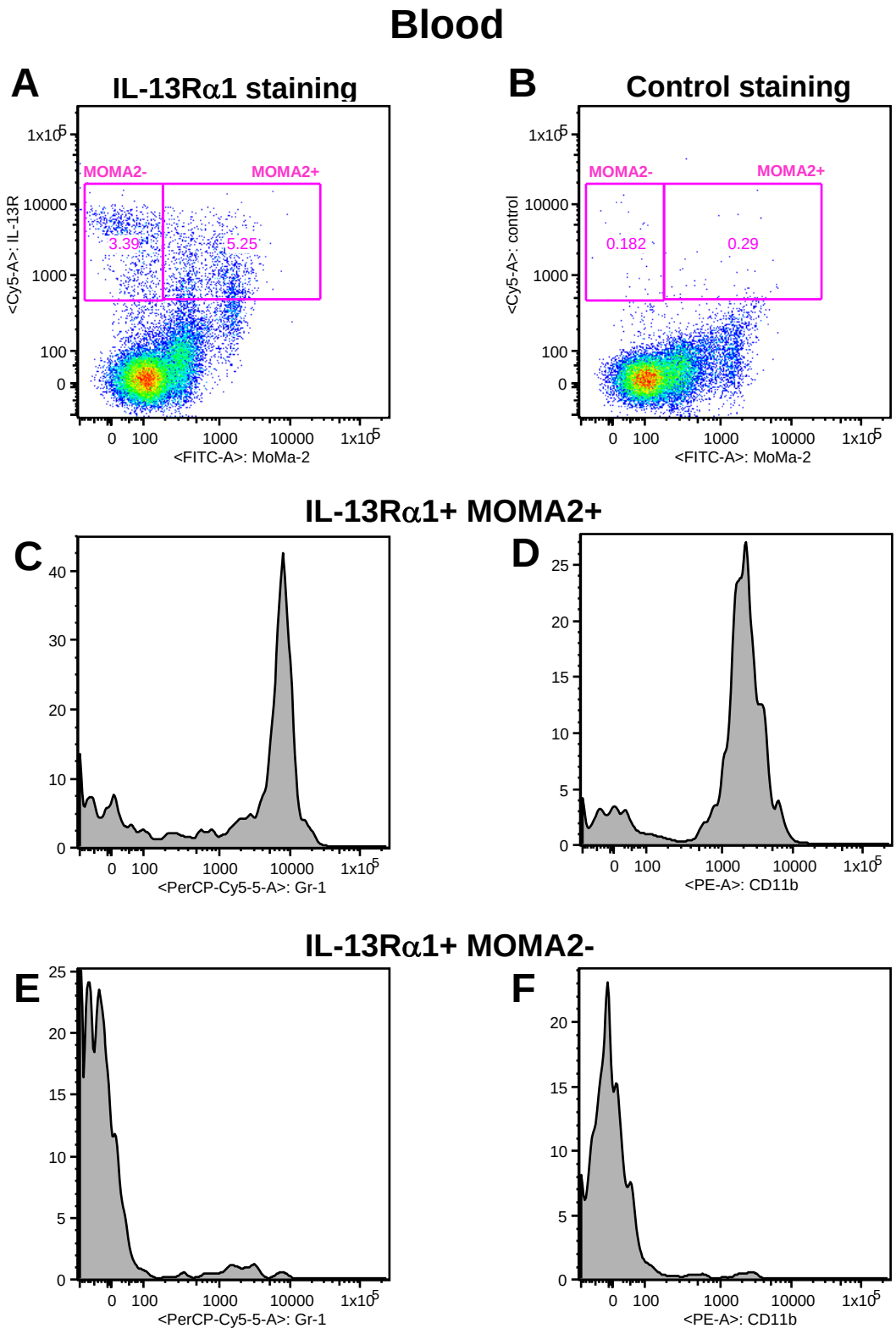


Figure 5.19 Detection of IL-13Rα1+ cells in naïve blood. Blood was taken from naïve mice. (A-B) Representative dot plots of IL-13Rα1 staining (A) and control (B). (C-D) Gr-1 (C) and CD11b (D) expression on IL-13Rα1+ MOMA2+ cells. (E-F) Gr-1 (E) and CD11b (F) expression on IL-13Rα1+ MOMA2- cells. n = 3 mice.

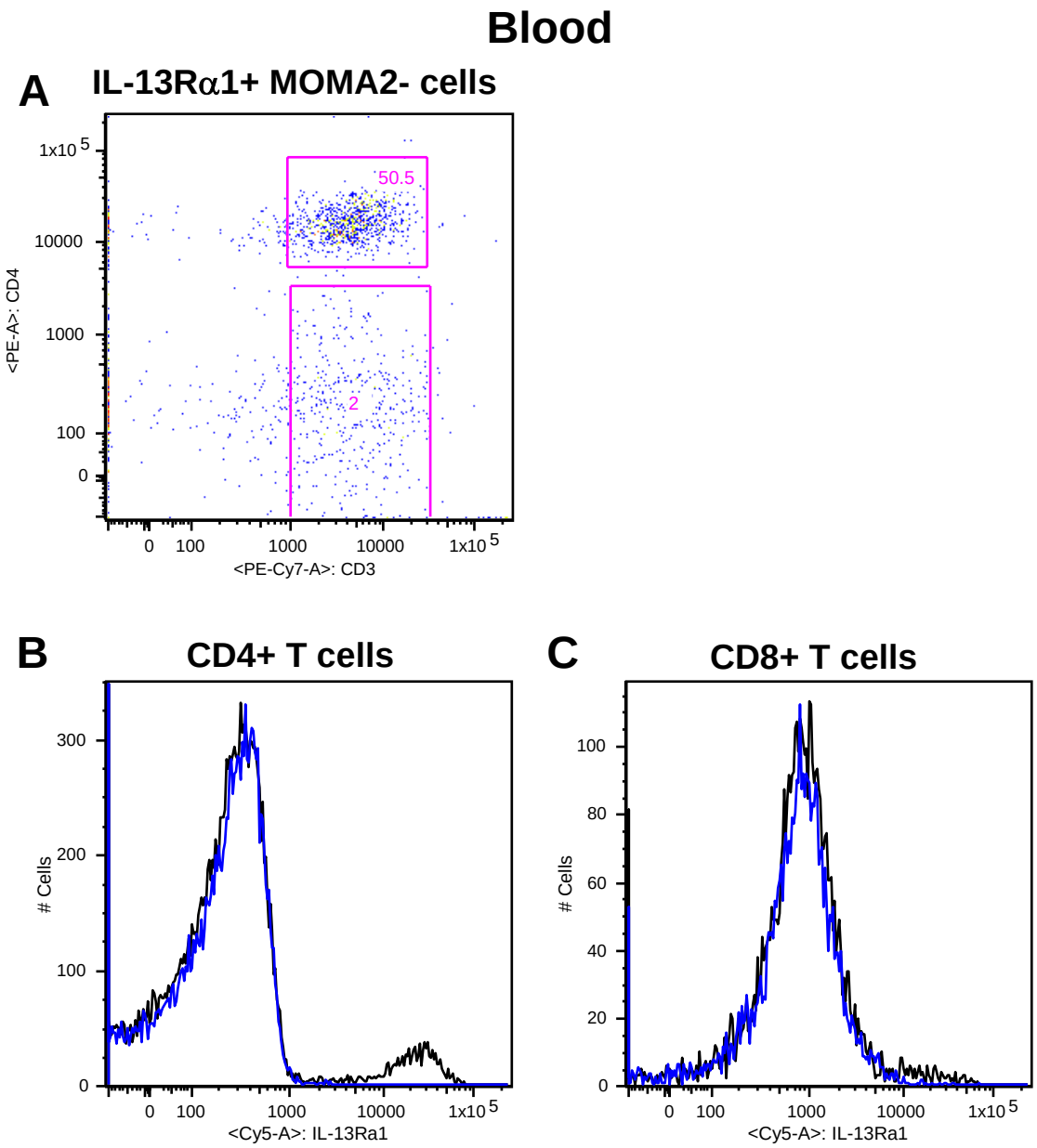


Figure 5.20 IL-13Rα1 expression on T cells in naïve blood. Blood was taken from naïve mice. (A) Representative dot plot of CD3 and CD4 expression on IL-13Rα1+ MOMA2- cells. (B-C) IL-13Rα1 staining (black line) or control (blue line) on naïve blood CD4+ (B) and CD8+ (C) T cells. n = 3 mice.

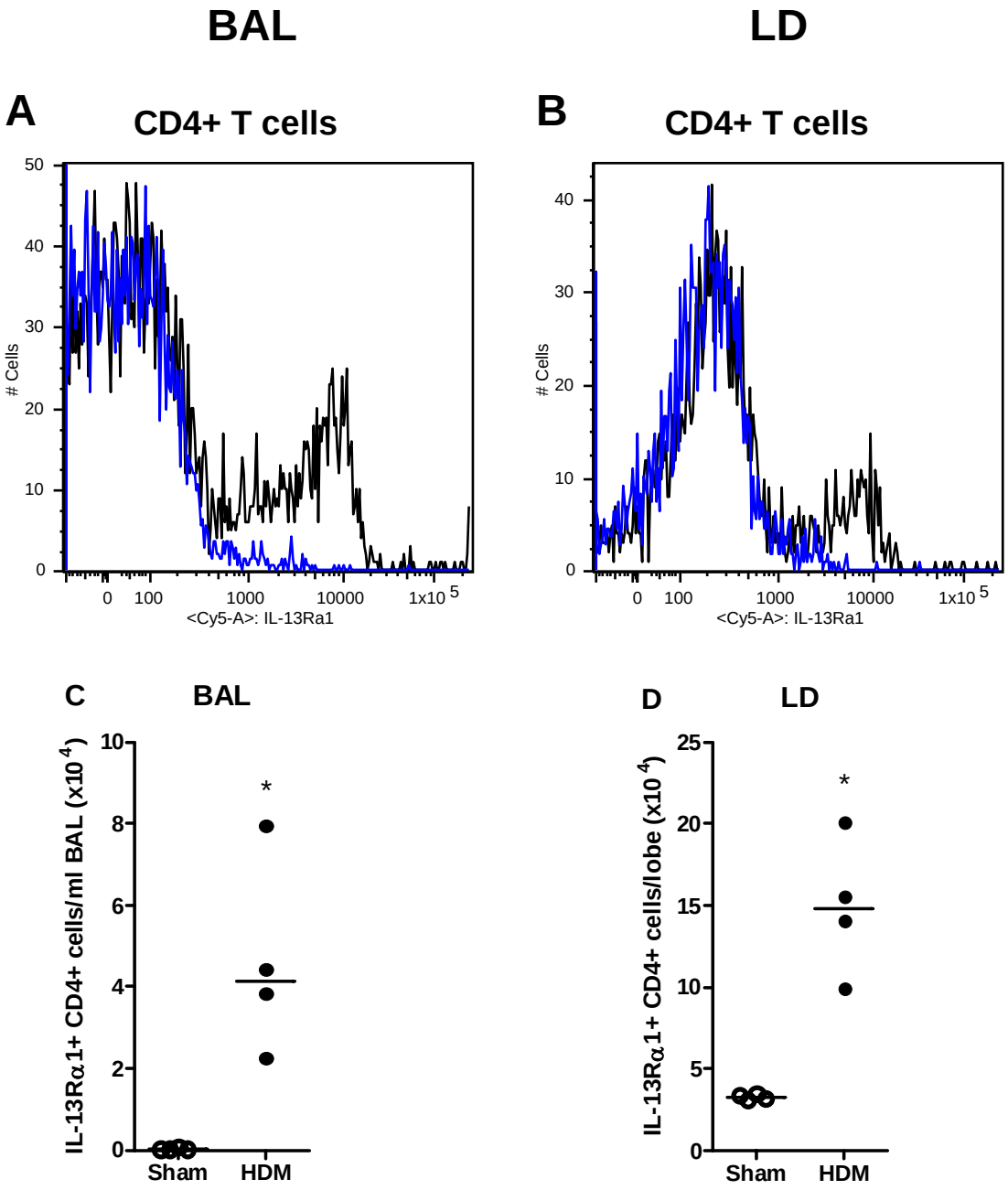


Figure 5.21 IL-13Rα1 expression on CD4+ T cells in BAL and LD from HDM exposed mice. BAL and lungs were taken after 5 weeks of HDM exposure, 24 hours after the last HDM instillation. IL-13Rα1+ cells were quantified by flow cytometry. (A-B) Representative histograms of IL-13Rα1 expression (black line) or control staining (blue line) on CD4+ T cells from BAL (A) and LD (B). (C-D) The number of IL-13Rα1+ CD4+ T cells in BAL (C) and LD (D). n = 4 mice/group, bar represents median, data represents one of two experiments. * $p<0.05$ by Mann Whitney test.

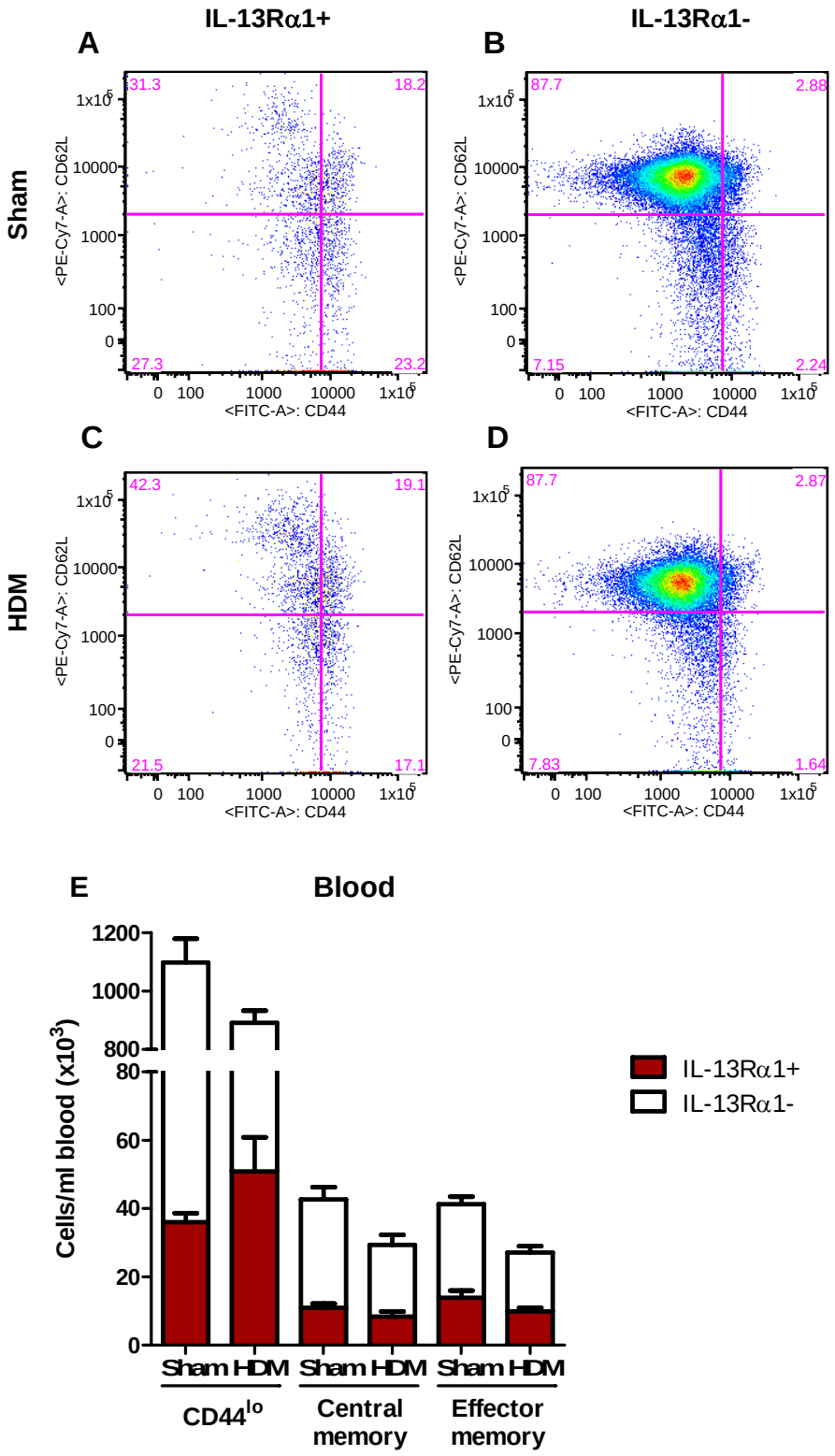


Figure 5.22 Phenotype of IL-13Rα1+ CD4+ T cells in blood from sham and HDM exposed mice. Blood was taken after 5 weeks of HDM exposure, 24 hours after the last HDM instillation. IL-13Rα1+ cells were quantified and phenotyped by flow cytometry. (A-D) Representative dot plots of IL-13Rα1+ (A, C) and IL-13Rα1- (B, D) CD4+ T cells from sham (A-B) and HDM (C-D) exposed mice. (E) Numbers of IL-13Rα1+ naïve, central memory and effector memory T cells in blood. n = 6 mice/group, mean ± SEM.

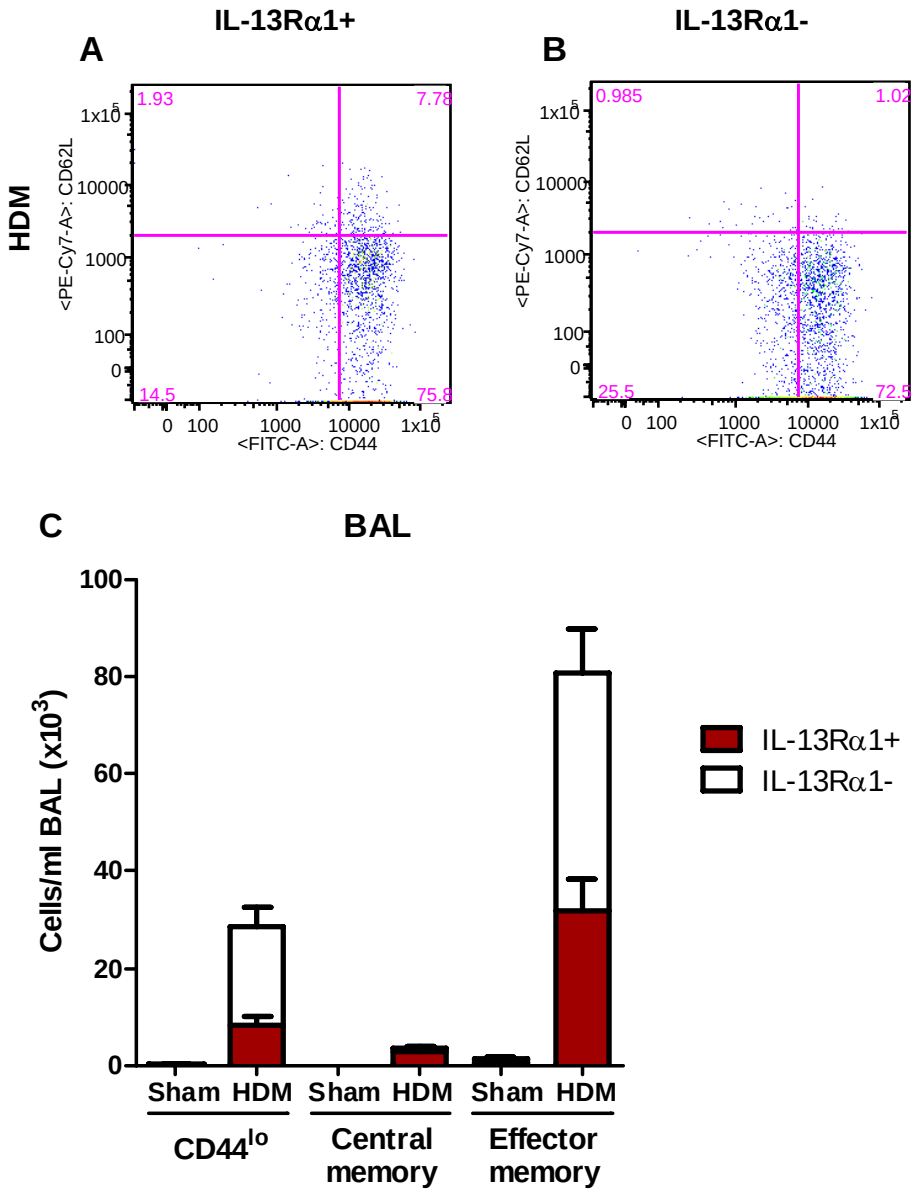


Figure 5.23 Phenotype of IL-13Rα1+ CD4+ T cells in BAL from sham and HDM exposed mice. BAL was taken after 5 weeks of HDM exposure, 24 hours after the last HDM instillation. IL-13Rα1+ cells were quantified and phenotyped by flow cytometry. (A-B) Representative dot plots of IL-13Rα1+ (A) and IL-13Rα1- (B) CD4+ T cells from HDM exposed mice. (C) Numbers of IL-13Rα1+ naïve, central memory and effector memory T cells in BAL. n = 6 mice/group, mean ± SEM.

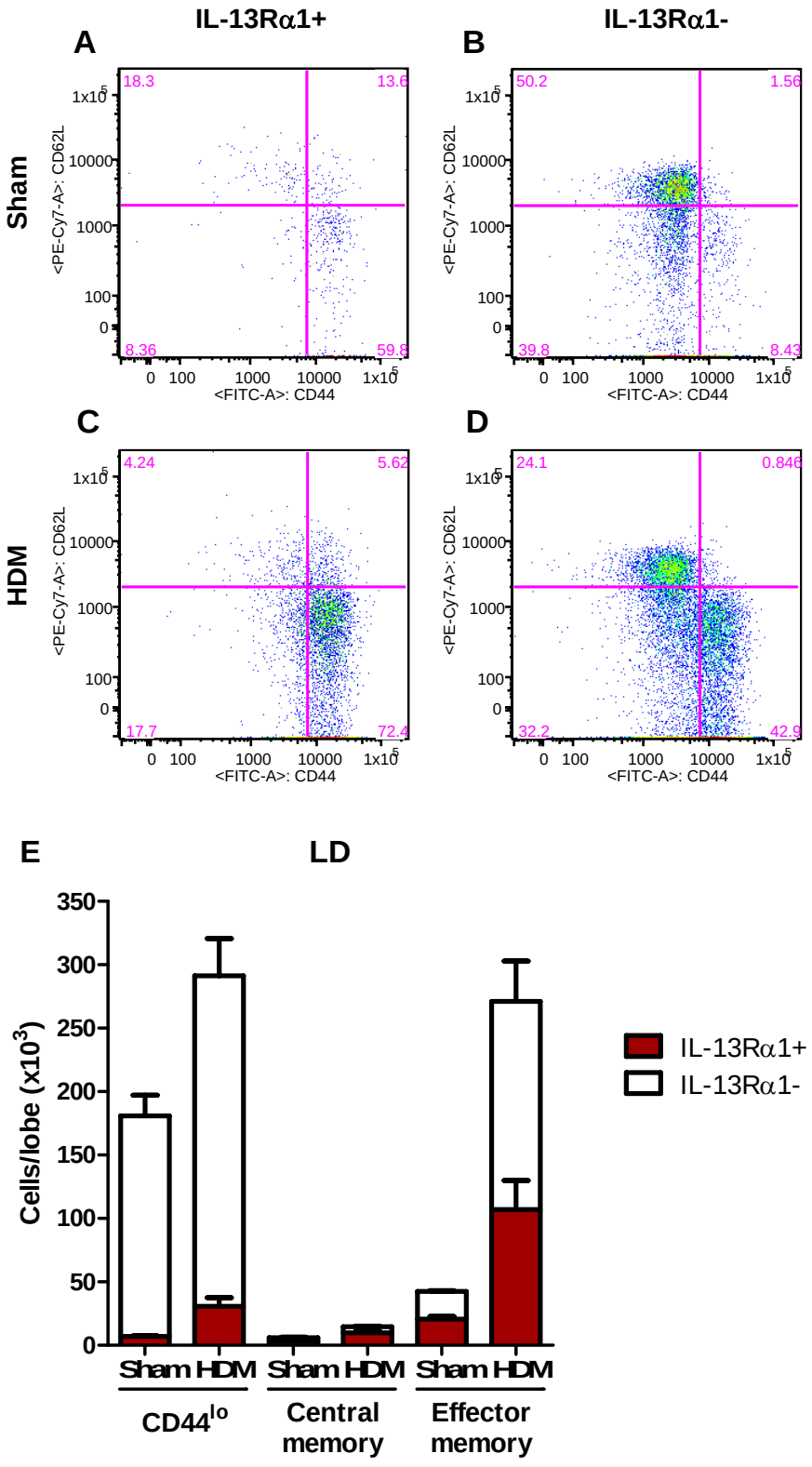


Figure 5.24 Phenotype of IL-13Rα1+ CD4+ T cells in LD from sham and HDM exposed mice. Lungs were taken after 5 weeks of HDM exposure, 24 hours after the last HDM instillation. IL-13Rα1+ cells were quantified and phenotyped by flow cytometry. (A-D) Representative dot plots of IL-13Rα1+ (A, C) and IL-13Rα1- (B, D) CD4+ T cells from sham (A-B) and HDM (C-D) exposed mice. (E) Numbers of IL-13Rα1+ naïve, central memory and effector memory T cells in LD. n = 6 mice/group, mean ± SEM.

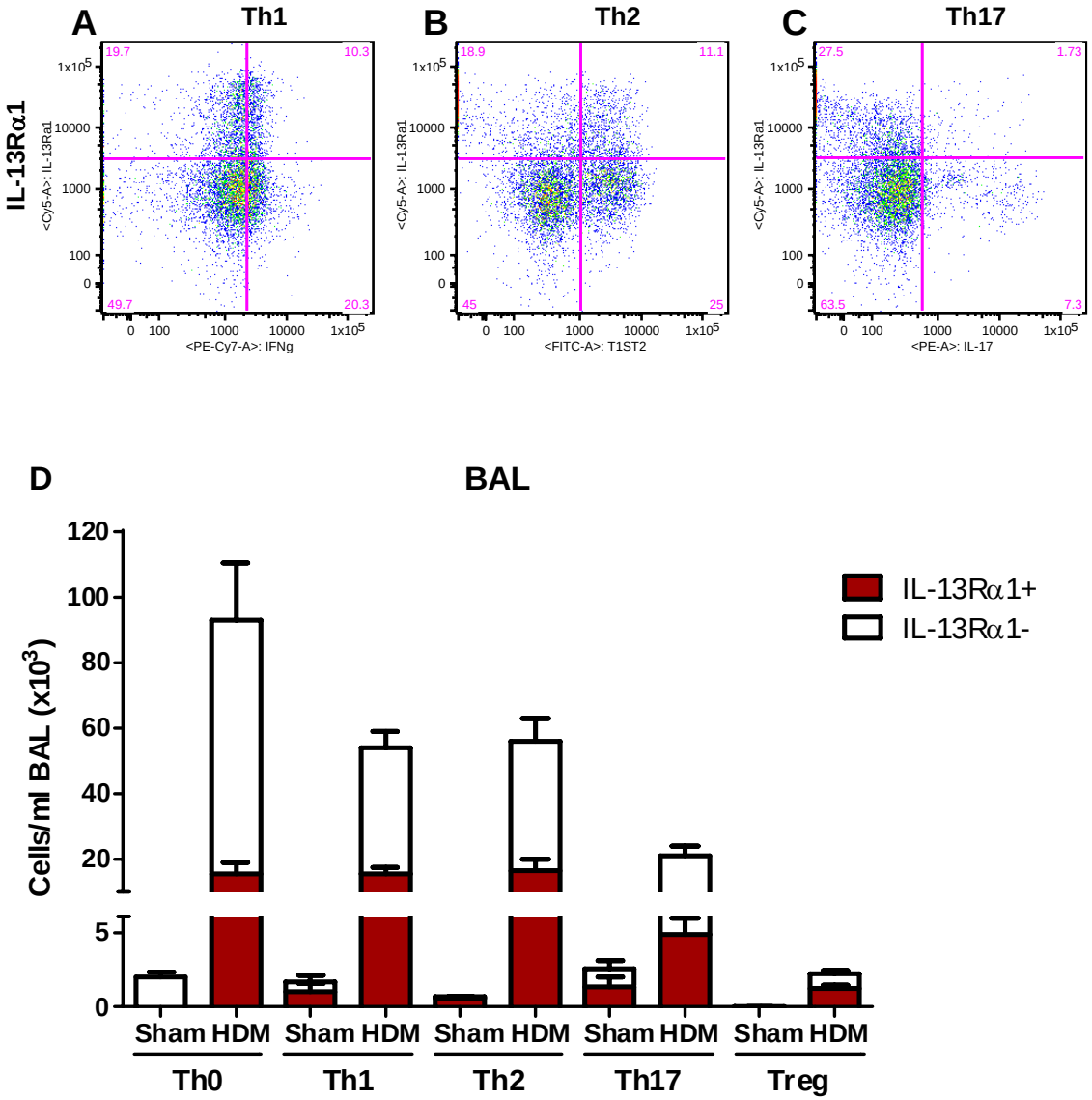


Figure 5.25 Phenotype of IL-13Rα1+ T helper cells in BAL from HDM exposed mice. BAL was taken after 5 weeks of HDM exposure, 24 hours after the last HDM instillation. IL-13Rα1+ cells were quantified and phenotyped by flow cytometry. (A-C) Representative dot plots of IL-13Rα1 expression on Th1 (A), Th2 (B) and Th17 (C) cells from HDM exposed mice. The number of IL-13Rα1+ Th0, Th1, Th2, Th17 and Treg cells in LD (D) n = 6 mice/group, mean ± SEM.

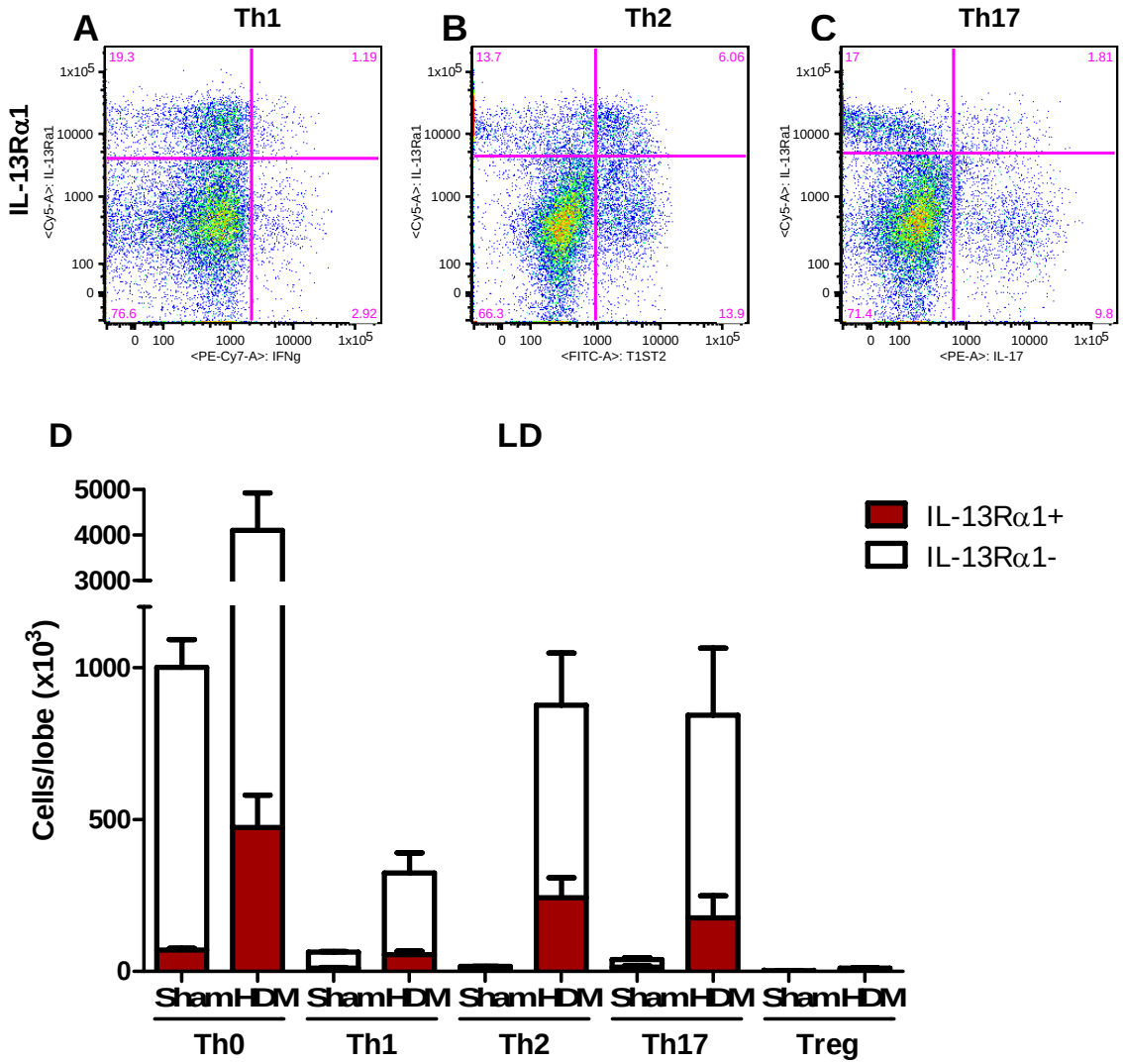


Figure 5.26 Phenotype of IL-13Rα1+ T helper cells in LD from HDM exposed mice. Lungs were taken after 5 weeks of HDM exposure, 24 hours after the last HDM instillation. IL-13Rα1+ cells were quantified and phenotyped by flow cytometry. (A-C) Representative dot plots of IL-13Rα1 expression on Th1 (A), Th2 (B) and Th17 (C) cells from HDM exposed mice. The number of IL-13Rα1+ Th0, Th1, Th2, Th17 and Treg cells in LD (D) n = 6 mice/group, mean ± SEM.

5.4 Discussion

Many cells types, both haematopoietic and stromal, have been reported to be responsive to IL-13. The aim of this chapter was to identify IL-13 receptor expressing cells within the lungs and circulation of HDM exposed mice to determine the cell types implicated in IL-13 driven pathology. Thus, further elucidating the mechanisms involved in anti-IL-13 mAb efficacy in AAD.

IL-13 has two known binding proteins; IL-13Rα1 and IL-13Rα2. The effects of IL-13 are predominantly mediated via the type II IL-4 receptor, comprising of IL-13Rα1 and IL-4Rα. IL-13Rα2 has no known co-receptors and is proposed to function primarily as a soluble decoy receptor. However, membrane associated IL-13Rα2 can deliver a pro-fibrotic signal under certain circumstances (Fichtner-Feigl *et al.*, 2006) and has been reported to impede signalling via the type II IL-4 receptor by sequestration of IL-4Rα (Andrews *et al.*, 2006). Expression of IL-13Rα1, IL-13Rα2 and IL-4Rα mRNA in lung tissue during HDM exposure was assessed by real-time PCR. Exposure to HDM over a 5 week period did not significantly modulate IL-13Rα1 mRNA expression compared to sham, however analysis was only conduced 4 hours post-HDM therefore any transient changes in IL-13Rα1 expression following HDM exposure may not have been captured. Conversely, IL-13Rα2 mRNA expression was highly up-regulated following exposure to HDM. Distinct from IL-13Rα1, IL-4Rα mRNA expression was also modestly elevated after chronic exposure to HDM.

5.4.1 IL-13Rα2 expression

In mice IL-13Rα2 may be membrane bound or soluble. Soluble IL-13Rα2 (sIL-13Rα2) is generated from cleavage of membrane bound IL-13Rα2 or translation and secretion of a distinct IL-13Rα2 splice variant (Tabata *et al.*, 2006;Daines *et al.*, 2007;Chen *et al.*, 2009). The expression of sIL-13Rα2 and membrane IL-13Rα2 transcripts are differentially regulated (Tabata *et al.*, 2006). Furthermore, due to the putative roles of sIL-13Rα2 as a decoy receptor and membrane IL-13Rα2 as a pro-fibrotic signalling receptor, these two forms of IL-13Rα2 may play opposing roles in AAD and IL-13 induced pathology.

Soluble IL-13Rα2 protein concentrations were assessed in BAL, LH supernatants and serum by ELISA and IL-13Rα2 was localised in the lungs by IF staining. The up-regulation of IL-13Rα2 mRNA in lung tissue upon HDM exposure was corroborated by an increase in sIL-13Rα2 in LH detected by ELISA. Moreover, sIL-13Rα2 expression appeared further elevated by increasing the period of HDM exposure. Despite this, BAL sIL-13Rα2 was not elevated above sham levels. A modest increase in sIL-13Rα2 protein was also detected in the serum of mice exposed to HDM for 3 weeks; however this was not evident at week 5. There is some disparity in the magnitude of IL-13Rα2 mRNA and protein up-regulation in the lung tissue. After 5 weeks of HDM exposure IL-13Rα2 mRNA was over 150-fold greater than that in sham mice, whereas sIL-13Rα2 protein levels in HDM exposed mice were less than 2-fold higher than sham. This could indicate IL-13Rα2 translation is subject to a high degree of post-transcriptional control; that sIL-13Rα2 protein is short lived in allergic mice or that the majority of IL-13Rα2 protein is membrane associated and thus not present in the LH supernatants assayed. Within the lung tissue, IL-13Rα2 IF staining was apparent in airway epithelial cells from both sham and HDM mice. Following HDM exposure IL-13Rα2 was present throughout the lung tissue. This signal could be due to expression of IL-13Rα2 by all lung cells or elevated secretion of sIL-13Rα2 by specific cell types and its subsequent dispersal throughout the tissue. IF staining for IL-13Rα2 did not allow discrimination between sIL-13Rα2 and membrane associated IL-13Rα2 hence the relative abundances of sIL-13Rα2 and membrane IL-13Rα2 are unknown. Therefore, it is not possible to determine whether the IL-13Rα2+ cells identified by IF are capable of responding to IL-13. Further investigation is required to determine whether the expression of IL-13Rα2 in airway epithelial cells in sham mice and IL-13Rα2 expression throughout the lung tissue following HDM exposure renders these cells IL-13 responsive.

In agreement with the present study, IL-13Rα2 up-regulation following stimulation with allergen or Th2 cytokines has been previously reported in mice. IL-13Rα2 mRNA was up-regulated in the lungs of mice sensitised and challenged with OVA or SEA (Wilson *et al.*, 2007;Yasunaga *et al.*, 2003;Chiba *et al.*, 2010). The latter study also observed an increase in serum sIL-13Rα2 following allergen challenge. IL-

13Rα2 mRNA has been localised specifically to the airway epithelium and pulmonary macrophages in transgenic mice with lung targeted IL-13 or IL-4 over-expression. In addition to IL-13 or IL-4 stimulation, IL-10 and IFNγ are also capable of up-regulating IL-13Rα2 (Zheng *et al.*, 2003). Furthermore, Tabata *et al.* demonstrated *ex vivo* stimulation of lung cells with IL-4 or IL-13 induced expression of mRNA transcripts for both soluble and membrane forms of IL-13Rα2 (Tabata *et al.*, 2006). Elevated concentrations of sIL-13Rα2 in BAL and serum have been demonstrated in mice sensitised and challenged with HDM compared to unsensitised mice (Tabata *et al.*, 2006). Upon quantitative RT-PCR analysis of the lung tissue from these mice, both IL-13Rα2 transcripts were up-regulated following HDM sensitisation and challenge. Interestingly, addition of HDM to IL-13Rα2 over-expressing cells *in vitro* induces the release of sIL-13Rα2 in an allergen specific, protease dependent manner (Daines *et al.*, 2007). Accordingly, a single administration of HDM into the airways *in vivo* resulted in an elevation of sIL-13Rα2 in BAL. However, repeated administration of protease active HDM into the airways could result in degradation of sIL-13Rα2 which may account for the discrepancies in sIL-13Rα2 BAL concentrations between these two latter, acute HDM studies and the present, chronic HDM study. Taken together with the present data, these observations suggest both soluble and membrane bound forms of IL-13Rα2 are up-regulated in HDM induced AAD. The sIL-13Rα2 protein detectable following HDM exposure in the present study is likely to result from both translation of the sIL-13Rα2 transcript and cleavage of membrane IL-13Rα2. The resultant pool of sIL-13Rα2 is capable of neutralising IL-13 and thus limiting IL-13 driven pathology. The levels of membrane bound IL-13Rα2 protein in the current study remain unknown; hence the role of IL-13 induced IL-13Rα2 signalling in HDM induced AAD is undetermined.

In contrast to mice, no alternatively spliced transcripts for sIL-13Rα2 have been discovered in human tissue. Generation of human sIL-13Rα2 is solely dependent upon cleavage of membrane IL-13Rα2 (Chen *et al.*, 2009). Levels of sIL-13Rα2 in BAL and serum are undetectable in asthmatics and healthy controls (O'Toole *et al.*, 2008). The presence and hence the role of IL-13Rα2 and regulation of IL-13 signalling in humans are likely to be quite distinct from the systems involved in mice; thus, complicating the extrapolation of observations and mechanisms between the two

species. Nevertheless, IL-13Rα2 expression by bronchial epithelial cells has previously been demonstrated in primary human cells and is up-regulated by IL-4 or IL-13 stimulation (Yasunaga *et al.*, 2003;Tanabe *et al.*, 2008). Similarly, IL-13Rα2 has been detected on the cell surface of primary human fibroblasts, and is up-regulated by pre-treatment with IL-13 or IL-4 (Andrews *et al.*, 2006). However, Konstantinidis *et al.* reveal IL-13Rα2 expression by epithelial cells is greater than that of fibroblasts (Konstantinidis *et al.*, 2008). Reports of the localisation of IL-13Rα2 within the cell are variable and may thus depend on culture conditions, in particular the degree of differentiation and stimulation. In human epithelial cells IL-13Rα2 has been demonstrated on the cell surface; as predominantly intracellular; as a secreted soluble form and as nuclear and perinuclear staining (Andrews *et al.*, 2006;Konstantinidis *et al.*, 2008;Tanabe *et al.*, 2008;White *et al.*, 2010). Hence, the cellular localisation, signalling capabilities, modulation and function of IL-13Rα2 in man remain elusive. However, a role for IL-13Rα2 has recently been demonstrated in clearance of IL-13 in man (Kasaian *et al.*, 2011). Thus, as sIL-13Rα2 modulates IL-13 activity in mice by acting as a decoy receptor, membrane IL-13Rα2 regulates IL-13 availability in humans by acting as an IL-13 scavenger.

5.4.2 IL-13Rα1 expression

Since IL-13Rα1 forms part of the principal IL-13 receptor signalling complex the vast majority of evidence pertaining to IL-13Rα1 expression on cell subsets is derived from functional responses to IL-13 rather than analysis of expression of IL-13Rα1 protein. Many cell types have been reported to respond to stimulation with IL-13, including monocytes, macrophages, fibroblasts, eosinophils, mast cells, basophils, dendritic cells, smooth muscle cells, endothelial cells and epithelial cells but the data available on IL-13Rα1 expression is limited. In the present study, IF and flow cytometry analysis of BAL, LD and blood cells were conducted to identify IL-13Rα1 expressing cells in sham and HDM exposed mice.

IF staining revealed IL-13Rα1+ cells throughout the lung parenchyma in sham and HDM exposed mice. The majority of these cells were identified as macrophages, although IL-13Rα1 was also detected on subsets of T cells and monocytes. However, it is likely cells expressing low levels of IL-13Rα1 may have been masked by the

high level of background staining observed, particularly in lungs from HDM exposed mice. Thus, while the current studies have focused on cells emitting the brightest IL-13Rα1 signal, these are not likely to represent the only cell types expressing IL-13Rα1 in the lung.

5.4.2.1 IL-13Rα1 expression on macrophages.

IL-13Rα1 expression in the lung parenchyma was co-localised to CD68 by IF staining and hence attributed to macrophages. Further analysis by flow cytometry defined these macrophages as AM based on CD11c and F4/80 expression. Interestingly, IF staining for IL-13Rα1 appeared brighter in lungs from HDM exposed mice than sham mice despite no significant changes in the levels of IL-13Rα1 mRNA in HDM lungs compared to sham lungs at the time-points assessed. Analysis of IL-13Rα1 expression by flow cytometry and microscopy revealed IL-13Rα1 was lost from the cell surface after exposure to HDM but present inside the cell indicating receptor internalisation may be occurring following allergen exposure. Accordingly, IF staining for IL-13Rα1 in sham lungs was closely associated with the intracellular marker CD68 but did not co-localise precisely, whereas IL-13Rα1 staining in lungs from HDM exposed mice was observed within the CD68+ cytoplasmic regions of macrophages. This suggests IL-13Rα1 may be predominantly expressed on macrophage processes in sham mice and subsequently internalised into vesicles following HDM exposure. Quantification of BAL macrophages revealed a modest elevation in the number of IL-13Rα1+ macrophages following HDM exposure; however intensity of receptor staining was diminished. Furthermore, the proportion of BAL macrophages expressing IL-13Rα1 fell from approximately 65% to 27% after exposure to HDM. This is likely to be due to a combination of loss of surface receptor and the diluting effect of infiltrating IL-13Rα1- macrophages accumulating in the BAL of HDM mice.

IL-13Rα1 was expressed on AM in the lung tissue and BAL, although the intensity of staining was greatest on BAL AM. Negligible IL-13Rα1 expression was detected on IM in the lung tissue. Again, surface expression of IL-13Rα1 on LD AM was lost upon exposure to HDM. Analysis of whole BAL macrophages from HDM exposed mice described above revealed intracellular IL-13Rα1 staining by both flow

cytometry and fluorescence microscopy, thus indicating receptor internalisation is occurring on exposure to HDM. The type II IL-4 receptor has previously been demonstrated to be internalised into endosomes following IL-4 or IL-13 stimulation of fibroblasts *in vitro* (Doucet *et al.*, 1998). HDM exposure is known to elevate both IL-4 and IL-13 concentrations in the lung tissue; hence this mechanism may also be responsible for the loss of surface IL-13Rα1 on macrophages *in vivo*. Alternatively, it is possible IL-13Rα1 staining is diminished because the detection antibody does not recognise IL-13Rα1 in the presence of IL-13. However, the anti-IL-13Rα1 antibody employed for these studies was a polyclonal and thus should recognise multiple IL-13Rα1 epitopes. Whilst it is unlikely every epitope would be masked by IL-13 binding, this could be confirmed by pre-incubating IL-13Rα1 expressing AM or whole lung sections with IL-13 prior to IL-13Rα1 staining.

Taken together, these observations may illustrate a negative feedback mechanism in which IL-13Rα1 is internalised following IL-13 binding and thus potentially limiting IL-13 driven pathology. Fate of IL-13Rα1 following internalisation is currently unknown, however further analysis of the type of endosomes containing IL-13Rα1 would indicate whether the receptor is recycled back onto the cell membrane or degraded via lysosomes. Furthermore, these data suggest IL-13Rα1 expression is controlled predominantly at the cell membrane rather than at the transcription level, since no significant modulation of IL-13Rα1 mRNA was observed during inflammation. An increase in the intensity of receptor staining in permeabilised cells from HDM mice compared to sham mice, in the absence of mRNA up-regulation, indicates some control of IL-13Rα1 expression may also occur at the translation level.

Further analysis of the phenotype of IL-13Rα1+ AM revealed expression of both macrophage and DC markers, consistent with the phenotype of AM. HDM exposure elevated the expression of CD206, CD205 and Dectin-1 in AM, indicating activation. Specifically, up-regulation of Dectin-1 and the mannose receptor, CD206 are indicative of alternative activation (Menzies *et al.*, 2010). However, these molecules are early markers of alternative activation, and hence alternative activation should be verified by the additional analysis of late markers such as RELMα (FIZZ1) and YM-1. Furthermore, alternatively activated macrophages are reported to secrete IL-10,

TGFβ and Th2 cytokines such as IL-13 (Holtzman *et al.*, 2009;Gordon, 2003), however no changes in the levels of intracellular IL-13, IL-10 or TGFβ were detected in AM following HDM exposure in the present study, although low levels of IL-10 and TGFβ were detected in AM from sham and HDM exposed mice. Thus, AM display signs of alternative activation following exposure to HDM. This is in accordance with the induction of Th2 immunity and up-regulation of the alternatively activating cytokines IL-4 and IL-13 upon HDM exposure demonstrated in chapter 3.

Macrophages are well documented to respond to IL-13 in a manner that induces alternative activation (Gordon & Martinez, 2010). Alternative activation of macrophages is stimulated by IL-4 or IL-13 and results in a multitude of changes that promote humoral immunity, allergic and anti-parasite responses and tissue repair. These include up-regulation of mannose receptor, RELMα, YM-1 and MHC class II which results in increased endocytic activity. Furthermore, arginase-1 is up-regulated leading to the differential use of L-arginine to produce, amongst other products, proline for collagen synthesis (Gordon, 2003). Despite these established effects of IL-13 on macrophages, limited analysis of IL-13Rα1 expression by these cells has been conducted. Kim *et al.* described IL-13Rα1 mRNA and protein expression in lungs from mice with virally induced chronic lung inflammation (Kim *et al.*, 2008). And furthermore, identified the majority of IL-13Rα1 expression in this model was localised to CD68+ macrophages in the lung. Expression of IL-13Rα1 mRNA and protein has also been demonstrated in human monocyte derived macrophages and mouse peritoneal macrophages (Junttila *et al.*, 2008;Martinez-Nunez *et al.*, 2011). AM exhibit a unique phenotype and verification of their response to IL-13 has not been directly studied. The function of AM has been described as "ambidextrous"; being able to suppress or promote inflammatory responses to inhaled microbes and proteins in a manner appropriate to their potential pathogenicity (Peters-Golden, 2004). Thus, the role AM in asthma pathogenesis and their response to allergen challenge is complex and not well understood. The present data illustrate naïve AM express receptors for IL-13 and are therefore likely to respond to IL-13, thereby implicating AM in IL-13 dependent AAD pathology. Since IL-13Rα1 expression was significantly diminished on AM from allergic mice, the role of this IL-13/AM interaction in AAD pathogenesis is more likely to be in the initiation rather than

maintenance of AAD. The role of AM in mice following exposure to exogenous IL-13 or HDM is the subject of the forthcoming chapter.

5.4.2.2 IL-13Rα1 expression on monocytes

IL-13Rα1 was detected on the surface of a subset of monocytes in naïve blood; identified as MOMA2+ Gr-1+ CD11b+. Akin to macrophages, it is well established that monocytes also respond to IL-13 stimulation, however the subsequent effects of IL-13 stimulation are multifaceted. Pro-inflammatory actions of IL-13 on monocytes include up-regulation of various adhesion molecules, CD23, MHC class II, CD80 and CD86 (Zurawski & de Vries, 1994;de Vries, 1998). Conversely, IL-13 down-regulates the expression of pro-inflammatory mediators IL-1α, IL-1β, IL-6, IL-12, TNFα, IL-8, MIP-1α, MIP-1β and MCP-3; induces expression of 15-lipoxygenase and inhibits COX-2 induction in monocytes. In addition, IL-13Rα1 mRNA expression in human monocytes has been demonstrated to be down-regulated upon *in vitro* differentiation into macrophages (Hart *et al.*, 1999) and surface expression of IL-13Rα1 on human monocytes down-regulated by incubation with IL-13 or IL-4 (Graber *et al.*, 1998). This down-regulation of IL-13Rα1 expression upon maturation/activation is supported by the earlier observation in the present study that CD68+ macrophages infiltrating into the lungs of HDM exposed mice do not express IL-13Rα1 and is paralleled by the loss of surface IL-13Rα1 on AM after HDM exposure. This indicates monocytes and macrophages, once activated, may lose the ability to respond to IL-13 stimulation. Hence implying a limited role for the actions of IL-13 on activated monocytes and macrophages in the perpetuation of AAD in the lung tissue.

5.4.2.3 IL-13Rα1 expression on T cells

Unexpectedly, IL-13Rα1 was also found to be present on the surface of a small proportion of CD4+ T cells. This population of IL-13Rα1+ CD4+ T cells was present in blood from naïve and HDM exposed mice and could also be detected infiltrating the BAL and lung tissue of HDM mice. Attempts to identify the phenotype of this population revealed the majority of IL-13Rα1+ CD4+ cells in the blood were naïve T cells, however the IL-13Rα1+ CD4+ population was enriched for memory cells compared with the whole CD4+ T cell population. Induction of HDM induced AAD

resulted in negligible changes in the respective sizes of these population. Following HDM exposure the majority of IL-13Rα1+ CD4+ T cells in BAL and LD were effector cells. Naïve and central memory cells in the lungs and BAL also expressed IL-13Rα1; in fact the majority of central memory cells were IL-13Rα1+. Further analysis of IL-13Rα1+ CD4+ effector T cells in BAL and LD indicated IL-13Rα1 expression was not specific to a particular T helper phenotype, but could be detected on subsets of Th1, Th2, Th17 and Tregs. Thus, IL-13 may have direct actions on T cells present in the BAL and LD of allergic mice. However, effects of IL-13Rα1 ligation on specific T cell subsets and the involvement of these pathways in the pathogenesis of HDM induced AAD are largely unknown.

Until recently it was believed CD4+ T cells did not express IL-13Rα1 at the cell surface, despite IL-13Rα1 mRNA and intracellular protein being present in human peripheral blood T cells (Gauchat *et al.*, 1997;Graber *et al.*, 1998). Newcomb *et al.* have since demonstrated elevated IL-13Rα1 mRNA and protein specifically in murine Th17, but not Th0, Th1 or Th2 cells, polarised *in vitro* (Newcomb *et al.*, 2009). Furthermore, Th17 cells responded to IL-13 stimulation by further up-regulating IL-13Rα1 mRNA, reducing IL-17A and IL-21 production, down-regulating retinoic acid receptor-related orphan receptor-γt (ROR-γt) and up-regulating GATA-binding protein 3 (GATA3) expression. This IL-13 dependent negative regulation was not observed in Th1 or Th2 polarised populations. Equivalent data has been obtained in polarised human T cell populations in which surface expression of IL-13Rα1 was demonstrated in addition to elevated mRNA and a functional response to IL-13 (Newcomb *et al.*, 2011). In addition, Newcomb *et al.* demonstrate the combination of TGF-β, IL-1β and IL-23 (but not IL-6) used for *in vitro* polarisation of Th17 cells is responsible for the up-regulation of IL-13Rα1. This data appears contrary to observations in the present study in which IL-13Rα1 expression is observed in all T helper cell populations from mice with HDM induced AAD and is not unique to Th17 cells. However, Newcomb *et al.* rely heavily on *in vitro* polarisation of T cells, using very specific conditions, without analysing T cells polarised *in vivo* during an ongoing immune response. It is possible the observed up-regulation of IL-13Rα1 is driven by TGF-β, IL-1β and IL-23 and is coincident with Th17 polarisation rather than specific to Th17 cells. In support of this, chronic exposure to HDM up-regulates the

expression of TGF-β and IL-1β (unpublished observation, data not shown) in the lungs, potentially providing a favourable environment for IL-13Rα1 up-regulation (Fattouh *et al.*, 2008). This hypothesis requires further investigation; of particular interest would be determination of IL-23 concentrations in the lungs following exposure to HDM and determination of the effects of TGFβ, IL-1β and IL-23 stimulation on cells previously polarised to Th1 and Th2 phenotypes *in vitro*. In addition, further analysis of *in vivo* polarised Th0, Th1, Th2 and Th17 cells and their responses to *ex vivo* IL-13 stimulation would be help elucidate the function of IL-13Rα1 on T cells.

In summary, IL-13Rα2 is constitutively expressed by airway epithelium in mice, and was up-regulated in HDM induced AAD, however, whether this IL-13Rα2 expression renders these cells responsive to IL-13 remains to be determined. IL-13Rα1 is expressed by AM but lost from the cell surface following HDM exposure. In addition, a proportion of blood monocytes and CD4+ T cells express IL-13Rα1, although the function of IL-13 signalling in these cell types requires further investigation. The role of AM in IL-13 and HDM induced airway inflammation will be explored in the following chapter.

6. THE ROLE OF AM IN HDM INDUCED AAD

6.1 Introduction

The previous chapter established AM as one of the key cell types in the lung expressing the primary IL-13 signalling receptor subunit IL-13Rα1. Thus indicating AM may play a role in IL-13 dependent lung pathology. Hence, the objective of this chapter was to investigate the role of AM in the pathogenesis of AAD. To address this required the development of a protocol for specific AM depletion.

Colony-stimulating factor-1 receptor (CSF-1R) blockade was used to deplete AM in preliminary studies. CSF-1 is reported to be a survival factor for tissue macrophages hence blockade of this signal results in the loss of macrophages evident in *Csf1*^{op}/*Csf1*^{op} mice which lack functional CSF-1 and in mice dosed with a mAb to CSF-1R (Wiktor-Jedrzejczak *et al.*, 1992;Roth *et al.*, 1998;MacDonald *et al.*, 2010)

As an alternative approach to AM depletion clodronate (dichloromethylene-bisphosphonate) filled liposomes were employed. Clodronate induces apoptosis in phagocytes that engulf and digest the liposomes, hence intra-tracheal (i.t.) administration of clodronate liposomes depletes AM present in the airway spaces (van Rooijen & Sanders, 1994). Liposomes cannot cross epithelial or endothelial barriers and hence do not deplete IM or other macrophage populations residing outside the lungs (Thepen *et al.*, 1989). Furthermore, DC are not depleted by liposomes, thus i.t. administration of clodronate liposomes elicits specific depletion of AM (Jakubzick *et al.*, 2006).

To investigate the role of AM in IL-13 dependent disease pathology initial studies were conducted in a simple model of lung inflammation induced by i.t. delivery of exogenous IL-13. Administration of IL-13 directly into the airways induces accumulation of eosinophils and neutrophils in BAL, goblet cell up-regulation and AHR, moreover these effects are also evident in RAG1$^{-/-}$ mice implicating resident lung cells in the response to IL-13 (Wills-Karp *et al.*, 1998;Grunig *et al.*, 1998). Establishing this model in AM deficient mice and assessing the ensuing pathology would indicate whether AM are involved in the elicitation of IL-13 stimulated lung pathology.

Following on from assessing the role of AM in IL-13 stimulated lung pathology, HDM induced AAD was employed to explore the role of AM in IL-13 dependent lung pathology. Although AM depletion in HDM induced AAD has not previously been reported, a small number of studies have investigated the effects of AM depletion in various other models of lung inflammation with conflicting outcomes. AM depletion has been demonstrated to exacerbate, ameliorate or not affect lung inflammation and AHR (Thepen *et al.*, 1989;Thepen *et al.*, 1991;Thepen *et al.*, 1992;Tang *et al.*, 2001a;Bang *et al.*, 2011;Nagarkar *et al.*, 2010;Yang *et al.*, 2010;Careau & Bissonnette, 2004;Bedoret *et al.*, 2009). It is likely the inconsistency of these results arises from a multitude of differences in animal models, species, depletion approaches and time of AM depletion. In the present studies AM depletion was conducted prior to HDM exposure and continued throughout the study to investigate the role of AM in the development of the allergic response. In addition, AM depletion was conducted "therapeutically", after the initiation of the allergic response, to determine the role of AM in the maintenance of AAD.

6.1.1 Aim

4. Use the appropriate cell types identified in chapter 5 to characterise the underlying mechanisms of IL-13 inhibition *in vivo* by specific cell depletion.

The initial aims of this chapter were to establish protocols for specific AM depletion and IL-13 induced lung inflammation and to subsequently determine the effects of AM depletion on IL-13 induced lung pathology. Furthermore, to investigate the effects of both prophylactic and therapeutic AM depletion on the development and maintenance of HDM induced AAD, respectively, in order to determine whether AM play a role in IL-13 dependent lung pathology.

6.2 Methods

6.2.1 Macrophage depletion.

6.2.1.1 Anti-CSF-1R treatment

Blockade of the macrophage survival factor CSF-1 was accomplished by treatment with a high affinity anti-mouse CSF-1R mAb generated by UCB, CA019_00486 (mAb 535). Mice were dosed with 10mg/kg 535 s.c., 3 times per week for up to 14 days; a dose previously demonstrated to be fully efficacious in murine disease models (unpublished data from UCB). Control mice received 10mg/kg isotype control (101.4) s.c., 3 times per week for 14 days. After 3, 7, 10 or 14 days of treatment mice were bled by cardiac puncture and killed for collection of BAL and lungs. Cells were liberated from the lung tissue by digestion as detailed in materials and methods. Staining of monocytes and macrophages in blood, BAL and LD for analysis by flow cytometry was conducted according to materials and methods. Identification of eosinophils was based solely on forward and side-scatter characteristics.

6.2.1.2 Administration of clodronate liposomes

Mice were dosed with 50µl of liposome encapsulated clodronate (ClodronateLiposomes.org, The Netherlands) i.t. once or twice per week, commencing two days prior to administration of IL-13 or HDM. Control mice received PBS filled liposomes according to the same dosing schedule.

6.2.2 IL-13 induced lung inflammation

An IL-13 induced lung inflammation protocol was adapted from Wills-Karp and Grunig (Wills-Karp *et al.*, 1998;Grunig *et al.*, 1998). Mice were dosed with 5µg IL-13 i.t. for 3 consecutive days and killed 15 hours after the last administration for collection of BAL and lungs (Figure 6.1). Control mice received i.t. vehicle (PBS + 1% FCS). Analysis of BAL and LD cellularity was conducted by flow cytometry as previously described in materials and methods. Mice receiving liposomes were dosed once, two days prior to the first IL-13 administration.

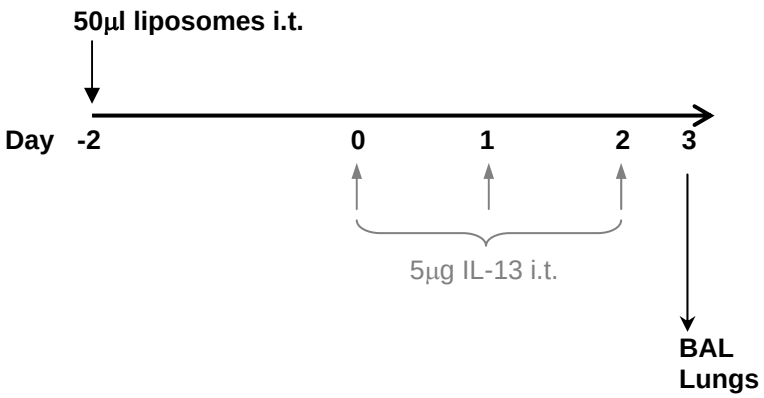


Figure 6.1 Experimental protocol for IL-13 induced lung inflammation. Mice were administered i.t. IL-13 on 3 consecutive days. Control mice received i.t. saline alone. Mice were dosed with i.t. liposomes 2 days prior to IL-13 administration. Mice were culled 15 hours after the final IL-13 administration for collection of BAL and lung samples.

6.2.3 Clodronate liposome treatment of HDM exposed mice

To determine the role of macrophages in AAD prophylactic or therapeutic administration of liposomes was conducted in mice exposed to HDM for 3 weeks. Mice dosed prophylactically received 50µl liposomes i.t., two days prior to the first HDM exposure and once weekly thereafter (Figure 6.2 A). AHR to MCh was assessed by WBP on day 11, 24 hours post HDM. Mice dosed therapeutically received 50µl liposomes i.t., twice weekly during the third week of HDM exposure (Figure 6.2 B). AHR to MCh was assessed by WBP on day 16, 24 hours post HDM, prior to administration of liposomes. Under both protocols mice were bled by cardiac puncture and killed 4 hours after the last HDM exposure for collection of BAL and lung samples.

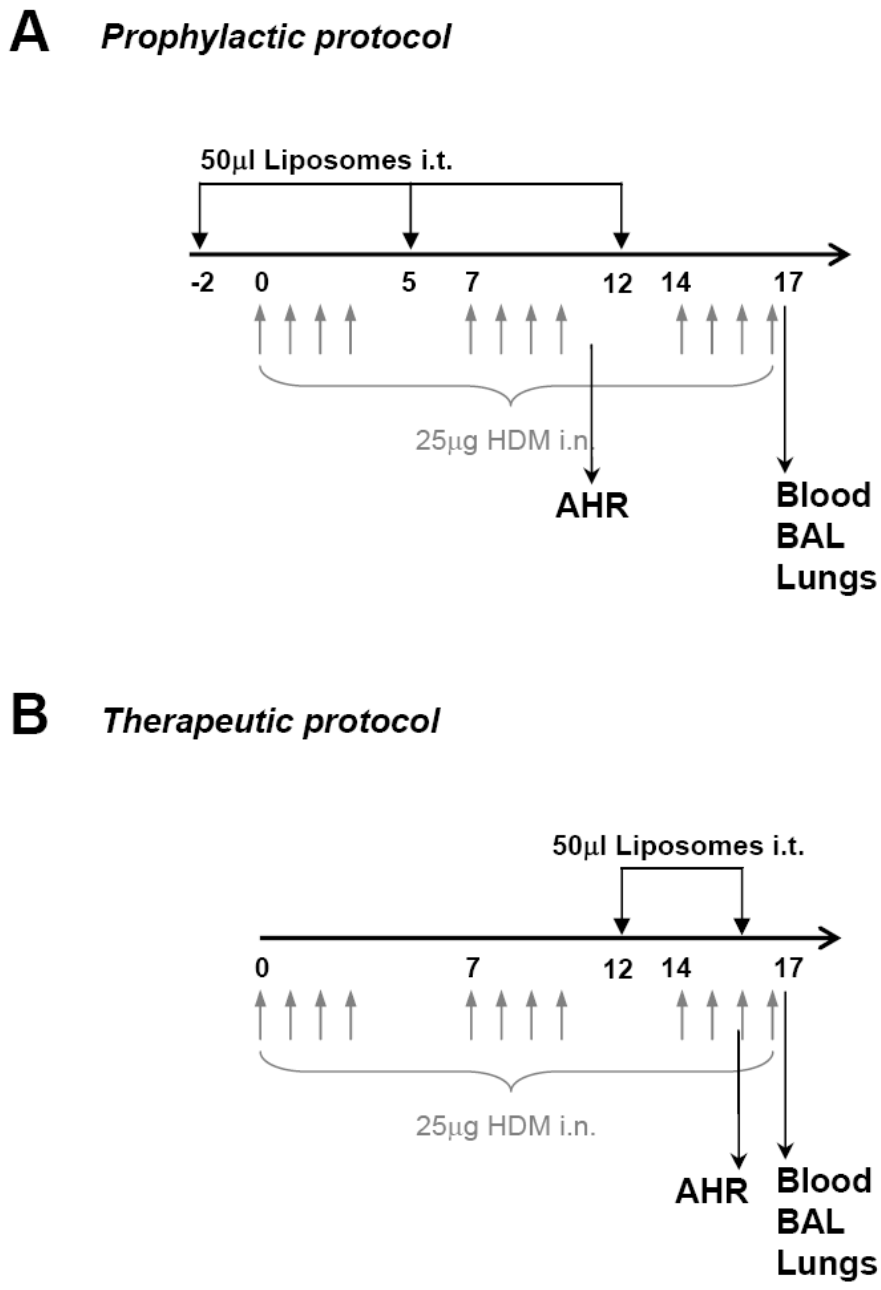


Figure 6.2 Experimental protocol for macrophage depletion during HDM induced lung inflammation. Mice were exposed to HDM 4 times/week for 3 weeks. Sham exposed mice received i.n. saline alone. (A) Prophylactic protocol; mice were dosed with i.t. liposomes 2 days prior to the first HDM exposure and weekly thereafter. AHR to MCh was assessed by WPB on day 11. (B) Therapeutic protocol; mice were dosed with i.t. liposomes on day 12 and 16 of HDM exposure. AHR to MCh was assessed by WBP on day 16. In both protocols mice were bled via cardiac puncture and killed 4 hours after the final HDM exposure for collection of BAL and lung samples.

6.3 Results

6.3.1 Anti-CSF-1 receptor induced macrophage depletion

In an attempt to deplete alveolar macrophages, blockade of the macrophage survival factor CSF-1 was conducted by repeated administration of an anti-CSF-1 receptor mAb, 535. 535 treatment had no significant effects on the total number of BAL macrophages over the 14 day dosing period (Figure 6.3 A), however a partial reduction in the number of LD macrophages was observed from day 3 (Figure 6.3 B). This was accounted for by a modest decline in the number of LD AM, apparent from day 7, and a more robust reduction in LD IM evident after just one dose of 535 (Figures 6.3 D and F, respectively). No significant effects on the number of BAL AM were observed (Figure 6.3 C) however BAL IM were reduced from 3 days of receptor blockade (Figure 6.3 E). The number of circulating monocytes in the blood was also significantly decreased after a single dose of 535 (Figure 6.4 A), however a significant increase in the number of circulating eosinophils was noted in the blood after 10 days of treatment which was further elevated by day 14 (Figure 6.4 B). This elevation in eosinophils was also evident in LD (Figure 6.4 C) but not BAL (data not shown). Due to the incomplete depletion of AM and the greater number of circulating eosinophils observed with 535 treatment, alternative approaches for macrophage depletion were sought.

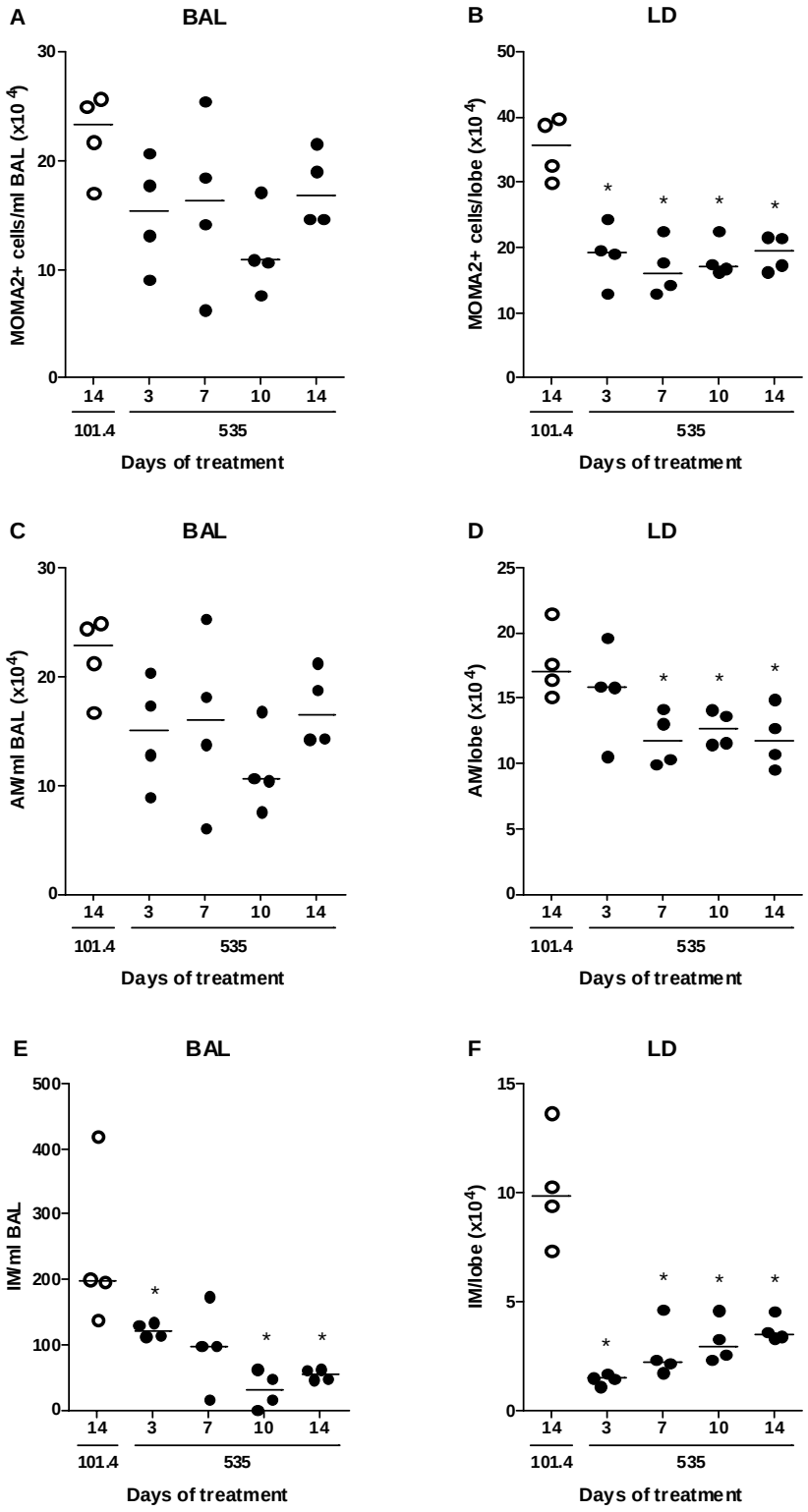


Figure 6.3 Effects of anti-CSF-1 receptor treatment on BAL macrophage frequency. Mice were dosed with 10mg/kg 535 or isotype control (101.4) s.c., 3 times a week for 3, 7, 10 or 14 days. BAL and lungs were taken 2 days after the last administration of 535 treatment. Total macrophages (A-B), AM (C-D) and IM (E-F) in BAL (A, C, E) and LD (B, D, F) were identified and quantified by flow cytometry. n = 4 mice/group, bar represents median. * $p<0.05$ relative to 101.4 group by Mann Whitney test.

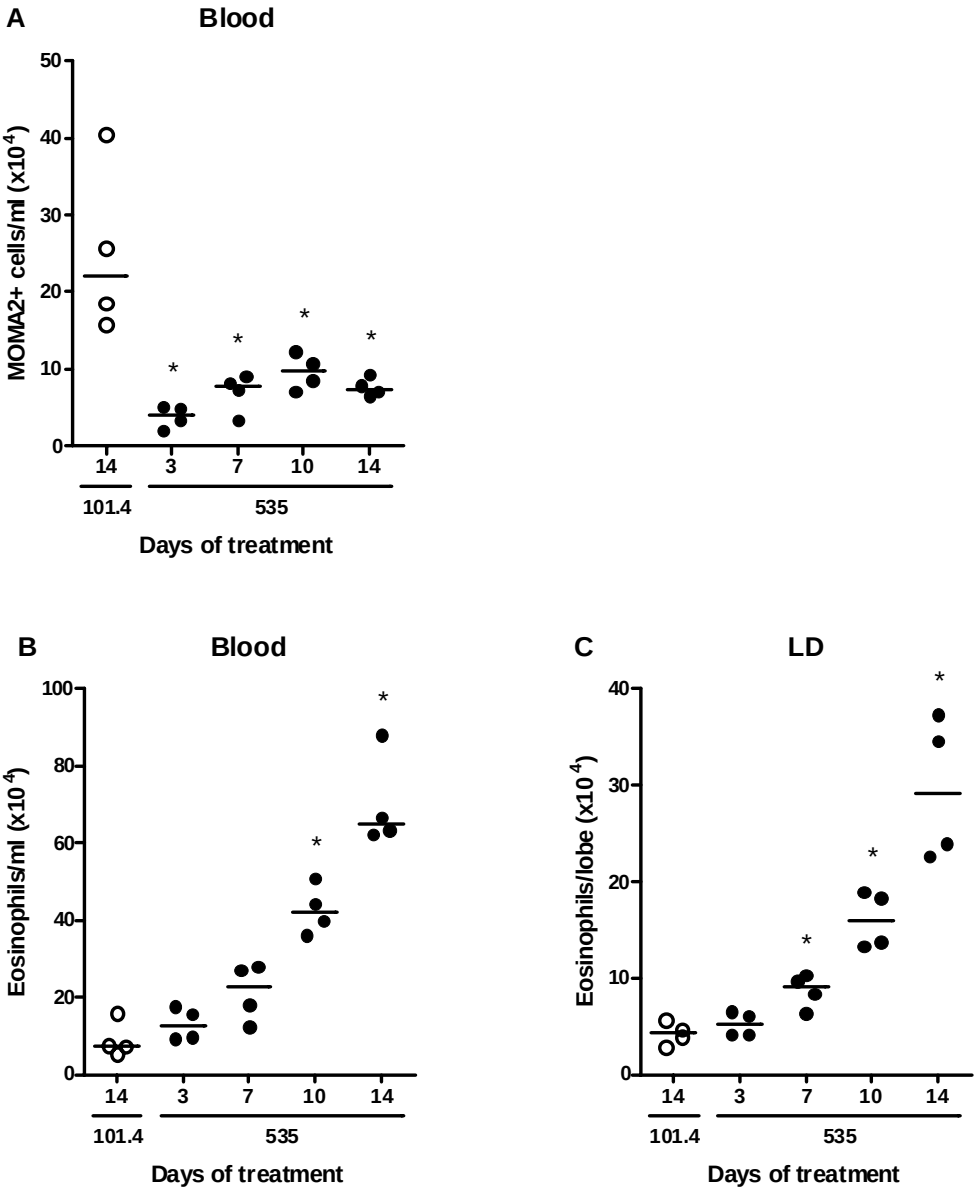


Figure 6.4 Effects of anti-CSF-1 receptor treatment on blood monocytes and eosinophils. Mice were dosed with 10mg/kg 535 or isotype control (101.4) s.c., 3 times a week for 3, 7, 10 or 14 days. Blood and lungs were taken 2 days after the last administration of 535 treatment. Total blood monocytes (A) and eosinophils (B) and LD eosinophils (C) were identified and quantified by flow cytometry. n = 4 mice/group, bar represents median. * $p<0.05$ relative to 101.4 group by Mann Whitney test.

6.3.2 Clodronate liposome mediated macrophage depletion

Clodronate encapsulated liposomes were employed to deplete AM. Initial studies were conducted to determine the volume of i.t. liposomes required for adequate macrophage depletion. Thereafter the time-course of macrophage depletion was established to inform dose frequency required for subsequent studies. Administration of i.t. clodronate liposomes reduced the number of macrophages in BAL by approximately 83% 2 days after dosing, but did not affect the total number of LD macrophages (Figure 6.5 A-B). AM were depleted in BAL (85%) and partially depleted in LD (65%; Figure 6.5 C-D), yet no effects were observed on IM in BAL or LD (Figure 6.5 E-F). The standard protocol for macrophage depletion uses 100µl of liposomes i.t. however Home Office restrictions limited i.t. administration to 50µl (Thepen *et al.*, 1989). Therefore this initial study sought to determine the effects of one or two doses of 50µl of liposomes. No differences in macrophage depletion at day 2 were observed between one dose of 50µl and two doses of 50µl one hour apart (Figure 6.5), demonstrating one dose of 50µl of clodronate liposomes i.t. was adequate to deplete AM in naïve mice. Furthermore, two consecutive i.t. doses of clodronate liposomes was less well tolerated than one dose, resulting in 3 mice being culled prior to the end of the experiment. In addition, two consecutive doses of PBS liposomes elicited a non-significant trend towards reduced total macrophages and AM in LD (Figure 6.5 B and D). Subsequently, macrophage depletion was assessed for a week following one dose of i.t. liposomes. A significant reduction in the number of total macrophages in BAL was apparent from day 1 and persisted until at least day 7 (Figure 6.6 A). This was mirrored by the numbers of BAL AM which were reduced by 75% at day 1, 83% at day 4 and 67% at day 7 (Figure 6.6 C). In contrast, the numbers of BAL IM were elevated slightly from day 4 of liposome administration (Figure 6.6 E). In LD i.t. liposomes had no effect on the total number of macrophages (Figure 6.6 B) however, AM were reduced at day 4 (65%) and 7 (63%; Figure 6.6 D). Akin to BAL, a small increase in the number of IM was observed in LD at day 4 (Figure 6.6 F). Since AM depletion in the lung tissue was not apparent until at least day 2, liposome dosing for prophylactic depletion of macrophages *in vivo* would commence 2 days prior to the start of the experiment in subsequent studies. Furthermore, there was some evidence of BAL AM repopulating by day 7 after

clodronate liposome administration therefore liposomes would be dosed weekly in future studies.

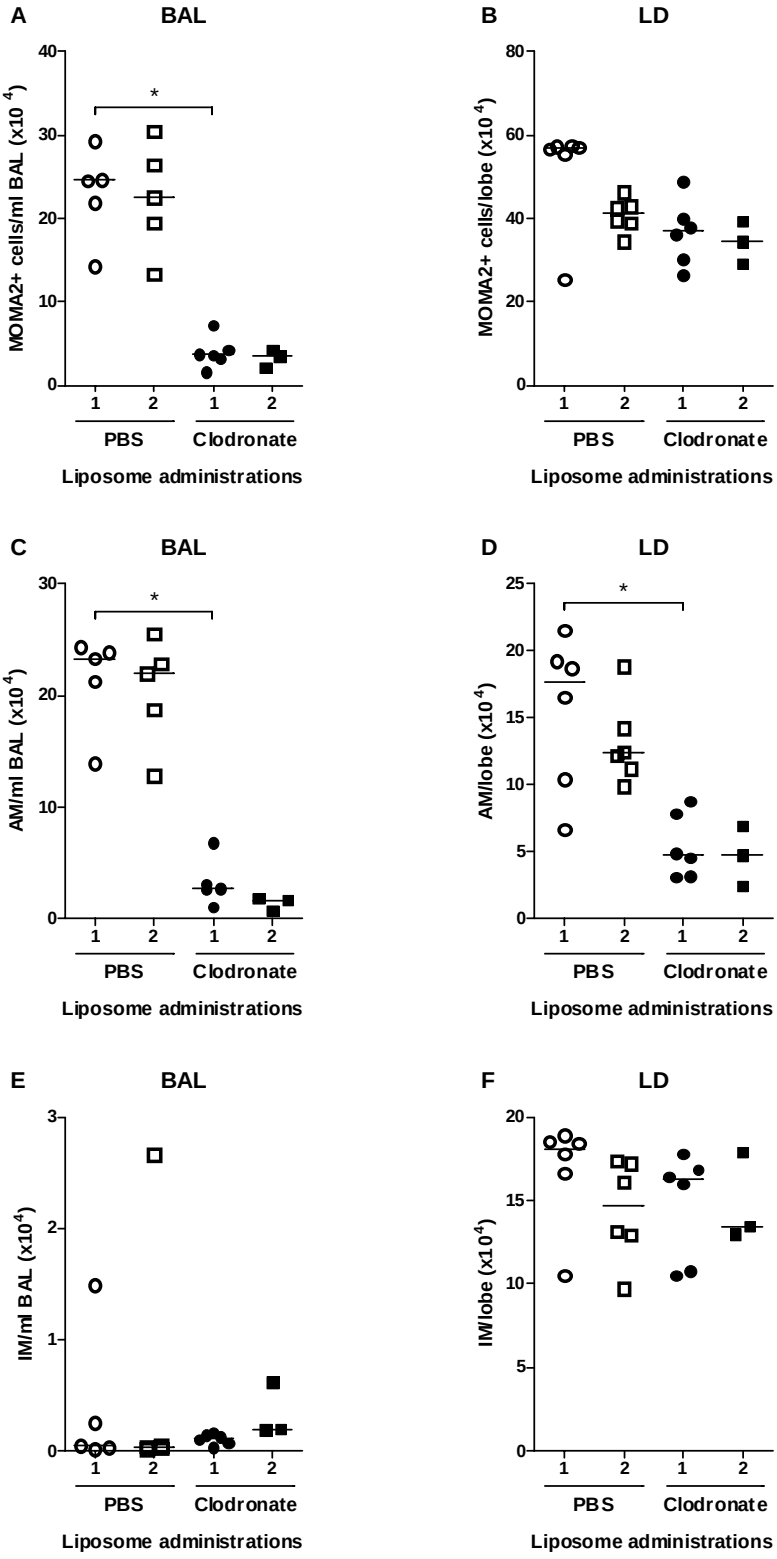


Figure 6.5 Effects of 1 or 2 doses of clodronate liposomes on BAL and LD macrophages. Mice were dosed with 50µl clodronate liposomes or control (PBS liposomes) i.t., once or twice. BAL and lungs were taken 2 days after liposome administration. Total macrophages (A-B), AM (C-D) and IM (E-F) in BAL (A, C, E) and LD (B, D, F) were identified and quantified by flow cytometry. n = 3-6 mice/group, bar represents median. * $p<0.05$ by Kruskal-Wallis ANOVA with Dunn's post test.

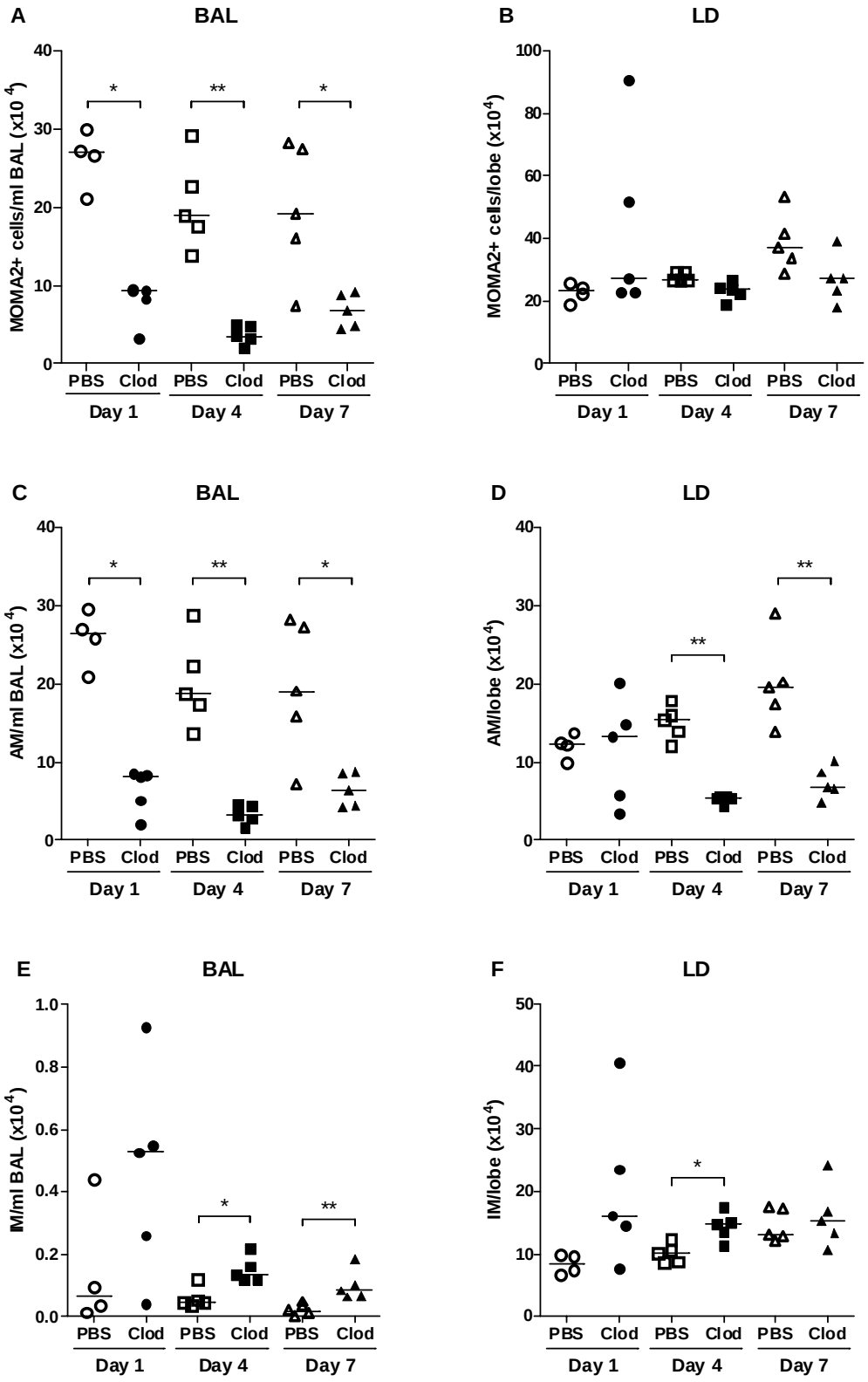


Figure 6.6 Time course of clodronate induced macrophage depletion. Mice were dosed with 50µl clodronate liposomes (Clod) or control (PBS) liposomes i.t., once. BAL and lungs were taken 1, 4 and 7 days after liposome administration. Total macrophages (A-B), AM (C-D) and IM (E-F) in BAL (A, C, E) and LD (B, D, F) were identified and quantified by flow cytometry. n = 4-5 mice/group, bar represents median. * $p<0.05$ and ** $p<0.01$ by Mann Whitney test.

6.3.3 IL-13 induced lung inflammation

A short term model of IL-13 induced lung inflammation was established to enable the subsequent investigation of the role of AM in the response to IL-13. Administration of 5μg IL-13 i.t. on 3 consecutive days induced accumulation of eosinophils, T cells and specifically CD4+ T cells in the BAL 15 hours after the last IL-13 instillation (Figure 6.7 A, C and E). This dosing regime did not induce any significant changes in tissue eosinophil or T cell numbers (Figure 6.7 B, D and F). IL-13 administration had no effects on the total numbers of leukocytes in BAL and LD (Figure 6.8 A-B) or on the number of macrophages in BAL and LD (Figure 6.8 C-D). A non-significant trend towards BAL neutrophilia was observed in IL-13 treated mice although there was no change in the number of LD neutrophils (Figure 6.8 E-F).

Analysis of BAL cytokines and chemokines revealed i.t. IL-13 administration did not induce IL-4 or IL-5 release (Figure 6.9 A-B). IL-13 induced a non-significant elevation in IL-10 concentration (Figure 6.9 C) and significant release of IL-12, eotaxin and KC (Figure 6.9 D-F). In addition, administration of IL-13 increased tissue IL-33 but had no effect on IL-25 or TSLP concentrations in LH (Figure 6.10).

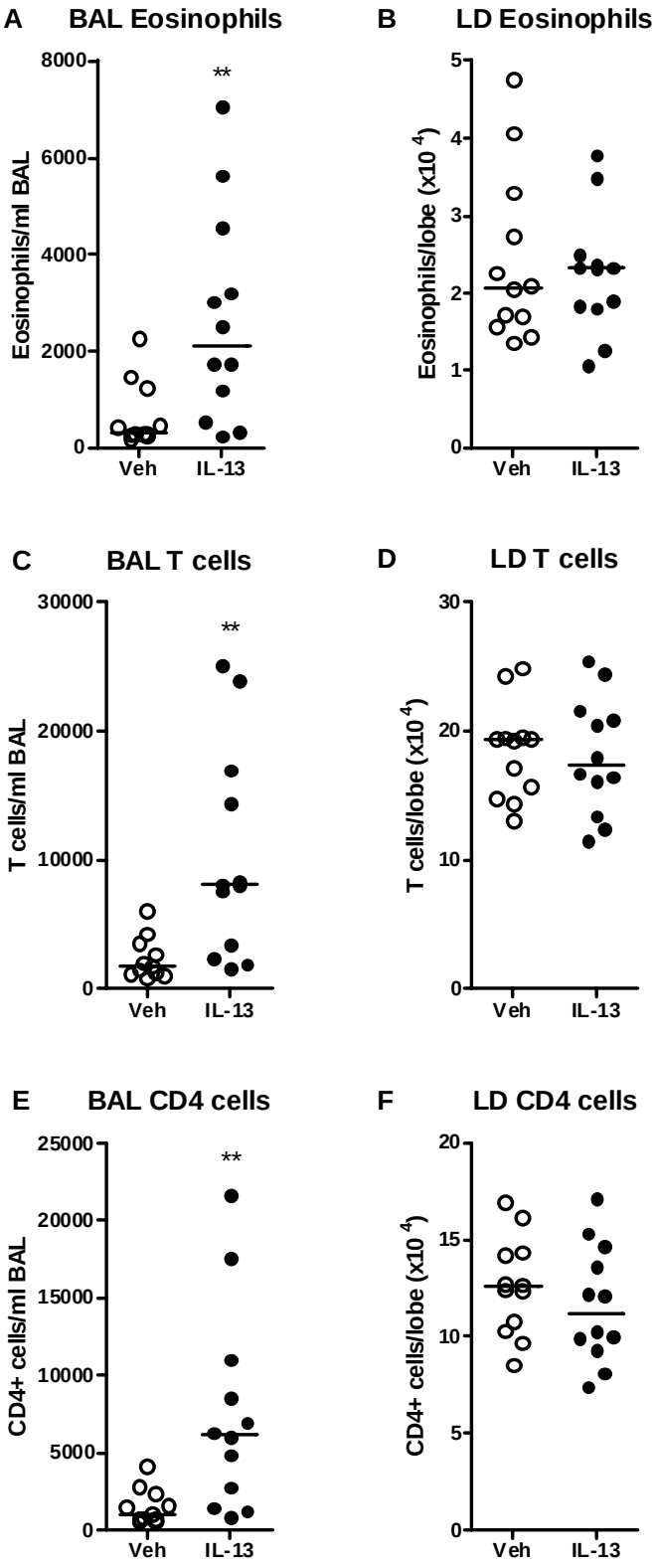


Figure 6.7 IL-13 induced accumulation of eosinophils and T cells. Mice were dosed with 5μg IL-13 or vehicle (Veh; PBS + 1% FCS) i.t., on 3 consecutive days. BAL and lungs were taken 15 hours after the last IL-13 administration. Eosinophils (A-B), CD3+ T cells (C-D) and CD4+ T cells (E-F) in BAL (A, C, E) and LD (B, D, F) were identified and quantified by flow cytometry. n = 11-12 mice/group, bar represents median. Data represents two independent experiments. ** $p<0.01$ by Mann Whitney test.

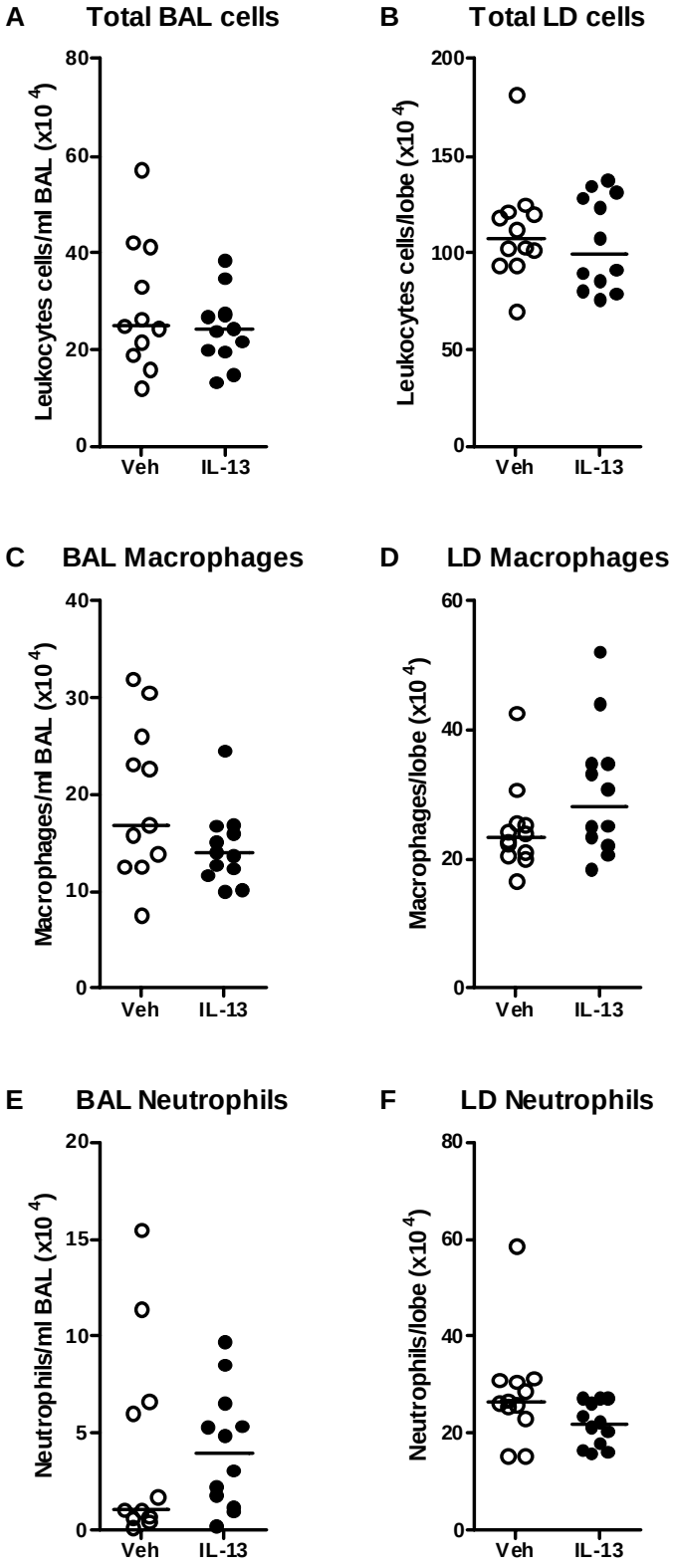


Figure 6.8 Effects of IL-13 on accumulation of total leukocytes, macrophages and neutrophils. Mice were dosed with 5µg IL-13 or vehicle (Veh; PBS + 1% FCS) i.t., on 3 consecutive days. BAL and lungs were taken 15 hours after the last IL-13 administration. Total leukocytes (A-B), macrophages (C-D) and neutrophils (E-F) in BAL (A, C, E) and LD (B, D, F) were identified and quantified by flow cytometry. n = 11-12 mice/group, bar represents median. Data represents two independent experiments.

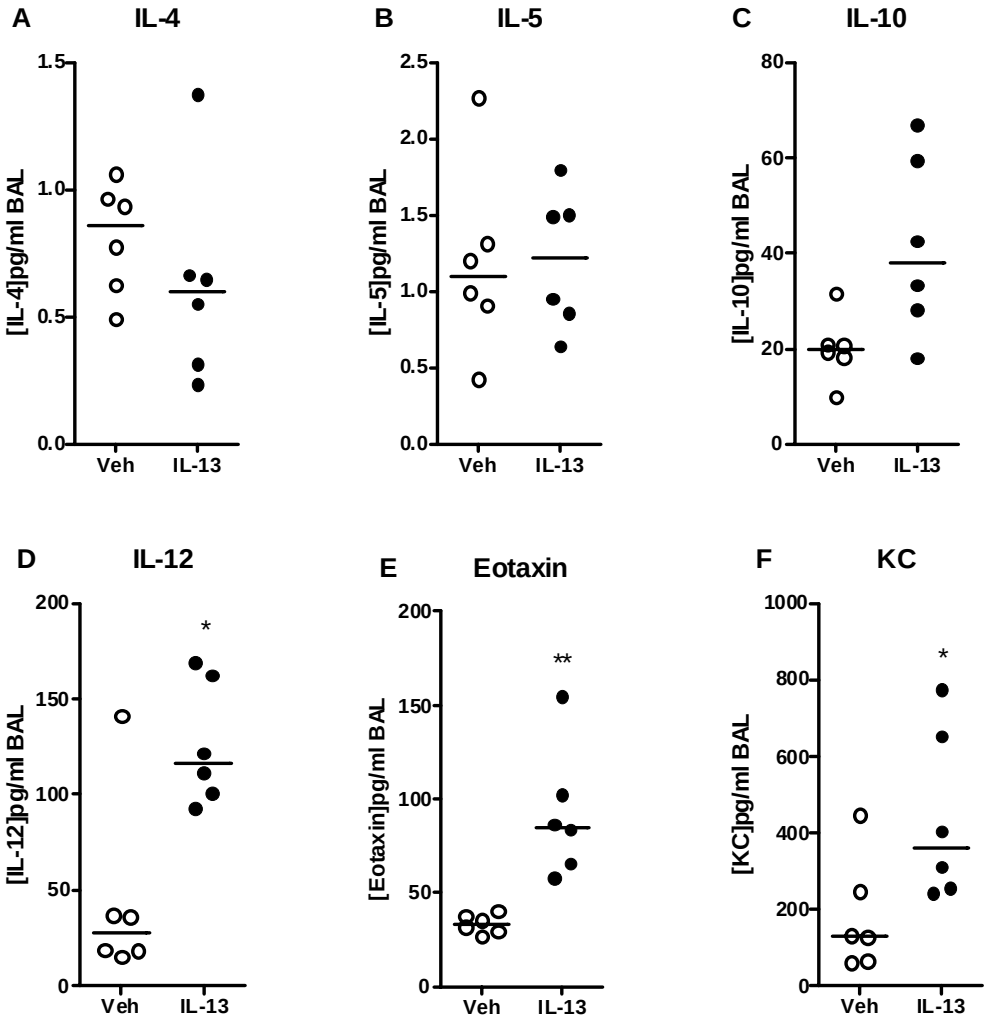


Figure 6.9 IL-13 induced mediator release. Mice were dosed with 5µg IL-13 or vehicle (Veh; PBS + 1% FCS) i.t., on 3 consecutive days. BAL was taken 15 hours after the last IL-13 administration. BAL IL-4 (A), IL-5 (B), IL-10 (C), IL-12 (D), eotaxin (E) and KC (F) were quantified by MSD multiplex assay (A-D, F) or ELISA (E). n = 6 mice/group, bar represents median. * $p<0.05$ and ** $p<0.01$ by Mann Whitney test.

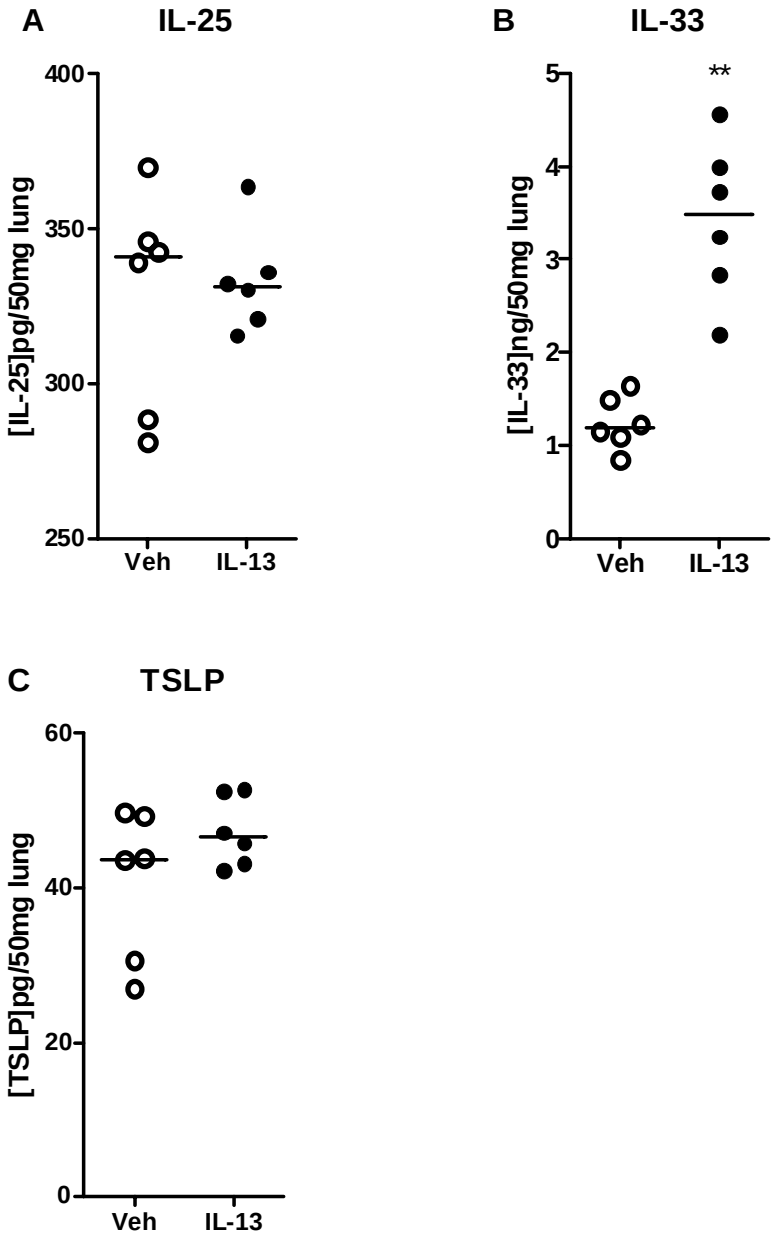


Figure 6.10 IL-13 induced release of epithelial cytokines. Mice were dosed with 5µg IL-13 or vehicle (Veh; PBS + 1% FCS) i.t., on 3 consecutive days. Lungs were taken 15 hours after the last IL-13 administration for generation of LH supernatant. LH IL-25 (A), IL-33 (B) and TSLP (C) were quantified by ELISA. n = 6 mice/group, bar represents median. ** $p<0.01$ by Mann Whitney test.

6.3.4 IL-13 induced lung inflammation in mice pre-treated with clodronate liposomes

Pre-treatment with clodronate liposomes depleted the majority of BAL AM in both vehicle and IL-13 dosed mice and partially depleted LD AM (Figure 6.11 C-D). As previously observed, a small increase in the number of BAL IM was evident in vehicle and IL-13 dosed mice treated with clodronate liposomes (Figure 6.11 E). To assess the total inflammatory infiltrate in BAL without the loss of macrophages skewing the data in clodronate treated mice, the number of macrophages was subtracted from total leukocyte counts. While IL-13 alone did not induce accumulation of leukocytes, IL-13 administration in clodronate pre-treated mice did induce significant accumulation of non-macrophage leukocytes in BAL (Figure 6.12 A). Furthermore, clodronate pre-treatment exacerbated IL-13 induced BAL eosinophilia (Figure 6.12 B). Treatment with clodronate or IL-13 alone induced small, non-significant increases in BAL neutrophils, however the effect of IL-13 in clodronate treated mice induced a more than additive BAL neutrophilia (Figure 6.12 C). Similarly, IL-13 administration to clodronate treated mice provoked an accumulation of T cells, CD4+ cells and Th2 cells that was greater than the added effect of IL-13 or clodronate alone (Figure 6.12 D-F).

IL-13 administration to clodronate pre-treated mice induced a trend towards elevated Th2 cytokines (IL-4 and IL-5) in BAL and a significant increase in the Th1 cytokines IFNγ and IL-12 (Figure 6.13 A-D). No significant modulation of IL-13 induced BAL IL-10 was observed with clodronate pre-treatment (Figure 6.13 E). Similarly, clodronate pre-treatment did not significantly affect IL-13 induced eotaxin and KC in BAL or IL-33 in LH (Figure 6.14).

Administration of IL-13 into the airways increased the frequency of goblet cells and induced up-regulation of muc5ac mRNA in lung tissue. Despite exacerbating airway inflammation, pre-treatment with clodronate liposomes had no significant effects on IL-13 induced goblet cell up-regulation, although a trend towards inhibition of muc5ac mRNA was observed (Figure 6.15).

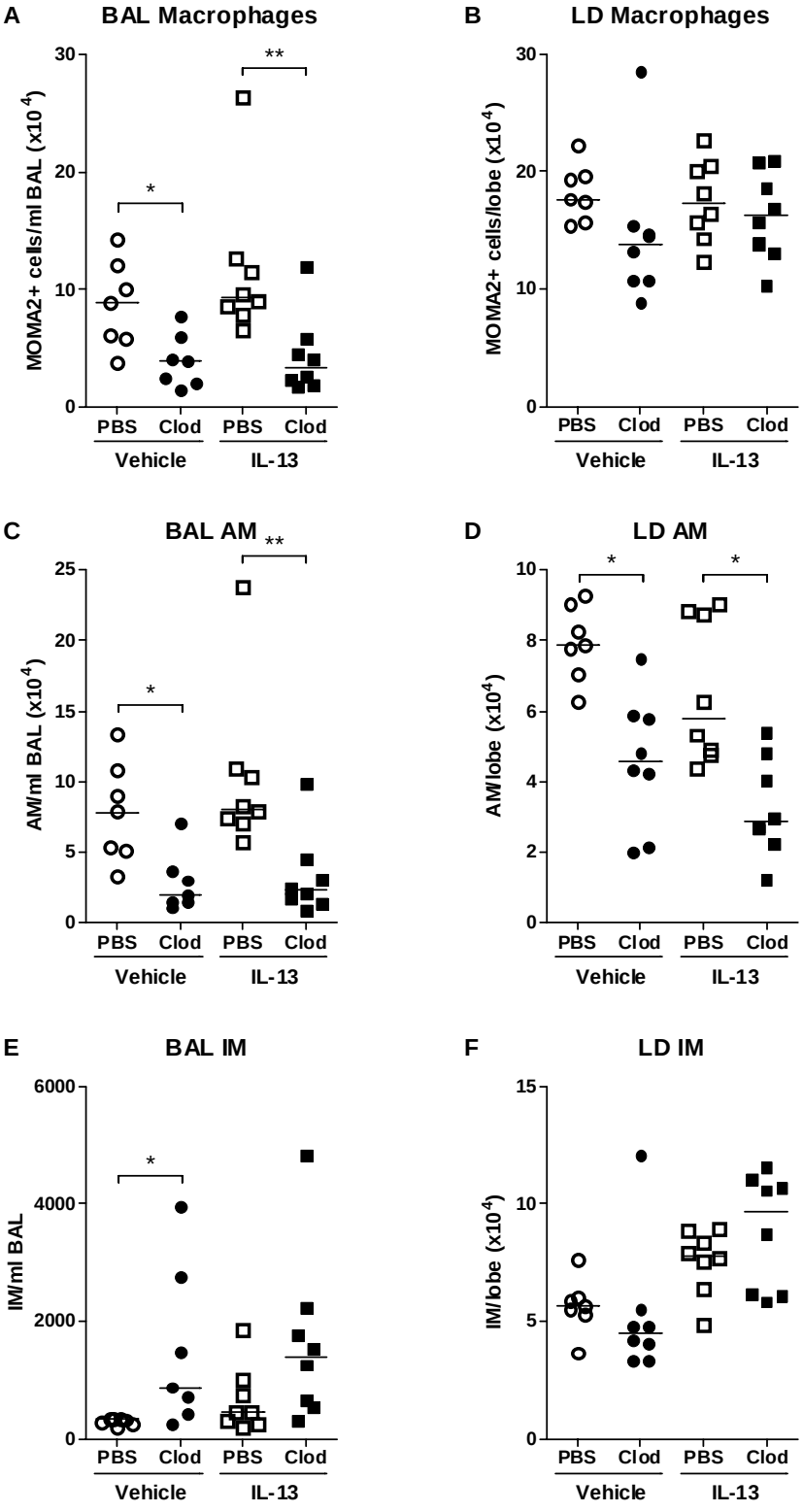


Figure 6.11 Administration of clodronate liposomes reduced AM in IL-13 treated mice. Mice were dosed with 5µg IL-13 or vehicle (Veh; PBS + 1% FCS) i.t., on 3 consecutive days. Mice were dosed with 50µl clodronate (Clod) or PBS filled liposomes i.t. 2 days prior to IL-13 administration. BAL and lungs were taken 15 hours after the last IL-13 administration. Total macrophages (A-B), AM (C-D) and IM (E-F) in BAL (A, C, E) and LD (B, D, F) were identified and quantified by flow cytometry. n = 7-8 mice/group, bar represents median, data represents one of two experiments. * $p<0.05$ and ** $p<0.01$ by Kruskal-Wallis test with Dunn's post test.

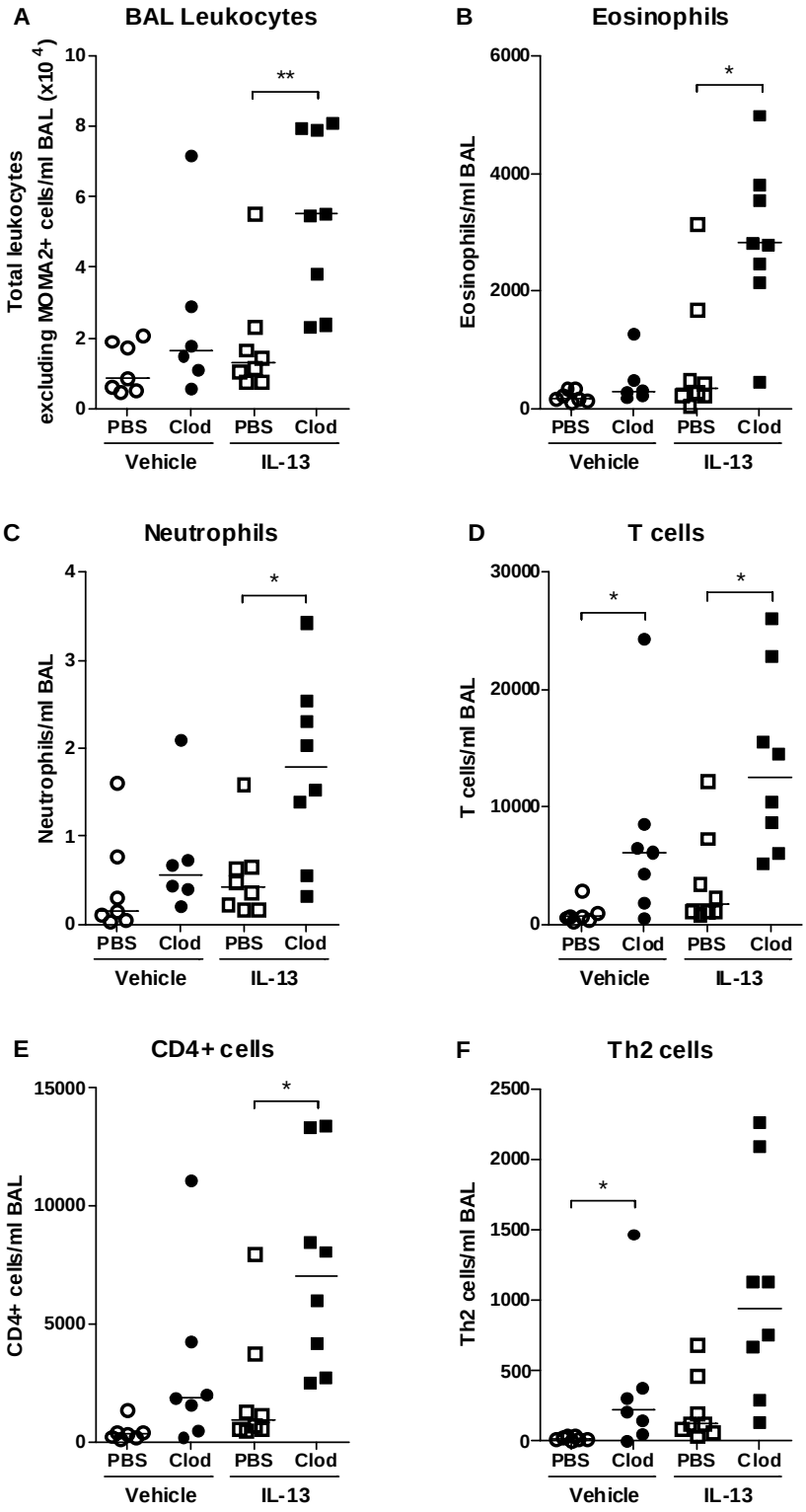


Figure 6.12 Administration of clodronate liposomes increased BAL cellularity in IL-13 treated mice. Mice were dosed with 5µg IL-13 or vehicle (Veh; PBS + 1% FCS) i.t., on 3 consecutive days. Mice were dosed with 50µl clodronate (Clod) or PBS filled liposomes i.t. 2 days prior to IL-13 administration. BAL was taken 15 hours after the last IL-13 administration. Total leukocytes (excluding macrophages) (A), eosinophils (B), neutrophils (C), T cells (D), CD4+ T cells (E) and Th2 cells (F) in BAL were identified and quantified by flow cytometry. n = 6-8 mice/group, bar represents median, data represents one of two experiments. * $p<0.05$ and ** $p<0.01$ by Kruskal-Wallis test with Dunn's post test.

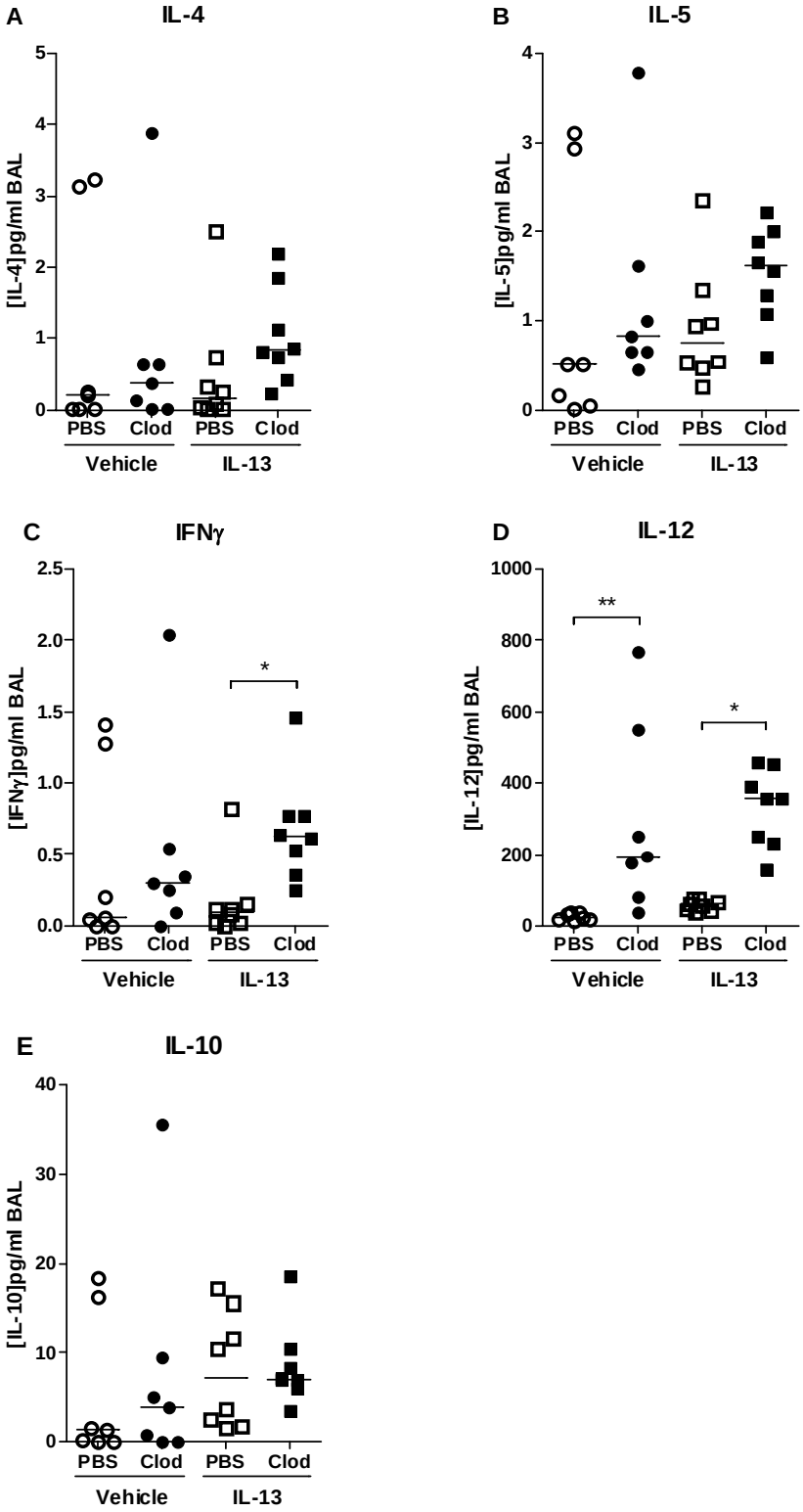


Figure 6.13 Effect of clodronate liposomes on IL-13 induced cytokines in BAL. Mice were dosed with 5µg IL-13 or vehicle (Veh; PBS + 1% FCS) i.t., on 3 consecutive days. Mice were dosed with 50µl clodronate (Clod) or PBS filled liposomes i.t. 2 days prior to IL-13 administration. BAL was taken 15 hours after the last IL-13 administration. Cytokines were quantified by MSD assay. n = 7-8 mice/group, bar represents median. * $p<0.05$ and ** $p<0.01$ by Kruskal-Wallis test with Dunn's post test.

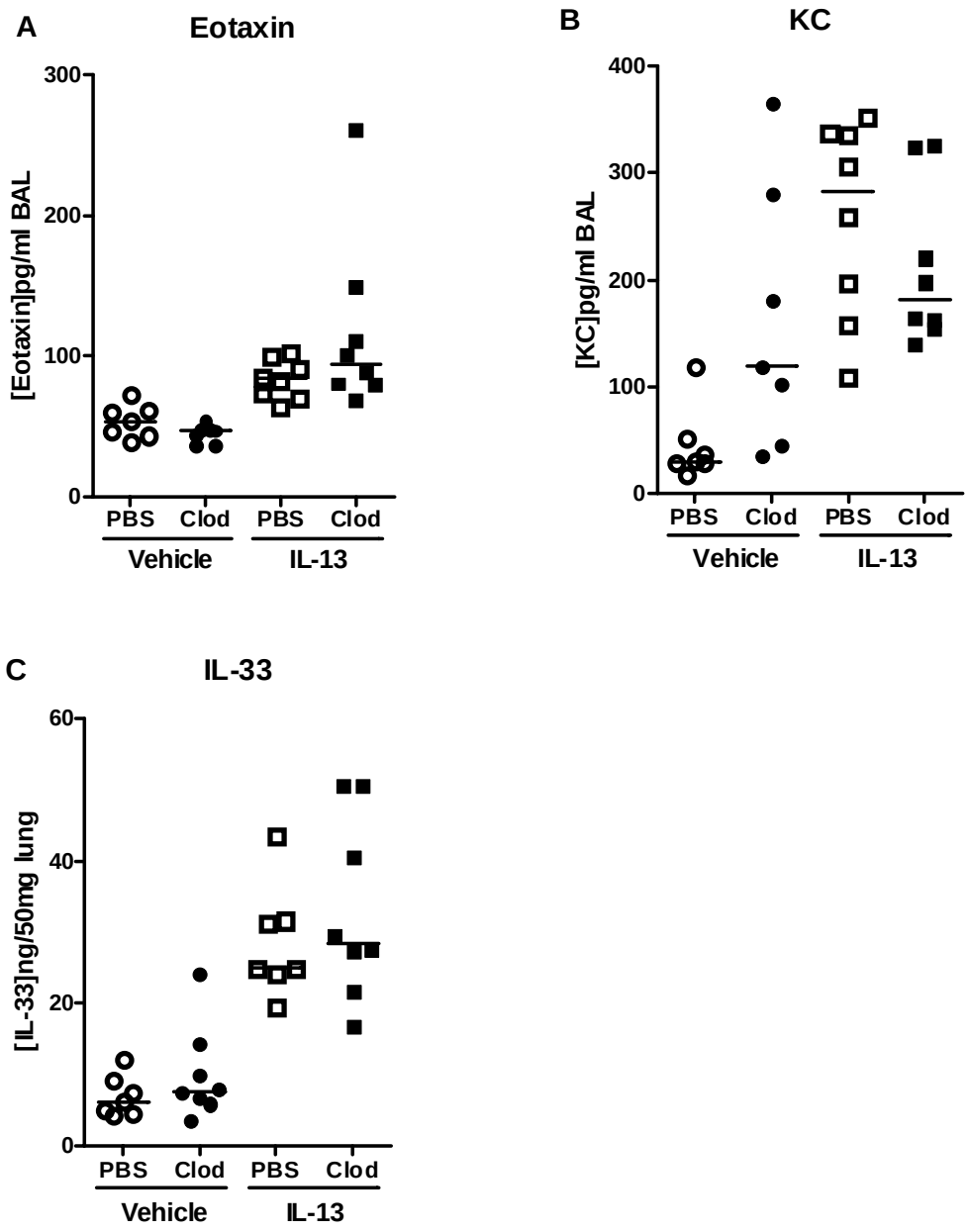


Figure 6.14 Effect of clodronate liposomes on IL-13 induced mediators. Mice were dosed with 5μg IL-13 or vehicle (Veh; PBS + 1% FCS) i.t., on 3 consecutive days. Mice were dosed with 50μl clodronate (Clod) or PBS filled liposomes i.t. 2 days prior to IL-13 administration. BAL and lungs were taken 15 hours after the last IL-13 administration. BAL eotaxin was quantified by ELISA (A), BAL KC by MSD assay (B) and LH IL-33 by ELISA (C). n = 7-8 mice/group, bar represents median.

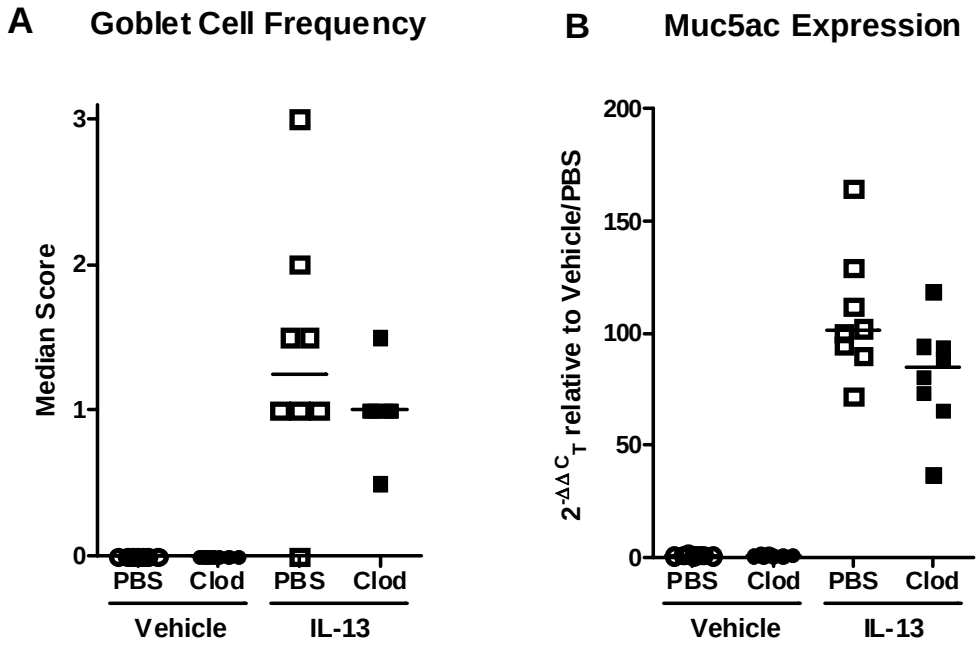


Figure 6.15 Effect of clodronate liposomes on IL-13 induced goblet cell up-regulation. Mice were dosed with 5μg IL-13 or vehicle (Veh; PBS + 1% FCS) i.t., on 3 consecutive days. Mice were dosed with 50μl clodronate (Clod) or PBS filled liposomes i.t. 2 days prior to IL-13 administration. Lungs were taken 15 hours after the last IL-13 administration. (A) Goblet cell frequency was scored in AB/PAS stained sections and (B) muc5ac mRNA was quantified in lung tissue by RT-PCR and normalised to Vehicle/PBS liposomes group. n = 7-8 mice/group, bar represents median.

6.3.5 Prophylactic administration of clodronate liposomes during HDM induced lung inflammation

To determine the role of AM in the development of AAD mice were dosed with clodronate liposomes i.t., commencing two days prior to the first HDM exposure and weekly thereafter for 3 weeks during continued HDM exposure. AHR was assessed by WBP after 2 weeks of HDM exposure. Prophylactic treatment with clodronate liposomes profoundly increased AHR in HDM exposed mice compared to HDM exposed mice receiving PBS liposomes (Figure 6.16). No changes in AHR were observed in sham exposed mice treated with clodronate liposomes compared to sham mice receiving PBS liposomes.

Analysis of the cellular infiltrate in BAL and LD after 3 weeks of prophylactic treatment with clodronate liposomes in HDM exposed mice revealed clodronate treatment significantly exacerbated HDM induced lung inflammation. As previously calculated, the number of macrophages was subtracted from the total number of leukocytes in BAL and LD to gauge the accumulation of inflammatory cells without macrophage depletion skewing the data. The number of BAL and LD leukocytes in clodronate treated, HDM exposed mice was at least 2 fold greater than in HDM exposed mice receiving PBS liposomes (Figure 6.17 A-B). Clodronate treatment increased HDM induced BAL and LD eosinophilia by 1.6 fold and 2.9 fold, respectively (Figure 6.17 C-D) and elevated HDM induced neutrophilia by 2.5 fold and 2.3 fold in BAL and LD, respectively (Figure 6.17 E-F). Moreover, accumulation of T cells, CD4+ cells and Th2 cells in BAL and LD was significantly greater in HDM exposed mice receiving clodronate liposomes than in those receiving PBS liposomes (Figure 6.18). However, quantification of BAL and LD macrophages revealed treatment with clodronate liposomes also elevated the total number of macrophages, AM and IM compared to PBS liposome treatment in HDM exposed mice (Figure 6.19). This effect was specific to HDM exposure as depletion of macrophages was apparent in BAL and LD from sham exposed clodronate treated mice. Scrutiny of the FACS data revealed AM present in HDM BAL (and LD; data not shown) from clodronate treated mice displayed a more variable phenotype with respect to the level of F4/80 and CD11c expression than AM from any of the other treatment groups (Figure 6.20 D compared to A-C). Furthermore, the majority of AM from clodronate treated, HDM exposed mice expressed CD11b whereas this double

positive population (CD11b+ CD11c+) was relatively small in HDM exposed mice treated with PBS liposomes and in sham mice treated with either liposome preparation (Figure 6.21). Quantification of CD11b+ AM demonstrated clodronate administration induced significant accumulation of CD11b+ AM in the BAL and LD of HDM exposed mice, but not sham mice (Figure 6.22 A-B). In addition, quantification of CD11b- AM (resident AM) demonstrated this population was depleted in BAL following clodronate administration to HDM or saline exposed mice (Figure 6.22 C), however CD11b- AM were not diminished in the LD of clodronate treated, HDM exposed mice (Figure 6.22 D).

Cytokine and chemokine concentrations in BAL and LH were assessed by MSD assay and ELISA. No changes in the HDM induced Th2 cytokines IL-4, IL-5 and IL-13 were detected following administration of clodronate liposomes (Figure 6.23). However, treatment with clodronate liposomes further increased HDM induced IFNγ and IL-10 in the BAL but not LH (Figure 6.24 A-D). Administration of clodronate liposomes to sham exposed mice stimulated IL-12 production in BAL and LH which was further elevated in HDM exposed mice, in a greater than additive manner (Figure 6.24 E-F).

HDM induced eotaxin was increased in BAL and LH following clodronate treatment (Figure 6.25 A-B). In addition, clodronate administration enhanced HDM induced production of KC in the lung tissue, however no significant effects were observed on the concentration of KC in BAL (Figure 6.25 C-D). Interestingly, clodronate treatment inhibited HDM induced IL-25 and enhanced HDM induced IL-33 in LH, but had no effects on TSLP (Figure 6.26 A-C).

Analysis of total serum IgE and HDM specific antibodies in terminal serum following clodronate administration to HDM exposed mice revealed an exacerbated antibody response. Total serum IgE and HDM specific IgE, IgG1 and IgG2b were all significantly elevated following clodronate treatment of HDM exposed mice compared to HDM mice receiving control liposomes (Figure 6.27 A-C and E). Clodronate administration did not affect the generation of HDM specific IgG2a (Figure 6.27 D).

Histological analysis of lung sections stained with AB/PAS revealed clodronate liposome treatment of HDM exposed mice partially reduced goblet cell frequency, despite exacerbating cellular inflammation (Figure 6.28). Clodronate treatment had no significant effects on HDM induced peribronchial collagen deposition (Figure 6.29).

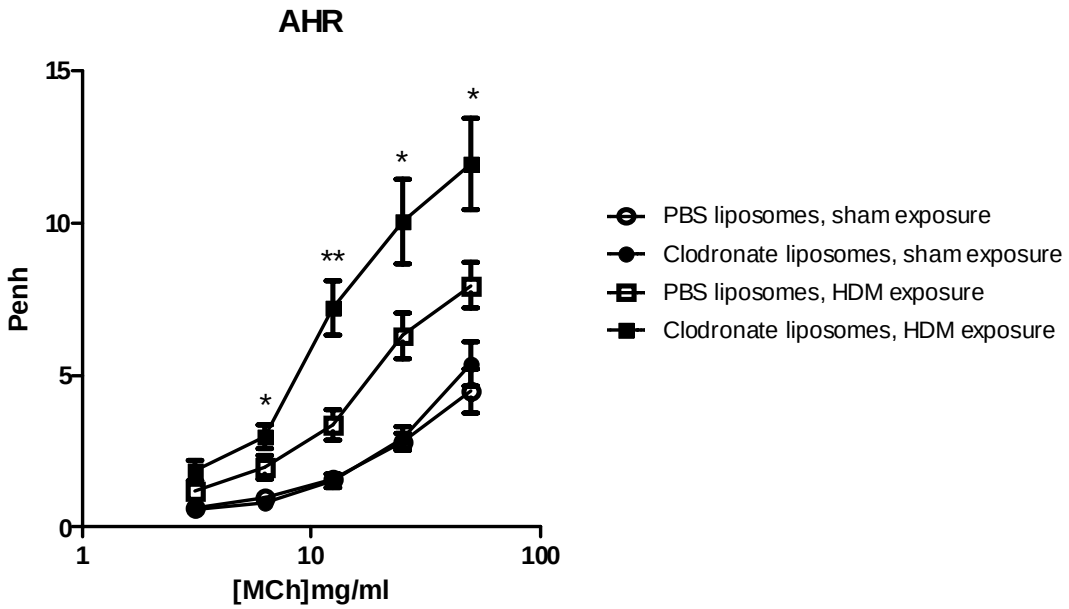


Figure 6.16 Administration of clodronate liposomes increased HDM induced AHR. HDM exposed mice were dosed with 50µl clodronate (Clod) or PBS filled liposomes i.t. prophylactically. AHR to MCh was determined as changes in Penh measured by WBP after the second week of HDM exposure, 24 hours post HDM. Data are shown as mean ± SEM, n = 6-8 mice/group. * $p<0.05$ and ** $p<0.01$ relative to PBS/HDM group by Mann Whitney test.

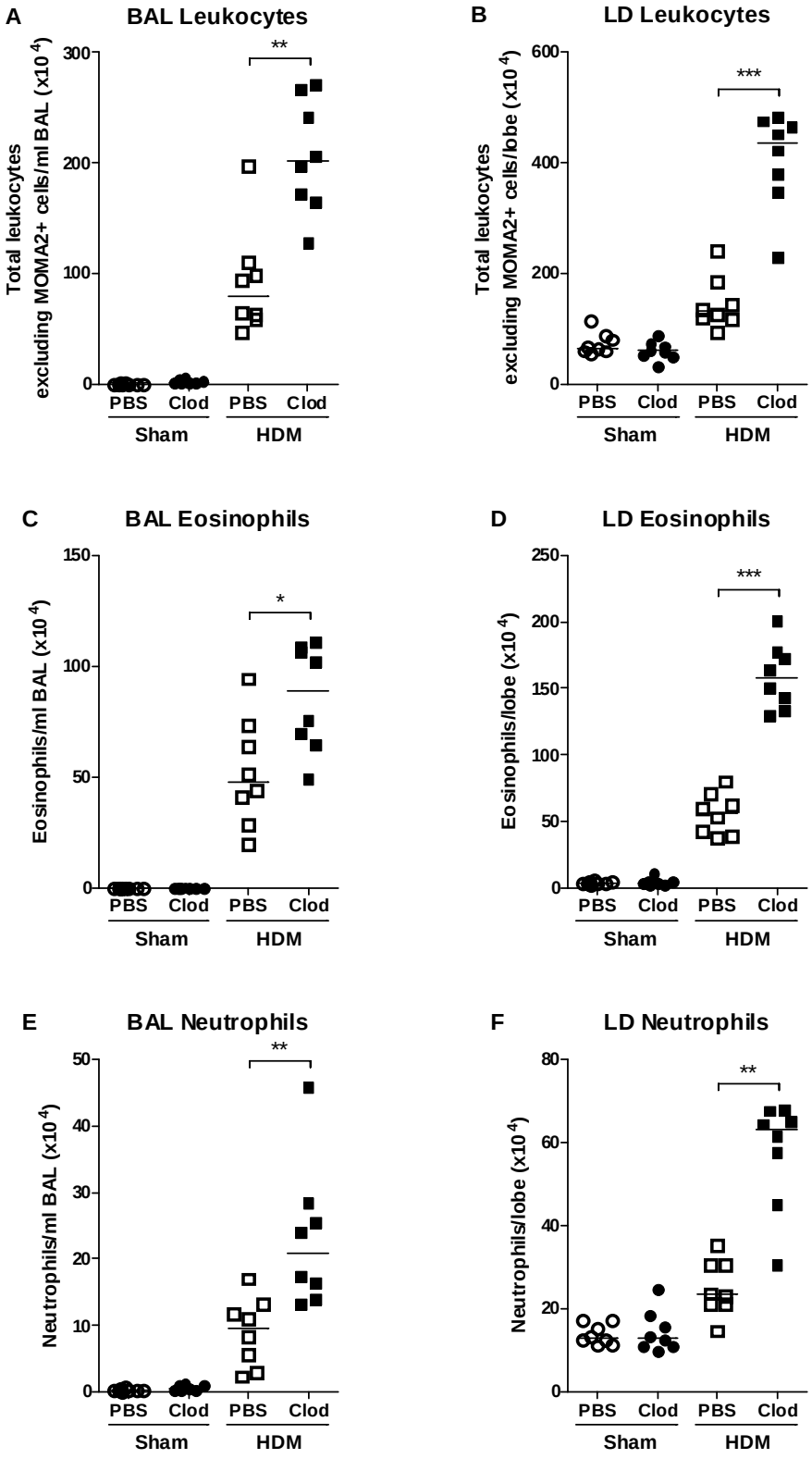


Figure 6.17 Administration of clodronate liposomes exacerbated HDM induced inflammation. HDM exposed mice were dosed with 50µl clodronate (Clod) or PBS filled liposomes i.t. prophylactically. BAL and lungs were taken 4 hours after the last HDM exposure. Total leukocytes, excluding macrophages (A-B), eosinophils (C-D) and neutrophils (E-F) in BAL (A, C, E) and LD (B, D, F) were identified and quantified by flow cytometry. n = 8 mice/group, bar represents median, data represents one of two experiments. * $p<0.05$, ** $p<0.01$ and *** $p<0.001$ by Mann Whitney test.

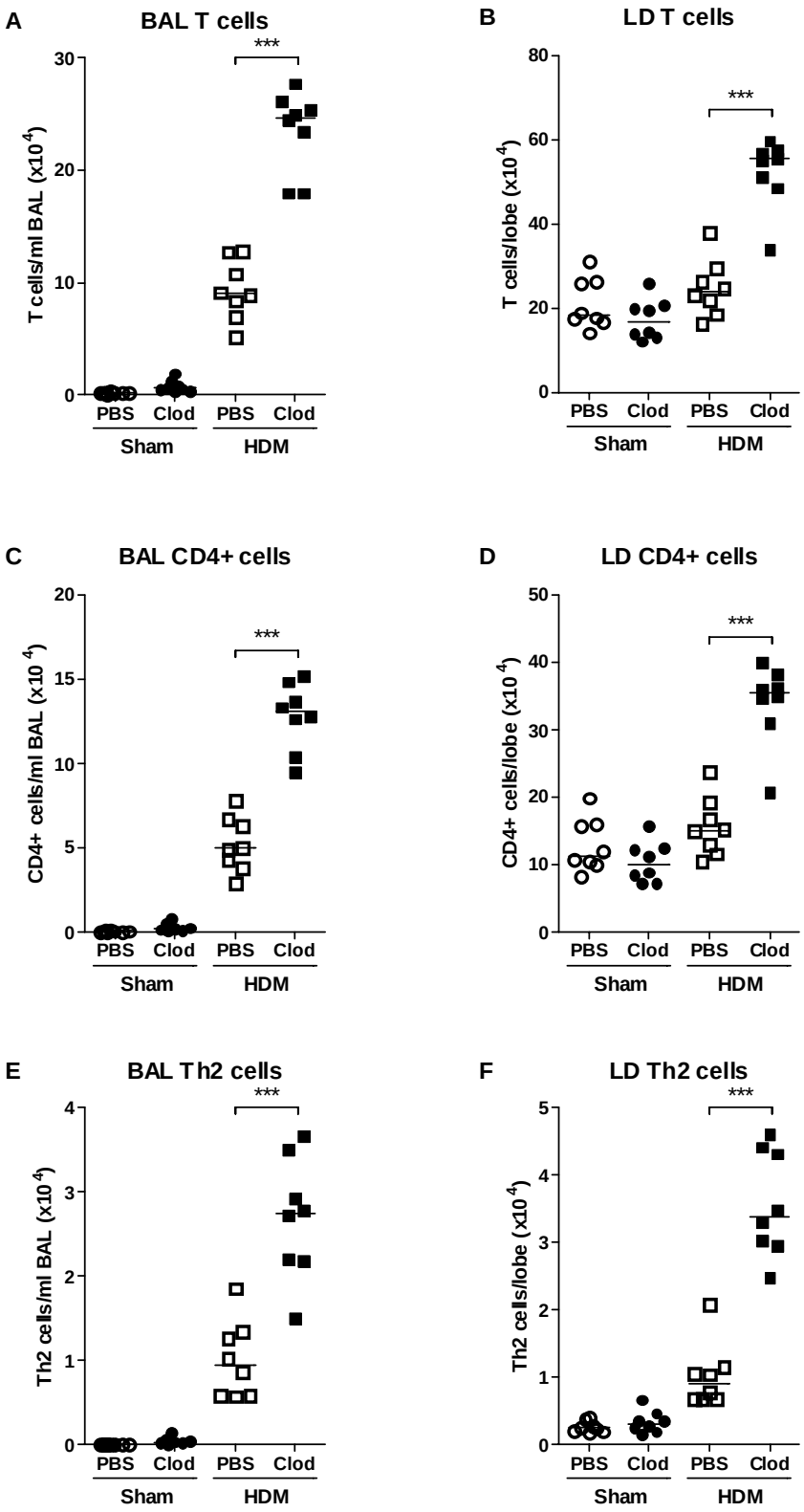


Figure 6.18 Administration of clodronate liposomes exacerbated T cell accumulation in HDM exposed mice. HDM exposed mice were dosed with 50µl clodronate (Clod) or PBS filled liposomes i.t. prophylactically. BAL and lungs were taken 4 hours after the last HDM exposure. T cells (A-B), CD4+ T cells (C-D) and Th2 cells (E-F) in BAL (A, C, E) and LD (B, D, F) were identified and quantified by flow cytometry. n = 8 mice/group, bar represents median, data represents one of two experiments. *** $p<0.001$ by Mann Whitney test.

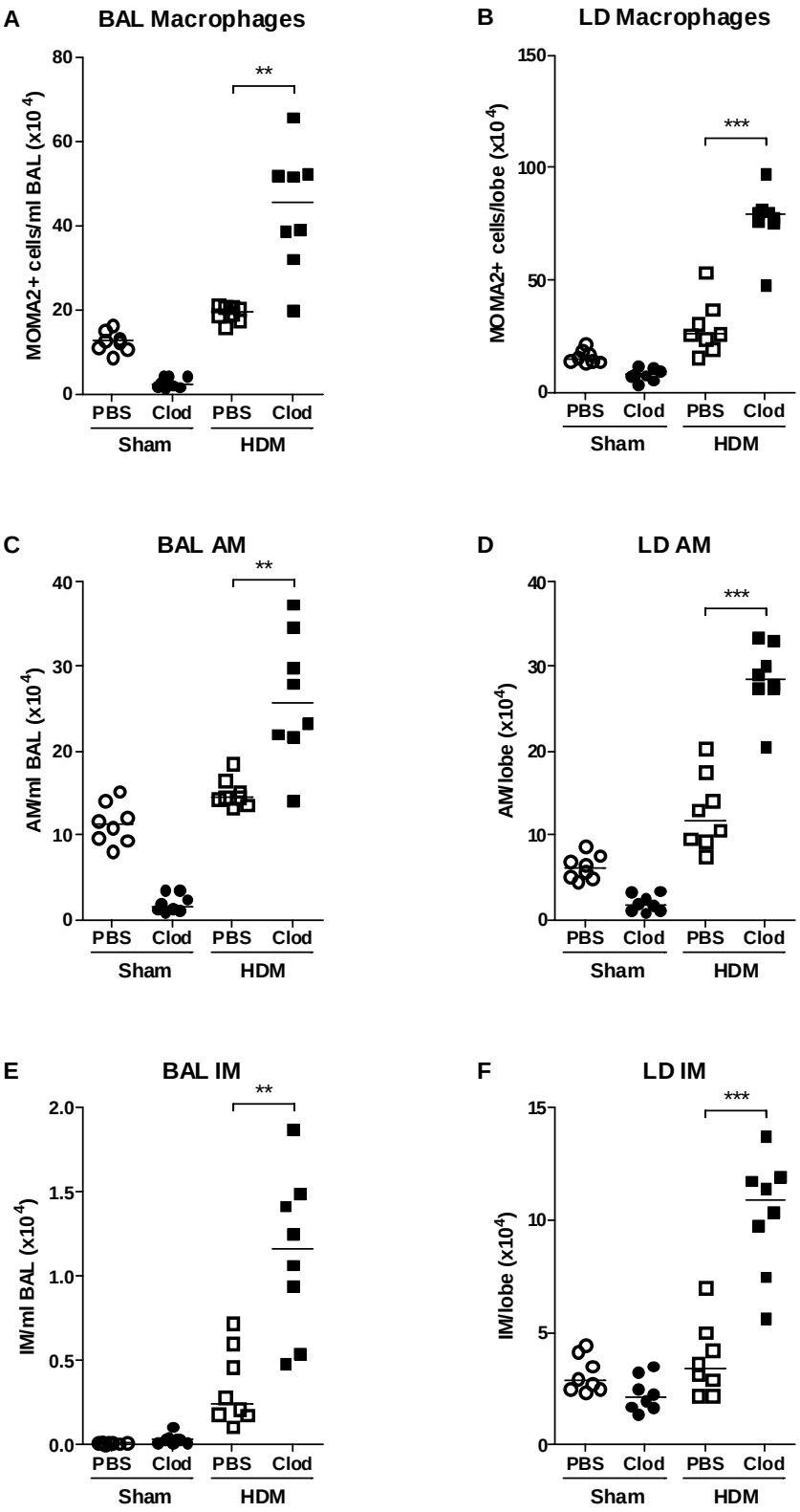


Figure 6.19 Administration of clodronate liposomes increased macrophage accumulation in HDM exposed mice. HDM exposed mice were dosed with 50µl clodronate (Clod) or PBS filled liposomes i.t. prophylactically. BAL and lungs were taken 4 hours after the last HDM exposure. Total macrophages (A-B), AM (C-D) and IM (E-F) in BAL (A, C, E) and LD (B, D, F) were identified and quantified by flow cytometry. n = 8 mice/group, bar represents median, data represents one of two experiments. ** $p<0.01$ and *** $p<0.001$ by Mann Whitney test.

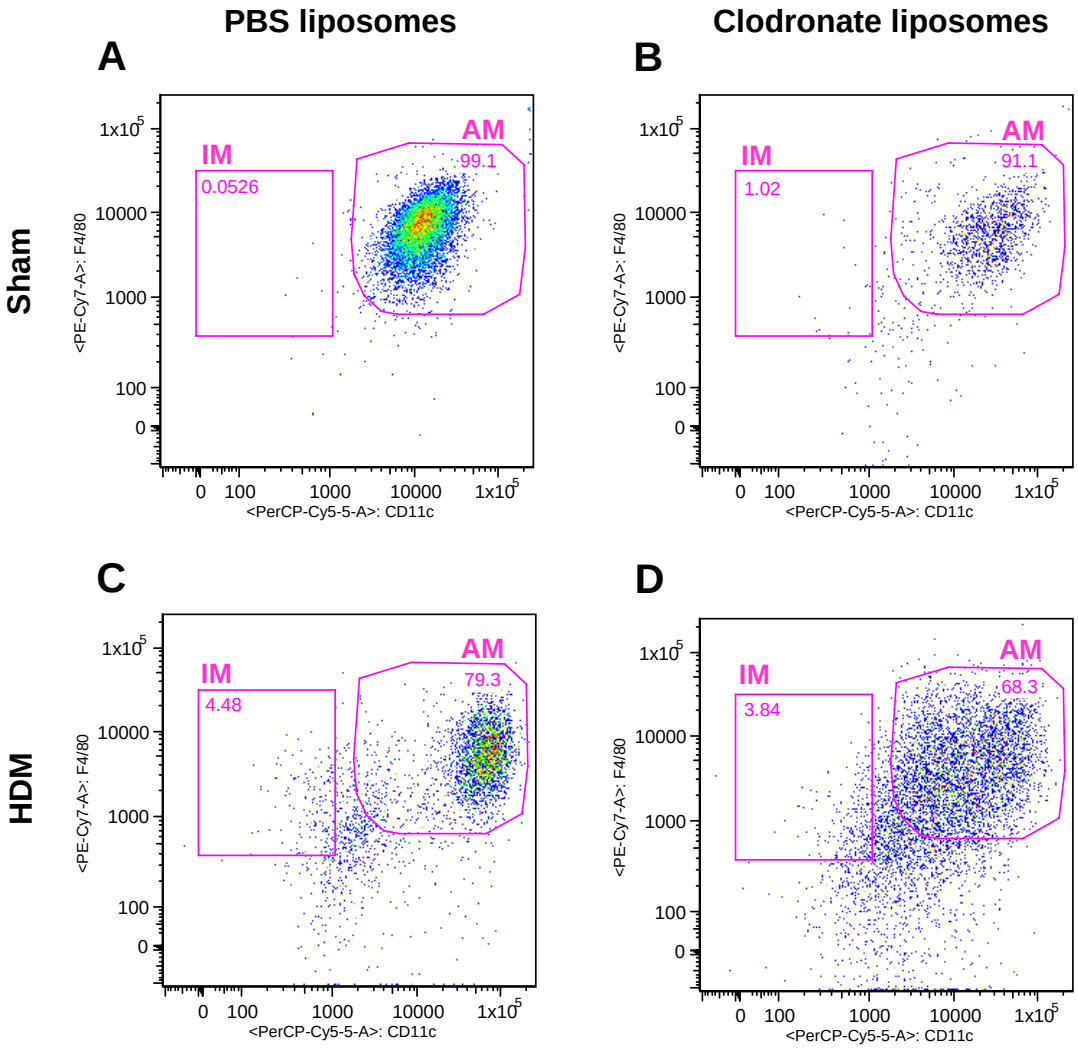


Figure 6.20 AM and IM frequencies following administration of clodronate liposomes to HDM exposed mice. HDM exposed mice were dosed with 50µl clodronate (Clod) or PBS filled liposomes i.t. prophylactically. BAL was taken 4 hours after the last HDM exposure; macrophages were identified by flow cytometry. Representative dot plots of BAL macrophages from sham exposed mice dosed with PBS (A) or clodronate liposomes (B) and HDM exposed mice dosed with PBS (C) or clodronate liposomes (D). n = 8 mice/group, data represents one of two experiments.

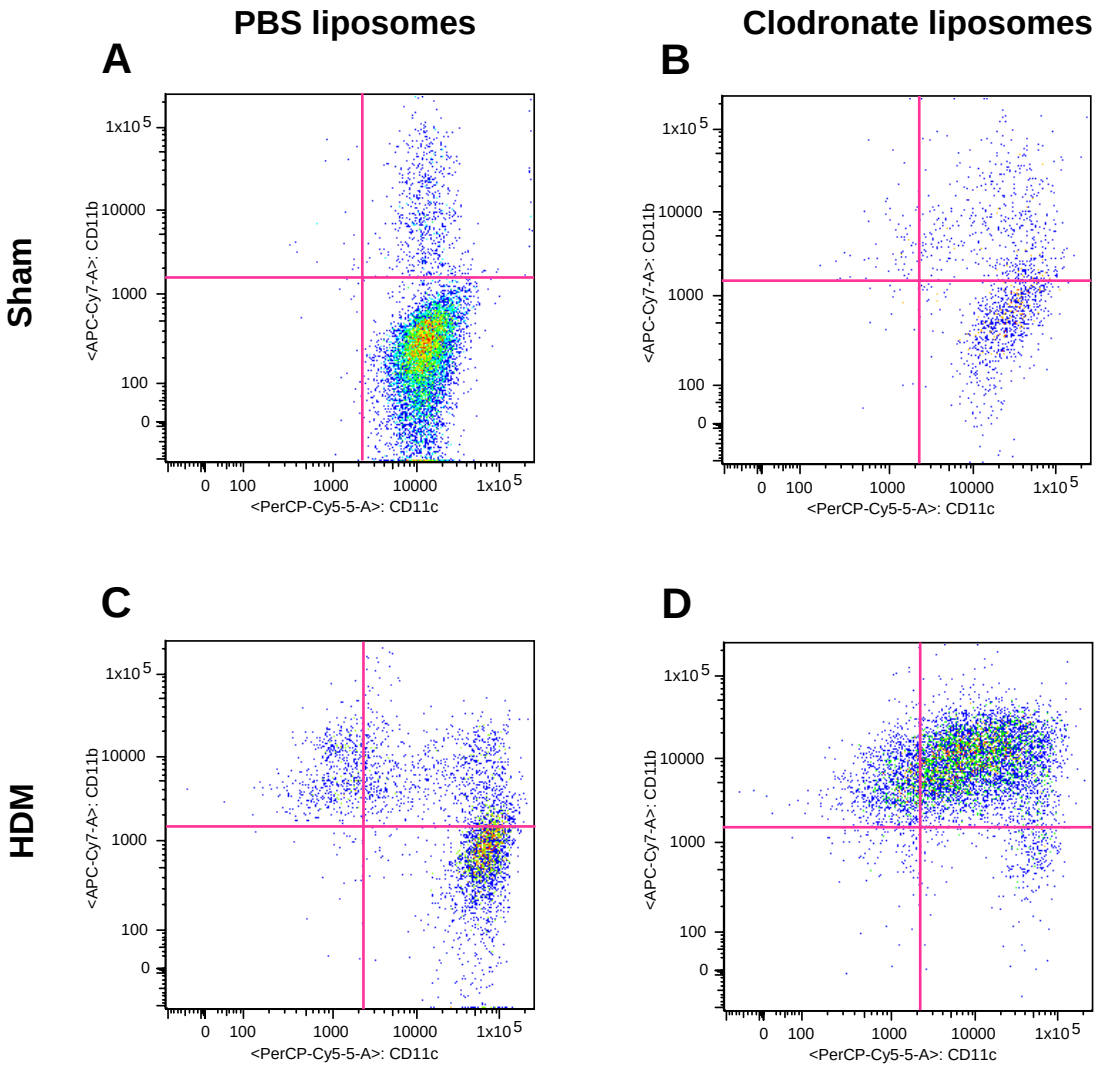


Figure 6.21 CD11b expression on pulmonary macrophages following administration of clodronate liposomes to HDM exposed mice. HDM exposed mice were dosed with 50µl clodronate (Clod) or PBS filled liposomes i.t. prophylactically. BAL was taken 4 hours after the last HDM exposure; macrophages were identified by flow cytometry. Representative dot plots of BAL macrophages from sham exposed mice dosed with PBS (A) or clodronate liposomes (B) and HDM exposed mice dosed with PBS (C) or clodronate liposomes (D). n = 8 mice/group, data represents one of two experiments.

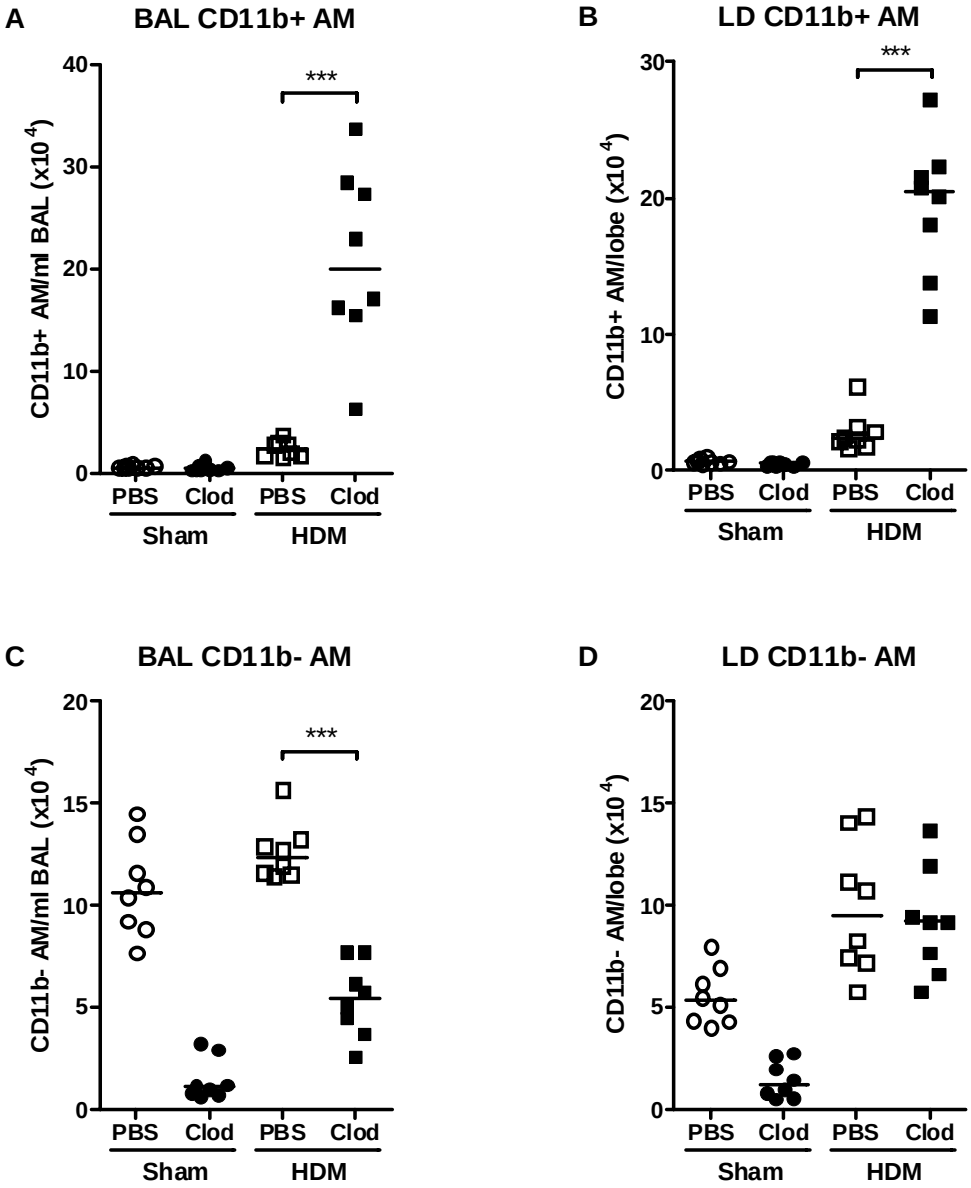


Figure 6.22 Clodronate liposomes increased accumulation of CD11b+ AM in HDM exposed mice. HDM exposed mice were dosed with 50µl clodronate (Clod) or PBS filled liposomes i.t. prophylactically. BAL and lungs were taken 4 hours after the last HDM exposure. CD11b+ AM (A-B) and CD11b- AM (C-D) in BAL (A, C) and LD (B, D) were identified and quantified by flow cytometry. n = 8 mice/group, bar represents median, data represents one of two experiments. *** $p<0.001$ by Mann Whitney test.

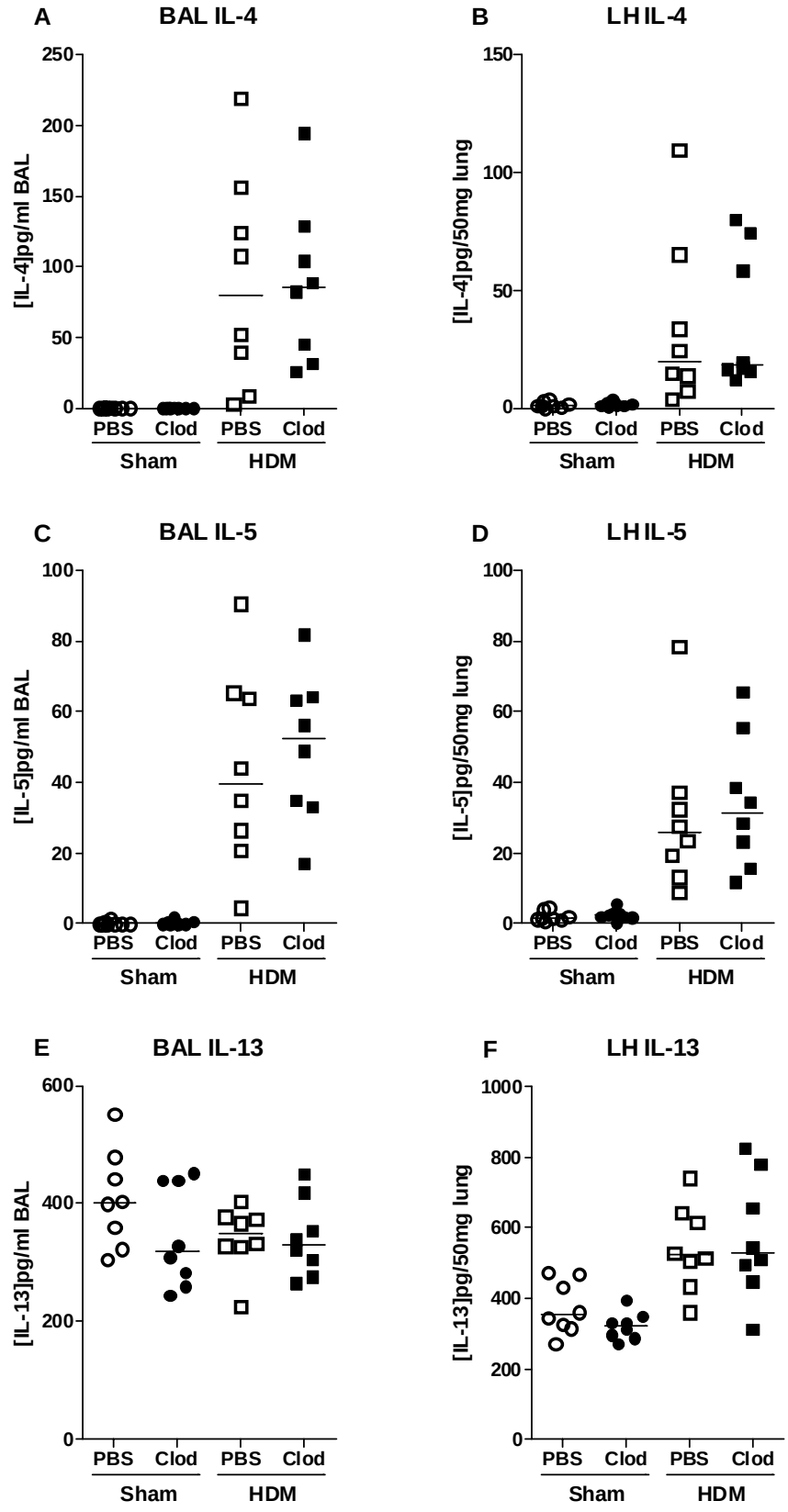


Figure 6.23 Effects of clodronate liposomes on HDM induced Th2 cytokines. HDM exposed mice were dosed with 50µl clodronate (Clod) or PBS filled liposomes i.t. prophylactically. BAL and lungs were taken 4 hours after the last HDM exposure. Cytokines were quantified in BAL and LH supernatants by MSD assay (A-D) or ELISA (E-F). n = 8 mice/group, bar represents median.

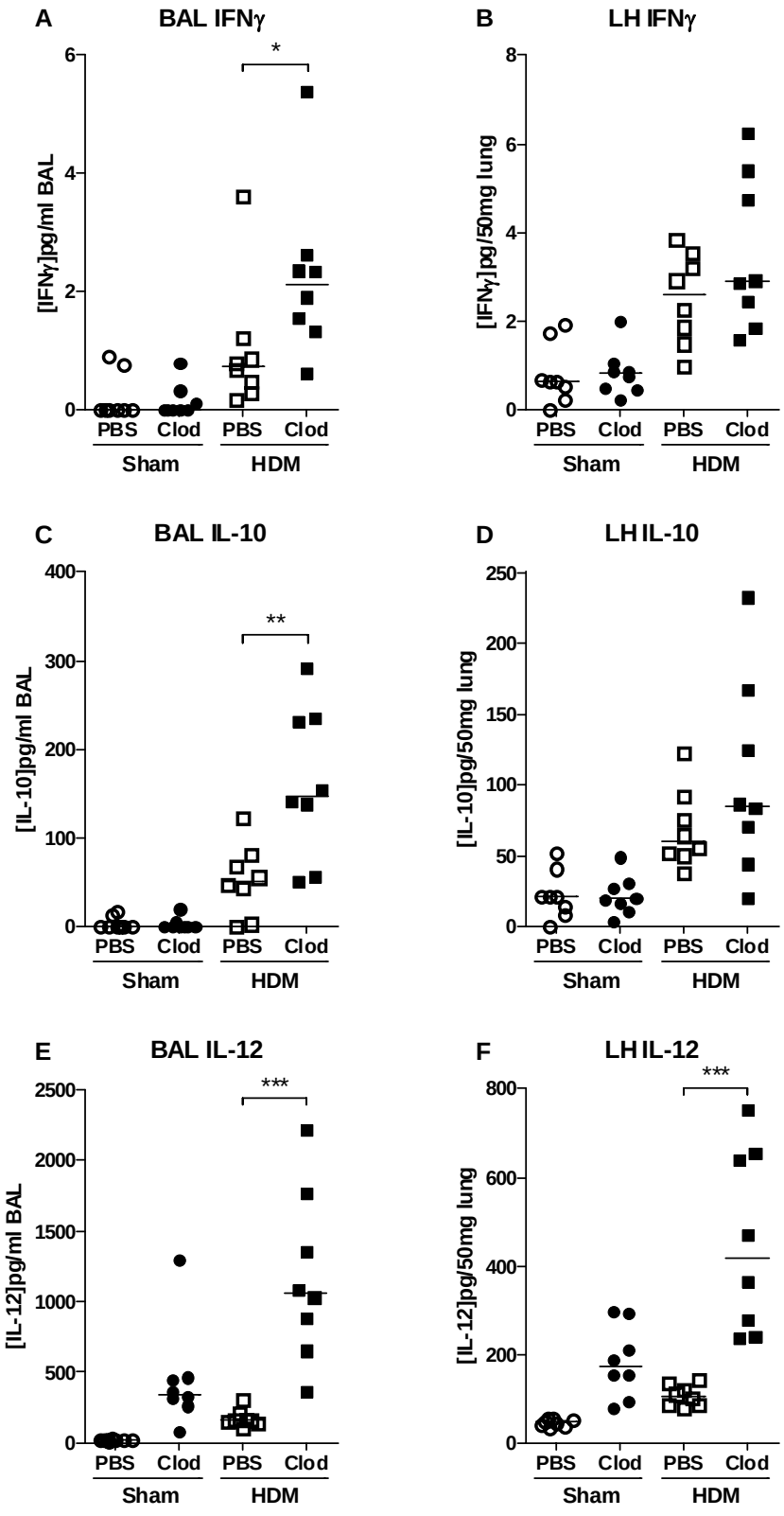


Figure 6.24 Effects of clodronate liposomes on HDM induced IFNγ, IL-10 and IL-12 production. HDM exposed mice were dosed with 50µl clodronate (Clod) or PBS filled liposomes i.t. prophylactically. BAL and lungs were taken 4 hours after the last HDM exposure. Cytokines were quantified in BAL and LH supernatants by MSD assay. n = 8 mice/group, bar represents median. * $p<0.05$, ** $p<0.01$ and *** $p<0.001$ by Mann Whitney test.

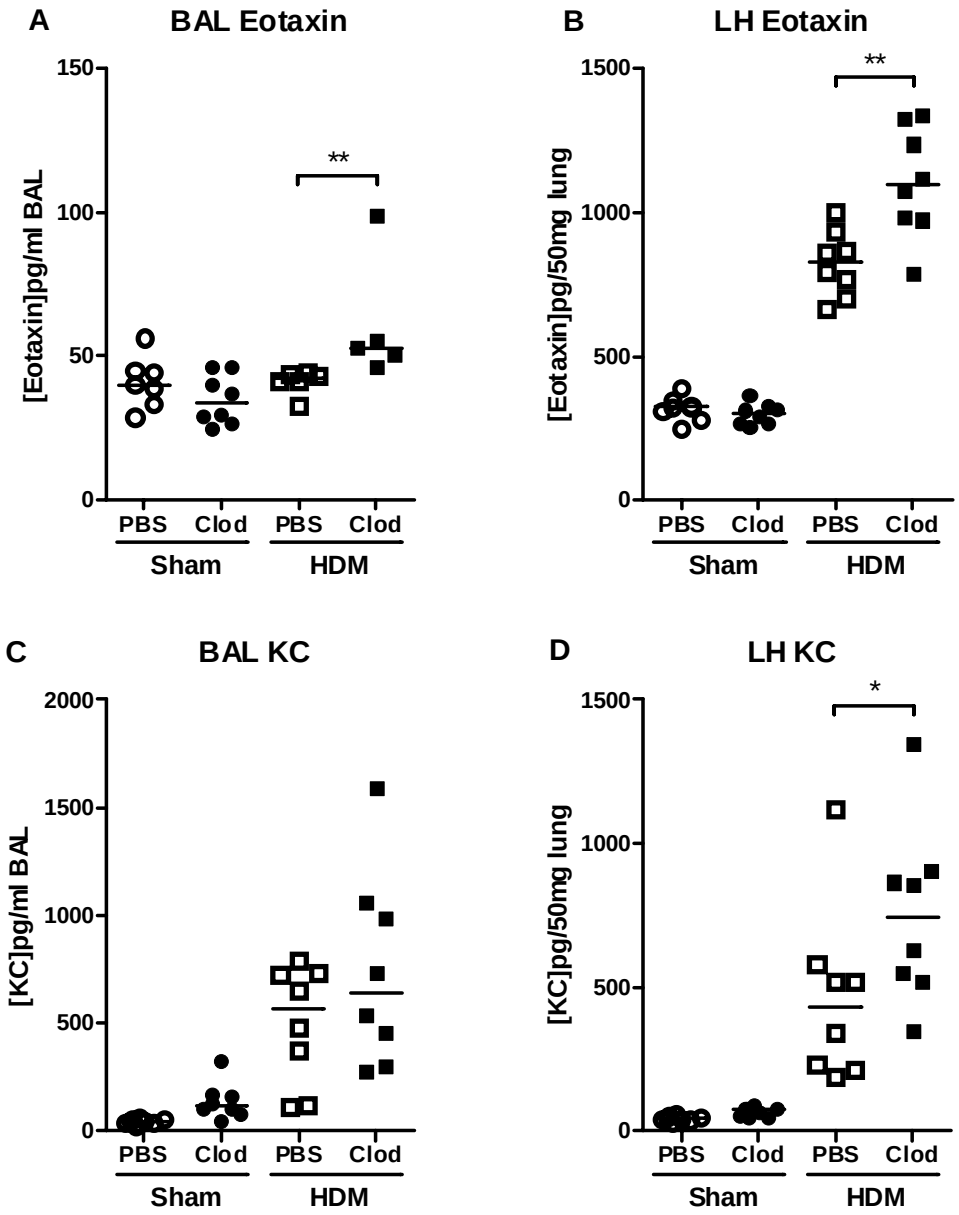


Figure 6.25 Effects of clodronate liposomes on HDM induced chemokines. HDM exposed mice were dosed with 50µl clodronate (Clod) or PBS filled liposomes i.t. prophylactically. BAL and lungs were taken 4 hours after the last HDM exposure. Chemokines were quantified in BAL and LH supernatants by ELISA (A-B) or MSD assay (C-D). n = 5-8 mice/group, bar represents median. * $p<0.05$ and ** $p<0.01$ by Mann Whitney test.

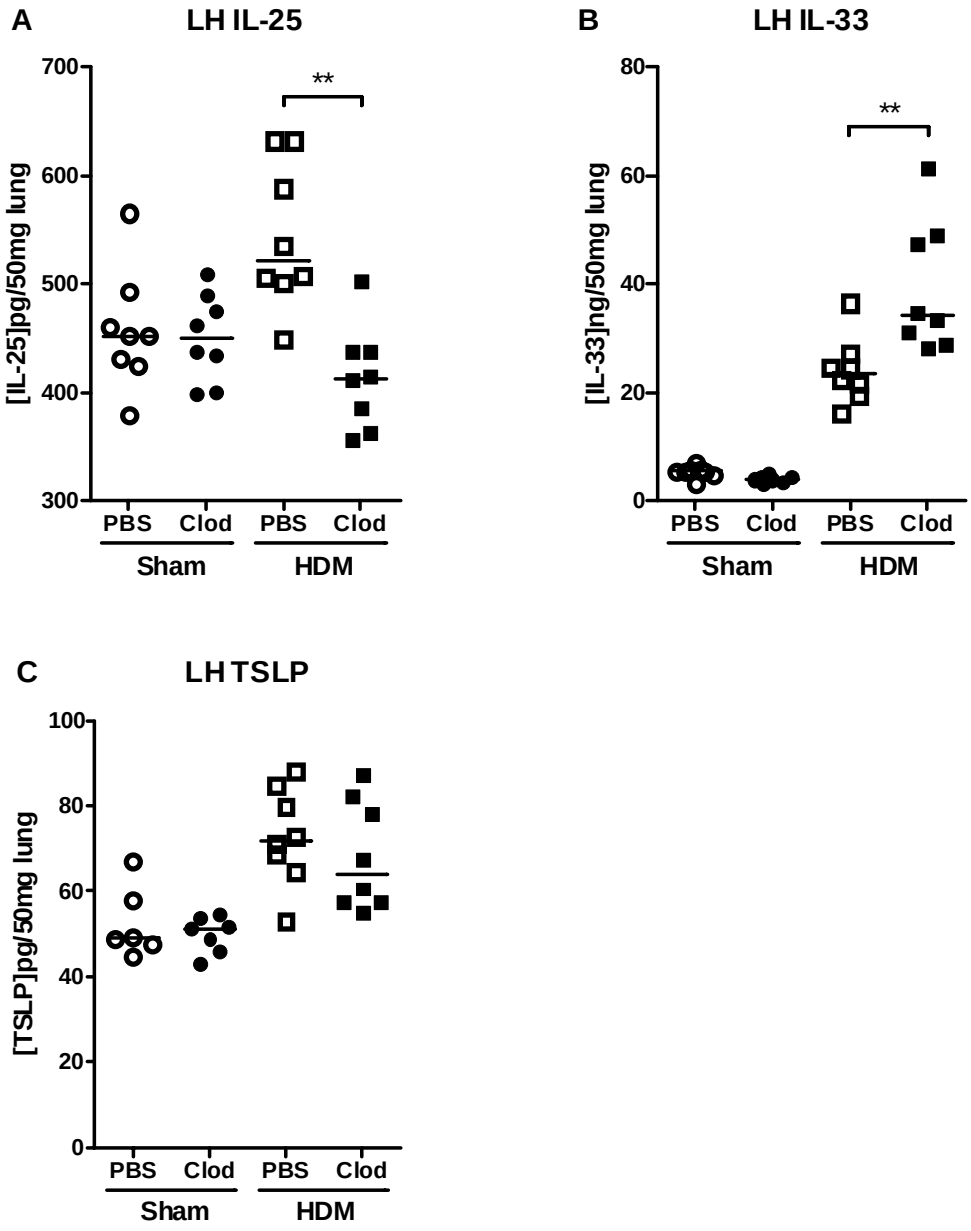


Figure 6.26 Effects of clodronate liposomes on HDM induced epithelial derived cytokines. HDM exposed mice were dosed with 50µl clodronate (Clod) or PBS filled liposomes i.t. prophylactically. Lungs were taken 4 hours after the last HDM exposure. Cytokines were quantified in LH supernatant by ELISA. n = 6-8 mice/group, bar represents median. ** $p<0.01$ by Mann Whitney test.

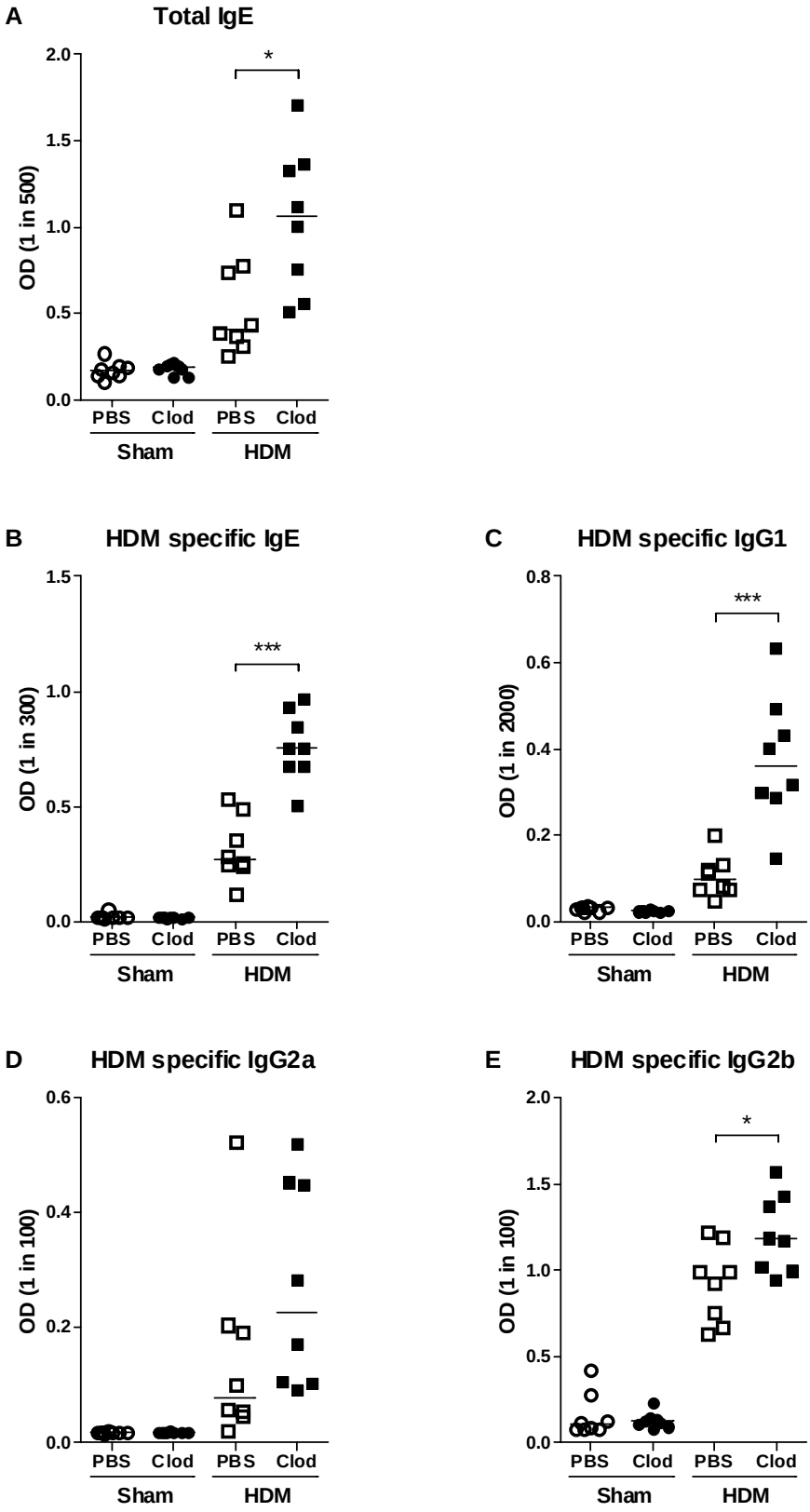


Figure 6.27 Effects of clodronate liposomes on the generation of HDM specific antibodies. HDM exposed mice were dosed with 50µl clodronate (Clod) or PBS filled liposomes i.t. prophylactically. Blood was taken 4 hours after the last HDM exposure. HDM specific antibodies were assessed in serum by ELISA. n = 8 mice/group, bar represents median. * $p<0.05$ and *** $p<0.001$ by Mann Whitney test.

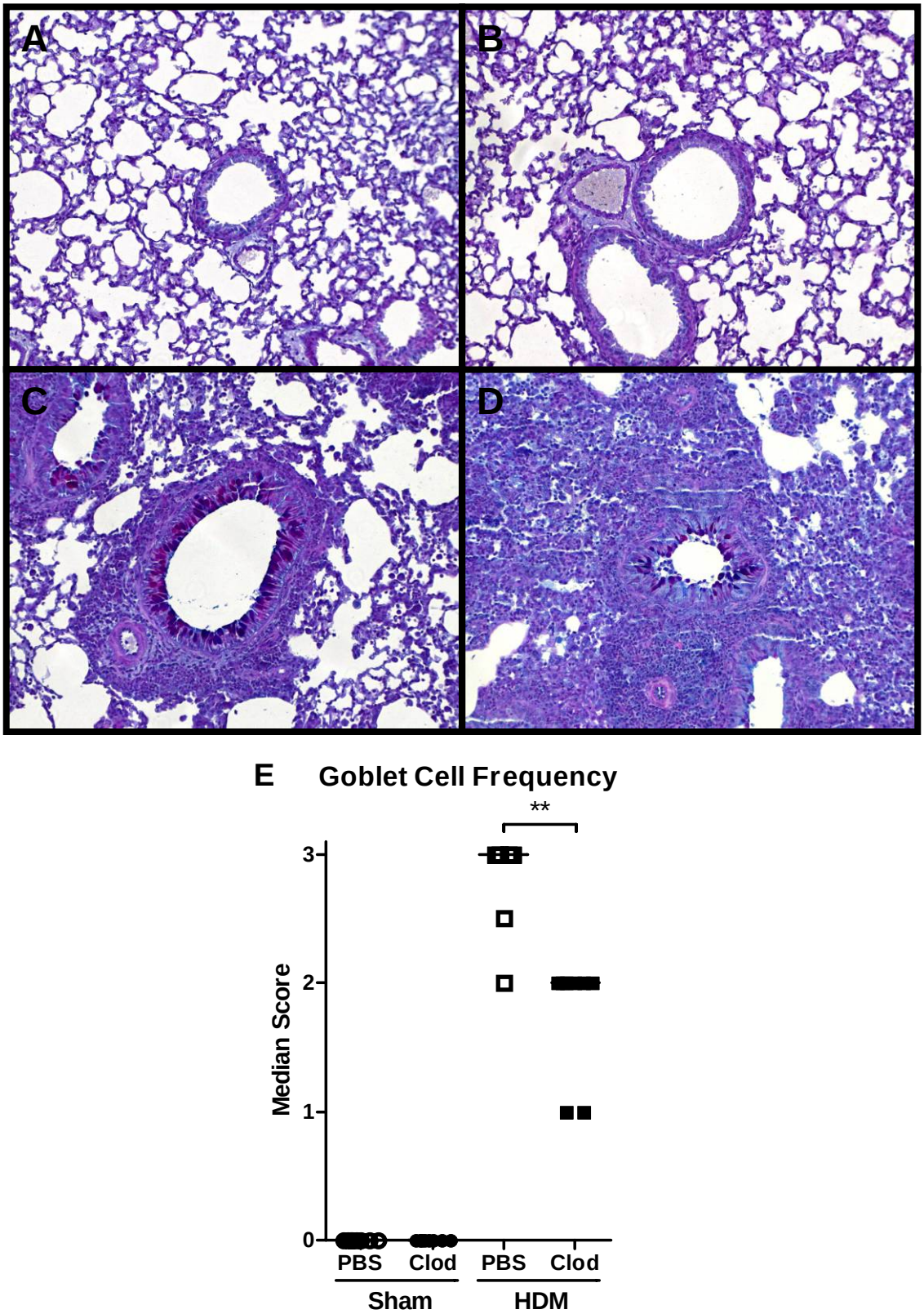


Figure 6.28 Effects of clodronate liposomes on HDM induced goblet cell hyperplasia. HDM exposed mice were dosed with 50µl clodronate (Clod) or PBS filled liposomes i.t. prophylactically. Lungs were taken 4 hours after the last HDM exposure. (A-D) Representative AB/PAS stained sections from sham exposed mice dosed with PBS (A) or clodronate liposomes (B) and HDM exposed mice dosed with PBS (C) or clodronate liposomes (D); original magnification x200. (E) Goblet cell frequency was scored in AB/PAS stained sections. n = 8 mice/group, bar represents median. ** $p<0.01$ by Mann Whitney test.

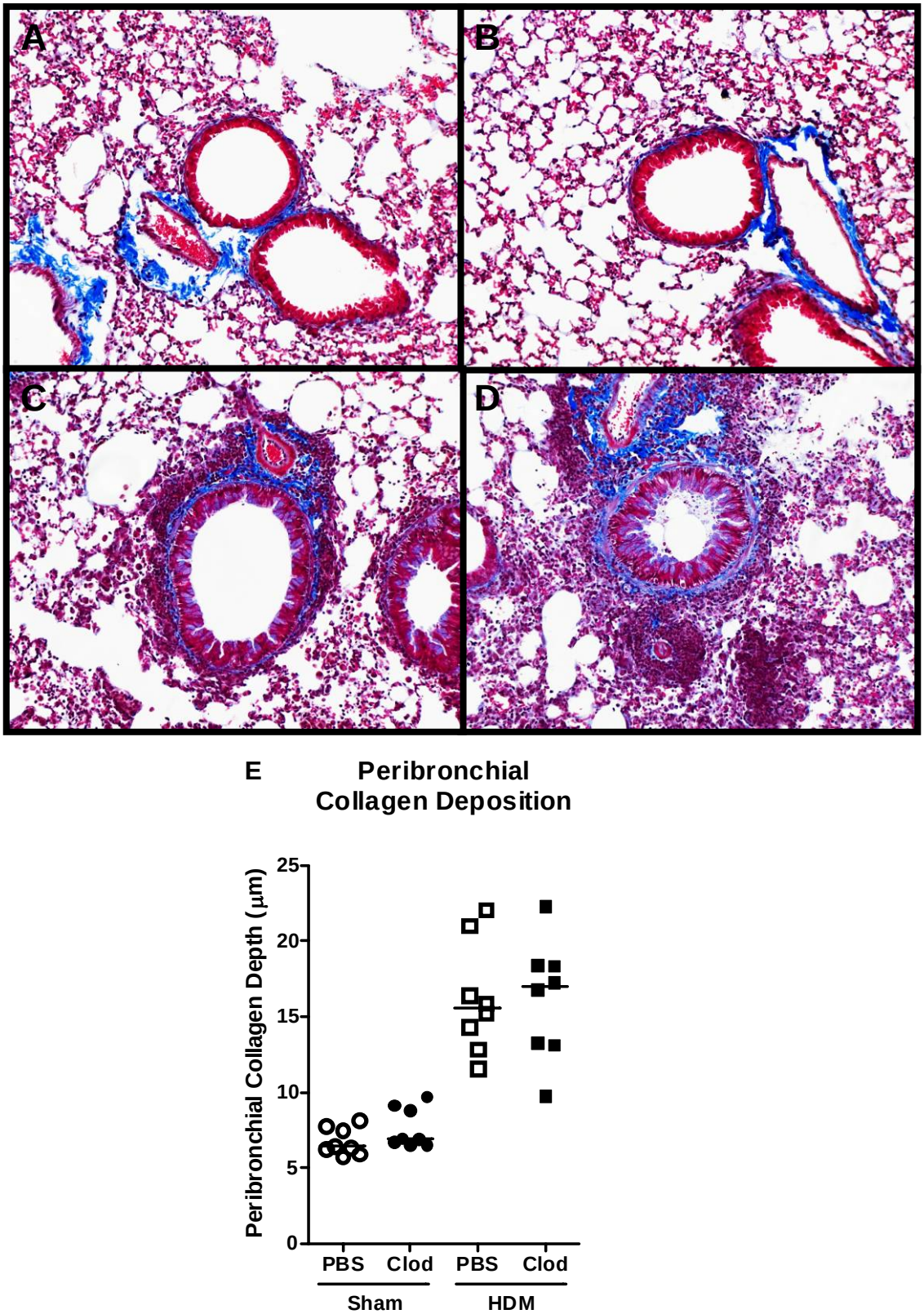


Figure 6.29 Effects of clodronate liposomes on HDM induced peribronchial collagen deposition. HDM exposed mice were dosed with 50µl clodronate (Clod) or PBS filled liposomes i.t. prophylactically. Lungs were taken 4 hours after the last HDM exposure. (A-D) Representative Masson's trichrome stained sections from sham exposed mice dosed with PBS (A) or clodronate liposomes (B) and HDM exposed mice dosed with PBS (C) or clodronate liposomes (D); original magnification x200. (E) Peribronchial collagen depth was measured in Masson's trichrome stained sections. n = 8 mice/group, bar represents median.

6.3.6 Therapeutic administration of clodronate liposomes during HDM induced lung inflammation

To determine the role of AM in the maintenance of AAD mice with established AAD were treated with clodronate liposomes for the third week of a 3 week HDM exposure period. Due to the increased number of macrophages observed in HDM exposed mice receiving clodronate liposomes in the previous study, mice were dosed with liposomes twice, rather than once, weekly during the final week of HDM exposure. AHR was assessed by WBP during the third week of HDM exposure, on day 16. Therapeutic treatment with clodronate liposomes had no significant effect on HDM induced AHR at this time point (Figure 6.30).

As previously demonstrated with prophylactic clodronate treatment, therapeutic administration of clodronate liposomes also exacerbated HDM induced lung inflammation. Clodronate treatment increased the number of non-macrophage leukocytes in BAL and LD from HDM exposed mice by over 2 fold compared to treatment with PBS liposomes (Figure 6.31 A-B). HDM induced eosinophilia in BAL and LD was further elevated following administration of clodronate liposomes by 2.2 fold and 3.2 fold, respectively (Figure 6.31 C-D). Similarly, HDM induced neutrophilia in BAL and LD was enhanced after clodronate treatment by 5.3 fold and 1.8 fold, respectively (Figure 6.31 E-F). In addition, therapeutic treatment with clodronate liposomes significantly increased HDM induced accumulation of T cells, CD4+ cells and Th2 cells in BAL and LD (Figure 6.32). Analysis of BAL and LD macrophages revealed the total number of LD macrophages was augmented in HDM exposed clodronate treated mice compared to HDM exposed mice treated with control liposomes, however this was not evident in BAL (Figure 6.33 A-B). Quantification of AM demonstrated administration of clodronate liposomes depleted BAL and LD AM in sham exposed mice. A modest reduction in the number of BAL AM in HDM exposed clodronate treated mice was observed, however this was not apparent in LD (Figure 6.33 C-D). Clodronate treatment of HDM exposed mice induced a significant accumulation of IM in BAL and LD (Figure 6.33 E-F). Further analysis of AM demonstrated clodronate administration to HDM but not sham exposed mice induced significant accumulation of CD11b+ AM in BAL and LD (Figure 6.34 A-B). In addition, quantification of CD11b- AM confirmed this population was depleted in

BAL and LD following clodronate administration to HDM or sham exposed mice (Figure 6.34 C-D).

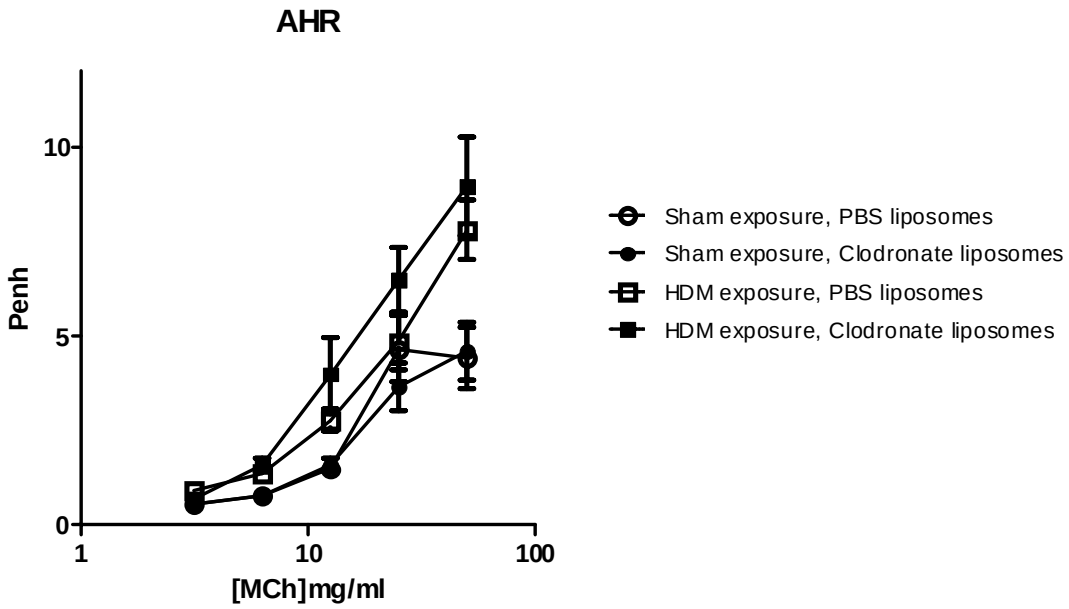


Figure 6.30 Therapeutic administration of clodronate liposomes does not affect HDM induced AHR. HDM exposed mice were dosed with 50µl clodronate (Clod) or PBS filled liposomes i.t. therapeutically, during the final week of HDM exposure. AHR to MCh was determined as changes in Penh measured by WBP on day 16 of HDM exposure, 24 hours post HDM. Data are shown as mean ± SEM, n = 6-8 mice/group.

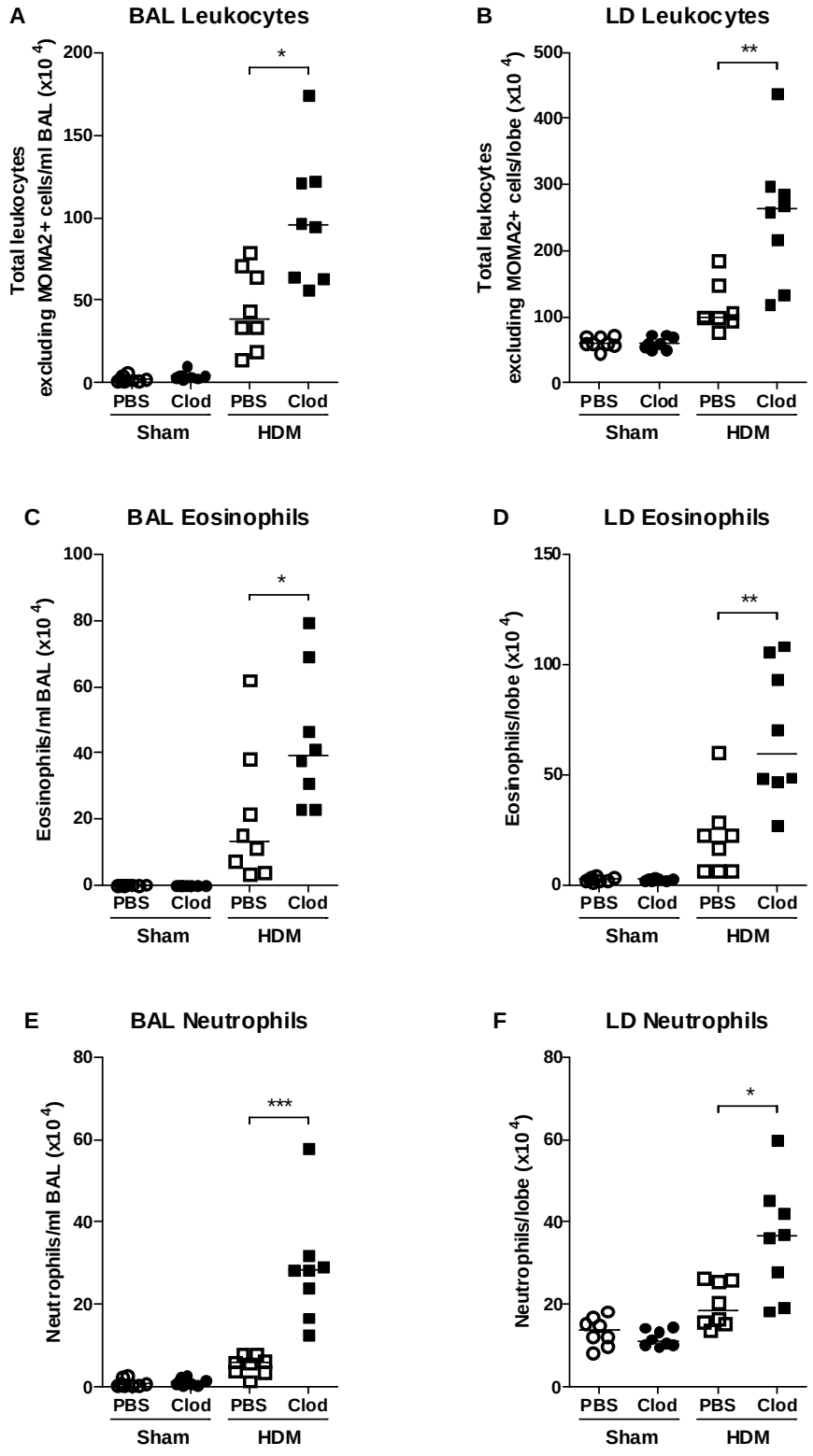


Figure 6.31 Therapeutic administration of clodronate liposomes exacerbated HDM induced inflammation. HDM exposed mice were dosed with 50µl clodronate (Clod) or PBS filled liposomes i.t. therapeutically, during the final week of HDM exposure. BAL and lungs were taken 4 hours after the last HDM exposure. Total leukocytes, excluding macrophages (A-B), eosinophils (C-D) and neutrophils (E-F) in BAL (A, C, E) and LD (B, D, F) were identified and quantified by flow cytometry. n = 8 mice/group, bar represents median, data represents one of two experiments. * $p<0.05$, ** $p<0.01$ and *** $p<0.001$ by Mann Whitney test.

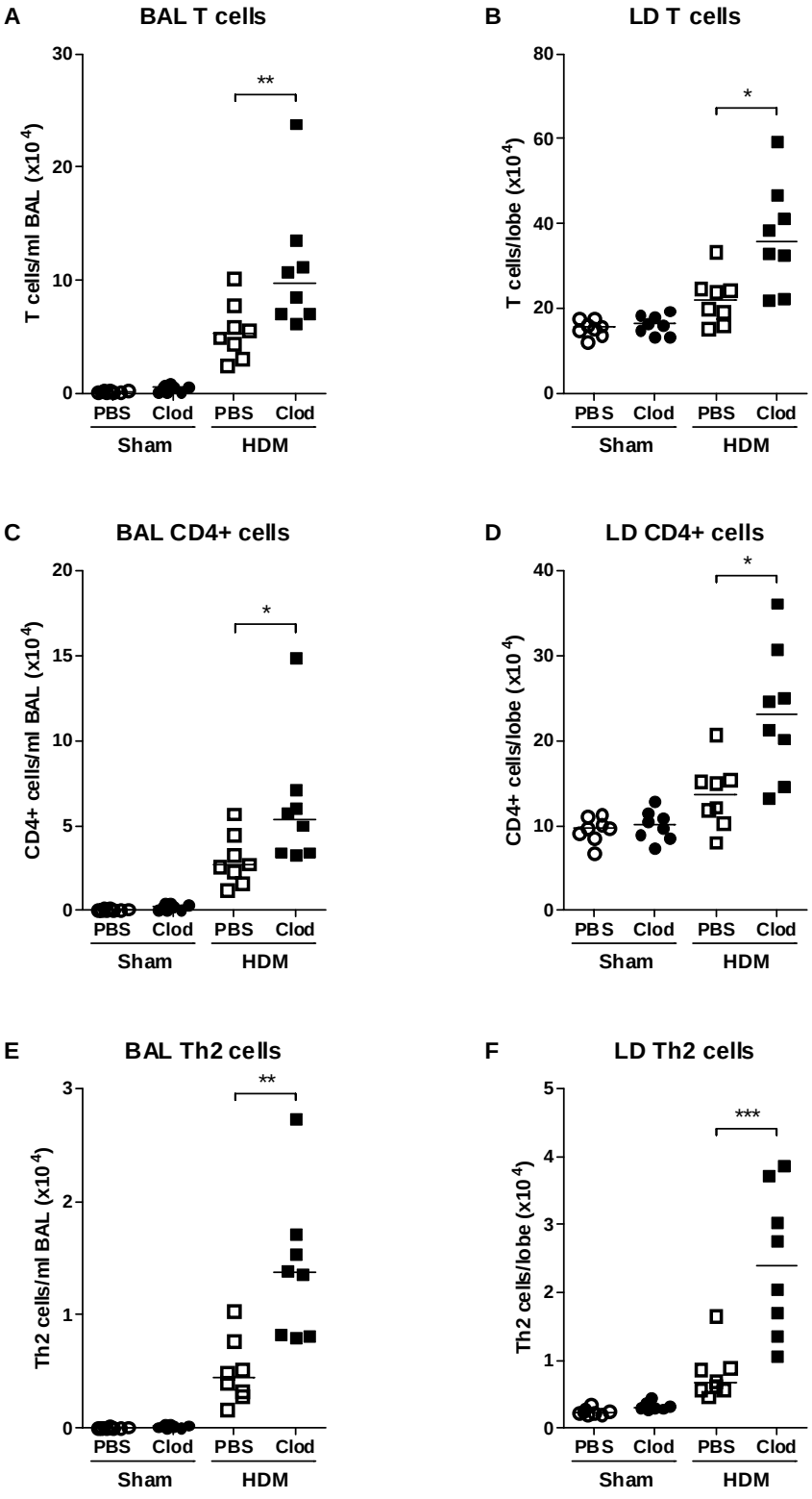


Figure 6.32 Therapeutic administration of clodronate liposomes exacerbated T cell accumulation in HDM exposed mice. HDM exposed mice were dosed with 50µl clodronate (Clod) or PBS filled liposomes i.t. therapeutically, during the final week of HDM exposure. BAL and lungs were taken 4 hours after the last HDM exposure. T cells (A-B), CD4+ T cells (C-D) and Th2 cells (E-F) in BAL (A, C, E) and LD (B, D, F) were identified and quantified by flow cytometry. n = 8 mice/group, bar represents median, data represents one of two experiments. * $p<0.05$, ** $p<0.01$ and *** $p<0.001$ by Mann Whitney test.

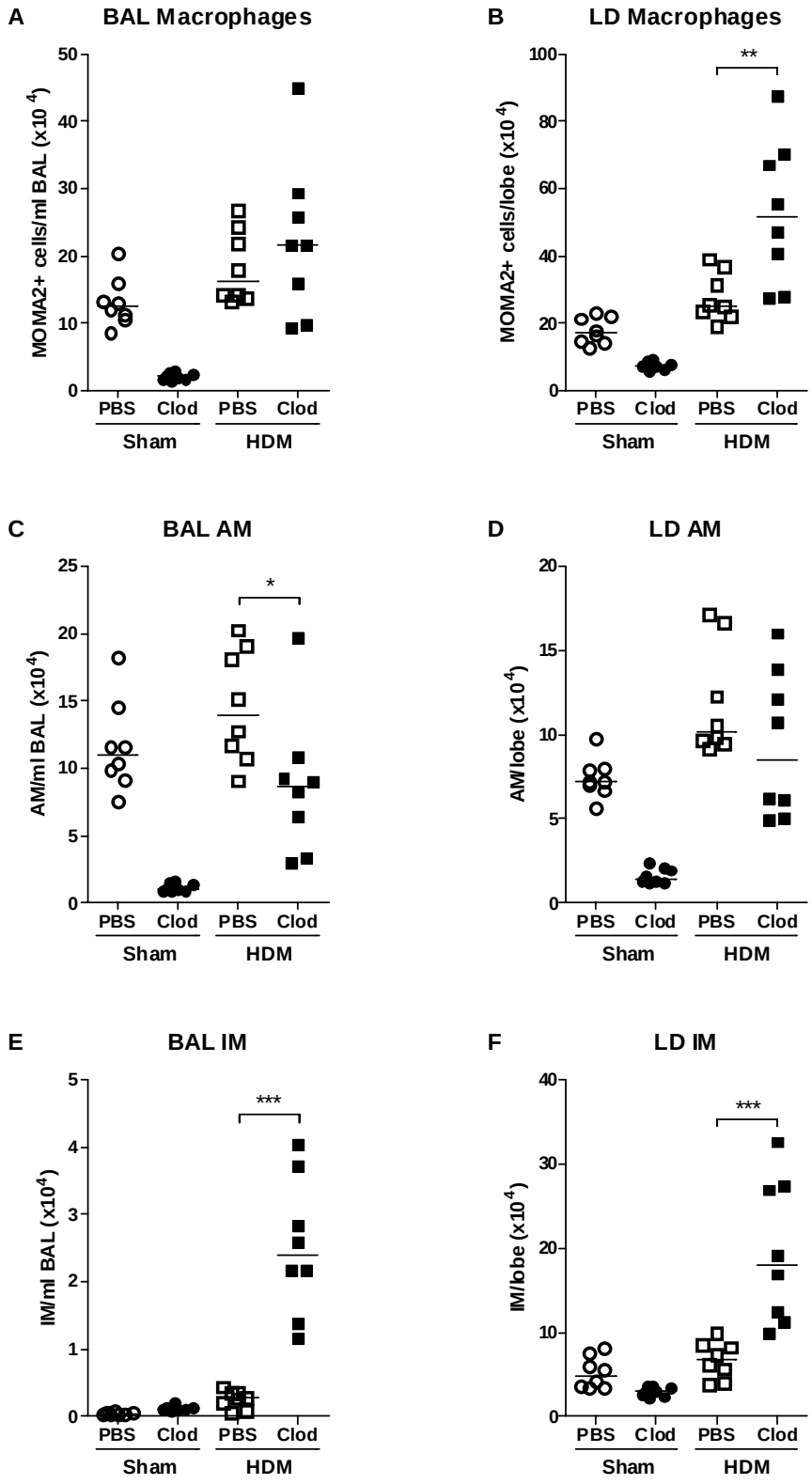


Figure 6.33 Effects of therapeutic clodronate liposomes on macrophage accumulation in HDM exposed mice. HDM exposed mice were dosed with 50µl clodronate (Clod) or PBS filled liposomes i.t. therapeutically, during the final week of HDM exposure. BAL and lungs were taken 4 hours after the last HDM exposure. Total macrophages (A-B), AM (C-D) and IM (E-F) in BAL (A, C, E) and LD (B, D, F) were identified and quantified by flow cytometry. n = 8 mice/group, bar represents median, data represents one of two experiments. * $p<0.05$, ** $p<0.01$ and *** $p<0.001$ by Mann Whitney test.

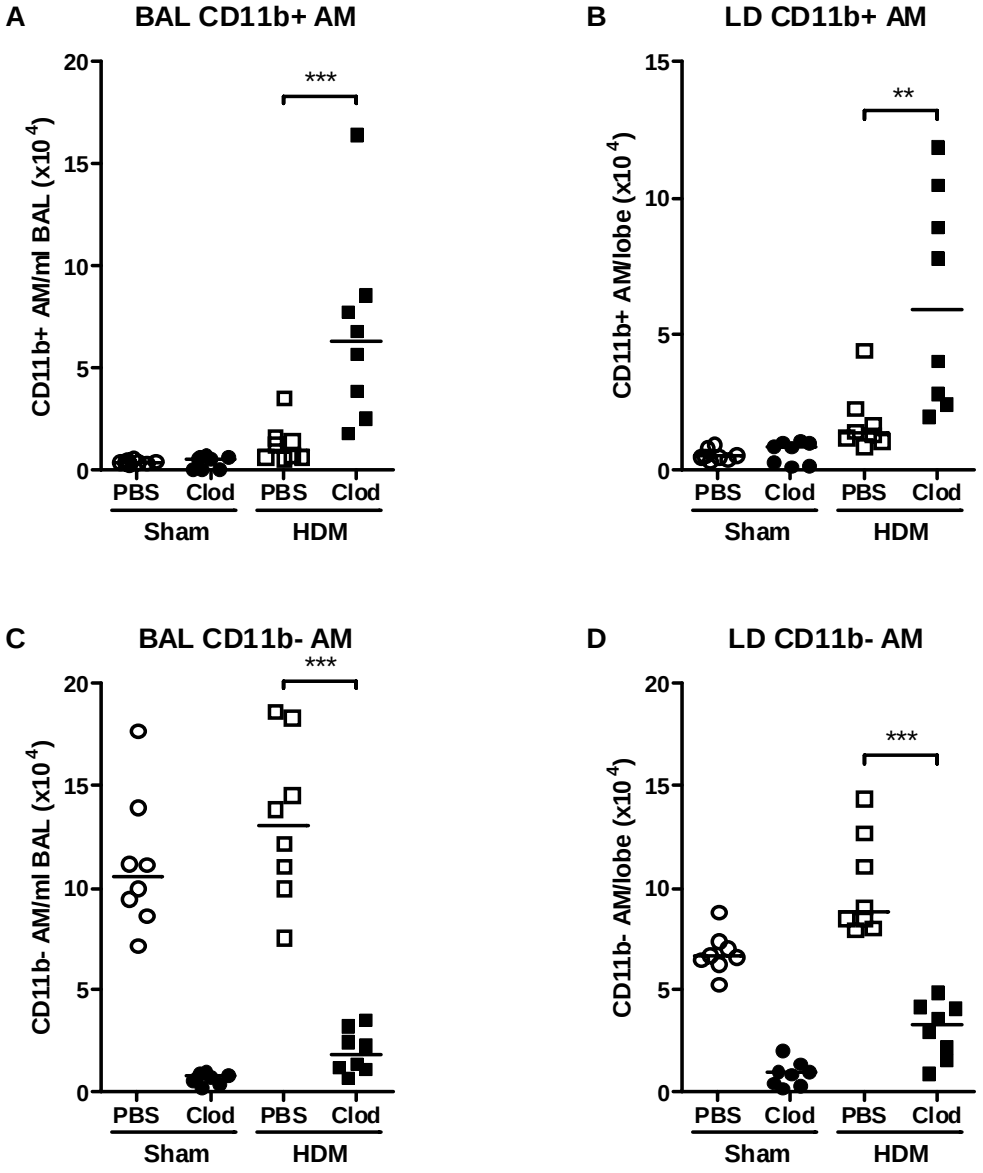


Figure 6.34 Therapeutic clodronate liposomes increased accumulation of CD11b+ AM in HDM exposed mice. HDM exposed mice were dosed with 50µl clodronate (Clod) or PBS filled liposomes i.t. therapeutically, during the final week of HDM exposure. BAL and lungs were taken 4 hours after the last HDM exposure. CD11b+ AM (A-B) and CD11b- AM (C-D) in BAL (A, C) and LD (B, D) were identified and quantified by flow cytometry. n = 8 mice/group, bar represents median, data represents one of two experiments. ** $p<0.01$ and *** $p<0.001$ by Mann Whitney test.

6.4 Discussion

Data in the previous chapter demonstrated that alveolar macrophages were the predominant population of IL-13Rα1+ cells within the lung. The aim of this chapter was to investigate the role of AM in the pathogenesis of lung inflammation induced by IL-13 and subsequently HDM by specific depletion of AM. Hence the initial objective was to establish a protocol for depletion of AM.

6.4.1 Anti-CSF-1R induced macrophage depletion

CSF-1, via its receptor CSF-1R, regulates the survival, proliferation and differentiation of macrophages hence disruption of this interaction results in diminished numbers of tissue macrophages (Wiktor-Jedrzejczak *et al.*, 1992;Cecchini *et al.*, 1994;Dai *et al.*, 2002). Specifically, mice lacking functional CSF-1 (*Csf1*^{op}/*Csf1*^{op}) exhibit significantly reduced numbers of macrophages in the lung tissue and BAL however, the number of AM is spontaneously corrected with age (Wiktor-Jedrzejczak *et al.*, 1992;Roth *et al.*, 1998;Shibata *et al.*, 2001). Disruption of the CSF-1 - CSF-1R interaction by administration of a mAb to CSF-1R has been reported to reduce the frequency of alveolar macrophages within the airway space, but not interstitial macrophages in the lung parenchyma (MacDonald *et al.*, 2010); however this study characterised alveolar and interstitial macrophages based on situation rather than CD11c expression. To determine whether administration of an anti-CSF-1R mAb could specifically deplete CD11c+ AM anti-CSF-1R mAb, 535, was dosed repeatedly for up to 14 days and the numbers of total macrophages, AM and IM assessed in BAL and LD at various intervals.

Treatment with 535 had no significant effects on the numbers of BAL macrophages or AM over the 14 day period. LD macrophages were reduced by approximately 50%; attributable to a 30% decline in AM and up to 85% reduction in IM. In both BAL and LD IM appeared to be more susceptible to CSF-1R blockade than AM. In addition, 535 treatment significantly reduced the frequency of circulating monocytes. However, 535 administration also induced a profound increase in the number of eosinophils in blood and LD which was further increased with prolonged treatment. No eosinophils were detected in BAL hence it is unlikely 535 itself induced lung inflammation and it is probable that the elevation in LD eosinophils is a consequence

of increased circulating eosinophils. Increased numbers of circulating granulocytes have previously been reported in *Csf1*^{op}*/Csf1*^{op} and *Csf1r*$^{-}$*/Csf1r*$^{-}$ mice (Ryan 2001, Dai 2002). Monocytes and granulocytes share a common progenitor cell (myeloblast) and thus preventing myeloblasts developing into monocytes by blocking CSF-1R may lead to increased granulopoiesis.

Due to the incomplete and non-specific depletion of AM together with induction of blood eosinophilia, CSF-1R blockade was considered an inappropriate approach for AM depletion.

6.4.2 Clodronate liposome mediated macrophage depletion

Administration of clodronate liposomes is an established technique for depleting phagocytes (van Rooijen & Sanders, 1994). Macrophages naturally phagocytose liposomes which are subsequently digested. This releases clodronate into the cell where it induces apoptosis. Liposomes cannot cross epithelial or endothelial barriers and consequently their site of action is restricted to the compartment into which they are administered. Hence i.t. administration of clodronate liposomes depletes AM but not IM in the lung (Thepen *et al.*, 1989). Preliminary studies indicated a dose of 50µl liposomes i.t. was sufficient for robust depletion of AM in BAL and LD at day 2, and did not affect the frequency of IM. A subsequent time-course demonstrated significant depletion of AM for at least 7 days after a single administration. However, a small increase in the number of BAL IM was also observed 4 and 7 days after clodronate administration which was also evident in LD on day 4. This apparent increase in the IM population may be due to a genuine rise in the number of IM, perhaps to compensate for the loss of AM, or the number of events acquired in the IM gate may be artificially increased by the inclusion of apoptotic AM that may have lost CD11c expression. Nevertheless, the effects of clodronate administration on the IM population are marginal compared to the effects on the AM population. Thus, a dosing regime of 50µl i.t. once weekly, commencing 2 days prior to induction of inflammation was established for use in subsequent studies.

6.4.3 IL-13 induced lung inflammation

To investigate the effects of AM depletion on the pathogenesis of IL-13 induced lung inflammation, a short term model of IL-13 induced inflammation was adapted from

Wills-Karp and Grunig (Wills-Karp *et al.*, 1998;Grunig *et al.*, 1998). Three daily administrations of i.t. IL-13 induced eosinophilia and T cell accumulation in BAL, but not LD. IL-13 did not affect the total number of BAL or LD leukocytes retrieved, nor the number of macrophages and neutrophils in BAL or LD. In addition IL-12, IL-10 (n.s.), eotaxin and KC were elevated in BAL and IL-33 was raised in LH. BAL eosinophilia and the associated elevation in eotaxin is an established effect of IL-13 administration (Grunig *et al.*, 1998;Wills-Karp *et al.*, 1998;Kibe *et al.*, 2003). However Grunig *et al.* amongst others, also reported IL-13 induced neutrophilia in BAL which was not significant in the present study, despite elevated levels of BAL KC (Grunig *et al.*, 1998). IL-13 induced recruitment of BAL T cells has not previously been reported, although IL-13 has been demonstrated to provoke accumulation of lymphocytes in BAL following adenoviral delivery of IL-13 into the lungs or transgenic overproduction of IL-13 in airway epithelium (Therien *et al.*, 2008;Kuperman *et al.*, 2002). In addition, adenoviral delivery of IL-13 into the lungs revealed elevated BAL KC, IL-12, IL-10 and eotaxin induced by IL-13, corroborating the present findings (Therien *et al.*, 2008). However, IL-13 induced IL-33 has not previously been reported and suggests the relationship between these two cytokines may be more complicated than previously suggested in light of the known property of IL-33 to induce IL-13 production (Kondo *et al.*, 2008;Kurowska-Stolarska *et al.*, 2009;Zhiguang *et al.*, 2010;Chang *et al.*, 2011). Furthermore, it is interesting to note that administration of exogenous IL-13 stimulated IL-33 production yet neutralisation of IL-13 did not inhibit HDM induced IL-33 (Figure 4.17). Thus demonstrating IL-13 is not the only mediator capable of stimulating IL-33 production and that redundancy exists in HDM induced IL-33 generation.

6.4.4 IL-13 induced lung inflammation in AM deficient mice

To determine the role of AM in IL-13 induced pulmonary responses, AM were depleted by administration of clodronate liposomes two days prior to IL-13 treatment. Depletion of AM was assessed at the end of the study and significant depletion of AM from BAL and LD was apparent in both vehicle and IL-13 treated groups receiving clodronate liposomes. As previously observed, administration of clodronate induced a marginal increase in BAL IM although this was not significant in IL-13 treated mice.

AM depletion exacerbated IL-13 induced inflammation in the lungs. Accumulation of eosinophils, neutrophils and T cells, including CD4+ cells and Th2 cells in BAL following IL-13 treatment was significantly greater in mice pre-treated with clodronate liposomes compared to those pre-treated with control liposomes. Pre-treatment with clodronate liposomes in vehicle treated mice elicited an increase in BAL T cells, however this response was further elevated in IL-13 treated mice. AM depletion had no significant effects on BAL IL-4, IL-5, IL-10, eotaxin or KC, or LH IL-33 in vehicle or IL-13 treated mice, yet BAL IFNγ and IL-12 concentrations were elevated in AM deficient IL-13 treated mice. Furthermore, clodronate liposome pre-treatment of vehicle dosed mice induced significant IL-12 production which may correspond to the accumulation of BAL T cells observed in the same mice. In addition, muc5ac mRNA expression and goblet cell frequency in the lung tissue was assessed in this study. As previously reported IL-13 induced muc5ac expression and increased goblet cell frequency (Kuperman *et al.*, 2002;Kibe *et al.*, 2003;Grunig *et al.*, 1998;Wills-Karp *et al.*, 1998). However, despite exacerbating inflammation AM depletion had no significant effects on IL-13 induced muc5ac up-regulation or goblet cell frequency.

Taken together, these data demonstrate AM are not required for the pathogenesis of IL-13 induced lung inflammation. Moreover, these data indicate AM may play a role in dampening the response to IL-13 in the lungs, hence the heightened inflammation in their absence. However an alternative explanation for AM depletion exacerbating inflammation is that clodronate liposomes or the accumulation of apoptotic cells in the airways is having an adjuvant effect and enhancing the response to IL-13.

6.4.5 Prophylactic clodronate treatment during HDM induced lung inflammation

To investigate the role of AM in the development of AAD, AM were depleted by pre-treatment with clodronate liposomes prior to HDM exposure. Mice were subsequently exposed to HDM for 3 weeks to induce AAD concomitant with weekly administration of clodronate liposomes to maintain AM depletion. Administration of clodronate liposomes induced a profound exacerbation of HDM induced AHR and inflammation. Total leukocytes, eosinophils, neutrophils, and T cells, including CD4+ cells and Th2 cells, in BAL and LD were all significantly elevated in HDM

exposed mice treated with clodronate liposomes compared to HDM mice treated with control liposomes. However, analysis of macrophage numbers at the end of the study indicated AM were not depleted by weekly clodronate treatment during HDM exposure, and were in fact increased compared to HDM mice receiving control liposomes. The numbers of total macrophages, AM and IM in BAL and LD from HDM mice were augmented by clodronate treatment. Conversely, this clodronate treatment regime was adequate for depletion of AM in sham exposed mice. Further analysis of the AM population from clodronate treated, HDM exposed mice revealed greater heterogeneity with respect to F4/80 and CD11c expression and up-regulation of CD11b compared to AM from HDM mice treated with control liposomes or sham exposed mice. Under normal circumstances AM are CD11b- although CD11b can be up-regulated upon activation (Guth *et al.*, 2009;Padilla *et al.*, 2005;Gonzalez-Juarrero *et al.*, 2003). In addition CD11b can be indicative of newly recruited macrophages (Gonzalez-Juarrero *et al.*, 2003). Quantification of CD11b+ AM showed this population was modestly increased in HDM compared to sham exposed mice and substantially amplified following clodronate treatment of HDM, but not sham mice. Furthermore, quantification of CD11b- AM revealed a significant reduction of this population in HDM BAL following clodronate liposome treatment. Taken together these results indicate two possible scenarios: Clodronate mediated depletion of AM is ineffective during inflammation, and the combination of HDM and clodronate liposomes merely alters the phenotype of AM perhaps by activation. Alternatively, clodronate liposomes are depleting resident AM but the replenishment of this population occurs more rapidly in an inflamed environment and the newly recruited AM exhibit an altered phenotype with high CD11b expression. In either case, exacerbation of inflammation is associated with loss of the CD11c+ CD11b- AM population and amplification of the CD11c+ CD11b+ AM population.

Upon analysis of inflammatory mediators in the lungs, there were no changes in the HDM induced Th2 cytokines IL-4, IL-5 and IL-13 following clodronate treatment despite significantly greater numbers of Th2 cells present in the lungs of HDM exposed, clodronate treated mice compared to HDM mice treated with control liposomes. However, concentrations of BAL IFNγ, BAL IL-10 and IL-12 in BAL and LH were elevated in HDM mice treated with clodronate liposomes compared to HDM mice receiving control liposomes.

The role of IFNγ in AAD is complex. IFNγ is a Th1 cytokine capable of suppressing Th2 responses. However, there is evidence suggesting IFNγ can drive AHR in AAD and augment expression of Th2 cytokines and eosinophilia in the lungs (Hessel *et al.*, 1997;Kumar *et al.*, 2004;Kim *et al.*, 2010;Koch *et al.*, 2006;Kim *et al.*, 2010). In contrast, IFNγ can reduce AHR and inhibit IL-13 induced goblet cell hyperplasia and eosinophilia (Koch *et al.*, 2006;Ford *et al.*, 2001). Under certain conditions IFNγ induces expression of IL-13Rα2 which may be the underlying mechanism for this IFNγ dependent inhibition of IL-13 induced pathology (Daines & Hershey, 2002). IFNγ is produced by T cells, amongst other inflammatory cells, and can induce lymphocyte accumulation at sites of inflammation. Therefore the elevated levels of BAL IFNγ in the current study could be a cause or effect of the increased accumulation of T cells observed in the lungs of HDM exposed, clodronate treated mice. In summary, elevated IFNγ provides a potential mechanism for the exacerbation of AHR and inflammation in the present study. However, this requires further investigation perhaps by determining the source of IFNγ or the effects of neutralising IFNγ in HDM exposed, clodronate treated mice.

IL-10 is an anti-inflammatory cytokine produced by many cell types including T cells, macrophages and DCs (Mosser & Zhang, 2008). IL-10 in the airways limits pathology associated with viral, bacterial and allergen challenge (Lloyd & Hawrylowicz, 2009). In models of AAD IL-10 can inhibit the production of Th2 cytokines, BAL eosinophilia and AHR (van Scott *et al.*, 2000;Fu *et al.*, 2006;Kosaka *et al.*, 2010). However, IL-10 has also been reported to concurrently exacerbate AHR (van Scott *et al.*, 2000). IL-10 plays an important role in the maintenance of homeostasis and the resolution of inflammation. In these capacities, both Tregs and macrophages represent key sources of IL-10. IL-10 is produced by various macrophage populations including regulatory (M2b) macrophages induced by TLR stimulation in the presence of IgG immune complexes; M2c macrophages induced by IL-10; and AM themselves (Martinez *et al.*, 2008;Mosser & Edwards, 2008). Furthermore, the generation of Tregs and M2c macrophages is dependent upon IL-10. However, the exacerbation of inflammation observed in AM depleted HDM exposed mice suggests a lack of regulation. Thus, assessment of Tregs and macrophage

subpopulations generated in HDM exposed clodronate treated mice could help determine the implications of elevated IL-10 in these mice.

IL-12 is predominantly produced by DC and macrophages and drives Th1 differentiation, thus is capable of down-regulating Th2 responses. Since IL-12 was up-regulated by clodronate treatment of sham and HDM mice in the present study it is likely to be a result of the accumulation of apoptotic bodies elicited by administration of clodronate liposomes. However, the combined effects of HDM and clodronate resulted in a more than additive production of IL-12 in BAL and LH. The role of IL-12 in HDM induced AAD is unknown and there are conflicting reports on the role of IL-12 using exogenous IL-12, *Il12rβ2*$^{-/-}$ mice and anti-IL-12 mAbs in various models of AAD driven by sheep red blood cells, OVA/alum or Der p 1/alum. IL-12 reduces Th2 cytokine production, inflammation, IgE and AHR partly by up-regulating IFNγ (Gavett *et al.*, 1995;Lee *et al.*, 2001;Kuribayashi *et al.*, 2002;Fu *et al.*, 2006). However, there is evidence from *Il12rβ2*$^{-/-}$ mice suggesting IL-12 is required for the development of allergen induced AHR and inflammation (Kim *et al.*, 2010). Furthermore, studies employing anti-IL-12 mAbs elucidate that IL-12 neutralisation during allergic sensitisation exacerbates AAD pathogenesis whereas IL-12 neutralisation in established AAD inhibits the production of Th2 cytokines, inflammation, antigen specific IgE and AHR in an IFNγ dependent manner (Meyts *et al.*, 2006). The converse of this latter finding implies excess IL-12 present in established AAD could exacerbate AHR and inflammation, via IFNγ. As suggested previously this mechanism could be responsible for the enhanced AHR and inflammation observed in HDM exposed clodronate treated mice in the present study, although further studies would be required to verify this.

In addition to the increased IFNγ, IL-10 and IL-12 in the present study; LH and BAL eotaxin, LH KC and IL-33 were also elevated in HDM exposed mice treated with clodronate liposomes compared to those treated with control liposomes. In contrast, LH IL-25 was reduced following clodronate treatment of HDM mice. Increased eotaxin is likely to account for the augmented accumulation of eosinophils in the BAL and lung tissue of HDM exposed clodronate treated mice. Similarly, the increase in KC corresponds to increased neutrophilia in HDM exposed clodronate treated mice. IL-33 can both amplify and directly induce innate and allergic responses by multiple

mechanisms including activation and recruitment of Th2 cells and eosinophils and activation of innate lymphoid cells. Hence, the increased concentration of IL-33 in LH from HDM mice following clodronate treatment may be contributing to the exacerbation of allergic inflammation in these mice. IL-25 also promotes Th2 immunity and activates innate lymphoid cells, however in contrast to IL-33; IL-25 is reduced in LH from HDM exposed mice treated with clodronate compared to control liposomes. That treatment with clodronate liposomes should inhibit HDM induced IL-25 is unexpected but may indicate that AM are required for IL-25 production. Interestingly, there is evidence suggesting AM are required for IL-25 induced inflammation, but not for IL-25 production (Claudio *et al.*, 2009).

In the present study the generation of Th2 associated serum antibodies, IgE and IgG1, in response to HDM exposure was significantly increased after AM depletion with clodronate liposomes. This was evident as elevated total IgE, HDM specific IgE and HDM specific IgG1. HDM specific IgG2b was also increased, but to a lesser extent. Heightened humoral responses following delivery of clodronate liposomes into the airways have previously been observed in immunised rats (Thepen *et al.*, 1989;Thepen *et al.*, 1992). Together these data indicate AM depletion with clodronate liposomes exacerbates the systemic immune response to HDM, and specifically Th2 immunity.

Surprisingly, despite exacerbated lung inflammation in HDM exposed mice treated with clodronate liposomes, and IL-13 production comparable to that in HDM exposed mice treated with control liposomes, clodronate liposome treatment reduced HDM induced goblet cell up-regulation. This may be attributable to the increased production of Th1 cytokines such as IFNγ which has previously been demonstrated to inhibit IL-13 induced goblet cell hyperplasia (Ford *et al.*, 2001). In addition, the elevated levels of IL-10 and IL-12 and reduced IL-25 may influence goblet cell differentiation. Alternatively, this data suggests AM may be required for HDM induced goblet cell up-regulation, however chemical depletion of AM after OVA challenge in pre-sensitised mice demonstrated AM are not required for the maintenance of goblet cells in AAD (Yang *et al.*, 2010). Administration of clodronate liposomes did not affect HDM induced peribronchial collagen deposition in the present study, indicating AM are not involved in this aspect of the remodelling

process, in this model. However, it is possible that the accumulating macrophages in the lung tissue following HDM exposure may contribute to collagen deposition.

In summary, these data demonstrate AM are not required for the pathogenesis of HDM induced AAD, and furthermore indicate AM may actually suppress the development of AAD in response to HDM exposure. Thus an exacerbated response to HDM ensues in the absence of AM. However, there are alternative explanations for this phenomenon which are discussed in section 6.4.7.

6.4.6 Therapeutic clodronate treatment during HDM induced lung inflammation

Having established the effects of prophylactic administration of clodronate liposomes on HDM induced AAD, the following study was conducted to investigate the effects of therapeutic administration of clodronate liposomes on established HDM induced AAD. Mice were dosed with i.t. liposomes twice during the final week of HDM exposure. Clodronate treatment had no significant effects on AHR however; lung inflammation was exacerbated in HDM exposed mice dosed with clodronate compared to control liposomes. As with prophylactic administration, but to a lesser extent, therapeutic administration of clodronate liposomes increased the accumulation of BAL and LD leukocytes, eosinophils, neutrophils and T cells, including CD4+ cells and Th2 cells in HDM exposed mice treated with clodronate compared to HDM exposed mice treated with control liposomes. The apparent discord between AHR and inflammation suggests the exacerbation of inflammation in the present study is not great enough to significantly affect AHR. Alternatively, AHR exacerbation may be independent of inflammation under these circumstances and driven by an alternative mechanism present during prophylactic clodronate dosing but absent in this therapeutic study. Determining the effects of dosing clodronate liposomes therapeutically, but for a longer period would indicate whether exacerbated AHR could be achieved or whether this phenomenon is due to the absence of AM specifically during the initiation of AAD.

Analysis of macrophage numbers at the end of the study demonstrated significant depletion of AM in BAL although the total numbers of macrophages in LD and IM in BAL and LD from HDM exposed mice were enhanced by treatment with clodronate liposomes. The increased frequency of liposome dosing in the current study elicited a

significant reduction in total BAL AM which was not achieved with once weekly prophylactic dosing in the previous study. As with prophylactic treatment, therapeutic treatment with clodronate increased the number of CD11b+ AM and reduced the number of CD11b- AM in HDM exposed mice compared to those dosed with control liposomes. This demonstrates clodronate liposomes are still capable of macrophage depletion in inflamed lungs. Hence when revisiting the possible explanations for the presence of AM in the previous study the latter scenario appears more plausible; in which weekly administration of clodronate liposomes depletes AM, but the replenishment of these cells is more rapid during inflammation and the recruited macrophages express CD11b. Thus, exacerbation of inflammation is associated with a reduction in the CD11c+ CD11b- AM population and an increase in the CD11c+ CD11b+ AM population. In the absence of inflammation, the AM population has been reported to be replenished by both local proliferation and migration of monocyte derived, tissue resident macrophages into the alveolar space, however this study only assessed CD11c+ CD11b- AM (Landsman & Jung, 2007). The expression of CD11b on recent AM and the balance between these two processes of replenishment is likely to be complicated by the presence of ongoing inflammation. To investigate whether the accumulation of CD11c+ CD11b+ AM arises from recruitment of monocytes and to explore the role of these cells during exacerbated inflammation, the present studies could be repeated in mice in which monocyte recruitment is impeded by blocking trafficking into the tissue or depleting monocytes themselves.

6.4.7 The role of AM in lung inflammation

Depletion of AM by administration of clodronate liposomes in models of lung inflammation driven by exogenous IL-13 or HDM invariably exacerbated inflammation and was associated with increased Th1 cytokines. Previous studies have reported comparable increases in immune responses in the lung following AM depletion by clodronate liposomes (Thepen *et al.*, 1989;Thepen *et al.*, 1992;Tang *et al.*, 2001a;Bang *et al.*, 2011). This heightened inflammation may be attributable to a number of potential mechanisms (Figure 6.30), each of which shall be discussed;

1. Clodronate liposomes may be acting as an adjuvant to enhance the response to IL-13/HDM.

2. The accumulation of apoptotic cells in the airways induced by administration of clodronate liposomes could have an adjuvant effect and elevate the response to IL-13/HDM.

3. Infiltrating macrophages recruited to replenish the depleted AM population are pro-inflammatory.

4. AM limit and subsequently resolve tissue inflammation by killing and phagocytosing pathogenic cells. In the absence of this clearance mechanism pathogenic cells are allowed to accumulate.

5. AM are immunosuppressive.

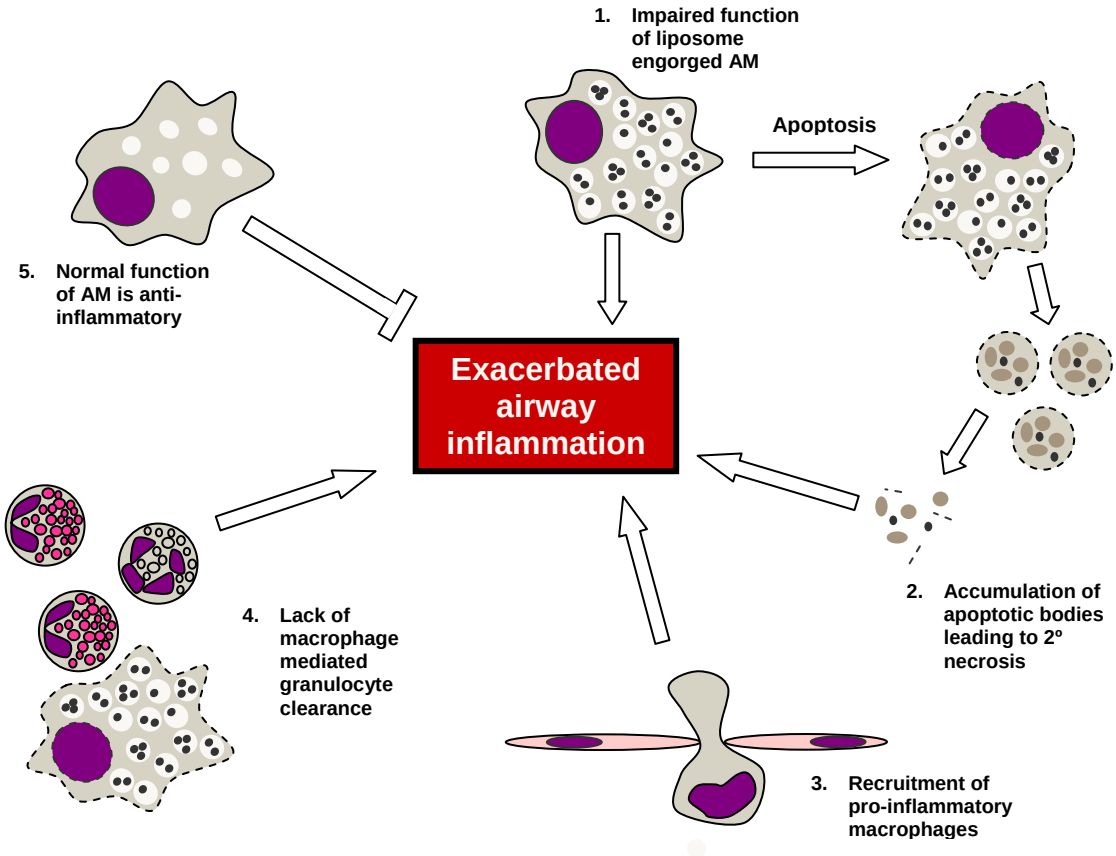


Figure 6.35 Potential mechanisms by which administration of clodronate liposomes may exacerbate airway inflammation.

6.4.7.1 Adjuvanticity of liposomes

The administration of liposomes alone can alter immune function. Phagocytosis of liposomes has been reported to suppress further phagocytic activity and migration in engorged macrophages and even stimulate immunity, however this is minimised by the use of zwitterionic liposomes to deliver clodronate (de Haan A. *et al.*, 1996). Furthermore, any effects of the liposomes themselves are controlled for in the present studies by use of PBS filled liposomes. Hence this mechanism is unlikely to be contributing to the exacerbated responses to IL-13 and HDM observed in mice treated with clodronate liposomes.

6.4.7.2 Adjuvanticity of apoptotic cells

Administration of clodronate liposomes induces apoptosis of macrophages however clearance of the resulting apoptotic cells may be insufficient due to the deficiency of macrophages themselves. Thus, whilst apoptosis is a silent death, the persistence of apoptotic cells leads to secondary necrosis (Medan *et al.*, 2002;Grainger *et al.*, 2004). This release of DAMPs would in turn amplify any ongoing immune response. In the present studies AM depletion induced by clodronate liposome treatment is not complete and the total number of macrophages in BAL and LD is actually greater in HDM mice treated with clodronate. Hence, the clearance of apoptotic cells may be adequate. Furthermore, phagocytosis of apoptotic cells can induce macrophages to release anti-inflammatory mediators, such as TGFβ, and down regulate pro-inflammatory mediators (Fadok *et al.*, 1998). Assessment of secondary necrosis in BAL or lungs could indicate whether clearance of apoptotic cells is sufficient in the present study and hence whether secondary necrosis is contributing to the enhanced inflammation observed in clodronate treated mice. In addition, assessing the functional phenotype of pulmonary macrophages from clodronate treated HDM mice *ex vivo* could indicate whether ingestion of apoptotic cells is inducing an anti-inflammatory profile. Specifically, the activity of these cells could be determined by analysis of their phagocytic activity *in vitro* and assessment of cytokine production upon phagocytosis of beads or apoptotic bodies and following other activating stimuli such as LPS.

6.4.7.3 Pro-inflammatory macrophages replenish the AM population

Following depletion of AM with clodronate liposomes in HDM exposed mice this population is replaced by CD11b+ AM, indicative of activated and/or newly recruited macrophages. This effect is specific to HDM exposed mice as it is not apparent in AM depleted sham mice. Accumulation of CD11b+ CD11c+ macrophages has previously been associated with OVA induced AAD, furthermore adoptive transfer of these macrophages enhanced allergen induced inflammation, Th2 cytokine production and AHR (Moon *et al.*, 2007). It is not clear whether accumulation of CD11b+ AM in the present study is a consequence or cause of the exacerbated inflammation observed in HDM exposed clodronate treated mice. Further analysis of the phenotype of CD11b+ AM would indicate whether these cells are indeed pathogenic and by what mechanisms they may be contributing to allergic inflammation.

Also of note, is the substantial increase in BAL and LD IM in HDM exposed clodronate treated mice, not apparent in HDM exposed mice treated with control liposomes or sham exposed mice. IM are reported to inhibit allergic sensitisation by producing high levels of IL-10 and preventing DC maturation and migration (Bedoret *et al.*, 2009). In concurrence with this, the expansion of this population correlates with elevated IL-10 concentrations in the same mice. Thus, IM are unlikely to be contributing to the exacerbation of inflammation.

In the present study, clodronate liposome treatment of HDM exposed mice significantly increased the number of CD11b+ AM and IM in the lungs although the source of these macrophages is unknown. A recent study has demonstrated that the accumulation of macrophages in the tissue during Th2 inflammation is due to IL-4 dependent proliferation of local tissue macrophages whereas the accumulation of macrophages during a Th1 response occurs through the recruitment of monocytes (Jenkins *et al.*, 2011). Since the presence of both Th2 and Th1 cytokines has been demonstrated in the tissue of clodronate treated HDM mice in the current study it is likely that both of these processes are occurring. However, investigation into the relative contributions of proliferation and recruitment to both the AM and IM populations would aid our understanding of these macrophage populations and their origins.

6.4.7.4 Lack of macrophage mediated clearance of inflammatory cells

Macrophages play a key role in the limitation and resolution of inflammation by inducing apoptosis and subsequently phagocytosing granulocytes at sites of inflammation (Ying *et al.*, 1997;Kodama *et al.*, 1998). Upon AM depletion and hence loss of this clearance mechanism increased accumulation of granulocytes might be expected. However, in the present studies granulocyte chemoattractants were elevated indicating increased recruitment and not simply diminished clearance of granulocytes contributed to the enlargement of these populations. Furthermore, this clearance mechanism is relatively specific for granulocytes and hence does not explain the accompanying elevation in the number of lymphocytes observed in the current studies.

6.4.7.5 AM are immunosuppressive

The exacerbation in AAD in the absence of AM suggests one of the functions of AM is to dampen down the inflammatory response. Heightened inflammation resulted from both prophylactic and therapeutic administration of clodronate liposomes indicating AM may be continually limiting ongoing inflammation, and that this activity is not specific to the initiation of an allergic response. The inhibitory functions of AM in rodent models of lung inflammation have previously been reported. AM depleted mice and rats exhibit exacerbated immune responses to hapten and OVA, demonstrated by augmented humoral immunity, allergic inflammation, Th2 cytokine production and AHR (Thepen *et al.*, 1991;Thepen *et al.*, 1992;Thepen *et al.*, 1989;Tang *et al.*, 2001a;Bang *et al.*, 2011). Several mechanisms by which AM are capable of suppressing components of AAD pathophysiology have been identified. AM can inhibit DC function both *in vitro* and *in vivo* (Holt *et al.*, 1993;Jakubzick *et al.*, 2006). Via these effects on DCs or directly, AM restrict the reactivity of T cells resident in the lungs (Strickland *et al.*, 1993;Thepen *et al.*, 1992). Accordingly, the immunocompetence of these T cells is restored in the absence of AM (Strickland *et al.*, 1993). This corroborates the increased accumulation of T cells observed in the present study. Furthermore, analysis of pulmonary DC frequency and phenotype following AM depletion in HDM exposed mice could indicate whether this increased T cell accumulation is driven by enhanced DC activation.

AM have also been reported to suppress AHR under certain circumstances. Adoptive transfer of AM from allergy-resistant or naïve rats prevents AHR in AM deficient allergic rats, without affecting the accumulation of BAL cells (Careau & Bissonnette, 2004;Careau *et al.*, 2006;Careau *et al.*, 2010). Pouliot *et al.* suggested AM possess an intrinsic ability to inhibit AHR that is suppressed by the microenvironment of the allergic lung (Pouliot *et al.*, 2008). This was illustrated by the inhibition of AHR in allergic rats after receiving AM harvested from allergic rats and "re-programmed" *ex vivo* by exposure to classically activating stimulus. Thus, AM can transfer resistance to AHR however, this is dependent on the phenotype of AM, which is in turn dictated by the lung microenvironment. Accordingly, AM can also exacerbate AHR if they have been alternatively activated. Alternatively activated AM from mice sensitised and challenged with OVA maintain their phenotype upon viral challenge and hence exacerbate AAD via the inappropriate production of Th2 cytokines leading to enhanced eosinophilia and AHR (Nagarkar *et al.*, 2010). Consequently, AM depletion after allergen challenge and prior to viral infection in this model reduced eosinophilia and AHR. Similarly, depletion of AM post-allergen challenge prevented the development of prolonged AHR in mice sensitised and challenged with OVA; although this protocol did not affect short-term AHR or pulmonary inflammation (Yang *et al.*, 2010). Moreover, allergen challenge stimulates expression of pro-inflammatory cytokines from AM and consequently stimulates Th2 cytokine production from T cells (Herbert *et al.*, 2010). This dichotomy of AM functions and hence variable effects of AM depletion illustrates the significance of the activation state of the AM and hence lung microenvironment prior to cell depletion.

Collectively, these data suggest naïve macrophages and classically activated macrophages (CAM) suppress AAD and therefore their depletion would exacerbate AAD whereas alternatively activated macrophages (AAM) contribute to AAD and therefore their depletion would dampen AAD. Since macrophage depletion in the present studies resulted in exacerbated AAD this implies the AM may be classically activated in HDM exposed mice. However, analysis of AM phenotype following HDM exposure in the preceding chapter indicated alternative activation, in accordance with the predominance of Th2 immunity and the consequent up-regulation of the alternatively activating cytokines IL-4 and IL-13, despite exposure to significant levels of the classical activation stimulus LPS present in HDM extract.

AAM (or M2) do not represent a single, homogeneous population of macrophages but, due to their implicit plasticity, reflect a range of activation states induced by some common stimuli. Thus M2 macrophages can be further subdivided into M2a, M2b and M2c phenotypes based primarily upon polarising stimuli (Martinez *et al.*, 2008). Mosser and Edwards go further still and suggest all macrophages exist in a broad spectrum of activation states elicited by a multitude of environmental stimuli (Mosser & Edwards, 2008). Briefly, M2a macrophages arise following exposure to IL-4 or IL-13 and thus represent AAM involved in Th2 immunity. M2b macrophages are induced by stimulation with immune complexes in the presence of LPS or IL-1β and subsequently secrete high levels of IL-10 as well as pro-inflammatory mediators such as TNFα, IL-1β and IL-6. M2c macrophages differentiate in response to IL-10, TGFβ or glucocorticoid exposure and possess anti-inflammatory activities. During HDM induced AAD AM are likely to be exposed to a cocktail of IL-4, IL-13, LPS, IL-1β, immune complexes, IL-10 and TGFβ, thus it is possible M2a, M2b and M2c phenotypes are all generated (Mosser & Edwards, 2008;Martinez *et al.*, 2008). Moreover, the discrepancies observed following AM depletion in the present study compared to findings in other models of lung inflammation may be a reflection of the predominance of macrophage subtypes induced by HDM compared to OVA or hapten exposure.

IL-10 is up-regulated following HDM exposure which may indicate the presence of M2b and/or M2c macrophages in the current studies. Both M2b and M2c macrophages have the potential to regulate immune responses. Therefore depletion of these cells in AAD may exacerbate disease. Further definition of the phenotype of AM in HDM induced AAD would aid determination of the function of these cells *in vivo* and hence whether this is a plausible mechanism for the exacerbation of AAD observed following AM depletion. In addition, the employment of alternative strategies for AM depletion or adoptive transfer of polarised AM could verify whether AM are suppressing allergic inflammation.

The role of AM in the pathogenesis of asthma is still largely unknown. In healthy individuals the primary role of AM is in maintaining or restoring homeostasis however, there is evidence that AM are inappropriately or insufficiently activated in asthmatic patients (Moreira & Hogaboam, 2011). Analogous to AM in HDM induced

AAD, AM in asthmatics are also likely to be exposed to a range of stimuli, including LPS, immune complexes and cytokines, which potentially differentiate AM into multiple phenotypes. Plausibly, classical activation of AM could exacerbate inflammation by aiding the recruitment and activation of inflammatory cells, while alternatively activated AM could contribute specifically to Th2 inflammation and the fibrotic process. Thus, either phenotype might contribute to asthma pathogenesis. Several studies have endeavoured to distinguish the phenotype of AM from asthmatic patients compared to healthy controls. Analysis of cell markers shows no differences in the proportions of CD68, CD14, CD11b, CD83, CD64, CD80, CD86 or FIZZ1 expressing AM from mild asthmatics compared to healthy controls, indicating no changes in the activation status of AM and no change in the frequency of alternatively activated AM (St-Laurent *et al.*, 2009). However, many of these markers have been demonstrated to be up-regulated following allergen challenge; CD14, CD11b, CD80, CD86 (Lensmar *et al.*, 2006;Viksman *et al.*, 2002;Tang *et al.*, 2001b;Balbo *et al.*, 2001). St-Laurent *et al.* did demonstrate an increased proportion of RFD7+ cells in BAL from asthmatic patients, indicative of mature, phagocytic, tissue macrophages (St-Laurent *et al.*, 2009). Cytokine expression, assessed by mRNA, demonstrated asthmatic AM expressed higher levels of IL-6, IL-10 and TGFβ but lower IL-8 and TNFα than healthy controls, with no differences observed in IL-1, IL-4, IL-12, IL-13 and IFNγ expression (Prieto *et al.*, 2000;Pouliot *et al.*, 2005). Using the macrophage classification system described above this phenotype most closely resembles the pro-Th2, M2b cells which produce IL-6, IL-1β, TNFα, high levels of IL-10 and low levels of IL-12 (Martinez *et al.*, 2008). Furthermore, elevated secretion of IL-6, IL-1β, TNFα and IL-10 protein from AM, and low IL-12 production, has previously been demonstrated in AM from asthmatic compared to healthy controls (Tang *et al.*, 1999;Gosset *et al.*, 1991;Colavita *et al.*, 2000). Interestingly, impaired IL-12 production from AM from asthmatic individuals has been demonstrated to be due to lower levels of CD40 expression, both at rest and following activation (Tang *et al.*, 2001b). In healthy controls, this release of IL-12 inhibits IL-5 production from T cells whereas the diminished release of IL-12 from asthmatic AM permits IL-5 production. Thus, the M2b-like phenotype of AM observed in asthmatic patients could be contributing to the pathogenesis of disease via the direct production of pro-inflammatory and pro-fibrotic cytokines and the indirect production of Th2 cytokines.

However, the high levels of IL-10 produced by AM from asthmatic individuals could be regulating airway pathology. Thus, the net effects of AM activity and hence the role of AM in disease pathogenesis is difficult to predict.

Collectively, these data suggest the phenotype of AM in mouse AAD and human asthma may be similar, and therefore that depletion of AM, or inhibition of AM activity, in asthma could exacerbate disease as observed in mouse AAD. This hypothesis requires much further investigation into the understanding of the role of AM in asthma. However, elucidation of the mechanisms involved in AM suppression of AAD could provide insights and opportunities for the future treatment of asthma.

In summary, prophylactic or therapeutic treatment with clodronate liposomes induced exacerbation of AAD induced by IL-13 or HDM. Exacerbation of AAD was associated with increased expression of Th1 cytokines and loss of CD11b- CD11c+ AM. These data indicate the role of AM in AAD may be suppression of AAD, however further investigation is required to verify this function.

7. CONCLUDING DISCUSSION

7.1 Summary of findings

The working hypothesis for this thesis was that IL-13 is required for the initiation, development and maintenance of pulmonary inflammation, airway remodelling and AHR in mice chronically exposed to inhaled HDM allergen. In order to address this, a previously described murine model of HDM induced AAD with similarities to asthma was established (Johnson *et al.*, 2004). This model was characterised by a predominant Th2 response, allergen specific antibody generation, AHR, goblet cell up-regulation and airway remodelling. Furthermore, IL-13 was demonstrated to be up-regulated in allergen exposed mice. Hence, IL-13 neutralising antibodies were employed to determine the role IL-13 in this model of AAD. Prophylactic anti-IL-13 mAb treatment established IL-13 as indispensable for the development of airway eosinophilia, AHR, goblet cell up-regulation and subepithelial fibrosis. However, IL-13 was not required for the initiation of the allergen specific Th2 response. Therapeutic IL-13 neutralisation demonstrated IL-13 was essential for the maintenance of goblet cells and continued peribronchial collagen deposition during allergen exposure. In addition these studies demonstrated IL-13 also played a role in the maintenance of airway inflammation and AHR. Thus, the hypothesis can be accepted.

To further explore the mechanisms of action of IL-13 in HDM induced AAD the expression and distribution of IL-13 receptors were investigated. Airway epithelial cells were found to constitutively express IL-13Rα2; the expression of which was up-regulated upon exposure to allergen. However, the role of this receptor in AAD remains unknown. IL-13Rα1 was detected on AM and subsets of monocytes and T cells. Following allergen exposure IL-13Rα1 expression was not modulated at the gene level however; this receptor subunit was internalised from the surface of AM. As the principal IL-13Rα1 expressing cell type, the role of AM in IL-13 induced airway pathology and AAD was investigated by specific depletion of AM. Contrary to abrogating IL-13 dependent pathology, AM depletion exacerbated IL-13 and HDM induced airway pathophysiology. Thus, IL-13 dependent airway pathology was not driven by AM and the role of the IL-13—AM axis in AAD remains to be determined. Furthermore, these studies provided evidence that the predominant function of AM during AAD was anti-inflammatory.

7.2 Impact of project

The present studies have described for the first time the effects of IL-13 neutralisation in HDM induced AAD; a chronic murine model driven by the repeated administration of an environmentally relevant aeroallergen to the airways, in the absence of prior sensitisation with chemical adjuvants. The data substantiate IL-13 as a key mediator not only in the development of AAD but also in the maintenance of disease. Thus indicating that novel therapeutics inhibiting IL-13 activities in man may be beneficial in the treatment of established asthma, and furthermore have the potential to modify disease.

In addition, several novel findings were made which require future verification. Neutrophils were identified as a potential source of IL-13 during airway inflammation. Neutrophils from healthy humans cannot produce IL-13 however, the production of IL-13 from lung neutrophils derived from asthmatic patients would be a more appropriate analysis (Reglier *et al.*, 1998). This potential source of IL-13 could be significant in patients with pulmonary neutrophilia such as severe asthmatics or patients experiencing an exacerbation.

A significant proportion of CD4+ T cells were shown to express IL-13Rα1, however this expression was not restricted to Th17 cells as previously reported (Newcomb *et al.*, 2009). The data imply many T cell populations have the potential to respond to IL-13 which carries implications for numerous Th2 driven pathologies in which IL-13 is up-regulated, including asthma. However, IL-13Rα1 expression must first be demonstrated on human CD4+ T cells. Furthermore, elucidation of the down-stream effects of IL-13Rα1 ligation in various T cell populations would be of value in determining the significance of IL-13Rα1 expression on T cells.

Administration of IL-13 into the airways induced IL-33 production. This has not previously been reported and carries significant implications, not least because IL-33 can stimulate IL-13 production (Kondo *et al.*, 2008). This potentially creates a positive feedback loop in which both cytokines are capable of promoting Th2 associated immunopathology (Lloyd, 2010;Kurowska-Stolarska *et al.*, 2009). Investigation into the existence of this mechanism in man and its relevance in the

amplification and perpetuation of airway inflammation could provide valuable insights for developing future asthma therapies.

The present studies also report, for the first time, the effects of AM depletion on IL-13 and HDM induced AAD. The exacerbated response corroborates AM are potentially immunosuppressive, although confirmation of this capacity in alternative experimental systems is required (Thepen *et al.*, 1994). These findings have raised a multitude of unanswered questions that shall be addressed in future work. However, if AM are capable of immune suppression disclosing and exploiting the mechanisms involved could have vast therapeutic implications, not just for asthma, but potentially all inflammatory lung diseases.

7.3 Future work

7.3.1 Source of IL-13 during AAD

The present series of studies failed to identify sources of IL-13 in the lung tissue during AAD due to difficulties detecting IL-13 by IF. To overcome this *Il13-eGFP* (enhanced green fluorescent protein) transgenic mice could be employed (Neill *et al.*, 2010). Induction of AAD followed by imaging of the lung tissue would allow the localisation and identification of the principal IL-13 producing cells during the development and maintenance of AAD. This information would help to identify processes up-stream of IL-13 that may be significant in the pathogenesis of the disease. In particular, the presence of IL-13 producing innate lymphoid cells in the lungs of mice has recently been described (Chang *et al.*, 2011). These cells have been demonstrated to be potent inducers of AHR however their role in AAD and furthermore their existence in man is yet to be elucidated.

7.3.2 Macrophage population expansion following anti-IL-13 mAb treatment during HDM exposure

Anti-IL-13 mAb treatment significantly increased the number of BAL AM and lung AM and IM in HDM exposed mice compared to HDM exposed mice receiving isotype control. This effect was not seen in sham exposed mice treated with anti-IL-13 mAb. Thus indicating IL-13 may negatively regulate the size of pulmonary macrophage populations during AAD. The mechanisms involved and the implications of expanding these macrophage populations are unknown. However, given that both AM and IM are proposed to regulate pulmonary inflammation, it is

tempting to speculate that expansion of these populations may contribute to the therapeutic effects of anti-IL-13 mAb treatment in the present studies (Bedoret *et al.*, 2009;Thepen *et al.*, 1994). Assessment of the phenotype of AM and IM following IL-13 neutralisation in HDM exposed mice could indicate whether these macrophages are pathogenic or promote resolution of AAD. In addition, the functions of AM and IM isolated from anti-IL-13 mAb treated, HDM exposed mice could be assessed *in vitro* and furthermore *in vivo* by adoptive transfer of these populations into the lungs of mice with AAD to determine whether they are capable of modulating the pathogenesis of AAD. Elucidation of this pathway could provide a novel mechanism of action for anti-IL-13 therapeutics. Of particular interest would be to determine whether IL-13 neutralisation in ongoing clinical trials in asthma patients also leads to expansion of IM and AM populations.

7.3.3 Role of IL-13Rα2 in AAD

Studies in this thesis demonstrated IL-13Rα2 was up-regulated during HDM induced AAD. IL-13Rα2 was detected as a soluble molecule in the lung tissue and serum and in the lungs by IF; however the techniques used failed to establish whether tissue IL-13Rα2 was present as a membrane bound receptor in addition to its soluble form. This is key to determining whether IL-13Rα2 functions solely as a decoy receptor in HDM induced AAD or whether this receptor possesses additional functionality. Specifically, it is not yet known whether IL-13Rα2 can mediate IL-13 clearance in mice as has been reported in man or whether IL-13Rα2 is involved in allergen induced peribronchial collagen deposition, as it is in bleomycin induced lung fibrosis (Kasaian *et al.*, 2011;Fichtner-Feigl *et al.*, 2006). Assessment of IL-13Rα2 by flow cytometry analysis of macrophages and epithelial cells isolated from HDM exposed mice could indicate whether this receptor is membrane associated. Further *in vitro* IL-13Rα2 dependent functional assays and knockdown assays could subsequently determine the signalling capabilities of IL-13Rα2.

Evaluation of the effects of mAbs 582 and 587, that block or permit IL-13Rα2 binding, respectively, could also provide an indication of the function of IL-13Rα2 in AAD. However, it is not known whether IL-13 can stimulate IL-13Rα2 signalling or promote internalisation in the presence of 587 mAb. The capacity of IL-13Rα2 to

signal in the presence of 587 could be determined *in vitro* by assessment of TGFβ up-regulation in macrophages stimulated with IL-13 and TNFα (Fichtner-Feigl *et al.*, 2006). In addition, IL-13-IL-13Rα2 internalisation in the presence of 587 could be analysed using techniques similar to those of Kasaian *et al.* which would require the identification or engineering of a cell line expressing murine IL-13Rα2 (Kasaian *et al.*, 2011). Internalisation could subsequently be determined by depletion of IL-13 in culture media or IF of murine IL-13–FLAG. If these studies demonstrate 587 permits the regular function of membrane associated IL-13Rα2, *in vivo* studies in which 587 exhibited equivalent efficacy to 582 would indicate membrane IL-13Rα2 is unlikely to play a role in the pathogenesis of HDM induced AAD. It is important to establish the role of IL-13Rα2 in the pathogenesis of AAD and subsequently how this translates to man. As has been demonstrated by Kasaian *et al.*, the function of IL-13Rα2 has a significant bearing on the efficacy of anti-IL-13 mAbs and consequently will influence the design and selection of novel IL-13 neutralising entities for the treatment of asthma (Kasaian *et al.*, 2011).

7.3.4 IL-13Rα1 internalisation

A series of experiments assessing the expression of IL-13Rα1 on AM in this project indicated this receptor was internalised following HDM exposure, however this requires confirmation. Furthermore, identification of the stimuli inducing receptor internalisation and the fate of the receptor after internalisation would provide valuable information regarding this pathway and hence IL-13 responsiveness. IL-13Rα1 internalisation has previously been demonstrated *in vitro* in fibroblasts, thus assessment of IL-13Rα1 internalisation in AM *in vitro* would confirm these initial observations (Doucet *et al.*, 1998b). Furthermore, an *in vitro* system would allow analysis of both human and murine AM. This could be achieved by temporal analysis of HDM, IL-13 or IL-4 stimulated macrophages stained by IF and would establish whether internalisation is driven by receptor ligation. These mechanisms could be further verified *in vivo* by analysis of receptor staining in AM from mice administered IL-13 or IL-4 into the airways and from mice treated with anti-IL-13 mAb during exposure to HDM. Furthermore, the localisation of IL-13Rα1 within early, late or recycling endosomes following internalisation would indicate whether the receptor is degraded or recycled; this could be accomplished by counterstaining the cells for

endosome markers such as Rab proteins. In addition, determining whether this mechanism of IL-13Rα1 internalisation occurs in all IL-13Rα1 expressing cells following stimulation may have implications for IL-13 dependent pathology in AAD.

7.3.5 AM mediated immune suppression

The present series of experiments have demonstrated that AM depletion during AAD exacerbates disease, indicating one of the primary functions of AM is to dampen disease. Due to a number of caveats associated with the technique used for AM depletion (discussed in 6.4.7) these findings require confirmation in alternative experimental systems. In an ideal experimental system, specific AM depletion would be achieved avoiding the use of liposomes and the potential for accumulation of apoptotic bodies which may influence the immune response themselves. Furthermore, the absence of AM would be maintained for the duration of the study, without replenishment by tissue macrophages or circulating monocytes. It is difficult to envisage how current approaches to cell depletion, including GM technology, could be employed to fulfil these criteria. Therefore, in the absence of appropriate depletion techniques to study the function of AM, adoptive transfer of AM could be used to investigate their functions. If indeed, AM are capable of suppressing AAD, transfer of AM into the airways of mice with AAD may be able to ameliorate disease. Furthermore, adoptive transfer of AM permits more in-depth investigation into the mechanisms involved. Transfer of AM from sham versus HDM exposed donor mice would indicate whether AM require activation or polarisation into a specific phenotype to dampen AAD. If this is the case; which phenotype of AM confers immunosuppression? Can this phenotype by recapitulated by *in vitro* stimulation with particular mediators or a combination thereof? Moreover could this phenotype be induced, and enhanced, *in vivo* by administration of a specific cocktail of mediators? The mechanisms of AM immunosuppression and dependencies could be explored by transfer of AM from donors deficient in specific mediators such as IL-10 or TGFβ. Further investigation could explore whether this type of immunoregulation is specific to AM, or whether all macrophages have the potential to dampen inflammation by the same mechanisms. Is AM mediated immunoregulation specific to the lung microenvironment or can inflammation in other organs be controlled? Is it specific to Th2 responses or can AM suppress Th1 and Th17 responses?

In summary, many questions remain regarding the putative immunosuppressive activity of AM. Future work should focus on confirming the capacity of AM to suppress AAD and to further understand the underlying mechanisms. Elucidation of the pathways involved could reveal multiple targets for therapeutic intervention and thus provide future therapies for asthma and possibly other diseases characterised by excessive inflammation.

PUBLICATIONS

Tomlinson, KL, Davies, GCG, Catley, MC, Lloyd, CM & Palframan, RT. (2010). The expression of IL-13 and its receptor subunits in HDM sensitised mice. *Immunology,* **131** (S1): 155

Tomlinson, KL, Davies, GCG, Sutton, DJ & Palframan, RT. 2010. Neutralisation of interleukin-13 in mice prevents airway pathology caused by chronic exposure to house dust mite. *PLoS one,* **5** (10).

Tomlinson, KL, Airey, M, Berry, LM, Davies, GCG, Sutton, DJ, O'Dowd, V, Lightwood, D, Palframan, RT, Shaw, S, Foulkes, R & Gozzard, N. (2009). Anti-murine IL-13 monoclonal antibodies recognising distinct functional epitopes inhibit HDM induced airway inflammation, remodelling and hyperreactivity in mice. *Poster presented at Keystone Allergy and Asthma Symposia 2009.*

Berry, LM, Airey, M, Bracher, M, Bourne, T, Carrington, B, Cross, S, Davies, G, Finney, H, Foulkes, R, Gozzard, N, Griffin, R, Hailu, H, Lamour, S, Lawson, A, Lightwood, D, McKnight, AJ, O'Dowd, V, Oxbrow, A, Shaw, S, Stephens, P, Sweeney, B, Tomlinson, KL, Uhe, C & Palframan RT. (2009). *In vitro* and *in vivo* characterisation of anti-murine IL-13 antibodies recognising distinct functional epitopes. *International Immunopharmacology,* **9** (2): 201.

Berry, LM, Bracher, M, Davies, GCG, Airey, M, Tomlinson, KL, Lightwood, D, Carrington, B, O'Dowd, V, Finney, H, McKnight, AJ, Shaw, S, Bourne, T, Gozzard, N, Foulkes, R & Palframan, RT. (2008). *In vitro* and *in vivo* characterisation of anti-murine IL-13 antibodies recognising two distinct functional epitopes. *Fundamental & Clinical pharmacology* **22** (suppl. 2): P100. *Poster presented at the EPHAR congress.*

BIBLIOGRAPHY

Ahdieh, M, Vandenbos, T & Youakim, A. (2001). Lung epithelial barrier function and wound healing are decreased by IL-4 and IL-13 and enhanced by IFN-gamma. *Am J Physiol Cell Physiol*, **281**, C2029-C2038.

Akimoto, T, Numata, F, Tamura, M, Takata, Y, Higashida, N, Takashi, T, Takeda, K & Akira, S. (1998). Abrogation of bronchial eosinophilic inflammation and airway hyperreactivity in signal transducers and activators of transcription (STAT)6-deficient mice. *J Exp Med*, **187**, 1537-1542.

Al-Ramli, W, Prefontaine, D, Chouiali, F, Martin, JG, Olivenstein, R, Lemiere, C & Hamid, Q. (2009). T(H)17-associated cytokines (IL-17A and IL-17F) in severe asthma. *J Allergy Clin Immunol*, **123**, 1185-1187.

Andrews, AL, Holloway, JW, Puddicombe, SM, Holgate, ST & Davies, DE. (2002). Kinetic analysis of the interleukin-13 receptor complex. *J Biol Chem*, **277**, 46073-46078.

Andrews, AL, Nasir, T, Bucchieri, F, Holloway, JW, Holgate, ST & Davies, DE. (2006). IL-13 receptor alpha 2: a regulator of IL-13 and IL-4 signal transduction in primary human fibroblasts. *J Allergy Clin Immunol*, **118**, 858-865.

Antoniu, SA. (2010). Pitrakinra, a dual IL-4/IL-13 antagonist for the potential treatment of asthma and eczema. *Curr Opin Investig Drugs*, **11**, 1286-1294.

Asokananthan, N, Graham, PT, Stewart, DJ, Bakker, AJ, Eidne, KA, Thompson, PJ & Stewart, GA. (2002). House dust mite allergens induce proinflammatory cytokines from respiratory epithelial cells: the cysteine protease allergen, Der p 1, activates protease-activated receptor (PAR)-2 and inactivates PAR-1. *J Immunol*, **169**, 4572-4578.

Atherton, HC, Jones, G & Danahay, H. (2003). IL-13-induced changes in the goblet cell density of human bronchial epithelial cell cultures: MAP kinase and phosphatidylinositol 3-kinase regulation. *Am J Physiol Lung Cell Mol Physiol*, **285**, L730-L739.

Backman, KS, Greenberger, PA & Patterson, R. (1997). Airways obstruction in patients with long-term asthma consistent with 'irreversible asthma'. *Chest*, **112**, 1234-1240.

Balbo, P, Silvestri, M, Rossi, GA, Crimi, E & Burastero, SE. (2001). Differential role of CD80 and CD86 on alveolar macrophages in the presentation of allergen to T lymphocytes in asthma. *Clin Exp Allergy*, **31**, 625-636.

Bang, BR, Chun, E, Shim, EJ, Lee, HS, Lee, SY, Cho, SH, Min, KU, Kim, YY & Park, HW. (2011). Alveolar macrophages modulate allergic inflammation in a murine model of asthma. *Exp Mol Med*, **43**, 275-280.

Barrett, NA, Maekawa, A, Rahman, OM, Austen, KF & Kanaoka, Y. (2009). Dectin-2 recognition of house dust mite triggers cysteinyl leukotriene generation by dendritic cells. *J Immunol*, **182**, 1119-1128.

Batra, V, Musani, AI, Hastie, AT, Khurana, S, Carpenter, KA, Zangrilli, JG & Peters, SP. (2004). Bronchoalveolar lavage fluid concentrations of transforming growth factor (TGF)-beta1, TGF-beta2, interleukin (IL)-4 and IL-13 after segmental allergen challenge and their effects on alpha-smooth muscle actin and collagen III synthesis by primary human lung fibroblasts. *Clin Exp Allergy*, **34**, 437-444.

Bergeron, C, Al-Ramli, W & Hamid, Q. (2009). Remodeling in asthma. *Proc Am Thorac Soc*, **6**, 301-305.

Berry, M, Morgan, A, Shaw, DE, Parker, D, Green, R, Brightling, C, Bradding, P, Wardlaw, AJ & Pavord, ID. (2007). Pathological features and inhaled corticosteroid response of eosinophilic and non-eosinophilic asthma. *Thorax*, **62**, 1043-1049.

Berry, MA, Parker, D, Neale, N, Woodman, L, Morgan, A, Monk, P, Bradding, P, Wardlaw, AJ, Pavord, ID & Brightling, CE. (2004). Sputum and bronchial submucosal IL-13 expression in asthma and eosinophilic bronchitis. *J Allergy Clin Immunol*, **114**, 1106-1109.

Blease, K, Jakubzick, C, Westwick, J, Lukacs, N, Kunkel, SL & Hogaboam, CM. (2001). Therapeutic effect of IL-13 immunoneutralization during chronic experimental fungal asthma. *J Immunol*, **166**, 5219-5224.

Bochner, BS, Klunk, DA, Sterbinsky, SA, Coffman, RL & Schleimer, RP. (1995). IL-13 selectively induces vascular cell adhesion molecule-1 expression in human endothelial cells. *J Immunol*, **154**, 799-803.

Bonecchi, R, Bianchi, G, Bordignon, PP, D'Ambrosio, D, Lang, R, Borsatti, A, Sozzani, S, Allavena, P, Gray, PA, Mantovani, A & Sinigaglia, F. (1998). Differential expression of chemokine receptors and chemotactic responsiveness of type 1 T helper cells (Th1s) and Th2s. *J Exp Med*, **187**, 129-134.

Borowski, A, Kuepper, M, Horn, U, Knupfer, U, Zissel, G, Hohne, K, Luttmann, W, Krause, S, Virchow, JC, Jr. & Friedrich, K. (2008). Interleukin-13 acts as an apoptotic effector on lung epithelial cells and induces pro-fibrotic gene expression in lung fibroblasts. *Clin Exp Allergy*, **38**, 619-628.

Bosse, Y, Thompson, C, Audette, K, Stankova, J & Rola-Pleszczynski, M. (2008). Interleukin-4 and interleukin-13 enhance human bronchial smooth muscle cell proliferation. *Int Arch Allergy Immunol*, **146**, 138-148.

Bousquet, J, Chanez, P, Lacoste, JY, Barneon, G, Ghavanian, N, Enander, I, Venge, P, Ahlstedt, S, Simony-Lafontaine, J & Godard, P. (1990). Eosinophilic inflammation in asthma. *N Engl J Med*, **323**, 1033-1039.

Bree, A, Schlerman, FJ, Wadanoli, M, Tchistiakova, L, Marquette, K, Tan, XY, Jacobson, BA, Widom, A, Cook, TA, Wood, N, Vunnum, S, Krykbaev, R, Xu, X, Donaldson, DD, Goldman, SJ, Sypek, J & Kasaian, MT. (2007). IL-13 blockade

reduces lung inflammation after Ascaris suum challenge in cynomolgus monkeys. *J Allergy Clin Immunol*, **119**, 1251-1257.

Brightling, CE, Saha, S & Hollins, F. (2010). Interleukin-13: prospects for new treatments. *Clin Exp Allergy*, **40**, 42-49.

Brightling, CE, Symon, FA, Birring, SS, Bradding, P, Pavord, ID & Wardlaw, AJ. (2002). TH2 cytokine expression in bronchoalveolar lavage fluid T lymphocytes and bronchial submucosa is a feature of asthma and eosinophilic bronchitis. *J Allergy Clin Immunol*, **110**, 899-905.

Brightling, CE, Symon, FA, Holgate, ST, Wardlaw, AJ, Pavord, ID & Bradding, P. (2003). Interleukin-4 and -13 expression is co-localized to mast cells within the airway smooth muscle in asthma. *Clin Exp Allergy*, **33**, 1711-1716.

Bullens, DM, Truyen, E, Coteur, L, Dilissen, E, Hellings, PW, Dupont, LJ & Ceuppens, JL. (2006). IL-17 mRNA in sputum of asthmatic patients: linking T cell driven inflammation and granulocytic influx? *Respir Res*, **7**, 135.

Chang, YJ, Kim, HY, Albacker, LA, Baumgarth, N, McKenzie, AN, Smith, DE, DeKruyff, RH & Umetsu, DT. (2011). Innate lymphoid cells mediate influenza-induced airway hyper-reactivity independently of adaptive immunity. *Nat Immunol*, **12**, 631-638.

Chen, W, Sivaprasad, U, Tabata, Y, Gibson, AM, Stier, MT, Finkelman, FD & Hershey, GK. (2009). IL-13R alpha 2 membrane and soluble isoforms differ in humans and mice. *J Immunol*, **183**, 7870-7876.

Chiba, Y, Onoda, S, Todoroki, M, Nishida, Y & Misawa, M. (2010). Upregulation of interleukin-13 receptor chains in bronchial smooth muscle tissues of mouse experimental asthma. *J Smooth Muscle Res*, **46**, 49-55.

Chibana, K, Ishii, Y, Asakura, T & Fukuda, T. (2003). Up-regulation of cysteinyl leukotriene 1 receptor by IL-13 enables human lung fibroblasts to respond to leukotriene C4 and produce eotaxin. *J Immunol*, **170**, 4290-4295.

Chibana, K, Trudeau, JB, Mustovich, AT, Hu, H, Zhao, J, Balzar, S, Chu, HW & Wenzel, SE. (2008). IL-13 induced increases in nitrite levels are primarily driven by increases in inducible nitric oxide synthase as compared with effects on arginases in human primary bronchial epithelial cells. *Clin Exp Allergy*, **38**, 936-946.

Colavita, AM, Hastie, AT, Musani, AI, Pascual, RM, Reinach, AJ, Lustine, HT, Galati, SA, Zangrilli, JG, Fish, JE & Peters, SP. (2000). Kinetics of IL-10 production after segmental antigen challenge of atopic asthmatic subjects. *J Allergy Clin Immunol*, **106**, 880-886.

Corren, J, Lemanske, RF, Hanania, NA, Korenblat, PE, Parsey, MV, Arron, JR, Harris, JM, Scheerens, H, Wu, LC, Su, Z, Mosesova, S, Eisner, MD, Bohen, SP & Matthews, JG. (2011). Lebrikizumab Treatment in Adults with Asthma. *N Engl J Med*, (in press).

Cuff, CA, Rundell, L, Williamson, J, McCarthy, R, Perham, M, Erickson, J, Zhong, S, Miller, R, Guerin, M, Huelsman, R, Bose, S, Grinnell, C, Goedken, E, Cherniack, A, Schwartz, A, Tarcsa, E, Barlow, E & Wu, C. (2008). Neutralizing anti-IL-13 antibodies that block binding of IL-13 to both IL-13 Ralpha1 and Ralpha2 provide greater efficacy compared to an antibody that blocks binding to Ralpha1 alone. *ATS conference*, **A91**.

Daines, MO, Chen, W, Tabata, Y, Walker, BA, Gibson, AM, Masino, JA, Warrier, MR, Daines, CL, Wenzel, SE & Hershey, GK. (2007). Allergen-dependent solubilization of IL-13 receptor alpha2 reveals a novel mechanism to regulate allergy. *J Allergy Clin Immunol*, **119**, 375-383.

Daines, MO & Hershey, GK. (2002). A novel mechanism by which interferon-gamma can regulate interleukin (IL)-13 responses. Evidence for intracellular stores of IL-13 receptor alpha -2 and their rapid mobilization by interferon-gamma. *J Biol Chem*, **277**, 10387-10393.

Daines, MO, Tabata, Y, Walker, BA, Chen, W, Warrier, MR, Basu, S & Hershey, GK. (2006). Level of expression of IL-13R alpha 2 impacts receptor distribution and IL-13 signaling. *J Immunol*, **176**, 7495-7501.

de Haan A., Groen, G, Prop, J, van, RN & Wilschut, J. (1996). Mucosal immunoadjuvant activity of liposomes: role of alveolar macrophages. *Immunology*, **89**, 488-493.

de Saint-Vis, B, Fugier-Vivier, I, Massacrier, C, Gaillard, C, Vanbervliet, B, Ait-Yahia, S, Banchereau, J, Liu, YJ, Lebecque, S & Caux, C. (1998). The cytokine profile expressed by human dendritic cells is dependent on cell subtype and mode of activation. *J Immunol*, **160**, 1666-1676.

de Vries, JE. (1998). The role of IL-13 and its receptor in allergy and inflammatory responses. *J Allergy Clin Immunol*, **102**, 165-169.

de Waal, MR, Abrams, JS, Zurawski, SM, Lecron, JC, Mohan-Peterson, S, Sanjanwala, B, Bennett, B, Silver, J, de Vries, JE & Yssel, H. (1995). Differential regulation of IL-13 and IL-4 production by human CD8+ and CD4+ Th0, Th1 and Th2 T cell clones and EBV-transformed B cells. *Int Immunol*, **7**, 1405-1416.

de Waal, MR, Figdor, CG, Huijbens, R, Mohan-Peterson, S, Bennett, B, Culpepper, J, Dang, W, Zurawski, G & de Vries, JE. (1993). Effects of IL-13 on phenotype, cytokine production, and cytotoxic function of human monocytes. Comparison with IL-4 and modulation by IFN-gamma or IL-10. *J Immunol*, **151**, 6370-6381.

Deb, R, Shakib, F, Reid, K & Clark, H. (2007). Major house dust mite allergens Dermatophagoides pteronyssinus 1 and Dermatophagoides farinae 1 degrade and inactivate lung surfactant proteins A and D. *J Biol Chem*, **282**, 36808-36819.

Deshpande, DA, Dogan, S, Walseth, TF, Miller, SM, Amrani, Y, Panettieri, RA & Kannan, MS. (2004). Modulation of calcium signaling by interleukin-13 in human airway smooth muscle: role of CD38/cyclic adenosine diphosphate ribose pathway. *Am J Respir Cell Mol Biol*, **31**, 36-42.

Deslee, G, Charbonnier, AS, Hammad, H, Angyalosi, G, Tillie-Leblond, I, Mantovani, A, Tonnel, AB & Pestel, J. (2002). Involvement of the mannose receptor in the uptake of Der p 1, a major mite allergen, by human dendritic cells. *J Allergy Clin Immunol*, **110**, 763-770.

Doherty, TM, Kastelein, R, Menon, S, Andrade, S & Coffman, RL. (1993). Modulation of murine macrophage function by IL-13. *J Immunol*, **151**, 7151-7160.

Doucet, C, Brouty-Boye, D, Pottin-Clemenceau, C, Canonica, GW, Jasmin, C & Azzarone, B. (1998a). Interleukin (IL) 4 and IL-13 act on human lung fibroblasts. Implication in asthma. *J Clin Invest*, **101**, 2129-2139.

Doucet, C, Brouty-Boye, D, Pottin-Clemenceau, C, Jasmin, C, Canonica, GW & Azzarone, B. (1998b). IL-4 and IL-13 specifically increase adhesion molecule and inflammatory cytokine expression in human lung fibroblasts. *Int Immunol*, **10**, 1421-1433.

Eberl, G. (2010). Immunology: Close encounters of the second type. *Nature*, **464**, 1285-1286.

Emson, CL, Bell, SE, Jones, A, Wisden, W & McKenzie, AN. (1998). Interleukin (IL)-4-independent induction of immunoglobulin (Ig)E, and perturbation of T cell development in transgenic mice expressing IL-13. *J Exp Med*, **188**, 399-404.

Eum, SY, Maghni, K, Tolloczko, B, Eidelman, DH & Martin, JG. (2005). IL-13 may mediate allergen-induced hyperresponsiveness independently of IL-5 or eotaxin by effects on airway smooth muscle. *Am J Physiol Lung Cell Mol Physiol*, **288**, L576-L584.

Fahy, JV. (2009). Eosinophilic and neutrophilic inflammation in asthma: insights from clinical studies. *Proc Am Thorac Soc*, **6**, 256-259.

Farghaly, HS, Blagbrough, IS, Medina-Tato, DA & Watson, ML. (2008). Interleukin 13 increases contractility of murine tracheal smooth muscle by a phosphoinositide 3-kinase p110delta-dependent mechanism. *Mol Pharmacol*, **73**, 1530-1537.

Fattouh, R & Jordana, M. (2008). TGF-beta, eosinophils and IL-13 in allergic airway remodeling: a critical appraisal with therapeutic considerations. *Inflamm Allergy Drug Targets*, **7**, 224-236.

Fichtner-Feigl, S, Strober, W, Kawakami, K, Puri, RK & Kitani, A. (2006). IL-13 signaling through the IL-13alpha2 receptor is involved in induction of TGF-beta1 production and fibrosis. *Nat Med*, **12**, 99-106.

Fritz, DK, Kerr, C, Botelho, F, Stampfli, M & Richards, CD. (2009). Oncostatin M (OSM) primes IL-13- and IL-4-induced eotaxin responses in fibroblasts: regulation of the type-II IL-4 receptor chains IL-4Ralpha and IL-13Ralpha1. *Exp Cell Res*, **315**, 3486-3499.

Fu, CL, Ye, YL, Lee, YL & Chiang, BL. (2006). Effects of overexpression of IL-10, IL-12, TGF-beta and IL-4 on allergen induced change in bronchial responsiveness. *Respir Res*, **7**, 72.

Furmonaviciene, R, Ghaemmaghami, AM, Boyd, SE, Jones, NS, Bailey, K, Willis, AC, Sewell, HF, Mitchell, DA & Shakib, F. (2007). The protease allergen Der p 1 cleaves cell surface DC-SIGN and DC-SIGNR: experimental analysis of in silico substrate identification and implications in allergic responses. *Clin Exp Allergy*, **37**, 231-242.

Gauchat, JF, Schlagenhauf, E, Feng, NP, Moser, R, Yamage, M, Jeannin, P, Alouani, S, Elson, G, Notarangelo, LD, Wells, T, Eugster, HP & Bonnefoy, JY. (1997). A novel 4-kb interleukin-13 receptor alpha mRNA expressed in human B, T, and endothelial cells encoding an alternate type-II interleukin-4/interleukin-13 receptor. *Eur J Immunol*, **27**, 971-978.

Gauvreau, GM, Boulet, LP, Cockcroft, DW, Fitzgerald, JM, Carlsten, C, Davis, BE, Deschesnes, F, Duong, M, Durn, BL, Howie, KJ, Hui, L, Kasaian, MT, Killian, KJ, Strinich, TX, Watson, RM, Y N, Zhou, S, Raible, D & O'Byrne, PM. (2011). The Effects of IL-13 Blockade on Allergen-Induced Airway Responses in Mild Atopic Asthma. *Am J Respir Crit Care Med*, **183**, 1007-1014.

Gauvreau, GM, Boulet, LP, Fitzgerald, JM, Durn, B, Zhou, S, Burt, D, Watson, RM, Duong, M, Killian, KJ, Carlsten, C, Ronco, J, Hui, L, Y, N, Deschesnes, F, Prince, P, Raible, D & O'Byrne, P. (2008). The Effects of IMA-638 on Allergen Induced Airway Responses in Subjects with Mild Atopic Asthma.In *ERS Annual Congress 2008*. p. 827s.

Gavett, SH, O'Hearn, DJ, Li, X, Huang, SK, Finkelman, FD & Wills-Karp, M. (1995). Interleukin 12 inhibits antigen-induced airway hyperresponsiveness, inflammation, and Th2 cytokine expression in mice. *J Exp Med*, **182**, 1527-1536.

Ghaemmaghami, AM, Gough, L, Sewell, HF & Shakib, F. (2002). The proteolytic activity of the major dust mite allergen Der p 1 conditions dendritic cells to produce less interleukin-12: allergen-induced Th2 bias determined at the dendritic cell level. *Clin Exp Allergy*, **32**, 1468-1475.

Gibbs, BF, Haas, H, Falcone, FH, Albrecht, C, Vollrath, IB, Noll, T, Wolff, HH & Amon, U. (1996). Purified human peripheral blood basophils release interleukin-13 and preformed interleukin-4 following immunological activation. *Eur J Immunol*, **26**, 2493-2498.

GINA. (2006). Global Strategy for Asthma Management and Prevention. http://www.ginasthma.org/guidelines-archived-2006-revision.html.

Gonzalez-Juarrero, M, Shim, TS, Kipnis, A, Junqueira-Kipnis, AP & Orme, IM. (2003). Dynamics of macrophage cell populations during murine pulmonary tuberculosis. *J Immunol*, **171**, 3128-3135.

Gordon, S. (2003). Alternative activation of macrophages. *Nat Rev Immunol*, **3**, 23-35.

Gordon, S & Martinez, FO. (2010). Alternative activation of macrophages: mechanism and functions. *Immunity*, **32**, 593-604.

Gosset, P, Tsicopoulos, A, Wallaert, B, Vannimenus, C, Joseph, M, Tonnel, AB & Capron, A. (1991). Increased secretion of tumor necrosis factor alpha and interleukin-6 by alveolar macrophages consecutive to the development of the late asthmatic reaction. *J Allergy Clin Immunol*, **88**, 561-571.

Gough, L, Campbell, E, Bayley, D, Van, HG & Shakib, F. (2003). Proteolytic activity of the house dust mite allergen Der p 1 enhances allergenicity in a mouse inhalation model. *Clin Exp Allergy*, **33**, 1159-1163.

Graber, P, Gretener, D, Herren, S, Aubry, JP, Elson, G, Poudrier, J, Lecoanet-Henchoz, S, Alouani, S, Losberger, C, Bonnefoy, JY, Kosco-Vilbois, MH & Gauchat, JF. (1998). The distribution of IL-13 receptor alpha1 expression on B cells, T cells and monocytes and its regulation by IL-13 and IL-4. *Eur J Immunol*, **28**, 4286-4298.

Grainge, CL, Lau, LC, Ward, JA, Dulay, V, Lahiff, G, Wilson, S, Holgate, S, Davies, DE & Howarth, PH. (2011). Effect of bronchoconstriction on airway remodeling in asthma. *N Engl J Med*, **364**, 2006-2015.

Gregory, LG, Causton, B, Murdoch, JR, Mathie, SA, O'Donnell, V, Thomas, CP, Priest, FM, Quint, DJ & Lloyd, CM. (2009). Inhaled house dust mite induces pulmonary T helper 2 cytokine production. *Clin Exp Allergy*, **39**, 1597-1610.

Grunig, G, Warnock, M, Wakil, AE, Venkayya, R, Brombacher, F, Rennick, DM, Sheppard, D, Mohrs, M, Donaldson, DD, Locksley, RM & Corry, DB. (1998). Requirement for IL-13 independently of IL-4 in experimental asthma. *Science*, **282**, 2261-2263.

Grunstein, MM, Hakonarson, H, Leiter, J, Chen, M, Whelan, R, Grunstein, JS & Chuang, S. (2002). IL-13-dependent autocrine signaling mediates altered responsiveness of IgE-sensitized airway smooth muscle. *Am J Physiol Lung Cell Mol Physiol*, **282**, L520-L528.

Haldar, P, Pavord, ID, Shaw, DE, Berry, MA, Thomas, M, Brightling, CE, Wardlaw, AJ & Green, RH. (2008). Cluster analysis and clinical asthma phenotypes. *Am J Respir Crit Care Med*, **178**, 218-224.

Hamelmann, E, Schwarze, J, Takeda, K, Oshiba, A, Larsen, GL, Irvin, CG & Gelfand, EW. (1997). Noninvasive measurement of airway responsiveness in allergic mice using barometric plethysmography. *Am J Respir Crit Care Med*, **156**, 766-775.

Hammad, H, Chieppa, M, Perros, F, Willart, MA, Germain, RN & Lambrecht, BN. (2009). House dust mite allergen induces asthma via Toll-like receptor 4 triggering of airway structural cells. *Nat Med*, **15**, 410-416.

Hammad, H & Lambrecht, BN. (2008). Dendritic cells and epithelial cells: linking innate and adaptive immunity in asthma. *Nat Rev Immunol*, **8**, 193-204.

Hammad, H, Plantinga, M, Deswarte, K, Pouliot, P, Willart, MA, Kool, M, Muskens, F & Lambrecht, BN. (2010). Inflammatory dendritic cells--not basophils--are necessary and sufficient for induction of Th2 immunity to inhaled house dust mite allergen. *J Exp Med*, **207**, 2097-2111.

Heinzmann, A, Mao, XQ, Akaiwa, M, Kreomer, RT, Gao, PS, Ohshima, K, Umeshita, R, Abe, Y, Braun, S, Yamashita, T, Roberts, MH, Sugimoto, R, Arima, K, Arinobu, Y, Yu, B, Kruse, S, Enomoto, T, Dake, Y, Kawai, M, Shimazu, S, Sasaki, S, Adra, CN, Kitaichi, M, Inoue, H, Yamauchi, K, Tomichi, N, Kurimoto, F, Hamasaki, N, Hopkin, JM, Izuhara, K, Shirakawa, T & Deichmann, KA. (2000). Genetic variants of IL-13 signalling and human asthma and atopy. *Hum Mol Genet*, **9**, 549-559.

Heller, NM, Qi, X, Junttila, IS, Shirey, KA, Vogel, SN, Paul, WE & Keegan, AD. (2008). Type I IL-4Rs selectively activate IRS-2 to induce target gene expression in macrophages. *Sci Signal*, **1**, ra17.

Hirst, SJ, Hallsworth, MP, Peng, Q & Lee, TH. (2002). Selective induction of eotaxin release by interleukin-13 or interleukin-4 in human airway smooth muscle cells is synergistic with interleukin-1beta and is mediated by the interleukin-4 receptor alpha-chain. *Am J Respir Crit Care Med*, **165**, 1161-1171.

Holgate, ST, Davies, DE, Lackie, PM, Wilson, SJ, Puddicombe, SM & Lordan, JL. (2000). Epithelial-mesenchymal interactions in the pathogenesis of asthma. *J Allergy Clin Immunol*, **105**, 193-204.

Holtzman, MJ, Byers, DE, Benoit, LA, Battaile, JT, You, Y, Agapov, E, Park, C, Grayson, MH, Kim, EY & Patel, AC. (2009). Immune pathways for translating viral infection into chronic airway disease. *Adv Immunol*, **102**, 245-276.

Horie, S, Okubo, Y, Hossain, M, Sato, E, Nomura, H, Koyama, S, Suzuki, J, Isobe, M & Sekiguchi, M. (1997). Interleukin-13 but not interleukin-4 prolongs eosinophil survival and induces eosinophil chemotaxis. *Intern Med*, **36**, 179-185.

Huang, SK, Xiao, HQ, Kleine-Tebbe, J, Paciotti, G, Marsh, DG, Lichtenstein, LM & Liu, MC. (1995). IL-13 expression at the sites of allergen challenge in patients with asthma. *J Immunol*, **155**, 2688-2694.

Humbert, M, Durham, SR, Kimmitt, P, Powell, N, Assoufi, B, Pfister, R, Menz, G, Kay, AB & Corrigan, CJ. (1997). Elevated expression of messenger ribonucleic acid encoding IL-13 in the bronchial mucosa of atopic and nonatopic subjects with asthma. *J Allergy Clin Immunol*, **99**, 657-665.

Imai, T, Nagira, M, Takagi, S, Kakizaki, M, Nishimura, M, Wang, J, Gray, PW, Matsushima, K & Yoshie, O. (1999). Selective recruitment of CCR4-bearing Th2 cells toward antigen-presenting cells by the CC chemokines thymus and activation-regulated chemokine and macrophage-derived chemokine. *Int Immunol*, **11**, 81-88.

Ingram, JL, Antao-Menezes, A, Mangum, JB, Lyght, O, Lee, PJ, Elias, JA & Bonner, JC. (2006). Opposing actions of Stat1 and Stat6 on IL-13-induced up-regulation of early growth response-1 and platelet-derived growth factor ligands in pulmonary fibroblasts. *J Immunol*, **177**, 4141-4148.

Ingram, JL, Rice, A, Geisenhoffer, K, Madtes, DK & Bonner, JC. (2003). Interleukin-13 stimulates the proliferation of lung myofibroblasts via a signal transducer and activator of transcription-6-dependent mechanism: a possible mechanism for the development of airway fibrosis in asthma. *Chest*, **123**, 422S-424S.

Ingram, JL, Rice, AB, Geisenhoffer, K, Madtes, DK & Bonner, JC. (2004). IL-13 and IL-1beta promote lung fibroblast growth through coordinated up-regulation of PDGF-AA and PDGF-Ralpha. *FASEB J*, **18**, 1132-1134.

Ingram, JL, Slade, DJ, Church, TD, Beaver, DM & Kraft, M. (2009). Dexamethasone and IL-13 Modulate IL-13R{alpha}2 and IL-13R{alpha}1 Expression in Airway Fibroblasts in Asthma. *Proc Am Thorac Soc*, **6**, 333-334.

Jacobsen, EA, Taranova, AG, Lee, NA & Lee, JJ. (2007). Eosinophils: singularly destructive effector cells or purveyors of immunoregulation? *J Allergy Clin Immunol*, **119**, 1313-1320.

Jakubzick, C, Tacke, F, Llodra, J, van, RN & Randolph, GJ. (2006). Modulation of dendritic cell trafficking to and from the airways. *J Immunol*, **176**, 3578-3584.

James, AL, Palmer, LJ, Kicic, E, Maxwell, PS, Lagan, SE, Ryan, GF & Musk, AW. (2005). Decline in lung function in the Busselton Health Study: the effects of asthma and cigarette smoking. *Am J Respir Crit Care Med*, **171**, 109-114.

James, AL & Wenzel, S. (2007). Clinical relevance of airway remodelling in airway diseases. *Eur Respir J*, **30**, 134-155.

Jenkins, SJ, Ruckerl, D, Cook, PC, Jones, LH, Finkelman, FD, van, RN, MacDonald, AS & Allen, JE. (2011). Local macrophage proliferation, rather than recruitment from the blood, is a signature of TH2 inflammation. *Science*, **332**, 1284-1288.

Jia, HP, Kline, JN, Penisten, A, Apicella, MA, Gioannini, TL, Weiss, J & McCray, PB, Jr. (2004). Endotoxin responsiveness of human airway epithelia is limited by low expression of MD-2. *Am J Physiol Lung Cell Mol Physiol*, **287**, L428-L437.

John, RJ, Rusznak, C, Ramjee, M, Lamont, AG, Abrahamson, M & Hewitt, EL. (2000). Functional effects of the inhibition of the cysteine protease activity of the major house dust mite allergen Der p 1 by a novel peptide-based inhibitor. *Clin Exp Allergy*, **30**, 784-793.

Johnson, JR, Wiley, RE, Fattouh, R, Swirski, FK, Gajewska, BU, Coyle, AJ, Gutierrez-Ramos, JC, Ellis, R, Inman, MD & Jordana, M. (2004). Continuous exposure to house dust mite elicits chronic airway inflammation and structural remodeling. *Am J Respir Crit Care Med*, **169**, 378-385.

Jung, T, Wijdenes, J, Neumann, C, de Vries, JE & Yssel, H. (1996). Interleukin-13 is produced by activated human CD45RA+ and CD45RO+ T cells: modulation by interleukin-4 and interleukin-12. *Eur J Immunol*, **26**, 571-577.

Junttila, IS, Mizukami, K, Dickensheets, H, Meier-Schellersheim, M, Yamane, H, Donnelly, RP & Paul, WE. (2008). Tuning sensitivity to IL-4 and IL-13: differential expression of IL-4Ralpha, IL-13Ralpha1, and gammac regulates relative cytokine sensitivity. *J Exp Med*, **205**, 2595-2608.

Kariyawasam, HH & Robinson, DS. (2006). The eosinophil: the cell and its weapons, the cytokines, its locations. *Semin Respir Crit Care Med*, **27**, 117-127.

Kariyawasam, HH & Robinson, DS. (2007). The role of eosinophils in airway tissue remodelling in asthma. *Curr Opin Immunol*, **19**, 681-686.

Kasaian, MT & Miller, DK. (2008). IL-13 as a therapeutic target for respiratory disease. *Biochem Pharmacol*, **76**, 147-155.

Kasaian, MT, Raible, D, Marquette, K, Cook, TA, Zhou, S, Tan, XY & Tchistiakova, L. (2011). IL-13 Antibodies Influence IL-13 Clearance in Humans by Modulating Scavenger Activity of IL-13R{alpha}2. *J Immunol*, **187**, 561-569.

Kasaian, MT, Tan, XY, Jin, M, Fitz, L, Marquette, K, Wood, N, Cook, TA, Lee, J, Widom, A, Agostinelli, R, Bree, A, Schlerman, FJ, Olland, S, Wadanoli, M, Sypek, J, Gill, D, Goldman, SJ & Tchistiakova, L. (2008). Interleukin-13 neutralization by two distinct receptor blocking mechanisms reduces immunoglobulin E responses and lung inflammation in cynomolgus monkeys. *J Pharmacol Exp Ther*, **325**, 882-892.

Kaufman, J, Sime, PJ & Phipps, RP. (2004). Expression of CD154 (CD40 ligand) by human lung fibroblasts: differential regulation by IFN-gamma and IL-13, and implications for fibrosis. *J Immunol*, **172**, 1862-1871.

Kaur, D, Hollins, F, Woodman, L, Yang, W, Monk, P, May, R, Bradding, P & Brightling, CE. (2006). Mast cells express IL-13R alpha 1: IL-13 promotes human lung mast cell proliferation and Fc epsilon RI expression. *Allergy*, **61**, 1047-1053.

Kawakami, K, Taguchi, J, Murata, T & Puri, RK. (2001). The interleukin-13 receptor alpha2 chain: an essential component for binding and internalization but not for interleukin-13-induced signal transduction through the STAT6 pathway. *Blood*, **97**, 2673-2679.

Kay, AB. (2006). The role of T lymphocytes in asthma. *Chem Immunol Allergy*, **91**, 59-75.

Kibe, A, Inoue, H, Fukuyama, S, Machida, K, Matsumoto, K, Koto, H, Ikegami, T, Aizawa, H & Hara, N. (2003). Differential regulation by glucocorticoid of interleukin-13-induced eosinophilia, hyperresponsiveness, and goblet cell hyperplasia in mouse airways. *Am J Respir Crit Care Med*, **167**, 50-56.

Kim, EY, Battaile, JT, Patel, AC, You, Y, Agapov, E, Grayson, MH, Benoit, LA, Byers, DE, Alevy, Y, Tucker, J, Swanson, S, Tidwell, R, Tyner, JW, Morton, JD, Castro, M, Polineni, D, Patterson, GA, Schwendener, RA, Allard, JD, Peltz, G & Holtzman, MJ. (2008). Persistent activation of an innate immune response translates respiratory viral infection into chronic lung disease. *Nat Med*, **14**, 633-640.

Kim, YS, Choi, SJ, Choi, JP, Jeon, SG, Oh, SY, Lee, BJ, Gho, YS, Lee, CG, Zhu, Z, Elias, JA & Kim, YK. (2010). IL-12-STAT4-IFN-gamma axis is a key downstream pathway in the development of IL-13-mediated asthma phenotypes in a Th2 type asthma model. *Exp Mol Med*, **42**, 533-546.

Kodama, T, Matsuyama, T, Miyata, S, Nishimura, H, Nishioka, Y, Kitada, O & Sugita, M. (1998). Kinetics of apoptosis in the lung of mice with allergic airway inflammation. *Clin Exp Allergy*, **28**, 1435-1443.

Kondo, Y, Yoshimoto, T, Yasuda, K, Futatsugi-Yumikura, S, Morimoto, M, Hayashi, N, Hoshino, T, Fujimoto, J & Nakanishi, K. (2008). Administration of IL-33 induces airway hyperresponsiveness and goblet cell hyperplasia in the lungs in the absence of adaptive immune system. *Int Immunol*, **20**, 791-800.

Konstantinidis, AK, Puddicombe, SM, Mochizuki, A, Sheth, PD, Yang, IA, Yoshisue, H, Wilson, SJ, Davies, DE, Holgate, ST & Holloway, JW. (2008). Cellular localization of interleukin 13 receptor alpha2 in human primary bronchial epithelial cells and fibroblasts. *J Investig Allergol Clin Immunol*, **18**, 174-180.

Kotsimbos, TC, Ghaffar, O, Minshall, EM, Humbert, M, Durham, SR, Pfister, R, Menz, G, Kay, AB & Hamid, QA. (1998). Expression of the IL-4 receptor alpha-subunit is increased in bronchial biopsy specimens from atopic and nonatopic asthmatic subjects. *J Allergy Clin Immunol*, **102**, 859-866.

Kroegel, C, Julius, P, Matthys, H, Virchow, JC, Jr. & Luttmann, W. (1996). Endobronchial secretion of interleukin-13 following local allergen challenge in atopic asthma: relationship to interleukin-4 and eosinophil counts. *Eur Respir J*, **9**, 899-904.

Krug, N, Madden, J, Redington, AE, Lackie, P, Djukanovic, R, Schauer, U, Holgate, ST, Frew, AJ & Howarth, PH. (1996). T-cell cytokine profile evaluated at the single cell level in BAL and blood in allergic asthma. *Am J Respir Cell Mol Biol*, **14**, 319-326.

Kumar, RK, Herbert, C, Webb, DC, Li, L & Foster, PS. (2004). Effects of anticytokine therapy in a mouse model of chronic asthma. *Am J Respir Crit Care Med*, **170**, 1043-1048.

Kuperman, D, Schofield, B, Wills-Karp, M & Grusby, MJ. (1998). Signal transducer and activator of transcription factor 6 (Stat6)-deficient mice are protected from antigen-induced airway hyperresponsiveness and mucus production. *J Exp Med*, **187**, 939-948.

Kuperman, DA, Huang, X, Koth, LL, Chang, GH, Dolganov, GM, Zhu, Z, Elias, JA, Sheppard, D & Erle, DJ. (2002). Direct effects of interleukin-13 on epithelial cells cause airway hyperreactivity and mucus overproduction in asthma. *Nat Med*, **8**, 885-889.

Kuribayashi, K, Kodama, T, Okamura, H, Sugita, M & Matsuyama, T. (2002). Effects of post-inhalation treatment with interleukin-12 on airway hyper-reactivity, eosinophilia and interleukin-18 receptor expression in a mouse model of asthma. *Clin Exp Allergy*, **32**, 641-649.

Kurowska-Stolarska, M, Stolarski, B, Kewin, P, Murphy, G, Corrigan, CJ, Ying, S, Pitman, N, Mirchandani, A, Rana, B, van, RN, Shepherd, M, McSharry, C, McInnes, IB, Xu, D & Liew, FY. (2009). IL-33 amplifies the polarization of alternatively activated macrophages that contribute to airway inflammation. *J Immunol*, **183**, 6469-6477.

Lambrecht, BN & Hammad, H. (2009). Biology of lung dendritic cells at the origin of asthma. *Immunity*, **31**, 412-424.

Landsman, L & Jung, S. (2007). Lung macrophages serve as obligatory intermediate between blood monocytes and alveolar macrophages. *J Immunol*, **179**, 3488-3494.

Laoukili, J, Perret, E, Willems, T, Minty, A, Parthoens, E, Houcine, O, Coste, A, Jorissen, M, Marano, F, Caput, D & Tournier, F. (2001). IL-13 alters mucociliary differentiation and ciliary beating of human respiratory epithelial cells. *J Clin Invest*, **108**, 1817-1824.

Laporte, JC, Moore, PE, Baraldo, S, Jouvin, MH, Church, TL, Schwartzman, IN, Panettieri, RA, Jr., Kinet, JP & Shore, SA. (2001). Direct effects of interleukin-13 on signaling pathways for physiological responses in cultured human airway smooth muscle cells. *Am J Respir Crit Care Med*, **164**, 141-148.

LaPorte, SL, Juo, ZS, Vaclavikova, J, Colf, LA, Qi, X, Heller, NM, Keegan, AD & Garcia, KC. (2008). Molecular and structural basis of cytokine receptor pleiotropy in the interleukin-4/13 system. *Cell*, **132**, 259-272.

Lee, CG, Da Silva, CA, Lee, JY, Hartl, D & Elias, JA. (2008). Chitin regulation of immune responses: an old molecule with new roles. *Curr Opin Immunol*, **20**, 684-689.

Lee, YL, Ye, YL, Yu, CI, Wu, YL, Lai, YL, Ku, PH, Hong, RL & Chiang, BL. (2001). Construction of single-chain interleukin-12 DNA plasmid to treat airway hyperresponsiveness in an animal model of asthma. *Hum Gene Ther*, **12**, 2065-2079.

Leigh, R, Ellis, R, Wattie, J, Donaldson, DD & Inman, MD. (2004a). Is interleukin-13 critical in maintaining airway hyperresponsiveness in allergen-challenged mice? *Am J Respir Crit Care Med*, **170**, 851-856.

Leigh, R, Ellis, R, Wattie, JN, Hirota, JA, Matthaei, KI, Foster, PS, O'Byrne, PM & Inman, MD. (2004b). Type 2 cytokines in the pathogenesis of sustained airway dysfunction and airway remodeling in mice. *Am J Respir Crit Care Med*, **169**, 860-867.

Lensmar, C, Katchar, K, Eklund, A, Grunewald, J & Wahlstrom, J. (2006). Phenotypic analysis of alveolar macrophages and lymphocytes following allergen inhalation by atopic subjects with mild asthma. *Respir Med*, **100**, 918-925.

Lewis, CC, Aronow, B, Hutton, J, Santeliz, J, Dienger, K, Herman, N, Finkelman, FD & Wills-Karp, M. (2009). Unique and overlapping gene expression patterns driven by IL-4 and IL-13 in the mouse lung. *J Allergy Clin Immunol*, **123**, 795-804.

Little, SA, Sproule, MW, Cowan, MD, Macleod, KJ, Robertson, M, Love, JG, Chalmers, GW, McSharry, CP & Thomson, NC. (2002). High resolution computed tomographic assessment of airway wall thickness in chronic asthma: reproducibility and relationship with lung function and severity. *Thorax*, **57**, 247-253.

Livak, KJ & Schmittgen, TD. (2001). Analysis of relative gene expression data using real-time quantitative PCR and the 2(-Delta Delta C(T)) Method. *Methods*, **25**, 402-408.

Lloyd, CM. (2009). Dust mites' dirty dealings in the lung. *Nat Med*, **15**, 366-367.

Lloyd, CM. (2010). IL-33 family members and asthma - bridging innate and adaptive immune responses. *Curr Opin Immunol*, **22**, 800-806.

Lloyd, CM & Hawrylowicz, CM. (2009). Regulatory T cells in asthma. *Immunity*, **31**, 438-449.

Lloyd, CM & Hessel, EM. (2010). Functions of T cells in asthma: more than just T(H)2 cells. *Nat Rev Immunol*, **10**, 838-848.

Lohning, M, Stroehmann, A, Coyle, AJ, Grogan, JL, Lin, S, Gutierrez-Ramos, JC, Levinson, D, Radbruch, A & Kamradt, T. (1998). T1/ST2 is preferentially expressed on murine Th2 cells, independent of interleukin 4, interleukin 5, and interleukin 10, and important for Th2 effector function. *Proc Natl Acad Sci U S A*, **95**, 6930-6935.

Lordan, JL, Bucchieri, F, Richter, A, Konstantinidis, A, Holloway, JW, Thornber, M, Puddicombe, SM, Buchanan, D, Wilson, SJ, Djukanovic, R, Holgate, ST & Davies, DE. (2002). Cooperative effects of Th2 cytokines and allergen on normal and asthmatic bronchial epithelial cells. *J Immunol*, **169**, 407-414.

Luttmann, W, Knoechel, B, Foerster, M, Matthys, H, Virchow, JC, Jr. & Kroegel, C. (1996). Activation of human eosinophils by IL-13. Induction of CD69 surface antigen, its relationship to messenger RNA expression, and promotion of cellular viability. *J Immunol*, **157**, 1678-1683.

MacDonald, KP, Palmer, JS, Cronau, S, Seppanen, E, Olver, S, Raffelt, NC, Kuns, R, Pettit, AR, Clouston, A, Wainwright, B, Branstetter, D, Smith, J, Paxton, RJ, Cerretti, DP, Bonham, L, Hill, GR & Hume, DA. (2010). An antibody against the colony-stimulating factor 1 receptor depletes the resident subset of monocytes and tissue- and tumor-associated macrophages but does not inhibit inflammation. *Blood*, **116**, 3955-3963.

Malavia, NK, Mih, JD, Raub, CB, Dinh, BT & George, SC. (2008). IL-13 induces a bronchial epithelial phenotype that is profibrotic. *Respir Res*, **9**, 27.

Mamessier, E, Nieves, A, Lorec, AM, Dupuy, P, Pinot, D, Pinet, C, Vervloet, D & Magnan, A. (2008). T-cell activation during exacerbations: a longitudinal study in refractory asthma. *Allergy*, **63**, 1202-1210.

Martin, PL, Fisher, D, Glass, W, O'Neil, K, Das, A, Martin, EC & Li, L. (2008). Preclinical safety and pharmacology of an anti-human interleukin-13 monoclonal antibody in normal macaques and in macaques with allergic asthma. *Int J Toxicol*, **27**, 351-358.

Martinez, FO, Sica, A, Mantovani, A & Locati, M. (2008). Macrophage activation and polarization. *Front Biosci*, **13**, 453-461.

Maruo, K, Akaike, T, Ono, T, Okamoto, T & Maeda, H. (1997). Generation of anaphylatoxins through proteolytic processing of C3 and C5 by house dust mite protease. *J Allergy Clin Immunol*, **100**, 253-260.

Matsukura, S, Stellato, C, Georas, SN, Casolaro, V, Plitt, JR, Miura, K, Kurosawa, S, Schindler, U & Schleimer, RP. (2001). Interleukin-13 upregulates eotaxin expression

in airway epithelial cells by a STAT6-dependent mechanism. *Am J Respir Cell Mol Biol*, **24**, 755-761.

Mattes, J, Yang, M, Mahalingam, S, Kuehr, J, Webb, DC, Simson, L, Hogan, SP, Koskinen, A, McKenzie, AN, Dent, LA, Rothenberg, ME, Matthaei, KI, Young, IG & Foster, PS. (2002). Intrinsic defect in T cell production of interleukin (IL)-13 in the absence of both IL-5 and eotaxin precludes the development of eosinophilia and airways hyperreactivity in experimental asthma. *J Exp Med*, **195**, 1433-1444.

McKenzie, AN, Culpepper, JA, de Waal, MR, Briere, F, Punnonen, J, Aversa, G, Sato, A, Dang, W, Cocks, BG & Menon, S. (1993). Interleukin 13, a T-cell-derived cytokine that regulates human monocyte and B-cell function. *Proc Natl Acad Sci U S A*, **90**, 3735-3739.

Menzies, FM, Henriquez, FL, Alexander, J & Roberts, CW. (2010). Sequential expression of macrophage anti-microbial/inflammatory and wound healing markers following innate, alternative and classical activation. *Clin Exp Immunol*, **160**, 369-379.

Miloux, B, Laurent, P, Bonnin, O, Lupker, J, Caput, D, Vita, N & Ferrara, P. (1997). Cloning of the human IL-13R alpha1 chain and reconstitution with the IL4R alpha of a functional IL-4/IL-13 receptor complex. *FEBS Lett*, **401**, 163-166.

Minty, A, Chalon, P, Derocq, JM, Dumont, X, Guillemot, JC, Kaghad, M, Labit, C, Leplatois, P, Liauzun, P & Miloux, B. (1993). Interleukin-13 is a new human lymphokine regulating inflammatory and immune responses. *Nature*, **362**, 248-250.

Miyata, M, Nakamura, Y, Shimokawa, N, Ohnuma, Y, Katoh, R, Matsuoka, S, Okumura, K, Ogawa, H, Masuyama, K & Nakao, A. (2009). Thymic stromal lymphopoietin is a critical mediator of IL-13-driven allergic inflammation. *Eur J Immunol*, **39**, 3078-3083.

Molet, S, Hamid, Q, Davoine, F, Nutku, E, Taha, R, Page, N, Olivenstein, R, Elias, J & Chakir, J. (2001). IL-17 is increased in asthmatic airways and induces human bronchial fibroblasts to produce cytokines. *J Allergy Clin Immunol*, **108**, 430-438.

Moon, KA, Kim, SY, Kim, TB, Yun, ES, Park, CS, Cho, YS, Moon, HB & Lee, KY. (2007). Allergen-induced CD11b+ CD11c(int) CCR3+ macrophages in the lung promote eosinophilic airway inflammation in a mouse asthma model. *Int Immunol*, **19**, 1371-1381.

Moore, WC, Meyers, DA, Wenzel, SE, Teague, WG, Li, H, Li, X, D'Agostino, R, Jr., Castro, M, Curran-Everett, D, Fitzpatrick, AM, Gaston, B, Jarjour, NN, Sorkness, R, Calhoun, WJ, Chung, KF, Comhair, SA, Dweik, RA, Israel, E, Peters, SP, Busse, WW, Erzurum, SC & Bleecker, ER. (2010). Identification of asthma phenotypes using cluster analysis in the Severe Asthma Research Program. *Am J Respir Crit Care Med*, **181**, 315-323.

Moreira, AP & Hogaboam, CM. (2011). Macrophages in allergic asthma: fine-tuning their pro- and anti-inflammatory actions for disease resolution. *J Interferon Cytokine Res*, **31**, 485-491.

Moro, K, Yamada, T, Tanabe, M, Takeuchi, T, Ikawa, T, Kawamoto, H, Furusawa, J, Ohtani, M, Fujii, H & Koyasu, S. (2010). Innate production of T(H)2 cytokines by adipose tissue-associated c-Kit(+)Sca-1(+) lymphoid cells. *Nature*, **463**, 540-544.

Mosser, DM & Edwards, JP. (2008). Exploring the full spectrum of macrophage activation. *Nat Rev Immunol*, **8**, 958-969.

Mosser, DM & Zhang, X. (2008). Interleukin-10: new perspectives on an old cytokine. *Immunol Rev*, **226**, 205-218.

Moynihan, B, Tolloczko, B, Michoud, MC, Tamaoka, M, Ferraro, P & Martin, JG. (2008). MAP kinases mediate interleukin-13 effects on calcium signaling in human airway smooth muscle cells. *Am J Physiol Lung Cell Mol Physiol*, **295**, L171-L177.

Munitz, A, Brandt, EB, Mingler, M, Finkelman, FD & Rothenberg, ME. (2008). Distinct roles for IL-13 and IL-4 via IL-13 receptor alpha1 and the type II IL-4 receptor in asthma pathogenesis. *Proc Natl Acad Sci U S A*, **105**, 7240-7245.

Nagarkar, DR, Bowman, ER, Schneider, D, Wang, Q, Shim, J, Zhao, Y, Linn, MJ, McHenry, CL, Gosangi, B, Bentley, JK, Tsai, WC, Sajjan, US, Lukacs, NW & Hershenson, MB. (2010). Rhinovirus infection of allergen-sensitized and -challenged mice induces eotaxin release from functionally polarized macrophages. *J Immunol*, **185**, 2525-2535.

Nathan, AT, Peterson, EA, Chakir, J & Wills-Karp, M. (2009). Innate immune responses of airway epithelium to house dust mite are mediated through beta-glucan-dependent pathways. *J Allergy Clin Immunol*, **123**, 612-618.

Neill, DR, Wong, SH, Bellosi, A, Flynn, RJ, Daly, M, Langford, TK, Bucks, C, Kane, CM, Fallon, PG, Pannell, R, Jolin, HE & McKenzie, AN. (2010). Nuocytes represent a new innate effector leukocyte that mediates type-2 immunity. *Nature*, **464**, 1367-1370.

Newcomb, DC, Boswell, MG, Zhou, W, Huckabee, MM, Goleniewska, K, Sevin, CM, Khurana Hershey, GK, Kolls, JK & Peebles, RS, Jr. (2011). Human T(H)17 cells express a functional IL-13 receptor and IL-13 attenuates IL-17A production. *J Allergy Clin Immunol*, **127**, 1006-1013.

Newcomb, DC, Zhou, W, Moore, ML, Goleniewska, K, Hershey, GK, Kolls, JK & Peebles, RS, Jr. (2009). A functional IL-13 receptor is expressed on polarized murine CD4+ Th17 cells and IL-13 signaling attenuates Th17 cytokine production. *J Immunol*, **182**, 5317-5321.

Nicholson, GC, Kariyawasam, HH, Tan, AJ, Hohlfeld, JM, Quinn, D, Walker, C, Rodman, D, Westwick, J, Jurcevic, S, Kon, OM, Barnes, PJ, Krug, N & Hansel, TT. (2011). The effects of an anti-IL-13 monoclonal antibody on cytokine levels and nasal symptoms following nasal allergen challenge. *J Allergy Clin Immunol*, (in press).

Niimi, A, Matsumoto, H, Amitani, R, Nakano, Y, Mishima, M, Minakuchi, M, Nishimura, K, Itoh, H & Izumi, T. (2000). Airway wall thickness in asthma assessed by computed tomography. Relation to clinical indices. *Am J Respir Crit Care Med*, **162**, 1518-1523.

O'Byrne, PM & Inman, MD. (2003). Airway hyperresponsiveness. *Chest*, **123**, 411S-416S.

O'Toole, M, Legault, H, Ramsey, R, Wynn, TA & Kasaian, MT. (2008). A novel and sensitive ELISA reveals that the soluble form of IL-13R-alpha2 is not expressed in plasma of healthy or asthmatic subjects. *Clin Exp Allergy*, **38**, 594-601.

Ochensberger, B, Daepp, GC, Rihs, S & Dahinden, CA. (1996). Human blood basophils produce interleukin-13 in response to IgE-receptor-dependent and -independent activation. *Blood*, **88**, 3028-3037.

Oh, CK, Geba, GP & Molfino, N. (2010). Investigational therapeutics targeting the IL-4/IL-13/STAT-6 pathway for the treatment of asthma. *Eur Respir Rev*, **19**, 46-54.

Ordonez, CL, Khashayar, R, Wong, HH, Ferrando, R, Wu, R, Hyde, DM, Hotchkiss, JA, Zhang, Y, Novikov, A, Dolganov, G & Fahy, JV. (2001). Mild and moderate asthma is associated with airway goblet cell hyperplasia and abnormalities in mucin gene expression. *Am J Respir Crit Care Med*, **163**, 517-523.

Overton, WR. (1988). Modified histogram subtraction technique for analysis of flow cytometry data. *Cytometry*, **9**, 619-626.

Padilla, J, Daley, E, Chow, A, Robinson, K, Parthasarathi, K, McKenzie, AN, Tschernig, T, Kurup, VP, Donaldson, DD & Grunig, G. (2005). IL-13 regulates the immune response to inhaled antigens. *J Immunol*, **174**, 8097-8105.

Paul, WE & Zhu, J. (2010). How are T(H)2-type immune responses initiated and amplified? *Nat Rev Immunol*, **10**, 225-235.

Pene, J, Chevalier, S, Preisser, L, Venereau, E, Guilleux, MH, Ghannam, S, Moles, JP, Danger, Y, Ravon, E, Lesaux, S, Yssel, H & Gascan, H. (2008). Chronically inflamed human tissues are infiltrated by highly differentiated Th17 lymphocytes. *J Immunol*, **180**, 7423-7430.

Perrigoue, JG, Saenz, SA, Siracusa, MC, Allenspach, EJ, Taylor, BC, Giacomin, PR, Nair, MG, Du, Y, Zaph, C, van, RN, Comeau, MR, Pearce, EJ, Laufer, TM & Artis, D. (2009). MHC class II-dependent basophil-CD4+ T cell interactions promote T(H)2 cytokine-dependent immunity. *Nat Immunol*, **10**, 697-705.

Peters-Golden, M. (2004). The alveolar macrophage: the forgotten cell in asthma. *Am J Respir Cell Mol Biol*, **31**, 3-7.

Pope, SM, Fulkerson, PC, Blanchard, C, Akei, HS, Nikolaidis, NM, Zimmermann, N, Molkentin, JD & Rothenberg, ME. (2005). Identification of a cooperative mechanism involving interleukin-13 and eotaxin-2 in experimental allergic lung inflammation. *J Biol Chem*, **280**, 13952-13961.

Pouliot, P, Spahr, A, Careau, E, Turmel, V & Bissonnette, EY. (2008). Alveolar macrophages from allergic lungs are not committed to a pro-allergic response and can reduce airway hyperresponsiveness following ex vivo culture. *Clin Exp Allergy*, **38**, 529-538.

Price, AE, Liang, HE, Sullivan, BM, Reinhardt, RL, Eisley, CJ, Erle, DJ & Locksley, RM. (2010). Systemically dispersed innate IL-13-expressing cells in type 2 immunity. *Proc Natl Acad Sci U S A*, **107**, 11489-11494.

Prieto, J, Lensmar, C, Roquet, A, van, dP, I, Gigliotti, D, Eklund, A & Grunewald, J. (2000). Increased interleukin-13 mRNA expression in bronchoalveolar lavage cells of atopic patients with mild asthma after repeated low-dose allergen provocations. *Respir Med*, **94**, 806-814.

Punnonen, J, Aversa, G, Cocks, BG, McKenzie, AN, Menon, S, Zurawski, G, de Waal, MR & de Vries, JE. (1993). Interleukin 13 induces interleukin 4-independent IgG4 and IgE synthesis and CD23 expression by human B cells. *Proc Natl Acad Sci U S A*, **90**, 3730-3734.

Rahaman, SO, Sharma, P, Harbor, PC, Aman, MJ, Vogelbaum, MA & Haque, SJ. (2002). IL-13R(alpha)2, a decoy receptor for IL-13 acts as an inhibitor of IL-4-dependent signal transduction in glioblastoma cells. *Cancer Res*, **62**, 1103-1109.

Ramalingam, TR, Pesce, JT, Sheikh, F, Cheever, AW, Mentink-Kane, MM, Wilson, MS, Stevens, S, Valenzuela, DM, Murphy, AJ, Yancopoulos, GD, Urban, JF, Jr., Donnelly, RP & Wynn, TA. (2008). Unique functions of the type II interleukin 4 receptor identified in mice lacking the interleukin 13 receptor alpha1 chain. *Nat Immunol*, **9**, 25-33.

Reese, TA, Liang, HE, Tager, AM, Luster, AD, van, RN, Voehringer, D & Locksley, RM. (2007). Chitin induces accumulation in tissue of innate immune cells associated with allergy. *Nature*, **447**, 92-96.

Reglier, H, Arce-Vicioso, M, Fay, M, Gougerot-Pocidalo, MA & Chollet-Martin, S. (1998). Lack of IL-10 and IL-13 production by human polymorphonuclear neutrophils. *Cytokine*, **10**, 192-198.

Risse, PA, Jo, T, Suarez, F, Hirota, N, Tolloczko, B, Ferraro, P, Grutter, P & Martin, JG. (2011). Interleukin-13 inhibits proliferation and enhances contractility of human airway smooth muscle cells without change in contractile phenotype. *Am J Physiol Lung Cell Mol Physiol*, **300**, L958-L966.

Robinson, DS, Hamid, Q, Ying, S, Tsicopoulos, A, Barkans, J, Bentley, AM, Corrigan, C, Durham, SR & Kay, AB. (1992). Predominant TH2-like bronchoalveolar T-lymphocyte population in atopic asthma. *N Engl J Med*, **326**, 298-304.

Rothenberg, ME & Hogan, SP. (2006). The eosinophil. *Annu Rev Immunol*, **24**, 147-174.

Saenz, SA, Noti, M & Artis, D. (2010a). Innate immune cell populations function as initiators and effectors in Th2 cytokine responses. *Trends Immunol*, **31**, 407-413.

Saenz, SA, Siracusa, MC, Perrigoue, JG, Spencer, SP, Urban, JF, Jr., Tocker, JE, Budelsky, AL, Kleinschek, MA, Kastelein, RA, Kambayashi, T, Bhandoola, A & Artis, D. (2010b). IL25 elicits a multipotent progenitor cell population that promotes T(H)2 cytokine responses. *Nature*, **464**, 1362-1366.

Saha, SK, Berry, MA, Parker, D, Siddiqui, S, Morgan, A, May, R, Monk, P, Bradding, P, Wardlaw, AJ, Pavord, ID & Brightling, CE. (2008). Increased sputum and bronchial biopsy IL-13 expression in severe asthma. *J Allergy Clin Immunol*, **121**, 685-691.

Saito, A, Okazaki, H, Sugawara, I, Yamamoto, K & Takizawa, H. (2003). Potential action of IL-4 and IL-13 as fibrogenic factors on lung fibroblasts in vitro. *Int Arch Allergy Immunol*, **132**, 168-176.

Schmid-Grendelmeier, P, Altznauer, F, Fischer, B, Bizer, C, Straumann, A, Menz, G, Blaser, K, Wuthrich, B & Simon, HU. (2002). Eosinophils express functional IL-13 in eosinophilic inflammatory diseases. *J Immunol*, **169**, 1021-1027.

Schroeder, JT, Bieneman, AP, Chichester, KL, Breslin, L, Xiao, H & Liu, MC. (2010). Pulmonary allergic responses augment interleukin-13 secretion by circulating basophils yet suppress interferon-alpha from plasmacytoid dendritic cells. *Clin Exp Allergy*, **40**, 745-754.

Schulz, O, Laing, P, Sewell, HF & Shakib, F. (1995). Der p I, a major allergen of the house dust mite, proteolytically cleaves the low-affinity receptor for human IgE (CD23). *Eur J Immunol*, **25**, 3191-3194.

Schulz, O, Sewell, HF & Shakib, F. (1998). Proteolytic cleavage of CD25, the alpha subunit of the human T cell interleukin 2 receptor, by Der p 1, a major mite allergen with cysteine protease activity. *J Exp Med*, **187**, 271-275.

Semlali, A, Jacques, E, Koussih, L, Gounni, AS & Chakir, J. (2010). Thymic stromal lymphopoietin-induced human asthmatic airway epithelial cell proliferation through an IL-13-dependent pathway. *J Allergy Clin Immunol*, **125**, 844-850.

Shao, DD, Suresh, R, Vakil, V, Gomer, RH & Pilling, D. (2008). Pivotal Advance: Th-1 cytokines inhibit, and Th-2 cytokines promote fibrocyte differentiation. *J Leukoc Biol*, **83**, 1323-1333.

Singh, D, Kane, B, Molfino, NA, Faggioni, R, Roskos, L & Woodcock, A. (2010). A phase 1 study evaluating the pharmacokinetics, safety and tolerability of repeat dosing with a human IL-13 antibody (CAT-354) in subjects with asthma. *BMC Pulm Med*, **10**, 3.

Sokol, CL, Chu, NQ, Yu, S, Nish, SA, Laufer, TM & Medzhitov, R. (2009). Basophils function as antigen-presenting cells for an allergen-induced T helper type 2 response. *Nat Immunol*, **10**, 713-720.

Southam, DS, Ellis, R, Wattie, J & Inman, MD. (2007). Components of airway hyperresponsiveness and their associations with inflammation and remodeling in mice. *J Allergy Clin Immunol*, **119**, 848-854.

St-Laurent, J, Turmel, V, Boulet, LP & Bissonnette, E. (2009). Alveolar macrophage subpopulations in bronchoalveolar lavage and induced sputum of asthmatic and control subjects. *J Asthma*, **46**, 1-8.

Steinke, JW. (2004). Anti-interleukin-4 therapy. *Immunol Allergy Clin North Am*, **24**, 599-614.

Strickland, DH, Thepen, T, Kees, UR, Kraal, G & Holt, PG. (1993). Regulation of T-cell function in lung tissue by pulmonary alveolar macrophages. *Immunology*, **80**, 266-272.

Strober, W, Kitani, A, Fichtner-Feigl, S & Fuss, IJ. (2009). The signaling function of the IL-13Ralpha2 receptor in the development of gastrointestinal fibrosis and cancer surveillance. *Curr Mol Med*, **9**, 740-750.

Sun, G, Stacey, MA, Schmidt, M, Mori, L & Mattoli, S. (2001). Interaction of mite allergens Der p3 and Der p9 with protease-activated receptor-2 expressed by lung epithelial cells. *J Immunol*, **167**, 1014-1021.

Syed, F, Panettieri, RA, Jr., Tliba, O, Huang, C, Li, K, Bracht, M, Amegadzie, B, Griswold, D, Li, L & Amrani, Y. (2005). The effect of IL-13 and IL-13R130Q, a naturally occurring IL-13 polymorphism, on the gene expression of human airway smooth muscle cells. *Respir Res*, **6**, 9.

Tabata, Y, Chen, W, Warrier, MR, Gibson, AM, Daines, MO & Hershey, GK. (2006). Allergy-driven alternative splicing of IL-13 receptor alpha2 yields distinct membrane and soluble forms. *J Immunol*, **177**, 7905-7912.

Tanabe, T, Fujimoto, K, Yasuo, M, Tsushima, K, Yoshida, K, Ise, H & Yamaya, M. (2008). Modulation of mucus production by interleukin-13 receptor alpha2 in the human airway epithelium. *Clin Exp Allergy*, **38**, 122-134.

Tang, C, Inman, MD, van, RN, Yang, P, Shen, H, Matsumoto, K & O'Byrne, PM. (2001a). Th type 1-stimulating activity of lung macrophages inhibits Th2-mediated allergic airway inflammation by an IFN-gamma-dependent mechanism. *J Immunol*, **166**, 1471-1481.

Tang, C, Rolland, JM, Ward, C, Li, X, Bish, R, Thien, F & Walters, EH. (1999). Modulatory effects of alveolar macrophages on CD4+ T-cell IL-5 responses correlate with IL-1beta, IL-6, and IL-12 production. *Eur Respir J*, **14**, 106-112.

Tang, C, Ward, C, Reid, D, Bish, R, O'Byrne, PM & Walters, EH. (2001b). Normally suppressing CD40 coregulatory signals delivered by airway macrophages to TH2 lymphocytes are defective in patients with atopic asthma. *J Allergy Clin Immunol*, **107**, 863-870.

Taube, C, Duez, C, Cui, ZH, Takeda, K, Rha, YH, Park, JW, Balhorn, A, Donaldson, DD, Dakhama, A & Gelfand, EW. (2002). The role of IL-13 in established allergic airway disease. *J Immunol*, **169**, 6482-6489.

Thepen, T, Kraal, G & Holt, PG. (1994). The role of alveolar macrophages in regulation of lung inflammation. *Ann N Y Acad Sci*, **725**, 200-206.

Thepen, T, McMenamin, C, Girn, B, Kraal, G & Holt, PG. (1992). Regulation of IgE production in pre-sensitized animals: in vivo elimination of alveolar macrophages

preferentially increases IgE responses to inhaled allergen. *Clin Exp Allergy*, **22**, 1107-1114.

Thepen, T, van, RN & Kraal, G. (1989). Alveolar macrophage elimination in vivo is associated with an increase in pulmonary immune response in mice. *J Exp Med*, **170**, 499-509.

Therien, AG, Bernier, V, Weicker, S, Tawa, P, Falgueyret, JP, Mathieu, MC, Honsberger, J, Pomerleau, V, Robichaud, A, Stocco, R, Dufresne, L, Houshyar, H, Lafleur, J, Ramachandran, C, O'Neill, GP, Slipetz, D & Tan, CM. (2008). Adenovirus IL-13-induced airway disease in mice: a corticosteroid-resistant model of severe asthma. *Am J Respir Cell Mol Biol*, **39**, 26-35.

Tliba, O, Deshpande, D, Chen, H, Van, BC, Kannan, M, Panettieri, RA, Jr. & Amrani, Y. (2003). IL-13 enhances agonist-evoked calcium signals and contractile responses in airway smooth muscle. *Br J Pharmacol*, **140**, 1159-1162.

Tomkinson, A, Tepper, J, Morton, M, Bowden, A, Stevens, L, Harris, P, Lindell, D, Fitch, N, Gundel, R & Getz, EB. (2010). Inhaled vs subcutaneous effects of a dual IL-4/IL-13 antagonist in a monkey model of asthma. *Allergy*, **65**, 69-77.

Tomlinson, KL, Davies, GC, Sutton, DJ & Palframan, RT. (2010). Neutralisation of interleukin-13 in mice prevents airway pathology caused by chronic exposure to house dust mite. *PLoS One*, **5**.

Trompette, A, Divanovic, S, Visintin, A, Blanchard, C, Hegde, RS, Madan, R, Thorne, PS, Wills-Karp, M, Gioannini, TL, Weiss, JP & Karp, CL. (2009). Allergenicity resulting from functional mimicry of a Toll-like receptor complex protein. *Nature*, **457**, 585-588.

Ulrich, K, Hincks, JS, Walsh, R, Wetterstrand, EM, Fidock, MD, Sreckovic, S, Lamb, DJ, Douglas, GJ, Yeadon, M, Perros-Huguet, C & Evans, SM. (2008). Anti-inflammatory modulation of chronic airway inflammation in the murine house dust mite model. *Pulm Pharmacol Ther*, **21**, 637-647.

Van Hove, CL, Maes, T, Joos, GF & Tournoy, KG. (2007). Prolonged inhaled allergen exposure can induce persistent tolerance. *Am J Respir Cell Mol Biol*, **36**, 573-584.

van Rijt, LS, Jung, S, Kleinjan, A, Vos, N, Willart, M, Duez, C, Hoogsteden, HC & Lambrecht, BN. (2005). In vivo depletion of lung CD11c+ dendritic cells during allergen challenge abrogates the characteristic features of asthma. *J Exp Med*, **201**, 981-991.

van Rooijen, N & Sanders, A. (1994). Liposome mediated depletion of macrophages: mechanism of action, preparation of liposomes and applications. *J Immunol Methods*, **174**, 83-93.

van Scott, MR, Justice, JP, Bradfield, JF, Enright, E, Sigounas, A & Sur, S. (2000). IL-10 reduces Th2 cytokine production and eosinophilia but augments airway reactivity in allergic mice. *Am J Physiol Lung Cell Mol Physiol*, **278**, L667-L674.

Viksman, MY, Bochner, BS, Peebles, RS, Schleimer, RP & Liu, MC. (2002). Expression of activation markers on alveolar macrophages in allergic asthmatics after endobronchial or whole-lung allergen challenge. *Clin Immunol*, **104**, 77-85.

Vock, C, Hauber, HP & Wegmann, M. (2010). The other T helper cells in asthma pathogenesis. *J Allergy (Cairo)*, **2010**, 519298.

Walsh, ER, Thakar, J, Stokes, K, Huang, F, Albert, R & August, A. (2011). Computational and experimental analysis reveals a requirement for eosinophil-derived IL-13 for the development of allergic airway responses in C57BL/6 mice. *J Immunol*, **186**, 2936-2949.

Walsh, GM. (2010). Tralokinumab, an anti-IL-13 mAb for the potential treatment of asthma and COPD. *Curr Opin Investig Drugs*, **11**, 1305-1312.

Walter, DM, McIntire, JJ, Berry, G, McKenzie, AN, Donaldson, DD, DeKruyff, RH & Umetsu, DT. (2001). Critical role for IL-13 in the development of allergen-induced airway hyperreactivity. *J Immunol*, **167**, 4668-4675.

Wan, H, Winton, HL, Soeller, C, Tovey, ER, Gruenert, DC, Thompson, PJ, Stewart, GA, Taylor, GW, Garrod, DR, Cannell, MB & Robinson, C. (1999). Der p 1 facilitates transepithelial allergen delivery by disruption of tight junctions. *J Clin Invest*, **104**, 123-133.

Wang, Y & McCusker, CT. (2005). Interleukin-13-dependent bronchial hyper-responsiveness following isolated upper-airway allergen challenge in a murine model of allergic rhinitis and asthma. *Clin Exp Allergy*, **35**, 1104-1111.

Webb, DC, Cai, Y, Matthaei, KI & Foster, PS. (2007). Comparative roles of IL-4, IL-13, and IL-4Ralpha in dendritic cell maturation and CD4+ Th2 cell function. *J Immunol*, **178**, 219-227.

Wenzel, S. (2005). Severe asthma in adults. *Am J Respir Crit Care Med*, **172**, 149-160.

Wenzel, S, Wilbraham, D, Fuller, R, Getz, EB & Longphre, M. (2007). Effect of an interleukin-4 variant on late phase asthmatic response to allergen challenge in asthmatic patients: results of two phase 2a studies. *Lancet*, **370**, 1422-1431.

Wenzel, SE. (2006). Asthma: defining of the persistent adult phenotypes. *Lancet*, **368**, 804-813.

Wenzel, SE, Trudeau, JB, Barnes, S, Zhou, X, Cundall, M, Westcott, JY, McCord, K & Chu, HW. (2002). TGF-beta and IL-13 synergistically increase eotaxin-1 production in human airway fibroblasts. *J Immunol*, **169**, 4613-4619.

Willart, MA & Hammad, H. (2010). Alarming dendritic cells for allergic sensitization. *Allergol Int*, **59**, 95-103.

Wills-Karp, M. (2004). Interleukin-13 in asthma pathogenesis. *Immunol Rev*, **202**, 175-190.

Wills-Karp, M, Luyimbazi, J, Xu, X, Schofield, B, Neben, TY, Karp, CL & Donaldson, DD. (1998). Interleukin-13: central mediator of allergic asthma. *Science*, **282**, 2258-2261.

Wilson, MS, Elnekave, E, Mentink-Kane, MM, Hodges, MG, Pesce, JT, Ramalingam, TR, Thompson, RW, Kamanaka, M, Flavell, RA, Keane-Myers, A, Cheever, AW & Wynn, TA. (2007). IL-13Ralpha2 and IL-10 coordinately suppress airway inflammation, airway-hyperreactivity, and fibrosis in mice. *J Clin Invest*, **117**, 2941-2951.

Woltmann, G, McNulty, CA, Dewson, G, Symon, FA & Wardlaw, AJ. (2000). Interleukin-13 induces PSGL-1/P-selectin-dependent adhesion of eosinophils, but not neutrophils, to human umbilical vein endothelial cells under flow. *Blood*, **95**, 3146-3152.

Wood, N, Whitters, MJ, Jacobson, BA, Witek, J, Sypek, JP, Kasaian, M, Eppihimer, MJ, Unger, M, Tanaka, T, Goldman, SJ, Collins, M, Donaldson, DD & Grusby, MJ. (2003). Enhanced interleukin (IL)-13 responses in mice lacking IL-13 receptor alpha 2. *J Exp Med*, **197**, 703-709.

Woodruff, PG, Boushey, HA, Dolganov, GM, Barker, CS, Yang, YH, Donnelly, S, Ellwanger, A, Sidhu, SS, Dao-Pick, TP, Pantoja, C, Erle, DJ, Yamamoto, KR & Fahy, JV. (2007). Genome-wide profiling identifies epithelial cell genes associated with asthma and with treatment response to corticosteroids. *Proc Natl Acad Sci U S A*, **104**, 15858-15863.

Woodruff, PG, Modrek, B, Choy, DF, Jia, G, Abbas, AR, Ellwanger, A, Koth, LL, Arron, JR & Fahy, JV. (2009). T-helper type 2-driven inflammation defines major subphenotypes of asthma. *Am J Respir Crit Care Med*, **180**, 388-395.

Wynn, TA. (2003). IL-13 effector functions. *Annu Rev Immunol*, **21**, 425-456.

Xu, D, Chan, WL, Leung, BP, Huang, F, Wheeler, R, Piedrafita, D, Robinson, JH & Liew, FY. (1998). Selective expression of a stable cell surface molecule on type 2 but not type 1 helper T cells. *J Exp Med*, **187**, 787-794.

Yang, G, Li, L, Volk, A, Emmell, E, Petley, T, Giles-Komar, J, Rafferty, P, Lakshminarayanan, M, Griswold, DE, Bugelski, PJ & Das, AM. (2005). Therapeutic dosing with anti-interleukin-13 monoclonal antibody inhibits asthma progression in mice. *J Pharmacol Exp Ther*, **313**, 8-15.

Yang, G, Volk, A, Petley, T, Emmell, E, Giles-Komar, J, Shang, X, Li, J, Das, AM, Shealy, D, Griswold, DE & Li, L. (2004). Anti-IL-13 monoclonal antibody inhibits airway hyperresponsiveness, inflammation and airway remodeling. *Cytokine*, **28**, 224-232.

Yang, M, Hogan, SP, Henry, PJ, Matthaei, KI, McKenzie, AN, Young, IG, Rothenberg, ME & Foster, PS. (2001). Interleukin-13 mediates airways hyperreactivity through the IL-4 receptor-alpha chain and STAT-6 independently of IL-5 and eotaxin. *Am J Respir Cell Mol Biol*, **25**, 522-530.

Yang, M, Kumar, RK & Foster, PS. (2010). Interferon-gamma and pulmonary macrophages contribute to the mechanisms underlying prolonged airway hyperresponsiveness. *Clin Exp Allergy*, **40**, 163-173.

Yasunaga, S, Yuyama, N, Arima, K, Tanaka, H, Toda, S, Maeda, M, Matsui, K, Goda, C, Yang, Q, Sugita, Y, Nagai, H & Izuhara, K. (2003). The negative-feedback regulation of the IL-13 signal by the IL-13 receptor alpha2 chain in bronchial epithelial cells. *Cytokine*, **24**, 293-303.

Ying, S, Meng, Q, Taborda-Barata, L & Kay, AB. (1997). Association of apoptosis of neutrophils and eosinophils and their ingestion by macrophages with resolution of the allergen-induced cutaneous late-phase response in atopic human subjects. *Proc Assoc Am Physicians*, **109**, 42-50.

Yoshimoto, T, Yasuda, K, Tanaka, H, Nakahira, M, Imai, Y, Fujimori, Y & Nakanishi, K. (2009). Basophils contribute to T(H)2-IgE responses in vivo via IL-4 production and presentation of peptide-MHC class II complexes to CD4+ T cells. *Nat Immunol*, **10**, 706-712.

Zheng, T, Liu, W, Oh, SY, Zhu, Z, Hu, B, Homer, RJ, Cohn, L, Grusby, MJ & Elias, JA. (2008). IL-13 receptor alpha2 selectively inhibits IL-13-induced responses in the murine lung. *J Immunol*, **180**, 522-529.

Zheng, T, Zhu, Z, Liu, W, Lee, CG, Chen, Q, Homer, RJ & Elias, JA. (2003). Cytokine regulation of IL-13Ralpha2 and IL-13Ralpha1 in vivo and in vitro. *J Allergy Clin Immunol*, **111**, 720-728.

Zhiguang, X, Wei, C, Steven, R, Wei, D, Wei, Z, Rong, M, Zhanguo, L & Lianfeng, Z. (2010). Over-expression of IL-33 leads to spontaneous pulmonary inflammation in mIL-33 transgenic mice. *Immunol Lett*, **131**, 159-165.

Zhu, Z, Homer, RJ, Wang, Z, Chen, Q, Geba, GP, Wang, J, Zhang, Y & Elias, JA. (1999). Pulmonary expression of interleukin-13 causes inflammation, mucus hypersecretion, subepithelial fibrosis, physiologic abnormalities, and eotaxin production. *J Clin Invest*, **103**, 779-788.

Zurawski, G & de Vries, JE. (1994). Interleukin 13, an interleukin 4-like cytokine that acts on monocytes and B cells, but not on T cells. *Immunol Today*, **15**, 19-26.